THE SHAPES OF LEVEL CURVES OF REAL POLYNOMIALS NEAR STRICT LOCAL MINIMA

Miruna-Stefana Sorea

Université de Lille

Laboratoire Paul Painlevé

CEMPI CENTRE EUROPÉEN POUR LES MATHÉMATIQUES, LA PHYSIQUE ET LEURS INTERACTIONS

Thèse

présentée pour l'obtention du

Diplôme de Doctorat de l'Université de Lille

Discipline : **Mathématiques**

par **Miruna-Ştefana Sorea**

The shapes of level curves of real polynomials near strict local minima

Les formes des lignes de niveau des polynômes réels près d'un minimum local strict

Soutenue publiquement le 10 octobre 2018 devant le jury composé de :

Arnaud Bodin	Directeur	Université de Lille
Benoit Fresse	Examinateur	Université de Lille
Evelia R. García Barroso	Rapportrice	Université de La Laguna
Étienne Ghys	Examinateur	École Normale Supérieure de Lyon
Ilia Itenberg	Rapporteur	Sorbonne Université
Hélène Maugendre	Examinatrice	Université Grenoble Alpes
Patrick Popescu-Pampu	Directeur	Université de Lille

École Doctorale Sciences Pour l'Ingénieur
Laboratoire Paul Painlevé
Université de Lille

Thèse préparée au **Laboratoire Paul Painlevé (UMR CNRS 8524)**
Université de Lille
Cité Scientifique
59 655 Villeneuve d'Ascq CEDEX

grâce à un financement du **Labex CEMPI** et de la **Région Hauts-de-France**

Dédié à mes parents.

[This page intentionally left blank]

Acknowledgements

First of all, I would like to express my sincere gratitude to my PhD advisors, Arnaud Bodin and Patrick Popescu-Pampu, for their continuous support and guidance. They taught me with professionalism and patience how to look for the good paths in my research. They are a model for me both in academia and in life. Thank you for believing in me!

My grateful thanks are also going to the reviewers, Evelia R. García Barroso and Ilia Itenberg, for carefully reading the manuscript and for their valuable remarks. Many thanks should also go to Benoit Fresse, Étienne Ghys and Hélène Maugendre, for being part of my thesis committee.

I extend my sincere thanks to all the members of the Laboratoire Paul Painlevé, in particular to Pierre Dèbes, Stephan de Bièvre and Guoting Chen.

I would like to express my gratitude to my professors at Babeş-Bolyai University in Cluj-Napoca. Special thanks go to Dorin Andrica, Simion Breaz and Cornel Pintea, who offered me good advice, teachings and useful recommendations.

The completion of my thesis would not have been possible without the lifelong support of my beloved parents and family. I wish to thank my father for his continuous dedication in introducing me in the passionate world of mathematics. He is always giving me the motivation and enthusiasm to progress on the realm of research. I offer my thanks to my mother for guiding me towards the good balance in all aspects of life and for teaching me about altruism and the ambition to do my best.

I am extremely grateful to Dani for all his affection, encouragements, sense of humour, optimism and balance. The period spent in Lille wouldn't have been the same without you! Together we braided mathematics with the poetry of life!

Many thanks to my friends, especially to Florian and Antonietta and to all my PhD office colleagues for the memorable and enjoyable moments we shared.

Finally, I wish to thank all the persons who have ever had any contribution to my personal and professional development!

[This page intentionally left blank]

Abstract

We consider a real bivariate polynomial function vanishing at the origin and exhibiting a strict local minimum at this point. We work in a neighbourhood of the origin in which the non-zero level curves of this function are smooth Jordan curves. Whenever the origin is a Morse critical point, the sufficiently small levels become boundaries of convex disks. Otherwise, these level curves may fail to be convex, as was shown by Coste.

The aim of the present thesis is twofold. Firstly, to construct examples of non-Morse strict local minima whose sufficiently small level curves are far from being convex. And secondly, to study a combinatorial object measuring this non-convexity, namely the Poincaré-Reeb tree of the restriction of the first coordinate to the region bounded by a given level curve. These planar trees are rooted and their vertices roughly speaking correspond to points on the curve with vertical tangent lines.

The main objective of our study is to characterise all possible topological types of Poincaré-Reeb trees. To this end, we construct a family of examples realising a large class of such trees. As a preliminary step, we restrict our attention to the univariate case, using a tool inspired by Ghys' work. One of our main results gives a new and constructive proof of the existence of Morse polynomials whose associated permutation (the so-called "Arnold's snake") is separable.

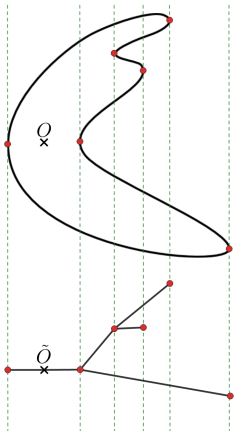

A variation of Coste's example: a level curve near a non-Morse strict minimum at the origin and a Poincaré-Reeb tree associated to it.

[This page intentionally left blank]

Résumé

Les formes des lignes de niveau des polynômes réels près d'un minimum local strict

Nous considérons une fonction polynomiale de deux variables réelles qui s'annule à l'origine et qui a un minimum local strict en ce point. Nous nous plaçons dans un voisinage de l'origine dans lequel les lignes de niveau non nulles de cette fonction sont des courbes de Jordan lisses. Chaque fois que l'origine est un point critique de Morse, les niveaux suffisamment petits deviennent des bords de disques convexes. Si l'origine n'est pas de Morse, ces courbes de niveau peuvent ne pas être convexes, comme l'a montré Coste.

Le but de cette thèse est double. Tout d'abord, nous nous intéressons à la construction d'exemples de minimums locaux stricts et non-Morse dont les lignes de niveau suffisamment petites sont loin d'être convexes. Et deuxièmement, nous étudions un objet combinatoire mesurant cette non-convexité : l'arbre de Poincaré-Reeb de la restriction de la première coordonnée à la région délimitée par une ligne de niveau donnée. Ces arbres planaires sont enracinés et leurs sommets correspondent en gros aux points de la courbe où les tangentes sont verticales.

L'objectif principal de notre étude est de caractériser tous les types topologiques possibles d'arbres de Poincaré-Reeb. À cette fin, nous construisons une famille d'exemples réalisant une grande classe de tels arbres. Dans un premier temps, nous concentrons notre attention sur le cas des polynômes d'une variable, en utilisant un outil inspiré du travail de Ghys. L'un de nos résultats principaux donne une preuve nouvelle et constructive de l'existence de polynômes de Morse dont la permutation associée (appelée «le serpent d'Arnold») est séparable.

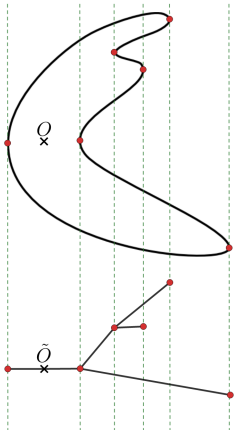

Une variante de l'exemple de Coste : une ligne de niveau d'un minimum strict et non-Morse à l'origine et un arbre de Poincaré-Reeb qui lui est associé.

[This page intentionally left blank]

Summary

Introduction - Version française

Contexte et motivation

Topologie locale des courbes algébriques dans le plan réel

Dans son livre récent ([Ghy17]), É. Ghys a étudié la topologie locale des courbes algébriques réelles. Il a décrit, en termes de permutations, les configurations locales possibles d'une famille $\{a_i(x)\}$ de polynômes réels d'une variable dans un voisinage de l'origine du plan réel. Les graphes de ces polynômes changent leurs position relative lorsqu'ils passent par un zéro commun (voir la Figure 3). Il a prouvé que les permutations pouvant être obtenues de cette manière sont exactement les permutations dites "séparables".

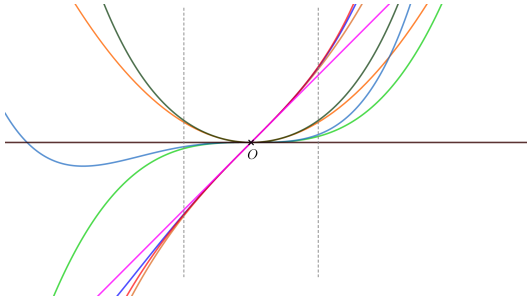

Figure 3: Les graphes des polynômes $a_i(x)$ dans un voisinage de l'origine.

Des chercheurs ont récemment montré un grand intérêt pour les permutations séparables (introduites dans [BBL98]), qui possèdent de belles propriétés algorithmiques et combinatoires (voir par exemple [Ghy17, page 27], [Bas+18], [Kit11, page 57]). Une permutation séparable est une permutation qui ne "contient" (voir par exemple [Ghy17, page 13, 18]) aucune des deux sous-permutations "interdites" suivantes:

$$\begin{pmatrix} 1 & 2 & 3 & 4 \\ 2 & 4 & 1 & 3 \end{pmatrix} \text{ ou } \begin{pmatrix} 1 & 2 & 3 & 4 \\ 3 & 1 & 4 & 2 \end{pmatrix}.$$

Un exemple de permutation qui n'est pas séparable est

$$\eta := \begin{pmatrix} 1 & 2 & 3 & 4 & 5 & 6 & 7 & 8 \\ 2 & 3 & 6 & 8 & 1 & 7 & 5 & 4 \end{pmatrix},$$

puisque η "contient" la sous-permutation $\begin{pmatrix} 1 & 2 & 3 & 4 \\ 3 & 1 & 4 & 2 \end{pmatrix}$. Il existe quatre indices $i_1 := 2$, $i_2 := 3$, $i_3 := 5$, $i_4 := 8$ tels que : $i_1 < i_2 < i_3 < i_4$, alors que nous avons (voir la Figure 4) : $\eta(i_3) \ll \eta(i_1) \ll \eta(i_4) \ll \eta(i_2)$.

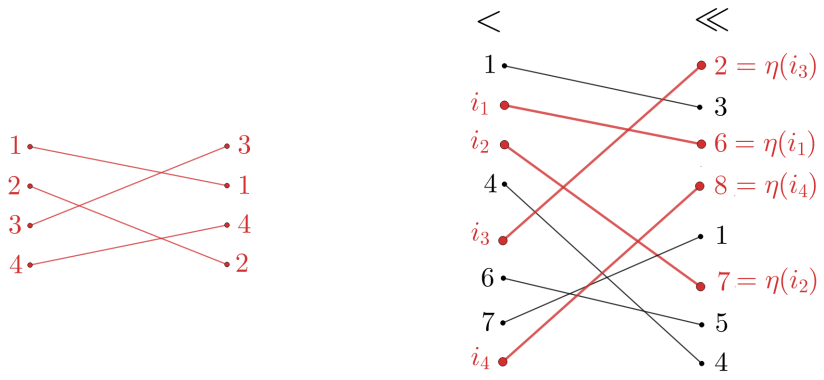

Figure 4: La permutation non séparable η contient l'une des deux permutations "interdites".

Une représentation alternative (inspirée de [Kit11, page 4]) de la permutation η, à travers son graphe, est dessinée dans la Figure 5, où nous marquons un point pour chaque paire $(i, \eta(i))$. La sous-permutation interdite est marquée par des triangles bleus.

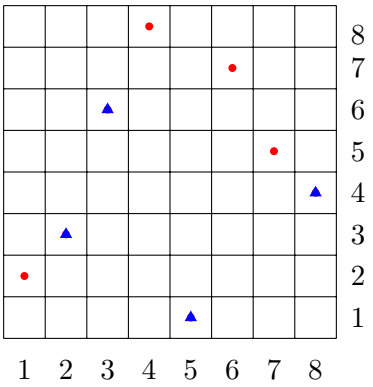

Figure 5: Une représentation alternative de la permutation η. La sous-permutation "interdite" est marquée par des triangles.

De plus, dans le même livre ([Ghy17]), E. Ghys a étudié les courbes algébriques réelles données par une équation polynomiale implicite $f(x, y) = 0$ en deux variables réelles. Il a codé leurs combinatoires en termes des "diagrammes de cordes" (voir la Figure 6).

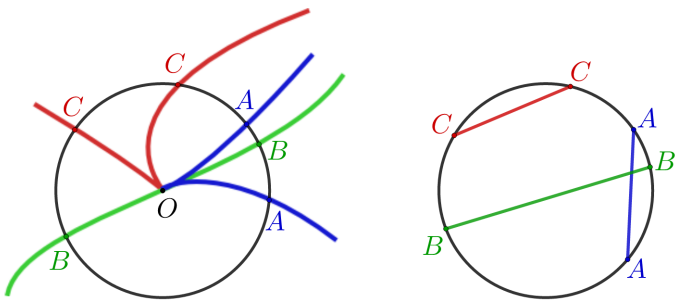

Figure 6: Une courbe singulière à trois branches (côté gauche) et son diagramme de cordes associé (côté droit).

Le but d'Étienne Ghys était de caractériser toutes les configurations topologiques possibles des branches d'une courbe algébrique dans un voisinage suffisamment petit de l'un de ses points singuliers. En collaboration avec Christopher-Lloyd Simon, il a prouvé:

Théorème. *[Ghy17, page 266 (Ghys et Simon)] Un diagramme de cordes donné est réalisable par une courbe plane algébrique réelle au voisinage d'un point singulier si et seulement si le diagramme de cordes ne contient aucun des sous-diagrammes de cordes illustrés ci-dessous (notez que le dernier sous-diagramme de cordes contient au moins cinq cordes):*

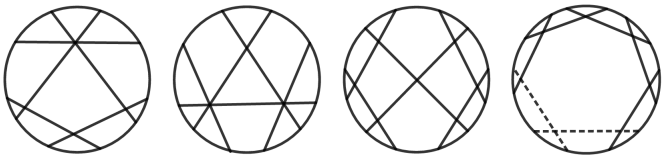

Le point de départ de cette thèse

Dans le travail de Ghys, la courbe était le lieu des zéros d'une fonction polynomiale réelle en deux variables. Nous allons considérer un polynôme avec le lieu des zéros réduit à un point (au moins dans un voisinage assez petit de l'origine). Nous étudierons les formes des courbes de niveau proches, qui peuvent être considérées comme les fibres de Milnor réelles du polynôme à l'origine.

Considérons une fonction polynomiale $f : \mathbb{R}^2 \to \mathbb{R}$ qui s'annule à l'origine O et qui présente un minimum local strict en ce point. Considérons l'ensemble $f^{-1}([0, \varepsilon])$ et notons par $\mathcal{D}_\varepsilon$ la composante connexe contenant l'origine. Pour $\varepsilon > 0$ suffisamment petit, $\mathcal{D}_\varepsilon$ est un disque topologique bordé par une courbe de Jordan lisse, notée $\mathcal{C}_\varepsilon$.

Chaque fois que l'origine est un minimum local strict de Morse (par exemple, $f(x, y) = x^2+y^2$) et $\varepsilon > 0$ est assez petit, le disque topologique $\mathcal{D}_\varepsilon$ est un disque convexe. Notez que les niveaux éloignés de l'origine peuvent être non convexes, comme le montre la Figure 7 ci-dessous.

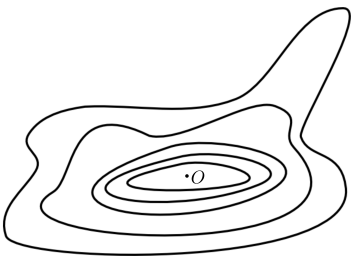

Figure 7: Des courbes de niveau suffisamment petites à proximité d'un minimum local strict de Morse deviennent des limites de disques topologiques convexes.

Le point de départ de cette recherche est la question suivante posée en juin 2004 par E. Giroux à P. Popescu-Pampu:

Question. Les petites courbes de niveau de f proches de minima locaux stricts sont-elles toujours des bords des disques convexes (même pour les singularités non-Morse) ?

La réponse à cette question est négative, comme le montre le contre-exemple suivant de M. Coste:

$$f(x, y) := x^2 + (y^2 - x)^2.$$

Cette fonction f est un polynôme réel bivarié avec un minimum local strict non-Morse à l'origine et dont les lignes de niveau suffisamment petites (voir la Figure 8) ne seront jamais convexes.

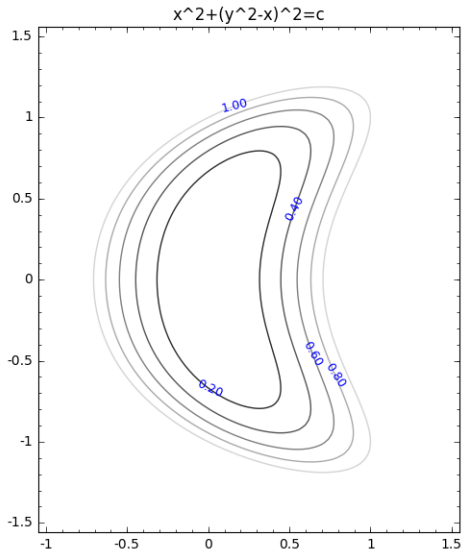

Figure 8: Quelques courbes de niveau de l'exemple de Coste.

Questions et objectifs

Notre première étape a été de construire quelques variantes de l'exemple de Coste (par exemple, celui donné dans la Figure 9).

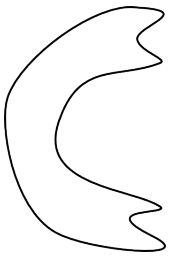

Figure 9: Une courbe de niveau $\mathcal{C}_\varepsilon$, pour $f(x, y) := x^6 + (y^4 + y^2 - x)^2(y^2 - x)^2$.

La question centrale suivante est apparue:

> Question. Quel objet combinatoire peut coder la forme en mesurant la non-convexité d'une composante connexe lisse et compacte d'une courbe algébrique réelle dans $\mathbb{R}^2$? Quelles sont les caractéristiques de cet objet - à la fois dans un contexte général et dans un contexte asymptotique (c'est-à-dire pour une famille de lignes de niveau convergeant vers un minimum local strict d'une fonction polynomiale) ?

Réponse : Nous prenons la topologie quotient donnée par la relation d'équivalence suivante dans $\mathbb{R}^2$: deux points de $\mathcal{D}_\varepsilon$ sont équivalents s'ils appartiennent à la même composante connexe d'une fibre de la projection $\Pi : \mathbb{R}^2 \to \mathbb{R}$, $\Pi(x, y) := x$. De cette façon, nous construisons un objet appelé graphe de Poincaré-Reeb, qui est un type spécial d'arbre plan (voir la Figure 10). Le

graphe de Poincaré-Reeb est en fait l'image du disque $\mathcal{D}_\varepsilon$ sous cette topologie quotient, plongée dans l'espace quotient de $\mathbb{R}^2$, qui est homéomorphe à $\mathbb{R}^2$.

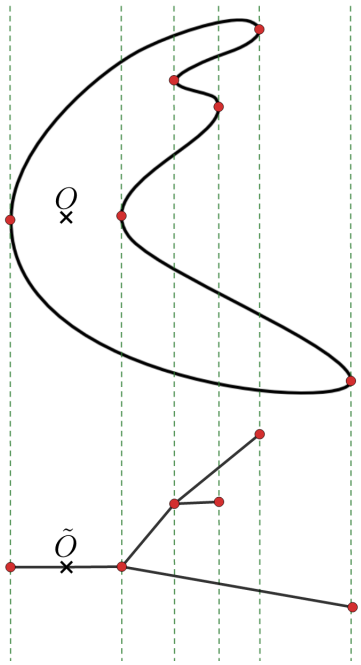

Figure 10: Une variante de l'exemple de Coste : une ligne de niveau d'un minimum strict non-Morse à l'origine et l'arbre de Poincaré-Reeb qui lui est associé.

Notez que les arêtes ouvertes de l'arbre de Poincaré-Reeb sont transverses aux feuilles verticales. Appelons **arbre transverse générique enraciné** un arbre binaire complet enraciné dont les arêtes ouvertes sont transverses au feuilletage trivial, orienté et coorienté du plan, induit par la fonction x, de sorte que ses sommets sont munis d'une relation d'ordre totale induite par ce feuilletage et que cet ordre est monotone sur chaque géodésique à partir de la racine.

QUESTION. Etant donné un arbre transverse générique enraciné, existe-t-il une équation d'un polynôme réel en deux variables avec un minimum isolé à l'origine qui réalise l'arbre donné sous la forme d'un arbre de Poincaré-Reeb ?

RÉPONSE : Nous donnons une famille de polynômes en deux variables qui réalise une grande classe de tels arbres.

À cette fin, nous étudions la **courbe polaire** f par rapport à la direction x :

$$\Gamma(f,x) := \left\{ (x,y) \in \mathbb{R}^2 \;\middle|\; \frac{\partial f}{\partial y}(x,y) = 0 \right\}.$$

C'est l'ensemble des points où la tangente à une ligne de niveau est verticale (voir Figure 11).

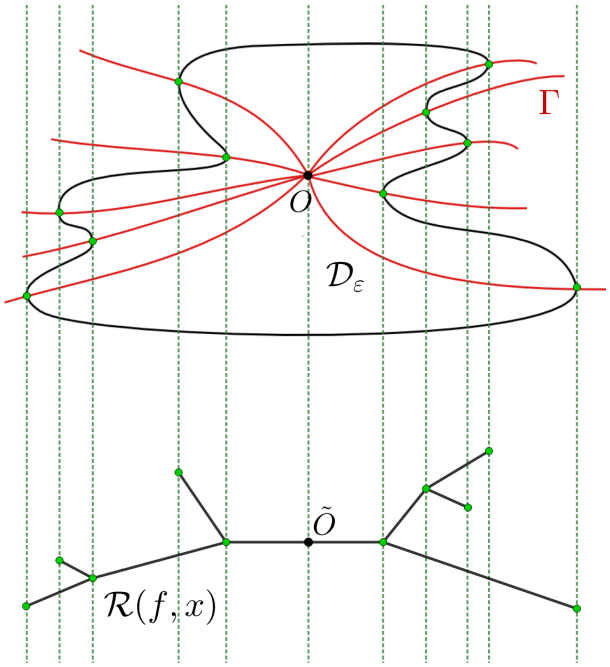

Figure 11: Un arbre de Poincaré-Reeb.

Notez que les sommets de l'arbre de Poincaré-Reeb sont des images des points de la courbe avec des tangentes verticales. Lorsque nous étudions la famille des lignes de niveau, les points de tangence verticale se déplacent le long des branches de la courbe polaire $\Gamma(f,x)$ (voir Figure 12). C'est la raison pour laquelle la courbe polaire jouera un rôle crucial dans notre recherche.

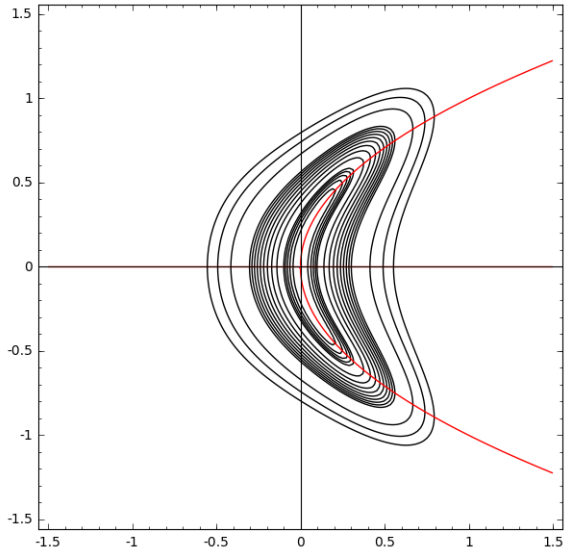

Figure 12: La courbe polaire pour l'exemple de Coste est $\Gamma(f,x) = \{(x,y) \in \mathbb{R}^2 \mid y(y-x^2) = 0\}$.

La notion de courbe polaire remonte au XIXème siècle, apparaissant dans les travaux de J.-V. Poncelet ([Pon17]) et M. Plücker ([Plü37]) dans la période 1813-1830 (voir par exemple [Tei90], [Tei77], [TF16]). À partir des années 1970, la théorie des courbes polaires (voir [BK86, page 589]) a été renouvelée grâce à d'importantes recherches et contributions dues à Lê ([LMW89]), Teissier, Merle, Eggers, Delgado, García Barroso ([GB00], [GB98], [GB96]), Płoski, Gwoździewicz, Casas-Alvero, Michel, Weber, Maugendre ([Mau99]), Hefez entre autres.

Des recherches considérables sur les courbes polaires ont été menées dans le cadre complexe.

Cependant, on en sait moins sur les courbes polaires réelles.

Cas univarié

La manière dont nous avons accès à la structure de l'arbre de Poincaré-Reeb consiste à étudier les formes asymptotiques des **graphes d'un polynôme d'une variable** $f_x(y)$, quand x tend vers zéro. Cela nous a amenés à étudier le cas univarié.

Notez que, dans le cas univarié, des recherches sur les courbes réelles ont été effectuées, où Davis ([Dav57]), Arnold ([Arn92]) et Douady ([Dou97]) ont chacun trouvé des preuves d'existence pour des formes données de graphes de polynômes. Cependant, ils n'ont pas construit les équations polynomiales associées. Présentons brièvement leurs résultats, après avoir introduit intuitivement deux outils nécessaires : les "suites alternées de nombres réels" et les "serpents".

• Un exemple de suite alternée de nombres réels est présenté dans la Figure 13 ci-dessous.

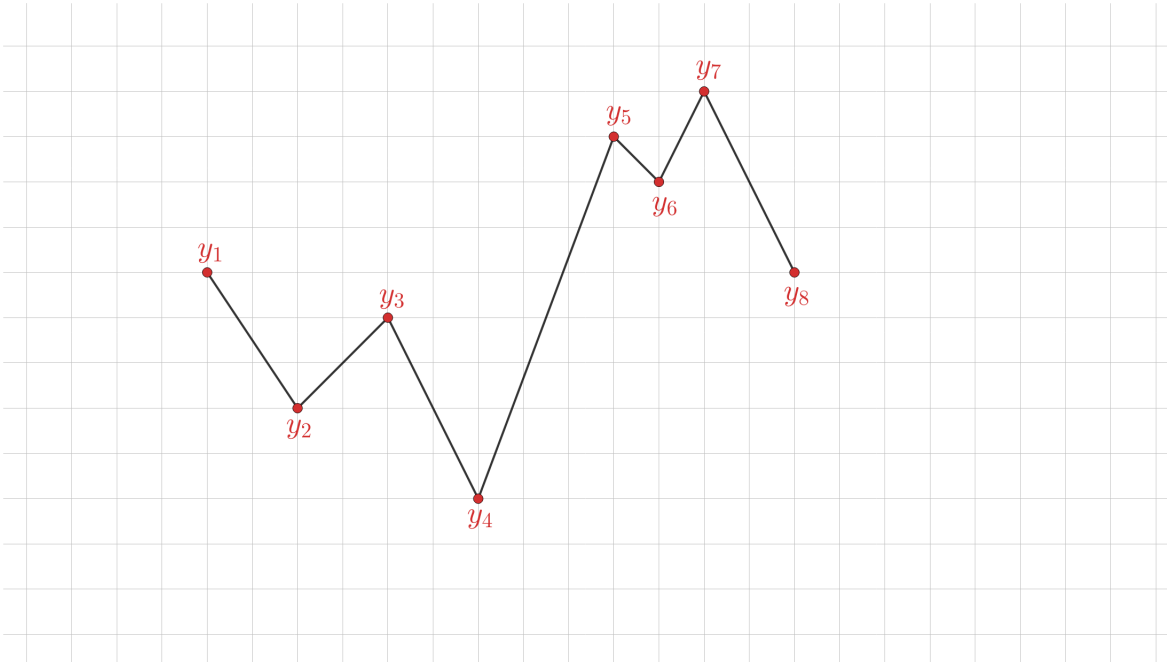

Figure 13: Une suite alternée de nombres réels $y_1 > y_2 < y_3 > y_4 < y_5 > y_6 < y_7 > y_8$

Si nous autorisons les égalités entre des nombres réels consécutifs, nous aurons une **suite faiblement alternée**.

Théorème. *[Dav57; Dou97] Soit une suite faiblement alternée de n nombres réels. Il existe un polynôme de degré $n+1$ dont la suite de valeurs critiques est la suite donnée.*

Notez que pour un polynôme $P \in \mathbb{R}[x]$, ses valeurs critiques sont les images des points critiques.

• Néanmoins, Arnold a utilisé des suites alternées spéciales d'éléments de l'ensemble $\{1, 2, \ldots, n\}$, où $n \in \mathbb{N}^*$, qui sont des permutations alternées. Plus précisément, il a appelé une permutation

$$\sigma : \{1, 2, \ldots, n\} \to \{1, 2, \ldots, n\}$$

un **serpent** si $[\sigma(1), \sigma(2), \ldots, \sigma(n)]$ est une suite alternée.

Par exemple, $\sigma_1 = \begin{pmatrix} 1 & 2 & 3 & 4 \\ 2 & 1 & 4 & 3 \end{pmatrix}$ ou $\sigma_2 = \begin{pmatrix} 1 & 2 & 3 & 4 \\ 3 & 2 & 4 & 1 \end{pmatrix}$ sont des serpents.

Definition. [Lan03, page 64] Fixons $n \geq 1$. Nous disons qu'un polynôme $P : \mathbb{R} \to \mathbb{R}$ est un **n-polynôme de Morse** s'il remplit les conditions suivantes:

(a) $\deg P = n$;

(b) P est monique, c'est-à-dire que le coefficient principal de P est égal à 1;

(c) ses points critiques (c'est-à-dire les valeurs $x_i \in \mathbb{C}$ telles que $P'(x_i) = 0$) sont réelles et simples;

(d) ses valeurs critiques (c'est-à-dire les valeurs $P(x_i)$, où x_i est un point critique) sont toutes distinctes.

Dans la Figure 14 ci-dessous, nous montrons comment associer un serpent $\sigma := \begin{pmatrix} 1 & 2 & 3 & 4 & 5 \\ 4 & 5 & 1 & 3 & 2 \end{pmatrix}$ à un polynôme de Morse (voir [Lan03, page 67]), en considérant deux relations d'ordre totales sur l'ensemble de ses points critiques : un ordre est le canonique, lu sur l'axe des x, tandis que l'autre ordre est celui donné par leurs valeurs critiques correspondantes.

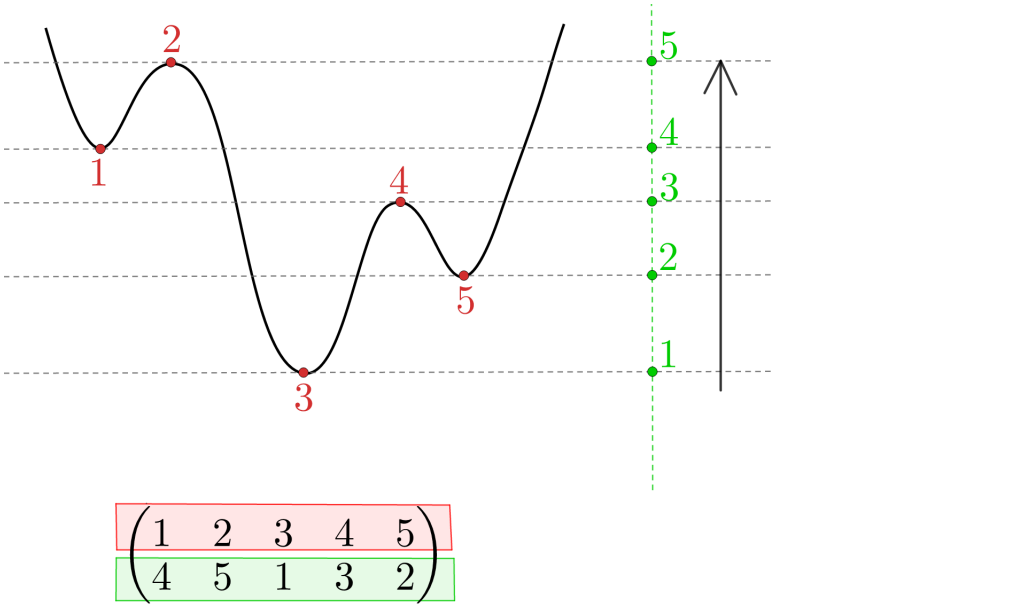

Figure 14: Associer un serpent à un polynôme de Morse en définissant deux relations d'ordre totales sur l'ensemble de ses points critiques.

Théorème. *[Arn92, Théorème 29, page 37] Le nombre de serpents de n éléments est égal au nombre de polynômes de Morse topologiquement inéquivalents de degré $n+1$ en une variable avec n valeurs critiques.*

Les résultats en bref

Expliquons maintenant nos résultats en bref.

A. Dans un premier temps, nous nous intéressons au cas des polynômes en une variable réelle.

Nous donnons une construction effective de tous les serpents séparables par des équations de polynômes de Morse réels univariés. En gros, notre résultat principal dans le cas univarié est le suivant:

Théorème. *Étant donné un serpent séparable σ, nous construisons une famille de polynômes de Morse $Q_x(y) \in \mathbb{R}[x][y]$, dont le serpent associé est σ, pour $x > 0$ suffisamment petit.*

Notez que, comme une amélioration des résultats antérieurs dans la littérature, nous donnons des formules explicites. Nos polynômes sont de la forme

$$Q_x(y) := \int_0^y \prod_{i=1}^{n} \big(t - a_i(x)\big)\mathrm{d}t,$$

pour un choix convenable des polynômes $a_i(x) \in \mathbb{R}[x]$.

B. Ensuite, nous nous concentrons sur le cas en deux variables. L'objectif principal de notre étude est de caractériser tous les types topologiques possibles de graphes de Poincaré-Reeb associés à une direction de projection x et à une composante connexe lisse et compacte d'une courbe algébrique réelle dans $\mathbb{R}^2$. Nous commençons par prouver que ces graphes sont des arbres planaires dont les **arêtes ouvertes sont transverses** aux feuilles verticales.

De plus, nous nous situons **dans le cas asymptotique**, c'est-à-dire que nous étudions les arbres de Poincaré-Reeb associés à des lignes de niveau $\mathcal{C}_\varepsilon$, pour $\varepsilon > 0$ assez petit, près d'un minimum isolé à l'origine. En utilisant la courbe polaire, nous montrons que lorsque $\varepsilon > 0$ est suffisamment petit, l'arbre de Poincaré-Reeb se stabilise de manière combinatoire. De plus, ses bords ne reculent pas. Ils ne font que s'éloigner de l'origine. L'arbre de Poincaré-Reeb est enraciné et c'est l'union d'un arbre positif (à droite de l'origine) et d'un arbre négatif (situé à gauche de l'origine). C'est ce que nous appelons **l'arbre asymptotique de Poincaré-Reeb**.

Si nous supposons aussi que la direction de la projection x est une **direction générique**, alors en utilisant les notions de crêtes et de vallées introduites par Coste et de la Puente (voir [CP01]), nous montrons que l'arbre asymptotique de Poincaré-Reeb est un arbre planaire binaire complet et que ses sommets sont totalement ordonnés par la foliation ambiante. Le préordre défini par le feuilletage x est un ordre total. Nous l'appelons **un arbre générique asymptotique de Poincaré-Reeb**. Voir la Figure 10. C'est un arbre transverse générique enraciné, dans le sens suivant:

Definition. Appelons **arbre transverse générique enraciné** un arbre binaire complet enraciné dont les arêtes ouvertes sont transverses au feuilletage trivial, orienté et coorienté du plan, induit par la fonction x, de sorte que ses sommets sont munis d'une relation d'ordre totale induite par ce feuilletage et que cet ordre est monotone sur chaque géodésique à partir de la racine.

Nous reviendrons plus tard sur la relation entre les arbres négatifs et positifs. Concentrons-nous maintenant sur le demi-plan $x > 0$, à savoir sur ce que nous appelons les **arbres positifs**.

L'un de nos principaux théorèmes est le suivant :

Théorème. *Chaque arbre transverse générique positif séparable est réalisable de manière effective par un minimum local strict d'une fonction polynomiale réelle en deux variables dans un voisinage suffisamment petit de l'origine.*

Notez que nous appelons ici "séparable" un arbre auquel nous pouvons associer une permutation séparable. En gros, pour associer une permutation à un arbre transverse générique enraciné, examinons son plongement vertical dans le plan réel, de telle sorte que sa racine soit au-dessus. On peut numéroter ses sommets de deux manières :

- l'ordre naturel sur l'ensemble de ses sommets : lisez d'abord les feuilles dans l'ordre induit par le plan réel; puis entre chaque paire de feuilles consécutives (a, b), intercalez le sommet de bifurcation interne $a \wedge b$;

- l'ordre vertical de ses sommets.

Ces deux relations d'ordre totale sur l'ensemble des sommets d'un arbre transverse générique enraciné fournissent une permutation (voir la Figure 15).

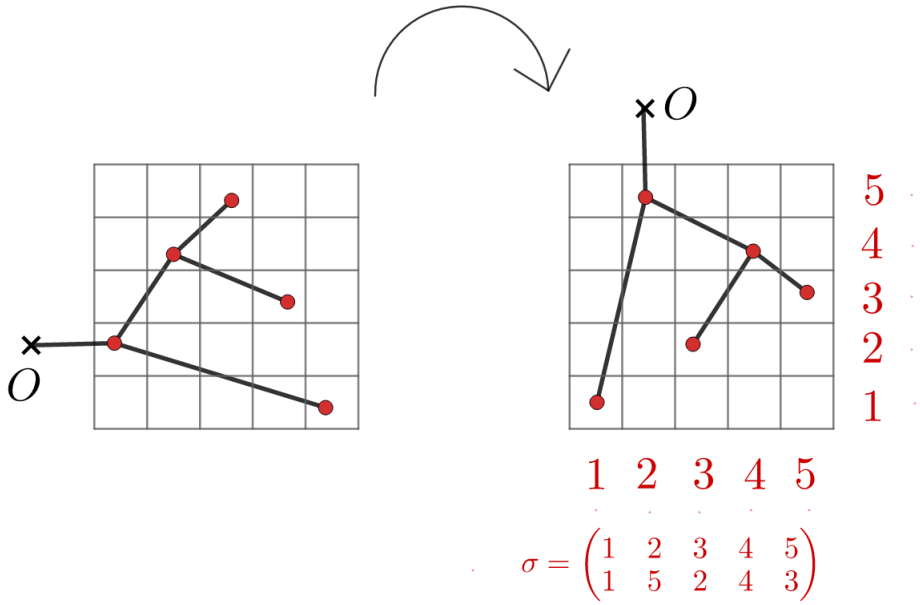

Figure 15: Associer une permutation à un arbre transverse générique enraciné.

Remarque. Notez que c'est une nouvelle manière d'associer une permutation à un arbre planaire, différente de celle définie dans [Ghy17], où Ghys a muni l'ensemble des graphes d'une famille finie donnée de polynômes dans un voisinage suffisamment petit d'un zéro commun de deux ordres totaux : un ordre donné par leur position pour $x > 0$ et l'autre par la position des polynômes pour $x < 0$, comme indiqué dans la Figure 16. Il a prouvé qu'une permutation peut être réalisée par des graphes de polynômes dans un voisinage d'un zéro commun si et seulement s'il s'agit d'une permutation séparable.

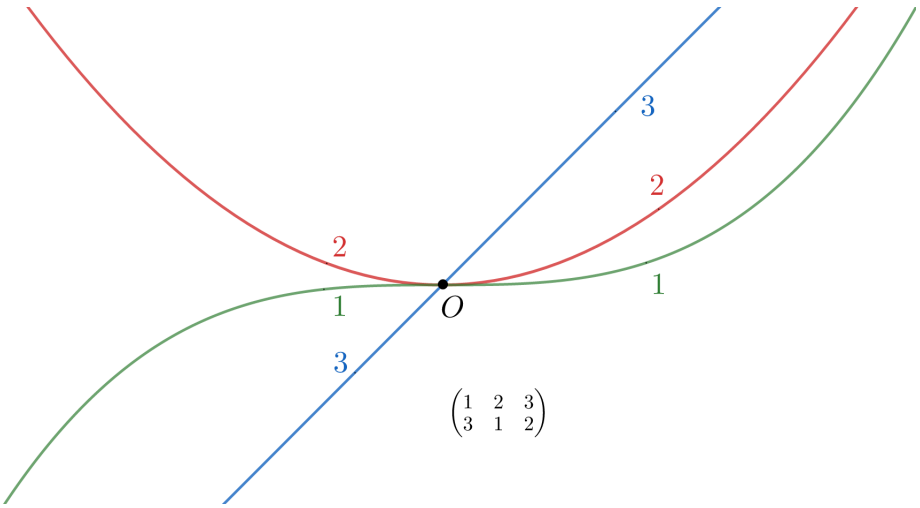

Figure 16: Associer une permutation à un ensemble de graphes de polynômes au voisinage d'un zéro commun.

Dans la preuve de notre théorème, nous utilisons la courbe polaire, qui est le lieu critique de l'application ϕ que nous détaillerons plus tard. L'allure à droite (c'est-à-dire pour $x > 0$) des lignes de niveau $\mathcal{C}_\varepsilon$, pour $\varepsilon > 0$ suffisamment petit, est déterminée par l'interaction combinatoire entre le lieu critique et l'image critique de l'application ϕ, qui ont tous deux un rôle crucial dans ce travail.

Enfin, nous nous intéressons simultanément aux arbres positifs et négatifs. Pour un arbre de Poincaré-Reeb positif séparable $\mathcal{T}$, nous présentons un nouvel algorithme dont le résultat est constitué de tous les arbres de Poincaré-Reeb négatifs qui forment des paires avec $\mathcal{T}$, par notre construction d'un minimum local strict.

Les résultats principaux en détail et la structure de la thèse

L'arbre de Poincaré-Reeb

Décrivons notre nouvelle construction de ce que nous appelons les graphes de Poincaré-Reeb, associés à une composante connexe lisse et compacte d'une courbe algébrique réelle dans $\mathbb{R}^2$ et à une direction de projection donnée x. Le **Chapitre** 2 est dédié à cet objet combinatoire, destiné à capturer la non-convexité des courbes. Il est inspiré de la construction classique introduite par H. Poincaré (voir [Poi10, 1904, page 221]), qui a été redécouverte par G. Reeb en 1946 (voir [Ree46]). Les deux l'ont utilisé comme outil dans la théorie de Morse. À savoir, étant donné une fonction de Morse sur une variété compacte sans bord, ils lui ont associé un graphe obtenu en quotiant la variété par la relation d'équivalence dont les classes sont les composantes connexes des niveaux de la fonction. Nous allons effectuer une construction analogue pour un type spécial de variété à bord.

• Considérons une composante connexe compacte et lisse $\mathcal{C}$ d'une courbe algébrique réelle contenue dans le plan $\mathbb{R}^2$ (voir Figure 17).

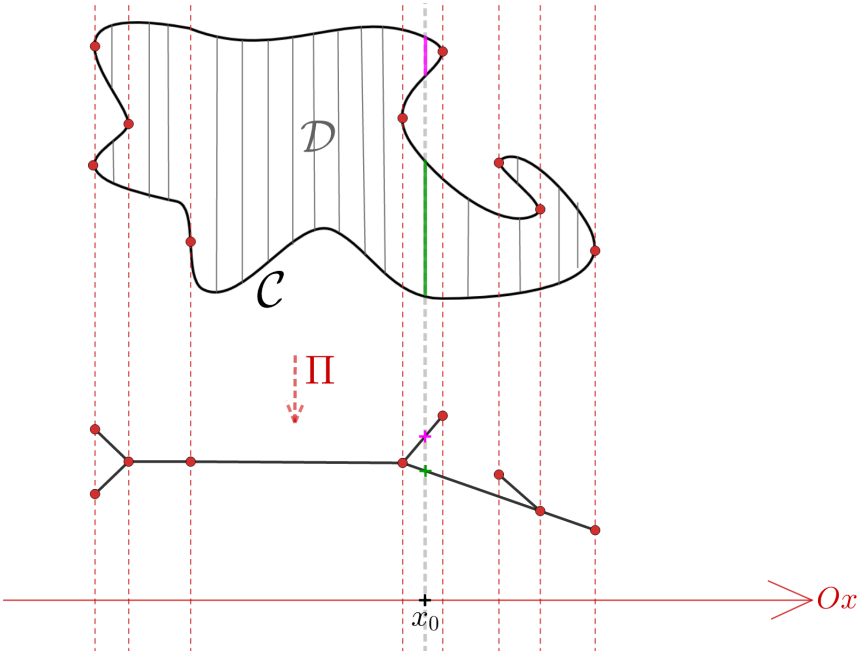

Figure 17: Le graphe de Poincaré-Reeb d'une composante connexe compacte et lisse $\mathcal{C}$ d'une courbe algébrique réelle contenue dans le plan $\mathbb{R}^2$.

On désigne par $\mathcal{D}$ le disque délimité par $\mathcal{C}$. Munissons le plan $\mathbb{R}^2$ de son orientation canonique et du feuilletage par des lignes verticales. La courbe $\mathcal{C}$, étant une composante connexe d'une courbe algébrique, n'a que un nombre fini de points de tangence verticale. Nous sommes prêts

pour la construction du graphe de Poincaré-Reeb. Ses sommets sont des images des points de la courbe ayant une tangente verticale. Considérez la projection $\Pi : \mathcal{D} \to \mathbb{R}$, $\Pi(x, y) := x$. Pour $x_0 \in \mathbb{R}$, si la fibre $\Pi^{-1}(x_0)$ n'est pas un ensemble vide, il s'agit d'une union finie de segments verticaux. Nous définissons une relation d'équivalence qui nous permet de contracter chacun de ces segments en un point. Par la topologie quotient, l'image du disque initial devient un sous-espace topologique connexe unidimensionnel plongé dans le plan réel. Plus précisément, il s'agit d'un graphe planaire connexe. Nous prouvons le résultat suivant:

Théorème 0.1 (voir Corollary 2.37)**.** *Le graphe de Poincaré-Reeb associé à une composante connexe compacte et lisse $\mathcal{C}$ d'une courbe algébrique réelle contenue dans le plan $\mathbb{R}^2$ et à une direction de projection x est un arbre planaire dont les arêtes ouvertes sont transverses au feuilletage induit par la fonction x. Ses sommets sont munis d'une relation de préordre totale induite par la fonction x.*

Dans la suite, nous l'appellerons **l'arbre de Poincaré-Reeb**. Notez que par **préordre** nous entendons une relation binaire, qui est réflexive et transitive.

Le principal outil utilisé dans la preuve du Théorème 0.1 est l'intégration par rapport à la caractéristique d'Euler.

• Limitons maintenant l'étude de cet arbre au cas asymptotique, c'est-à-dire, étudions les arbres de Poincaré-Reeb associés à des lignes de niveau suffisamment petites d'une fonction polynomiale bivariée réelle, proches d'un minimum local strict à l'origine. L'arbre se stabilise pour des lignes de niveau suffisamment petites. Appelez-le **l'arbre asymptotique de Poincaré-Reeb**.

Théorème 0.2 (voir Théorème 2.70)**.** *L'arbre asymptotique de Poincaré-Reeb est un arbre enraciné et la relation de préordre totale sur ses sommets, induite par la fonction x, est strictement monotone sur chaque géodésique à partir de la racine.*

Remarque. La monotonie stricte sur les géodésiques à partir de la racine implique que les courbes de niveau suffisamment petites $\mathcal{C}_\varepsilon$ ne présentent aucun phénomène de retournement ou de spirale. En particulier, pour $\varepsilon > 0$ suffisamment petit, il n'existe aucune forme $\mathcal{C}_\varepsilon$ semblable à celle de la Figure 18.

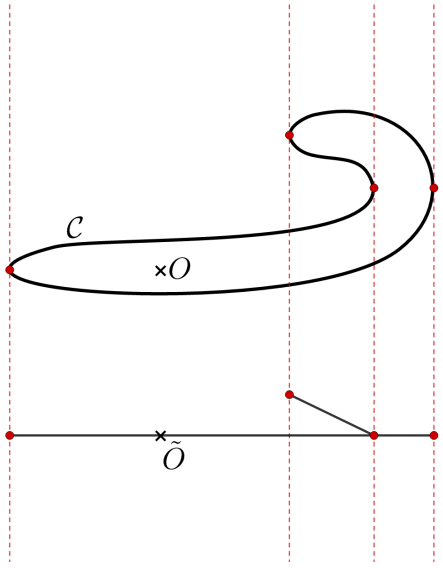

Figure 18: Forme interdite pour un $\varepsilon > 0$ assez pettit : on ne peut pas revenir en arrière comme ça.

Un arbre asymptotique de Poincaré-Reeb dont les sommets sont munis d'une relation de préordre induite par x est présenté dans la Figure 19 ci-dessous. C'est l'union d'un arbre positif (à droite de l'origine) et négatif (à gauche de l'origine), les deux derniers ayant une racine commune, c'est-à-dire l'image de l'origine. Nous ne parlons que d'une relation de préordre pour les sommets d'un arbre asymptotique de Poincaré-Reeb, car il pourrait y avoir plus d'un sommet au même niveau du feuilletage du plan donné par x.

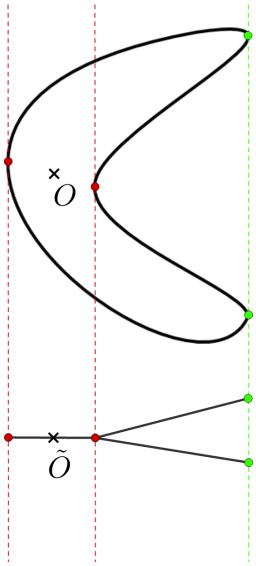

Figure 19: Un arbre asymptotique de Poincaré-Reeb dont les sommets sont dotés d'une relation de préordre induite par x : les deux sommets les plus à droite sont situés au même niveau.

• Plaçons-nous dans le cas asymptotique. Si, en plus, la direction x de la projection que nous considérons est générique, c'est-à-dire s'il s'agit d'une direction qui évite les bitangentes à $\mathcal{C}_\varepsilon$ et les tangentes d'inflexion verticales, alors nous obtenons ce que nous appelons **un arbre générique asymptotique de Poincaré-Reeb**.

Théorème 0.3 (voir Théorème 2.124)**.** *Outre les propriétés d'un arbre asymptotique de Poincaré-Reeb, un arbre asymptotique de Poincaré-Reeb générique présente les caractéristiques suivantes : le préordre défini par le feuilletage ambiant x est* ***une relation d'ordre totale*** *et il s'agit d'un arbre* ***binaire complet*** *(chaque sommet interne a exactement deux enfants).*

Exemple. Un exemple de deux arbres génériques asymptotiques de Poincaré-Reeb avec des relations d'ordre totales sur leurs sommets. Notez que les deux arbres sont des arbres de Poincaré-Reeb topologiquement inéquivalents.

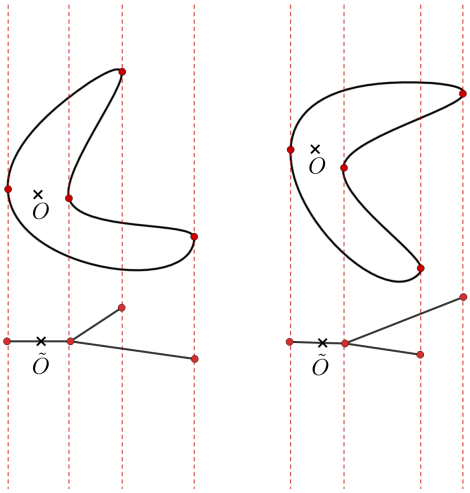

Figure 20: Deux arbres génériques asymptotiques de Poincaré-Reeb topologiquement inéquivalents.

En conclusion, nous avons construit et décrit un nouvel objet combinatoire, appelé arbre asymptotique de Poincaré-Reeb, dont le rôle est de quantifier la non-convexité des lignes de niveau suffisamment petites $\mathcal{C}_\varepsilon$. C'est un arbre transverse. Ensuite, notre objectif est de détecter quels arbres transverses peuvent être réalisés sous forme d'arbres asymptotiques de Poincaré-Reeb.

Le lien entre le cas bivarié et le cas univarié

Rappelons que, étant donné un arbre transverse générique enraciné $\mathcal{T}$, nous voulons construire une fonction polynomiale $f(x, y) \in \mathbb{R}[x, y]$ avec un minimum local strict à l'origine, tel que l'arbre asymptotique de Poincaré-Reeb associé à f et à la direction x soit $\mathcal{T}$. Dans la suite, nous allons expliquer la transition du cas bivarié au cas univarié. Nous présentons brièvement la relation géométrique et combinatoire entre les deux cas.

Pour le moment, limitons notre étude au demi-plan $x > 0$ du plan (Oxy) : le **Chapitre** 3 est dédié à la construction d'un polynôme réel avec un minimum local strict en O, qui réalise un serpent donné de la courbe de niveau $\mathcal{C}_\varepsilon$ à droite de l'origine (c'est-à-dire, pour $x > 0$).

• Tout d'abord, le serpent σ_ε indiqué dans la Figure 21 code la forme de $\mathcal{C}_\varepsilon \subset (Oxy)$ pour $x > 0$ (sous certaines hypothèses). Le serpent est déterminé par l'alternance de crêtes et de vallées.

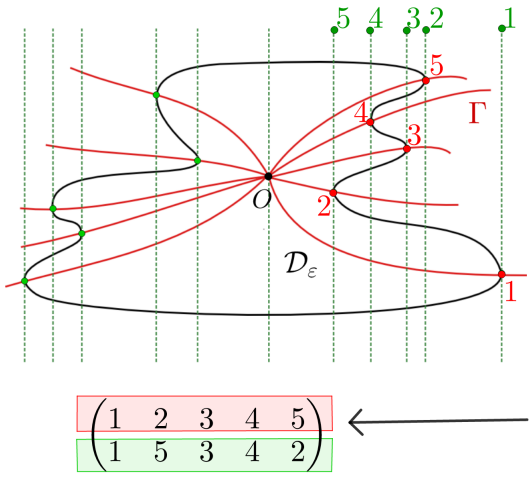

Figure 21: Le serpent asymptotique à droite.

• Deuxièmement, considérons le graphe de f :

$$\text{graph}(f) := \{(x, y, z) \in \mathbb{R}^3 \mid z = f(x, y)\}.$$

C'est une surface représentée dans la Figure 22. L'intersection de graph(f) avec le plan $x = x_0$, pour un $x_0 > 0$ suffisamment petit, consiste en une courbe algébrique plane qui est le graphe du polynôme univarié $f(x_0, y)$. Sous certaines hypothèses, il s'agit d'un polynôme de Morse auquel on peut associer un serpent, appelé τ.

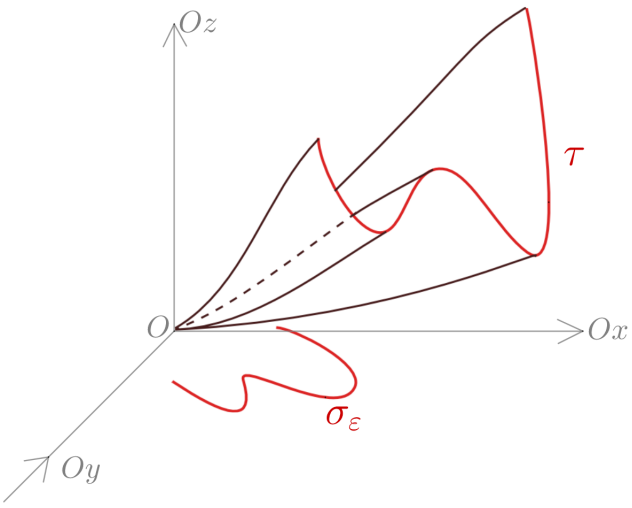

Figure 22: Serpents égaux : $\sigma_\varepsilon = \tau$.

Théorème 0.4 (voir Théorème 3.33)**.** *Sous certaines hypothèses (à préciser ultérieurement), les deux serpents sont égaux : $\sigma_\varepsilon = \tau$.*

L'idée principale est qu'à partir d'un serpent σ, afin de construire un polynôme $f(x, y) \in \mathbb{R}[x, y]$ qui réalise σ à droite, nous allons construire une famille asymptotique de polynômes d'une variable y avec des coefficients dans $\mathbb{R}[x]$, c'est-à-dire des polynômes dans $\mathbb{R}[x][y]$, tels que pour un $x > 0$ suffisamment petit le serpent τ est égal à σ.

Nous allons préciser les hypothèses mentionnées ci-dessus dans ce qui suit.

Étudions plus en détail la relation combinatoire entre le serpent σ_ε à droite et ce que nous appelons la courbe polaire "positive" par rapport à x.

Considérons l'application

$$\Phi : \mathbb{R}^2_{x,y} \to \mathbb{R}^2_{x,z}, \Phi(x, y) := (x, f(x, y)).$$

Le lieu critique de Φ est la courbe polaire $\Gamma(f, x)$.

Dans la Figure 23, nous voyons trois ensembles de courbes:

• la partie "positive" de la courbe polaire, notée $\Gamma_+ := \Gamma(f, x) \cap (x > 0)$;

• l'image critique (ou courbe discriminante) "positive" $\Delta_+ := \Phi(\Gamma_+)$ (en vert);

• le contour apparent sur la surface graph(f) (en rouge), lorsque le graphe est projeté sur le plan (Oxz).

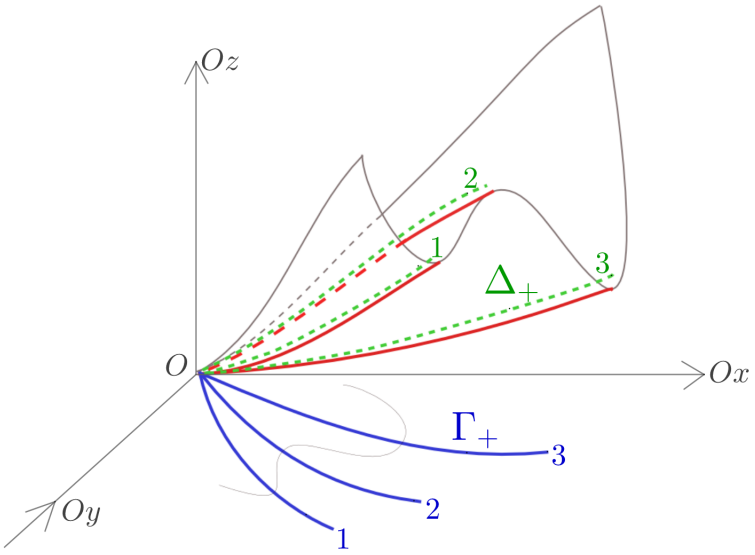

Figure 23: L'homéomorphisme entre la courbe polaire positive réduite Γ_+ et son image Δ_+.

Les polynômes que nous construisons satisfont les deux hypothèses de généricité suivantes:
- la courbe Γ_+ est réduite;
- l'application $\Phi_{|\Gamma_+} : \Gamma_+ \to \Delta_+$ est un homéomorphisme.

Nous obtiendrons le résultat suivant:

Théorème 0.5 (voir Proposition 3.32)**.** *Sous les hypothèses de généricité précédentes, la permutation réalisée par la bijection entre la courbe polaire positive Γ_+ et son image Δ_+ est égale au serpent σ_ε.*

Remarque. Intuitivement, pour associer une permutation à la bijection entre l'ensemble des branches de Γ_+ et l'ensemble des branches de Δ_+, examinons les deux relations d'ordre totales suivantes : les positions relatives des courbes dans Γ_+ et les positions relatives de leurs images dans Δ_+. L'interaction entre ces deux ensembles d'objets donne un serpent.

Nous dirigerons notre attention sur le passage inverse, c'est-à-dire sur le passage de polynômes en une variable aux polynômes en deux variables, seulement après avoir présenté ci-dessous le cas univarié.

Construction de polynômes en une variable

La stratégie que nous avons adoptée consistait à étudier les polynômes en deux variables dans $\mathbb{R}[x, y]$ comme familles asymptotiques de polynômes univariés $f_x(y) \in \mathbb{R}[x][y]$, pour un x suffisamment petit qui tend vers zéro. Par conséquent, nous consacrons le **Chapitre** 1 à la construction d'équations polynomiales univariées permettant de réaliser un serpent donné.

Théorème 0.6 (voir Théorème 1.149)**.** *Soit σ un serpent séparable, nous construisons explicitement une équation d'une famille de polynômes de Morse $Q_x(y) \in \mathbb{R}[x][y]$, $Q_x(y) := \int_0^y \prod_{i=1}^n (t - a_i(x))\mathrm{d}t$, telle que pour un $x > 0$ suffisamment petit le serpent associé à $Q_x(y)$ est σ.*

Notez que notre choix des polynômes $a_i(x) \in \mathbb{R}[x]$ est déterminé par les propriétés combinatoires du serpent séparable donné. La preuve repose sur la gestion d'un autre objet combinatoire présenté dans le Chapitre 1, appelé **l'arbre de contact**, associé à un ensemble fini de polynômes univariés réels $\{a_i(x)\}$. C'est un arbre enraciné dont les sommets internes sont décorés d'informations numériques extraites des polynômes donnés. Son rôle dans nos recherches est d'encoder la proximité entre différentes familles de polynômes réels à une variable.

Le principal défi consistait à déterminer le serpent (ou, de manière équivalente, l'arbre générique asymptotique de Poincaré-Reeb) en fonction de l'arbre de contact.

Construction de polynômes en deux variables, à droite

Revenons maintenant à notre objectif initial, en obtenant **le résultat principal de la thèse**, auquel nous dédions la dernière partie du **Chapitre** 3:

Théorème 0.7 (voir Théorème 3.34)**.** *Soit σ un serpent séparable.*

(a) Il existe un polynôme réel bivarié $f \in \mathbb{R}[x, y]$ avec un minimum isolé à l'origine dont le serpent à droite (c'est-à-dire pour $x > 0$ et $\varepsilon > 0$ les deux suffisamment petits) est le serpent donné σ.

(b) L'existence est réalisable de manière explicite, en suivant les deux étapes suivantes:

- *on construit le polynôme d'une variable $Q_x(y)$, avec $x > 0$ assez petit, dont le serpent associé est le serpent séparable donné σ, comme dans Théorème 0.6;*
- *on définit le polynôme à deux variables $f(x, y) := x^2 + Q_x(y)$.*

Nous prouvons que notre famille de polynômes a en effet un minimum local strict à l'origine, en utilisant un critère basé sur le polygone de Newton.

Pour donner l'équation du polynôme souhaité en deux variables, nous choisissons d'abord sa courbe polaire par rapport à x. Toutes les branches de la courbe polaire par rapport à x dans notre construction sont réelles, lisses et transverses à l'axe des y, de sorte que la courbe polaire vérifie les hypothèses de Théorème 0.5.

Paires d'arbres de Poincaré-Reeb négatifs-positifs obtenus avec notre méthode

Nous pouvons construire des équations qui permettent de réaliser tout arbre transverse générique enraciné séparable, positif (c'est-à-dire à droite de l'origine). Par symétrie, nous pouvons également réaliser l'un de ces arbres à gauche. Cependant, nous nous intéressons maintenant aux couples de ces arbres séparables qui peuvent être réalisés simultanément, en tant que paire d'arbres de Poincaré-Reeb négatifs-positifs à proximité d'un minimum isolé.

Question. Étant donné un arbre de Poincaré-Reeb séparable positif $\mathcal{T}$ (c'est-à-dire à droite de l'origine), quels sont les arbres de Poincaré-Reeb négatifs (c'est-à-dire à gauche de l'origine) qui forment des paires avec $\mathcal{T}$, dans notre construction ?

Réponse : Dans le **Chapitre** 4, nous fournissons un algorithme (voir Algorithme 4.25) dont le résultat est l'ensemble de tous les arbres de Poincaré-Reeb négatifs, que nous pouvons réaliser et qui forment des paires avec un arbre de Poincaré-Reeb positif séparable donné, en utilisant notre construction. Plus précisément, les arbres-unions ainsi formés sont explicitement réalisables par notre famille de polynômes en tant qu'arbres génériques asymptotiques de Poincaré-Reeb près d'un minimum local strict dans un voisinage suffisamment petit de l'origine (voir le Théorème 4.26).

Exemple. Considérons un arbre de Poincaré-Reeb positif séparable $\mathcal{T}$ (voir Figure 24).

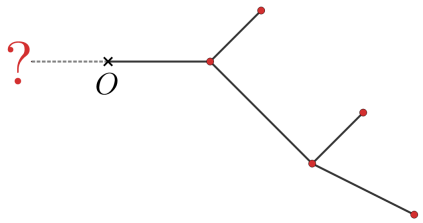

Figure 24: Quels sont les arbres de Poincaré-Reeb négatifs, qui forment des paires avec l'arbre de Poincaré-Reeb donné séparable $\mathcal{T}$, en utilisant notre construction ?

Toutes les paires d'arbres possibles de cet exemple et leurs lignes de niveau correspondantes $\mathcal{C}_\varepsilon$ sont montrées dans la Figure 25.

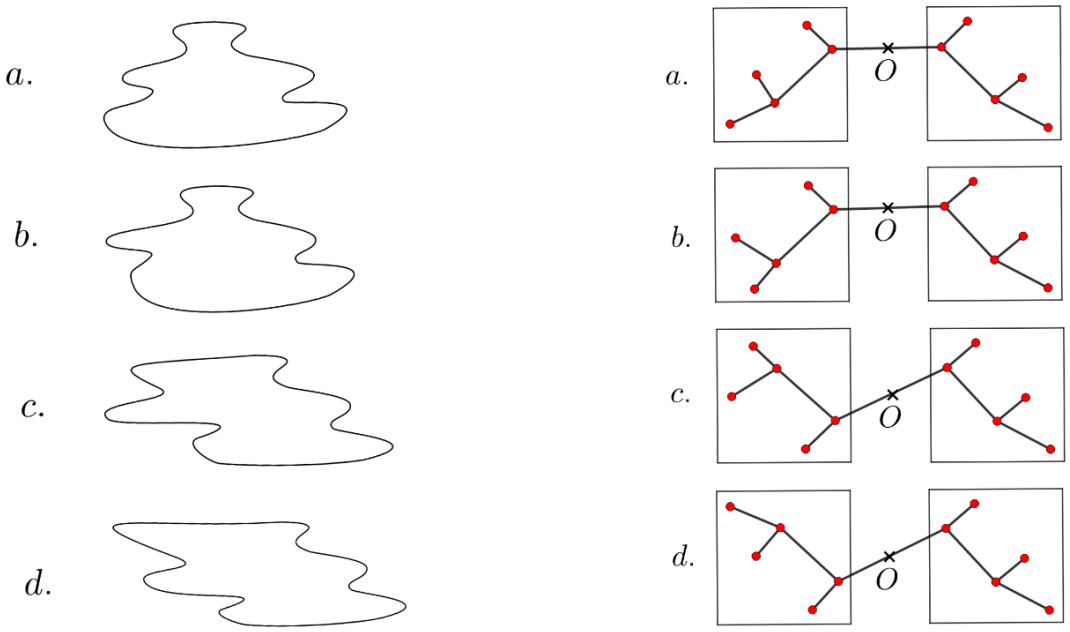

Figure 25: Lignes de niveau non convexes et leurs paires correspondantes d'arbres de Poincaré-Reeb négatifs-positifs réalisés avec notre construction par un minimum local strict à l'origine d'une fonction polynomiale en deux variables réelles, étant donné l'arbre de Poincaré-Reeb positif (l'arbre du côté droit de l'origine).

Par conséquent, en exécutant notre algorithme, nous fournissons tous les arbres de Poincaré-Reeb négatifs qui peuvent former une paire avec $\mathcal{T}$ et que nous pouvons réaliser effectivement par notre construction.

Introduction - English version

Context and motivation

Local topology of real plane algebraic curves

In his recent book [Ghy17], E. Ghys studied the local topology of real plane algebraic curves. He described, in terms of permutations, the possible local configurations of a family $\{a_i(x)\}$ of real polynomials in one variable near the origin of the real plane. The graphs of these polynomials change their relative positions when they pass through a common zero (see Figure 26). He proved that the permutations that can be obtained in this manner are exactly the so-called "separable" permutations.

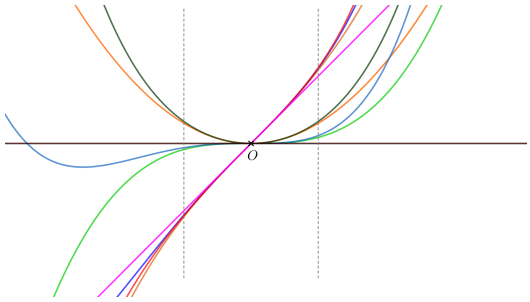

Figure 26: The graphs of the polynomials $a_i(x)$ in a neighbourhood of the origin.

Recently, researchers have shown increased interest in the separable permutations (introduced in [BBL98]), that have nice algorithmic and combinatorial properties (see for instance [Ghy17, page 27], [Bas+18], [Kit11, page 57]). A separable permutation is a permutation that does not "contain" (see for instance [Ghy17, page 13, 18]) either of the next two "forbidden" sub-permutations:

$$\begin{pmatrix} 1 & 2 & 3 & 4 \\ 2 & 4 & 1 & 3 \end{pmatrix} \text{ or } \begin{pmatrix} 1 & 2 & 3 & 4 \\ 3 & 1 & 4 & 2 \end{pmatrix}.$$

An example of a permutation that is not separable is

$$\eta := \begin{pmatrix} 1 & 2 & 3 & 4 & 5 & 6 & 7 & 8 \\ 2 & 3 & 6 & 8 & 1 & 7 & 5 & 4 \end{pmatrix},$$

since it "contains" the sub-permutation $\begin{pmatrix} 1 & 2 & 3 & 4 \\ 3 & 1 & 4 & 2 \end{pmatrix}$. Namely, there exist four indices $i_1 := 2$, $i_2 := 3$, $i_3 := 5$, $i_4 := 8$ such that: $i_1 < i_2 < i_3 < i_4$, while we have (see Figure 27): $\eta(i_3) \ll \eta(i_1) \ll \eta(i_4) \ll \eta(i_2)$.

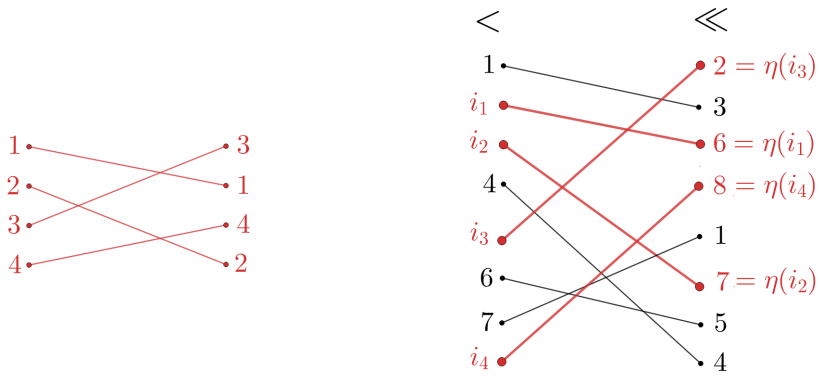

Figure 27: The nonseparable permutation η contains one of the two "forbidden" permutations.

An alternative representation (inspired from [Kit11, page 4]) of the permutation η, through its graph, is drawn in Figure 28, where we mark a dot for each pair $(i, \eta(i))$. The forbidden sub-permutation is marked by blue triangles.

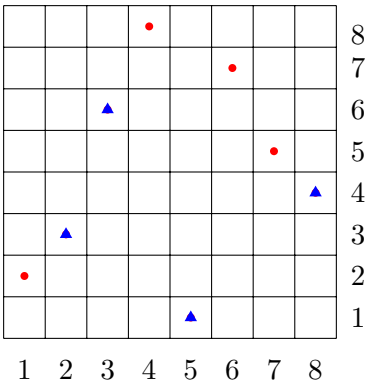

Figure 28: An alternative representation of the permutation η. The "forbidden" sub-permutation is marked by triangles.

Furthermore, in the same book ([Ghy17]), E. Ghys studied real algebraic curves given by an implicit polynomial equation $f(x, y) = 0$ in two real variables. He encoded their combinatorics in the so-called "chord diagrams" (see Figure 29).

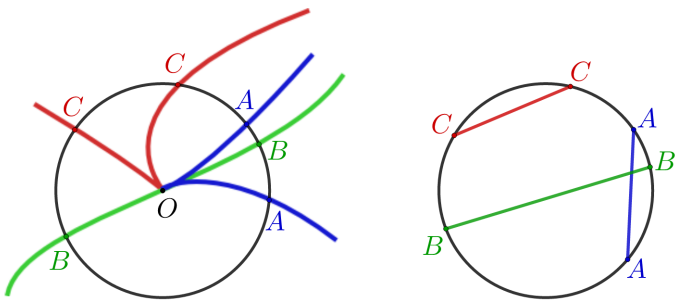

Figure 29: A singular curve with three branches (left side) and its associated chord diagram (right side).

Étienne Ghys' aim was to characterise all the possible topological configurations of the branches of an algebraic curve in a small enough neighbourhood of one of its singular points. In collaboration with Christopher-Lloyd Simon, he proved:

Theorem. *[Ghy17, page 266 (Ghys and Simon)] A given chord diagram is realisable by a real algebraic plane curve in a neighbourhood of a singular point if and only if the chord diagram does not contain any of the sub-chord diagrams illustrated below (note that the last sub-chord diagram contains at least five chords):*

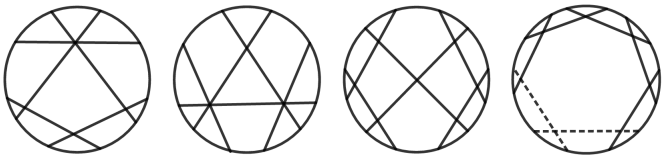

The starting point of this thesis

In Ghys' work the curve was the zero locus of a bivariate real polynomial function. Instead, we will consider a polynomial with the zero locus reduced to a point (at least in a small enough neighbourhood of the origin). We will study the shapes of the nearby level curves, which may be thought of as the real Milnor fibres of the polynomial at the origin.

Let us consider a polynomial function $f : \mathbb{R}^2 \to \mathbb{R}$ that vanishes at the origin O, exhibiting a strict local minimum at this point. Consider the set $f^{-1}([0, \varepsilon])$ and denote the connected component that contains the origin by $\mathcal{D}_\varepsilon$. For sufficiently small $\varepsilon > 0$, $\mathcal{D}_\varepsilon$ is a topological disk bounded by a smooth Jordan curve, denoted by $\mathcal{C}_\varepsilon$.

Whenever the origin is a Morse strict local minimum (for example, $f(x, y) = x^2 + y^2$), and $\varepsilon > 0$ is small enough, the topological disk $\mathcal{D}_\varepsilon$ is a convex disk. Note that the levels far from the origin can be non-convex, as we show in Figure 30 below.

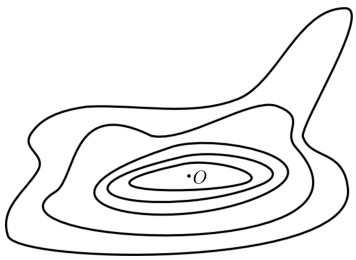

Figure 30: Small enough level curves near a Morse strict local minimum become boundaries of convex topological disks.

The starting point of this research is the following question posed in June 2004 by E. Giroux to P. Popescu-Pampu:

QUESTION. Are the small enough level curves of f near strict local minima always boundaries of convex disks (even for non-Morse singularities)?

The answer to this question is negative, as the following counterexample by M. Coste shows:

$$f(x, y) := x^2 + (y^2 - x)^2.$$

This function f is a bivariate real polynomial with a non-Morse strict local minimum at the origin and whose small enough level curves (see Figure 31) will never be convex.

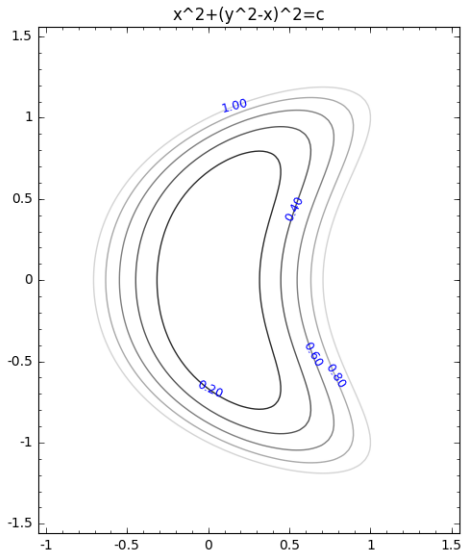

Figure 31: Some level curves of Coste's example.

Questions and goals

Our first step was to construct some variations of Coste's example (for instance, the one given in Figure 32).

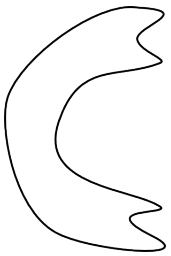

Figure 32: A level curve $\mathcal{C}_\varepsilon$, for $f(x,y) := x^6 + (y^4 + y^2 - x)^2(y^2 - x)^2$.

The following central question appeared:

> QUESTION. What combinatorial object can encode the shape by measuring the non-convexity of a smooth and compact connected component of a real algebraic curve in $\mathbb{R}^2$? What are the characteristics of this object - both in a general setting and in the asymptotic one (that is, for a family of level curves converging to a strict local minimum of a polynomial function)?

ANSWER: We take the quotient map given by the following equivalence relation in $\mathbb{R}^2$: two points of $\mathcal{D}_\varepsilon$ are equivalent if they belong to the same connected component of a fibre of the projection $\Pi : \mathbb{R}^2 \to \mathbb{R}$, $\Pi(x,y) := x$. In this way we construct an object called the Poincaré-Reeb graph, which is a special type of plane tree (see Figure 33). The Poincaré-Reeb graph is in fact the image of the disk $\mathcal{D}_\varepsilon$ under this quotient map, seen embedded in the quotient of $\mathbb{R}^2$, which is homeomorphic to $\mathbb{R}^2$.

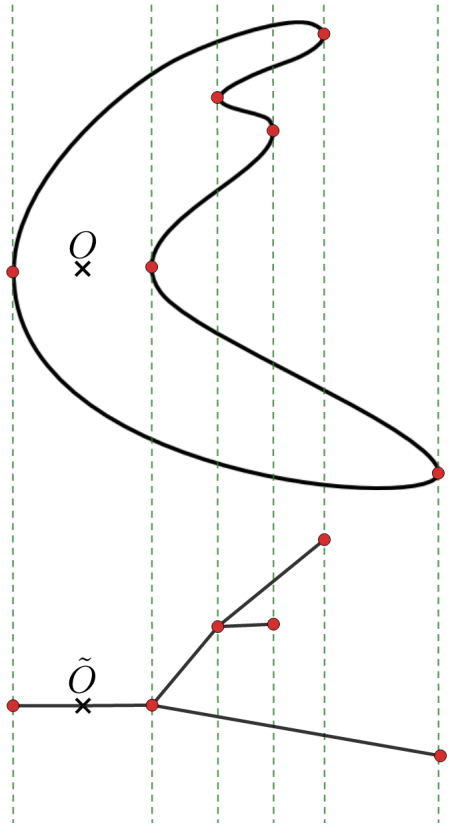

Figure 33: A variation of the Coste example: a level curve of a non-Morse strict minimum at the origin and the Poincaré-Reeb tree associated to it.

Note that the open edges of the Poincaré-Reeb tree are transverse to the vertical lines. Let us call **generic rooted transversal tree** a rooted plane complete binary tree whose open edges are transverse to the trivialisable, oriented and cooriented foliation of the plane induced by the function x, such that its vertices are endowed with a total order relation induced by this foliation and this order is monotone on each geodesic starting from the root.

> Question. Given a generic rooted transversal tree, does there exist an equation of a real bivariate polynomial with isolated minimum at the origin which realises the given tree as a Poincaré-Reeb tree?

Answer: We give a family of polynomials in two variables that realises a large class of such trees.

To this end, we study the so-called **polar curve** of f with respect to the direction x:

$$\Gamma(f,x) := \left\{ (x,y) \in \mathbb{R}^2 \;\middle|\; \frac{\partial f}{\partial y}(x,y) = 0 \right\}.$$

It is the set of points where the tangent to a level curve is vertical (see Figure 34).

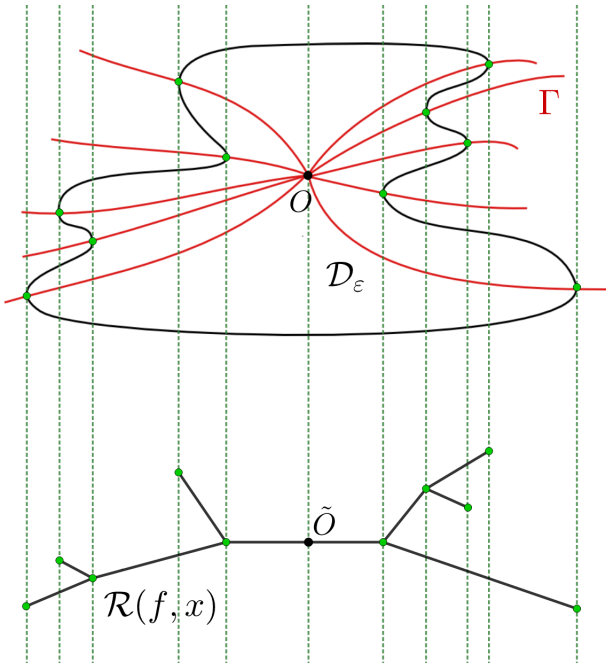

Figure 34: A Poincaré-Reeb tree.

Note that the vertices of the Poincaré-Reeb tree roughly speaking correspond to points on the curve with vertical tangent lines. When we study the family of level curves, the points of vertical tangency move along the branches of the polar curve $\Gamma(f,x)$ (see Figure 35). This is the reason why the polar curve will play a crucial role in our research.

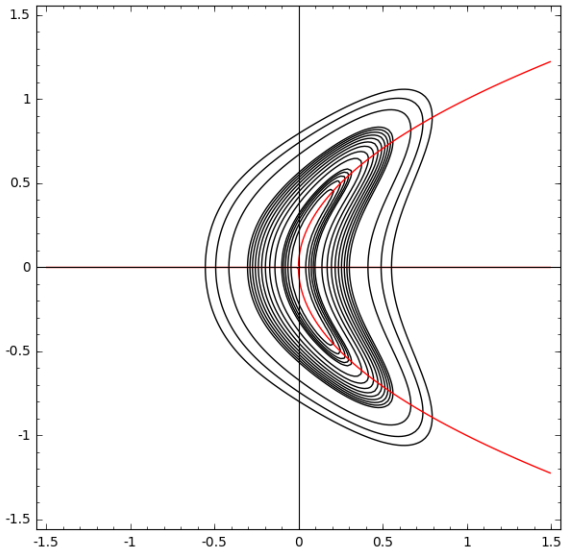

Figure 35: The polar curve for the Coste example is $\Gamma(f,x) = \{(x,y) \in \mathbb{R}^2 \mid y(y-x^2) = 0\}$.

The notion of a polar curve goes back to the XIXth century, appearing in the work of J.-V. Poncelet ([Pon17]) and M. Plücker ([Plü37]) in the period of 1813-1830 (see for instance [Tei90], [Tei77], [TF16]). Starting with the 1970s, the theory of polar curves (see [BK86, page 589]) was renewed by important investigations and contributions due to Lê ([LMW89]), Teissier, Merle, Eggers, Delgado, García Barroso ([GB00], [GB98], [GB96]), Płoski, Gwoździewicz, Casas-Alvero, Michel, Weber, Maugendre ([Mau99]), Hefez among others. Considerable research on the polar curves has been carried out in the complex setting. However, less is known about the real polar curves.

Univariate setting

The manner in which we have access to the structure of the Poincaré-Reeb tree is via the study of asymptotic forms of **the graphs of one variate polynomials** $f_x(y)$, for x tending to zero. This led us to the study of the univariate setting.

Note that in the univariate case some research on the subject of real curves has been carried, where Davis ([Dav57]), Arnold ([Arn92]) and Douady ([Dou97]) each found proofs of existence of given shapes of graphs of polynomials. However, they did not construct effectively the associated polynomial equations. Let us present briefly their results, after introducing intuitively two necessary tools, namely the "alternating sequences of real numbers" and the "snakes".

• An example of a given alternating sequence of real numbers is shown in Figure 36 below.

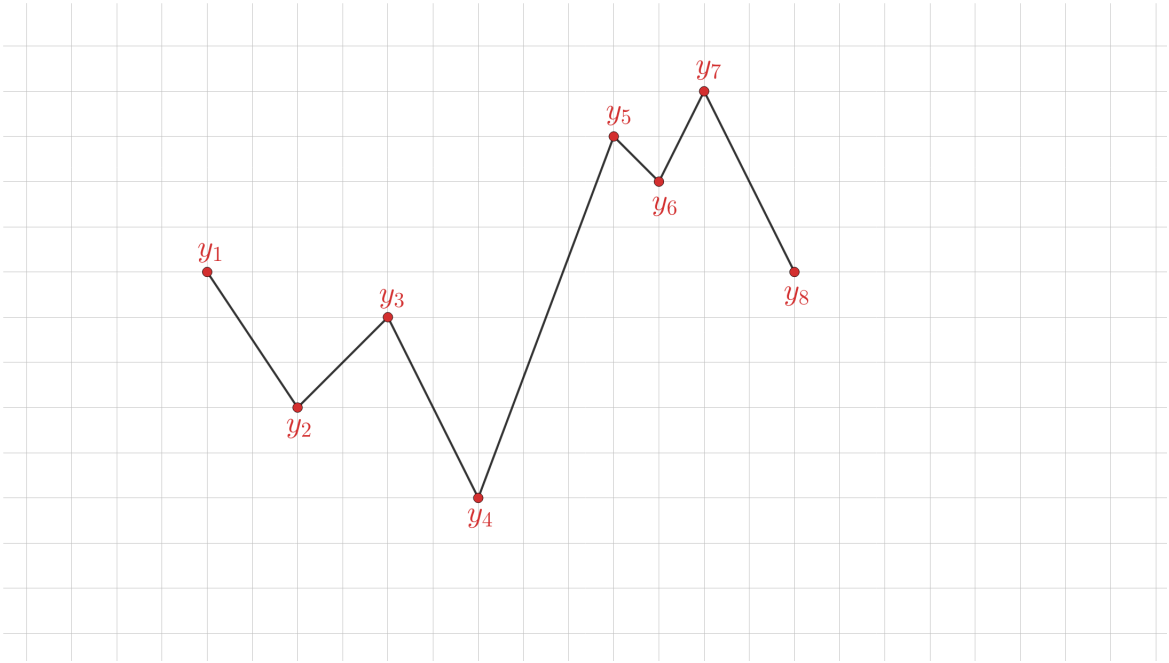

Figure 36: An alternating sequence of real numbers $y_1 > y_2 < y_3 > y_4 < y_5 > y_6 < y_7 > y_8$

If we allow equalities to take place between consecutive real numbers, we have a **weakly** alternating sequence.

Theorem. *[Dav57; Dou97] Given a weakly alternating sequence of n real numbers, there exists a polynomial of degree $n+1$ whose sequence of critical values is the given sequence.*

Note that for a polynomial $P \in \mathbb{R}[x]$, its critical values are the images of the critical points.

• Nevertheless, Arnold used special alternating sequences of elements of the set $\{1, 2, \ldots, n\}$, where $n \in \mathbb{N}^*$, which are alternating permutations. More precisely, he called a permutation

$$\sigma : \{1, 2, \ldots, n\} \to \{1, 2, \ldots, n\}$$

a **snake** if $[\sigma(1), \sigma(2), \ldots, \sigma(n)]$ is an alternating sequence.

For instance $\sigma_1 = \begin{pmatrix} 1 & 2 & 3 & 4 \\ 2 & 1 & 4 & 3 \end{pmatrix}$ or $\sigma_2 = \begin{pmatrix} 1 & 2 & 3 & 4 \\ 3 & 2 & 4 & 1 \end{pmatrix}$ are snakes.

Definition. [Lan03, page 64]Let us fix $n \geq 1$. We say that a polynomial $P : \mathbb{R} \to \mathbb{R}$ is an n-**Morse polynomial** if it satisfies the following conditions:

(a) $\deg P = n$;

(b) P is monic, i.e. the leading coefficient of P is equal to 1;

(c) its critical points (i.e. the values $x_i \in \mathbb{C}$ such that $P'(x_i) = 0$) are real and distinct;

(d) its critical values (i.e. the values $P(x_i)$, where x_i is a critical point) are all distinct.

In Figure 37 below, we show how one can associate a snake $\sigma := \begin{pmatrix} 1 & 2 & 3 & 4 & 5 \\ 4 & 5 & 1 & 3 & 2 \end{pmatrix}$ to a Morse polynomial (see [Lan03, page 67]), by considering two total order relations on the set of its critical points: one order is the canonical one, read on the Ox-axis, while the other order is the one given by their corresponding critical values.

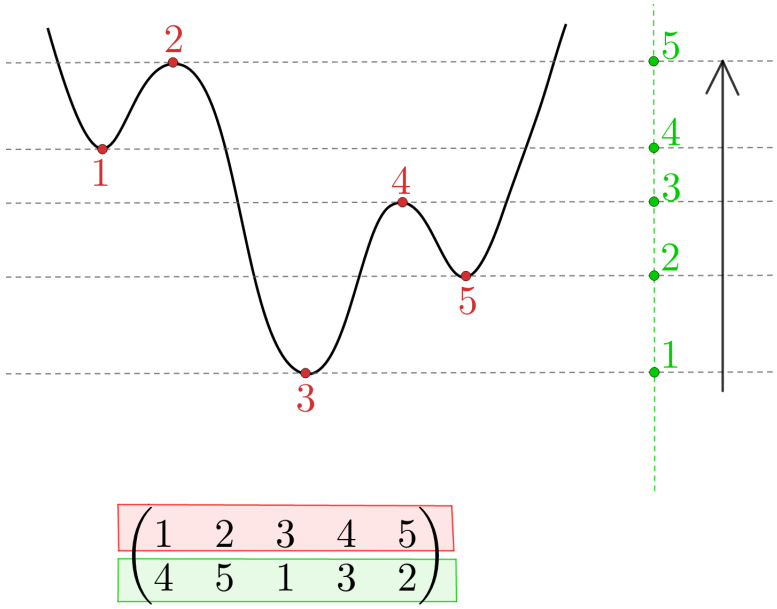

Figure 37: Associating a snake to a Morse polynomial by defining two total order relations on the set of its critical points.

Theorem. *[Arn92, Theorem 29, page 37] The number of snakes of n elements is equal to the number of topologically inequivalent Morse polynomials of degree $n+1$ in one variable with n critical values.*

The results in brief

Let us now explain our results in brief.

A. Firstly, we focus on the case of polynomials in one real variable.

We give an effective construction of all the separable snakes by equations of univariate real Morse polynomials. Roughly speaking, our main result in the univariate setting is the following:

Theorem. *Given a separable snake σ, we construct a family of Morse polynomials $Q_x(y) \in \mathbb{R}[x][y]$, whose associated snake is σ, for $x > 0$ sufficiently small.*

Notice that, as an improvement to earlier results in the literature, we write explicit formulae. Our polynomials are of the form

$$Q_x(y) := \int_0^y \prod_{i=1}^{n} \big(t - a_i(x)\big)\mathrm{d}t,$$

for a suitable choice of the polynomials $a_i(x) \in \mathbb{R}[x]$.

B. Then we focus on the bivariate case. The main objective of our study is to characterise all possible topological types of Poincaré-Reeb graphs associated to a direction of projection x and to a given smooth and compact connected component of a real algebraic curve in $\mathbb{R}^2$. We start by proving that these graphs are plane trees whose open **edges are transverse** to the vertical lines.

Furthermore we place ourselves **in the asymptotic setting**, namely we study the Poincaré-Reeb trees of level curves $\mathcal{C}_\varepsilon$, for $\varepsilon > 0$ small enough, near an isolated minimum at the origin. Using the polar curve, we show that when $\varepsilon > 0$ is sufficiently small, the Poincaré-Reeb tree combinatorically stabilises. In addition, its edges do not move backwards. They only move further from the origin. The Poincaré-Reeb tree is rooted and it is the union between a positive tree (to the right of the origin) and a negative tree (situated to the left of the origin). This is what we call **the asymptotic Poincaré-Reeb tree**.

If we suppose also that the direction of projection x is a **generic direction**, then using the notions of crests and valleys introduced by Coste and de la Puente (see [CP01]) we show that the asymptotic Poincaré-Reeb tree is moreover a complete binary plane tree and its vertices get totally ordered by the ambient foliation. Namely, the preorder defined by the foliation x is a total order. We call it **a generic asymptotic Poincaré-Reeb tree**. See Figure 33. It is a generic rooted transversal tree, in the following sense:

Definition. Let us call **generic rooted transversal tree** a rooted plane complete binary tree whose open edges are transverse to the trivialisable, oriented and cooriented foliation of the plane induced by the function x, such that its vertices are endowed with a total order relation induced by this foliation and this order is monotone on each geodesic starting from the root.

We will come back to the relation between the negative and positive trees later on. Let us now focus on the half-plane $x > 0$, namely on what we call **positive trees**.

One of our main theorems is the following:

> **Theorem.** *Every separable positive generic rooted transversal tree is realisable in an effective way by a strict local minimum of a bivariate real polynomial function in a small enough neighbourhood of the origin.*

Note that here we call "separable" a tree to which we can associate a separable permutation. Roughly speaking, to associate a permutation to a generic rooted transversal tree, let us look at its vertical embedding in the real plane, such that its root is on top. We can order its vertices in two manners:

- the natural order on the set of its vertices: first read the leaves in the order induced by the real plane; then between each pair of consecutive leaves (a, b), intercalate the internal bifurcation vertex $a \wedge b$;

- the vertical order of its vertices.

These two total order relations on the set of the vertices of a generic rooted transversal tree provide a permutation (see Figure 38).

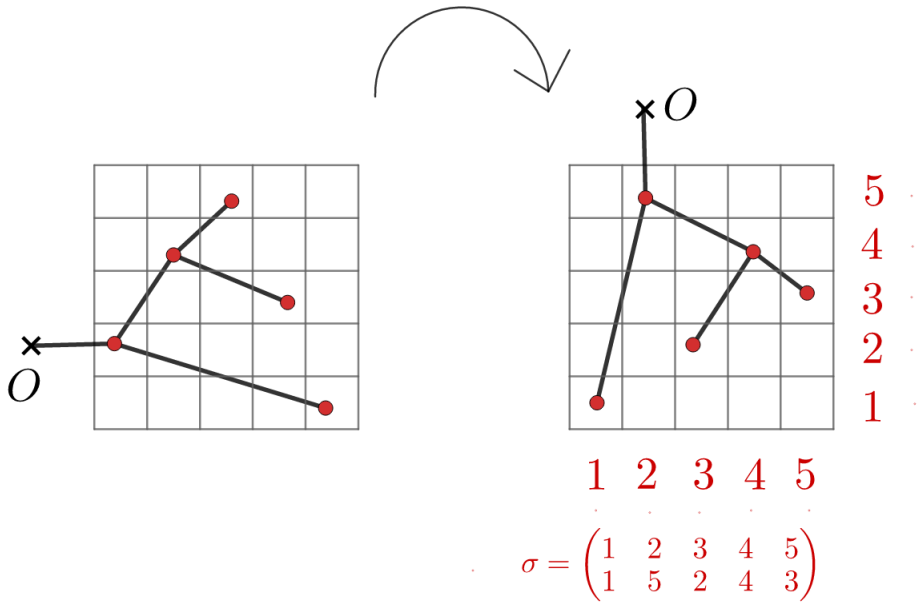

Figure 38: Associating a permutation to a generic rooted transversal tree.

Remark. Note that this is a new manner to associate a permutation to a plane tree, different to the one defined in [Ghy17], where Ghys endowed the set of graphs of a given finite family of polynomials in a small enough neighbourhood of a common zero with two total orders: one order given by their position for $x > 0$ and the other order given by the position of the polynomials for $x < 0$, as shown in Figure 39. He proved that a permutation can be realised by real polynomial graphs near a common zero if and only if it is a separable permutation.

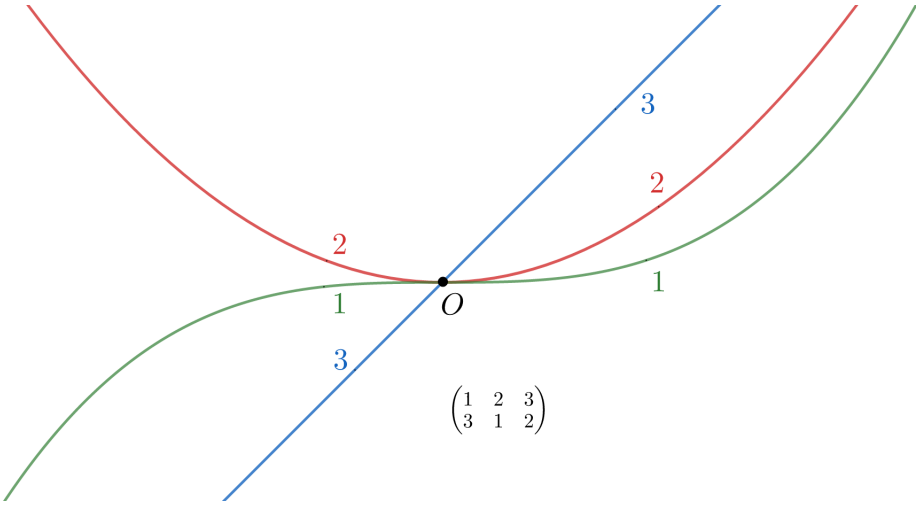

Figure 39: Associating a permutation to a set of graphs of polynomials near a common zero.

For the proof of our theorem, we rely on the polar curve, which is the critical locus of a map ϕ we introduce in more details later. The shape to the right (i.e. for $x > 0$) of the level curves $\mathcal{C}_\varepsilon$, for $\varepsilon > 0$ sufficiently small, is determined by the combinatorial interplay between the critical locus and the critical image of the map ϕ, which both have a crucial role in this work.

Finally, we are interested in both the positive and the negative trees simultaneously. For a given separable positive Poincaré-Reeb tree $\mathcal{T}$, we present a new algorithm whose output consists of all the negative Poincaré-Reeb trees that form pairs with $\mathcal{T}$, by our construction of a strict local minimum.

Main results in detail and structure of the thesis

The Poincaré-Reeb tree

Let us describe our new construction of what we call the Poincaré-Reeb graphs, associated to a smooth and compact connected component of a real algebraic curve in $\mathbb{R}^2$ and to a given projection direction x. **Chapter** 2 is dedicated to this combinatorial object, that is meant to capture the non-convexity of the curves. It is adapted from the classical construction introduced by H. Poincaré (see [Poi10, 1904, Fifth supplement, page 221]), which was rediscovered by G. Reeb in 1946 (in [Ree46]). Both used it as a tool in Morse theory. Namely, given a Morse function on a closed manifold, they associated it a graph as a quotient of the manifold by the equivalence relation whose classes are the connected components of the levels of the function. We will perform an analogous construction for a special type of manifold with boundary.

• Consider a compact and smooth connected component $\mathcal{C}$ of a real algebraic curve contained in the plane $\mathbb{R}^2$ (see Figure 40).

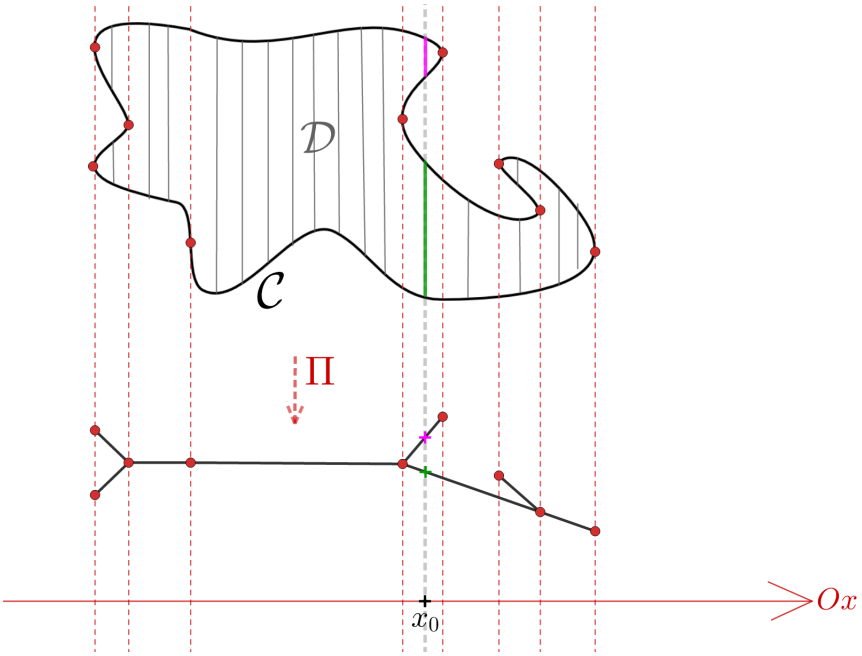

Figure 40: The Poincaré-Reeb graph of a smooth and compact connected component of a real algebraic curve in $\mathbb{R}^2$.

Denote by $\mathcal{D}$ the disk bounded by $\mathcal{C}$. Endow the plane $\mathbb{R}^2$ with its canonical orientation and with its foliation by vertical lines. The curve $\mathcal{C}$, being a connected component of an algebraic curve, has only finitely many points of vertical tangency. We are ready now for the construction of the Poincaré-Reeb graph. Its vertices correspond to the points of the curve having vertical tangent. Consider the projection $\Pi : \mathcal{D} \to \mathbb{R}$, $\Pi(x, y) := x$. For $x_0 \in \mathbb{R}$, if the fibre $\Pi^{-1}(x_0)$ is not the empty set, then it is a finite union of vertical segments. We define an equivalence relation that lets us contract each of these segments into a point. By the quotient map, the image of the initial disk becomes a one-dimensional connected topological subspace embedded in the real plane. More precisely, it is a connected plane graph. We prove the following result:

Theorem 0.1 (see Corollary 2.37)**.** *The Poincaré-Reeb graph associated to a compact and smooth connected component of a real algebraic plane curve and to a direction of projection x is a plane tree whose open edges are transverse to the foliation induced by the function x. Its vertices are endowed with a total preorder relation induced by the function x.*

In the sequel, we will call it **the Poincaré-Reeb tree**. Note that by **preorder** we mean a binary relation, that is reflexive and transitive.

The main tool used in the proof of Theorem 0.1 is the integration with respect to the Euler characteristic.

• Let us now restrict the study of this tree to the asymptotic setting, namely let us study the Poincaré-Reeb trees associated to small enough level curves of a real bivariate polynomial function, near a strict local minimum at the origin of the plane. The tree stabilises for sufficiently small level curves. Call it **the asymptotic Poincaré-Reeb tree**.

Theorem 0.2 (see Theorem 2.70)**.** *The asymptotic Poincaré-Reeb tree is a rooted tree and the total preorder relation on its vertices, induced by the function x, is strictly monotone on each geodesic starting from the root.*

Remark. The strict monotonicity on the geodesics starting from the root implies that the small enough level curves $\mathcal{C}_\varepsilon$ have no turning back or spiralling phenomena. In particular, for $\varepsilon > 0$ sufficiently small, there are no shapes $\mathcal{C}_\varepsilon$ like the one in Figure 41.

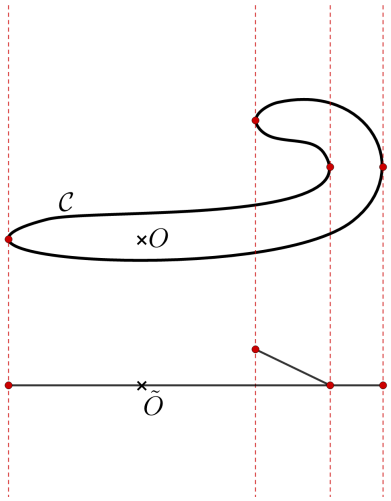

Figure 41: Forbidden shape for small enough $\varepsilon > 0$: there are no going backwards like this.

An asymptotic Poincaré-Reeb tree whose vertices are endowed with a preorder relation induced by x is shown in Figure 42 below. It is a union-tree of a positive tree (at the right of the origin) and a negative tree (at the left of the origin), the latter two having a common root, that is the image of the origin. We only speak about a preorder relation for the vertices of an asymptotic Poincaré-Reeb tree since there might be more than one vertex on the same level of the foliation of the plane given by x.

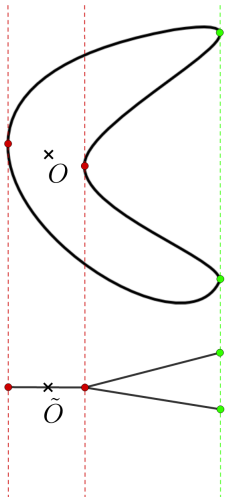

Figure 42: An asymptotic Poincaré-Reeb tree whose vertices are endowed with a preorder relation induced by x: the two rightmost vertices are situated on the same level.

• Let us place ourselves in the asymptotic case. If, in addition, the direction x of projection we consider is generic, namely if it is a direction that avoids bitangents to $\mathcal{C}_\varepsilon$ and tangents to vertical inflection points, then we obtain what we call **a generic asymptotic Poincaré-Reeb tree**.

Theorem 0.3 (see Theorem 2.124)**.** *Besides the properties of an asymptotic Poincaré-Reeb tree, a generic asymptotic Poincaré-Reeb tree has the following characteristics: the preorder defined by the ambient foliation x is* ***a total order*** *relation and it is a* ***complete binary*** *tree (i.e. each internal vertex has exactly two children).*

Example. An example of two generic asymptotic Poincaré-Reeb trees with total order relations endowing their vertices. Note that the two are topologically inequivalent Poincaré-Reeb trees.

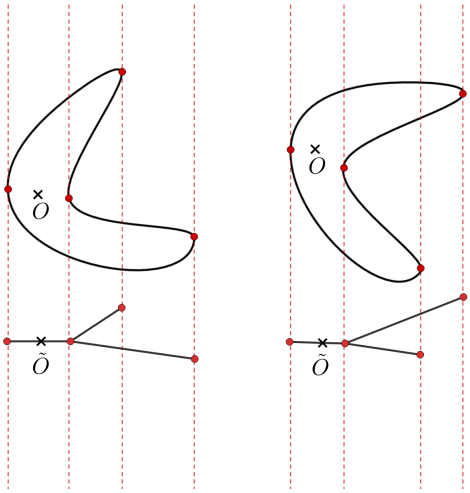

Figure 43: Two topologically inequivalent generic asymptotic Poincaré-Reeb trees.

In conclusion, we constructed and described a new combinatorial object, called the asymptotic Poincaré-Reeb tree, whose role is to quantify the non-convexity of small enough level curves $\mathcal{C}_\varepsilon$. It is a transversal tree. Next, our aim is to detect which transversal trees can be realised as asymptotic Poincaré-Reeb trees.

The connection between the bivariate case and the univariate case

Recall that, given a generic rooted transversal tree $\mathcal{T}$, we want to construct a polynomial function $f(x,y) \in \mathbb{R}[x,y]$ with a strict local minimum at the origin, such that the asymptotic Poincaré-Reeb tree associated to f and to the direction x is $\mathcal{T}$. In the sequel, we explain the transition from the bivariate setting to the univariate one. We present briefly the geometrical and combinatorial relation between the two settings.

For the moment, let us restrain our study to the half-plane $x > 0$ of the plane (Oxy): **Chapter** 3 is dedicated to the construction of a real polynomial with a strict local minimum at O, that realises a given snake of the level curve $\mathcal{C}_\varepsilon$ to the right of the origin (that is, for $x > 0$).

• First, the snake σ_ε shown in Figure 44 encodes the shape of $\mathcal{C}_\varepsilon \subset (Oxy)$ for $x > 0$ (under a certain hypothesis). The snake is determined by the alternating sequence of right crests and right valleys.

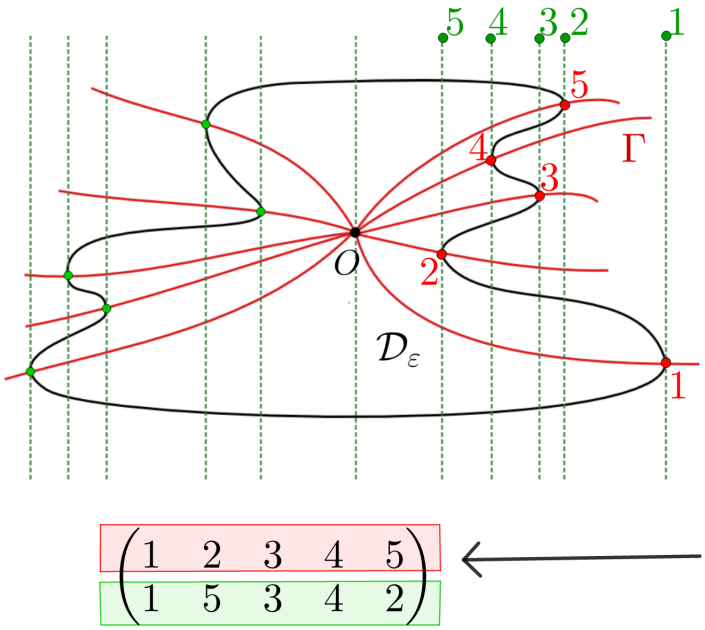

Figure 44: The right asymptotic snake.

• Secondly, consider the graph of f:

$$\text{graph}(f) := \{(x,y,z) \in \mathbb{R}^3 \mid z = f(x,y)\}.$$

It is a surface represented in Figure 45. The intersection of graph(f) with the plane $x = x_0$, for a sufficiently small $x_0 > 0$, consists of a plane algebraic curve which is the graph of the one variable polynomial $f(x_0, y)$. Under some hypotheses, this is a Morse polynomial and we can associate to it a snake, called τ.

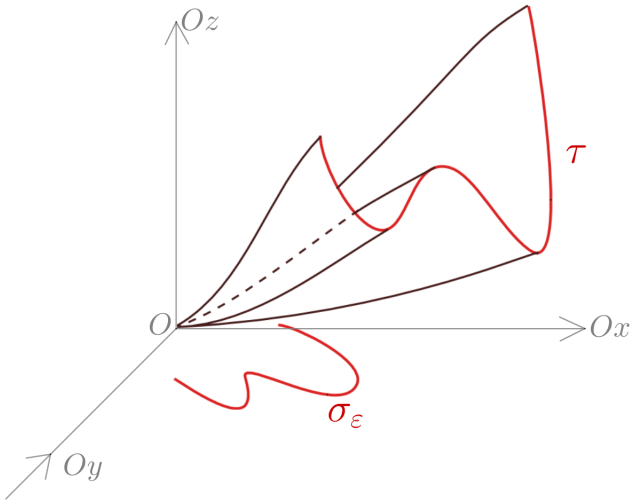

Figure 45: Equal snakes: $\sigma_\varepsilon = \tau$.

Theorem 0.4 (see Theorem 3.33)**.** *Under certain hypotheses (to be made precise later), the two snakes are equal:* $\sigma_\varepsilon = \tau$.

Roughly speaking, the key idea is that given a snake σ, in order to construct a polynomial $f(x, y) \in \mathbb{R}[x, y]$ that realises σ to the right, we will construct an asymptotic family of polynomials in one variable y with coefficients in x, that is, polynomials in $\mathbb{R}[x][y]$, such that for sufficiently small $x > 0$ the snake τ is equal to σ.

We will make the above mentioned hypotheses clear in what follows.

Let us further study the combinatorial relationship between the snake σ_ε to the right and what we call the "positive" polar curve with respect to x.

Consider the map

$$\Phi : \mathbb{R}^2_{x,y} \to \mathbb{R}^2_{x,z}, \Phi(x, y) := (x, f(x, y)).$$

The critical locus of Φ is the polar curve $\Gamma(f, x)$.

In Figure 46, we see three sets of curves:

- the "positive" part of the polar curve, denoted $\Gamma_+ := \Gamma(f, x) \cap (x > 0)$;
- the "positive" critical image (or discriminant curve) $\Delta_+ := \Phi(\Gamma_+)$ (in green);
- the apparent contour on the surface graph(f) (in red), when projected to the (Oxz)-plane.

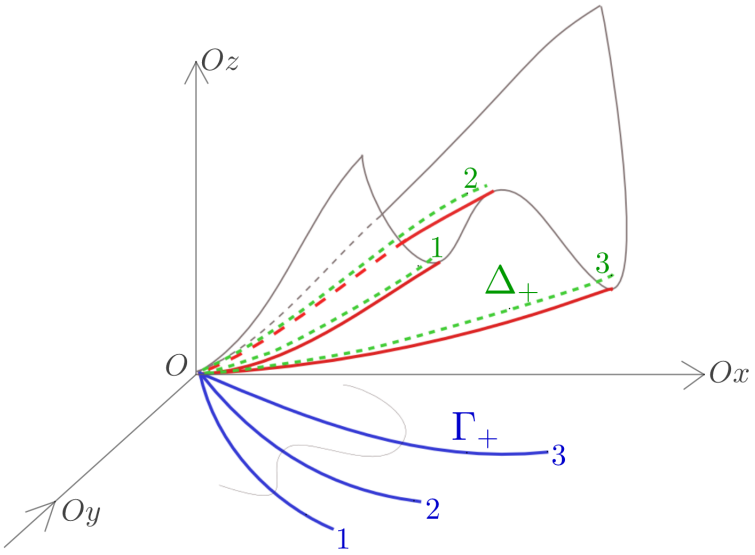

Figure 46: The homeomorphism between the reduced positive polar curve Γ_+ and its image Δ_+.

The polynomials that we construct satisfy the following two geometrical hypotheses:
- the curve Γ_+ is reduced;
- the map $\Phi_{|\Gamma_+} : \Gamma_+ \to \Delta_+$ is a homeomorphism.

We will obtain the following result:

Theorem 0.5 (see Proposition 3.32)**.** *Under the previous genericity hypotheses, the permutation realised by the bijection between the positive polar curve Γ_+ and its image Δ_+ is equal to the snake σ_ε.*

Remark. Intuitively, to associate a permutation to the bijection between the set of branches in Γ_+ and the set of branches in Δ_+, we look at the following two total order relations: the relative positions of the curves in Γ_+ and the relative positions of their images in Δ_+. The interplay between these two sets of objects yields a snake.

We shall direct our attention on the inverse transition, namely passing from one variable to two variable polynomials only after we will have presented the univariate case below.

Construction of one variable polynomials

The strategy we adopted was to study bivariate polynomials in $\mathbb{R}[x, y]$ as asymptotic families of univariate polynomials $f_x(y) \in \mathbb{R}[x][y]$, for sufficiently small x tending to zero. Hence we dedicate **Chapter** 1 to the construction of univariate polynomial equations that realise a given snake.

Theorem 0.6 (see Theorem 1.149)**.** *Given a separable snake σ, we construct explicitly an equation of a family of Morse polynomials $Q_x(y) \in \mathbb{R}[x][y]$, $Q_x(y) := \int_0^y \prod_{i=1}^n (t - a_i(x))\mathrm{d}t$, such that for sufficiently small $x > 0$ the snake associated to $Q_x(y)$ is σ.*

Note that our choice of the polynomials $a_i(x) \in \mathbb{R}[x]$ is determined by the combinatorial properties of the given separable snake. The proof is based on handling another combinatorial

object introduced in Chapter 1, called **the contact tree**, associated to a finite set of real univariate polynomials $\{a_i(x)\}$. It is a rooted plane tree whose internal vertices are decorated with numerical information extracted from the given polynomials. Its role in our research is to encode the proximity between different families of real one variable polynomials.

The main challenge was to determine the snake (or, equivalently, the generic asymptotic Poincaré-Reeb tree) in function of the contact tree.

Construction of polynomials in two variables, to the right

Let us return now to our initial objective, obtaining **the main result of the thesis**, to which we dedicate the last part of **Chapter** 3:

Theorem 0.7 (see Theorem 3.34)**.** *Let σ be a separable snake.*

(a) There exists a real bivariate polynomial $f \in \mathbb{R}[x, y]$ with an isolated minimum at the origin whose snake to the right (i.e. for $x > 0$ and $\varepsilon > 0$ both sufficiently small), denoted σ_ε, is the given snake σ.

(b) The existence is realisable in an explicit way, by following the next two steps:

- *construct the one variable polynomial $Q_x(y)$, with $x > 0$ small enough, whose associated snake is the given separable snake σ, as in Theorem 0.6;*
- *define the polynomial in two variables $f(x, y) := x^2 + Q_x(y)$.*

We prove that our family of polynomials has indeed a strict local minimum at the origin, using a criterion based on the Newton polygon.

To give the equation of the desired polynomial in two variables, we first choose its polar curve with respect to x. All the branches of the polar curve with respect to x in our construction are real, smooth and transverse to the Oy-axis, such that the polar curve satisfies the hypotheses of Theorem 0.5.

Pairs of negative-positive Poincaré-Reeb trees obtained with our method

We can construct equations that realise any given separable, positive (i.e. to the right of the origin) generic rooted transversal tree. By symmetry, we can also realise any of these trees to the left. However, we are now interested in which couples of these separable trees can be realised simultaneously, as a pair of negative-positive Poincaré-Reeb trees near an isolated minimum.

Question. Given a separable positive Poincaré-Reeb tree $\mathcal{T}$ (i.e. to the right of the origin), which are the negative Poincaré-Reeb trees (i.e. to the left of the origin) that form pairs with $\mathcal{T}$, in our construction?

Answer: In **Chapter** 4 we provide an algorithm (see Algorithm 4.25) whose output is the set of all the negative Poincaré-Reeb trees, that we can realise and that form pairs with a given separable positive Poincaré-Reeb tree, by using our construction. More precisely, the union-trees formed in this way are explicitly realisable by our family of polynomials as generic asymptotic Poincaré-Reeb trees near a strict local minimum in a small enough neighbourhood of the origin (see Theorem 4.26).

Example. Let us consider a given separable positive Poincaré-Reeb tree $\mathcal{T}$ (see Figure 47).

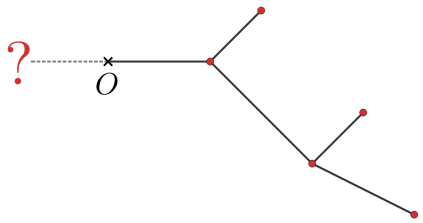

Figure 47: Which are the negative Poincaré-Reeb trees, that form pairs with the given separable, positive Poincaré-Reeb tree $\mathcal{T}$, using our construction?

All the possible pairs of trees of this example and their corresponding level curves $\mathcal{C}_\varepsilon$ are shown in Figure 48.

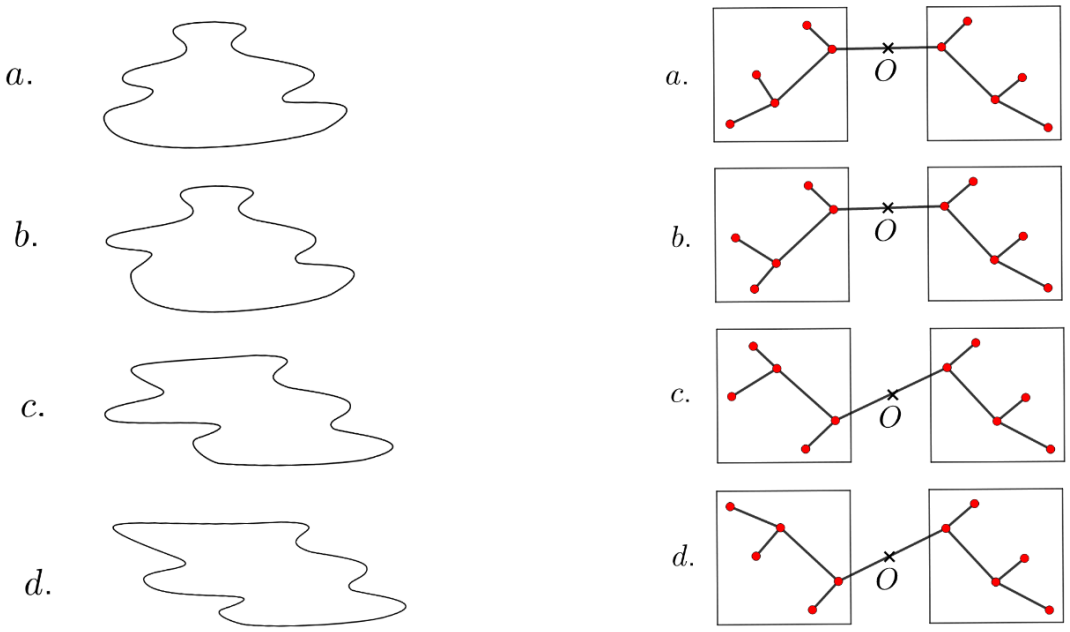

Figure 48: Non-convex level curves and their corresponding pairs of negative-positive Poincaré-Reeb trees realised with our construction by a strict local minimum at the origin of a polynomial function in two real variables, given the positive Poincaré-Reeb tree (the tree on the right side of the origin).

Therefore, by running our algorithm we provide all the negative Poincaré-Reeb trees that can form a pair with $\mathcal{T}$ and that we can realise effectively by our construction.

Chapter 1

The Poincaré-Reeb tree of univariate polynomial functions

In this chapter, we describe combinatorial objects that code geometrical and topological shapes. We start by coding the graph of a polynomial in one real variable.

1.1 Alternating sequences

Definition 1.1. Let $A := [a_1, a_2, \ldots, a_n]$ be a finite sequence of pairwise distinct real numbers, where $n \geq 1$.

We call it:

(a) **an α-down-up sequence** if $a_1 > a_2 < a_3 > a_4 < \ldots$;

(b) **an α-up-down sequence** if $a_1 < a_2 > a_3 < a_4 > \ldots$;

(c) **an ω-down-up sequence** if $\ldots a_{n-2} > a_{n-1} < a_n$;

(d) **an ω-up-down sequence** if $\ldots a_{n-2} < a_{n-1} > a_n$.

If A is of one of the previous kinds, we say simply that A is **an alternating sequence**.

Example 1.2. An alternating sequence of seven numbers is for instance

$$A := [3, 1, 6, -5, 0, -1, 100].$$

This alternating sequence is both an α-down-up sequence and an ω-down-up sequence.

Definition 1.3. Let $A := [a_1, a_2, \ldots, a_n]$ be a sequence of real numbers, where $n \geq 1$. We call it **a weakly alternating sequence** if we allow non strict inequalities between the real numbers a_i.

1.1.1 Some historical remarks

Remark 1.4. In the nineteenth century, André (see [And81], [And79]) introduced the notion of alternating permutation, as follows: he considered n distinct objects α_1, α_2, …, α_n and formed all the possible permutations of these elements. Take, for instance, the permutation

$$\alpha_{\pi(1)}, \alpha_{\pi(2)}, \alpha_{\pi(3)}, \ldots, \alpha_{\pi(n)}.$$

Let us consider the consecutive differences between the indices, namely $\pi(i+1) - \pi(i)$, for $i = 1, \ldots, n-1$. In [And81, page 168], André called the permutation $\alpha_{\pi(1)}, \alpha_{\pi(2)}, \alpha_{\pi(3)}, \ldots, \alpha_{\pi(n)}$

an alternating permutation if and only if one obtains an alternation of positive and negative differences of the indices of α, namely $\pi(i+1) - \pi(i)$, for $i = 1, \ldots, n-1$, such that no two consecutive positive (respectively negative) differences occur.

For instance, for $n = 5$, the permutation

$$\alpha_1, \alpha_4, \alpha_3, \alpha_5, \alpha_2$$

is an alternating permutation, while

$$\alpha_1, \alpha_3, \alpha_4, \alpha_2, \alpha_5$$

is not.

André proved that the number of alternating permutations is always even and denoted by $2A_n$ the number of alternating permutations of n elements. He gave a combinatorial interpretation of the coefficients of the Taylor development of $\tan(x)$ and of $\sec(x) = \frac{1}{\cos(x)}$ in [And79]:

$$\sec(x) = A_0 + A_2 \frac{x^2}{2!} + A_4 \frac{x^4}{4!} + \ldots$$

and

$$\tan(x) = A_1 \frac{x}{1!} + A_3 \frac{x^3}{3!} + A_5 \frac{x^5}{5!} + \ldots$$

Let us recall now from [Lan03, page 64] and [Arn00, page 60] the notion of *Bernoulli-Euler triangle*. Each entry of this triangle counts the number of possible paths from the top vertex to the given entry. The paths must be alternating left-right, starting always to the left. The left-hand edge of the Bernoulli-Euler triangle is called the Bernoulli side, while the right-hand edge is called the Euler side (see Figure 1.1).

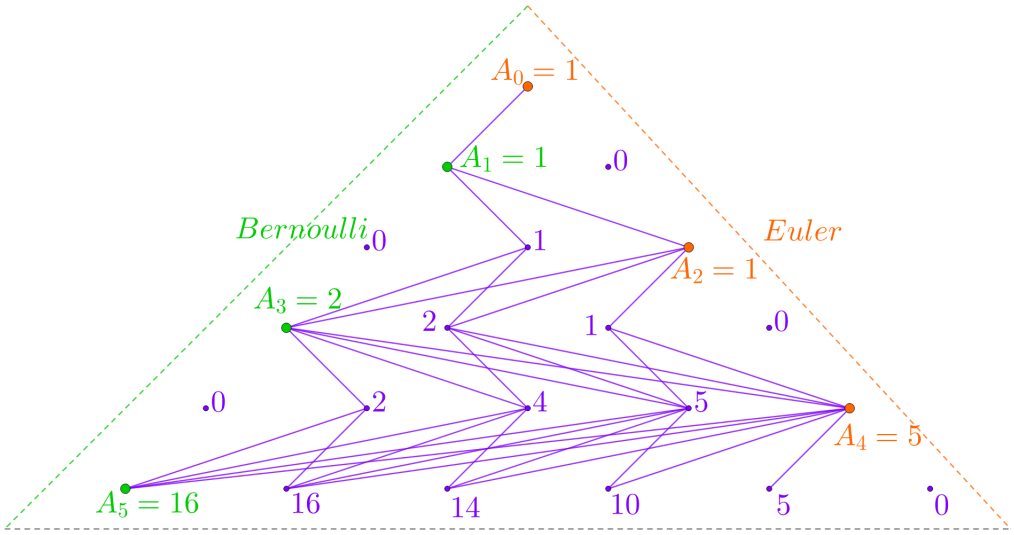

Figure 1.1: The Bernoulli-Euler triangle.

In [Lan03, page 70], the author proved that the above numbers A_n, for n odd, give the Bernoulli side of the Bernoulli-Euler triangle, while for n even, they give the Euler side of the Bernoulli-Euler triangle.

REMARK 1.5. In his survey [Sta10], Stanley used the notion of an alternating permutation (respectively reverse alternating permutation), as follows. Let $\sigma := \begin{pmatrix} 1 & 2 & \dots & n \\ \sigma(1) & \sigma(2) & \dots & \sigma(n) \end{pmatrix}$ be a permutation of $\{1, 2, \dots, n\}$. Stanley said that σ is:

(a) an alternating permutation, if $\sigma(i) < \sigma(i+1)$ for i even, while $\sigma(i) > \sigma(i+1)$ for i odd;

(b) a reverse alternating permutation, if $\sigma(i) > \sigma(i+1)$ for i even, while $\sigma(i) < \sigma(i+1)$ for i odd.

Nevertheless, we shall use only the terminology we introduce in Definition 1.1, Definition 1.3 and Definition 1.6.

1.2 Snakes

Let us present a related notion which was used by Arnold (see [Arn92, page 2], [Arn00]):

Definition 1.6. Let us consider a permutation $\sigma : \{1, 2, \dots, n\} \to \{1, 2, \dots, n\}$. We say that σ is **an n-snake** if $[\sigma(1), \sigma(2), \dots, \sigma(n)]$ is an alternating sequence in the sense of Definition 1.1. We call $(i, \sigma(i))$ **a critical point of the snake** σ.

REMARK 1.7. For a given snake $\sigma := \begin{pmatrix} 1 & 2 & \dots & n \\ \sigma(1) & \sigma(2) & \dots & \sigma(n) \end{pmatrix}$, let us take the set

$$\{(i, \sigma(i)) \mid i = 1, \dots, n\}$$

of points in the real plane. Then for each $i = 1, \dots, n-1$ let us connect the consecutive points $(i, \sigma(i))$ and $(i+1, \sigma(i+1))$ by an edge. This is the graphic representation of snakes that we shall use in what follows.

EXAMPLE 1.8. Let us give an example of a 3-snake: $\sigma := \begin{pmatrix} 1 & 2 & 3 \\ 2 & 1 & 3 \end{pmatrix}$, which is represented in Figure 1.2. Its alternating sequence is $[2 > 1 < 3]$.

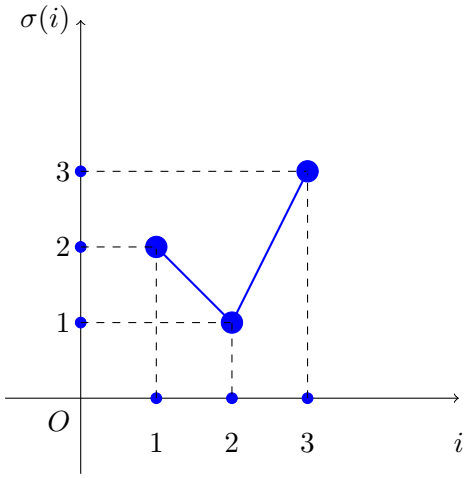

Figure 1.2: Example of a 3-snake σ.

Notation 1.9. *Let us denote by $\mathcal{A}_n$ the set of alternating sequences of n real numbers and by $\mathcal{S}_n$ the set of n-snakes.*

Definition 1.10. Let $A := [a_1, \ldots, a_n] \in \mathcal{A}_n$ be an alternating sequence of n distinct real numbers $a_i \in \mathbb{R}$. Consider a second sequence A' obtained by reordering the elements of A in a strictly increasing way. Define the **rank of** a_i, denoted rk (a_i), to be the position of a_i in this strictly increasing sequence A'. The **snake** φ_A **of** A is defined by

$$\varphi_A(i) := \text{rk } (a_i).$$

Now we can define the function $\varphi : \mathcal{A}_n \to \mathcal{S}_n$ as follows: $\varphi(A) := \varphi_A$.

Remark 1.11. The function φ is a surjection.

Example 1.12. Consider the following alternating sequence: $[3 > 1 < 4 > -1 < 6]$. Thus the set of the real numbers to be ordered is $\{3, 1, 4, -1, 6\}$. We obtain rank $(3) = 3$, rank $(1) = 2$, rank $(4) = 4$, rank $(-1) = 1$, rank $(6) = 5$. Hence, the 5-snake associated to $[3 > 1 < 4 > -1 < 6]$ is $\sigma := \begin{pmatrix} 1 & 2 & 3 & 4 & 5 \\ 3 & 2 & 4 & 1 & 5 \end{pmatrix}$, as one can observe in Figure 1.3.

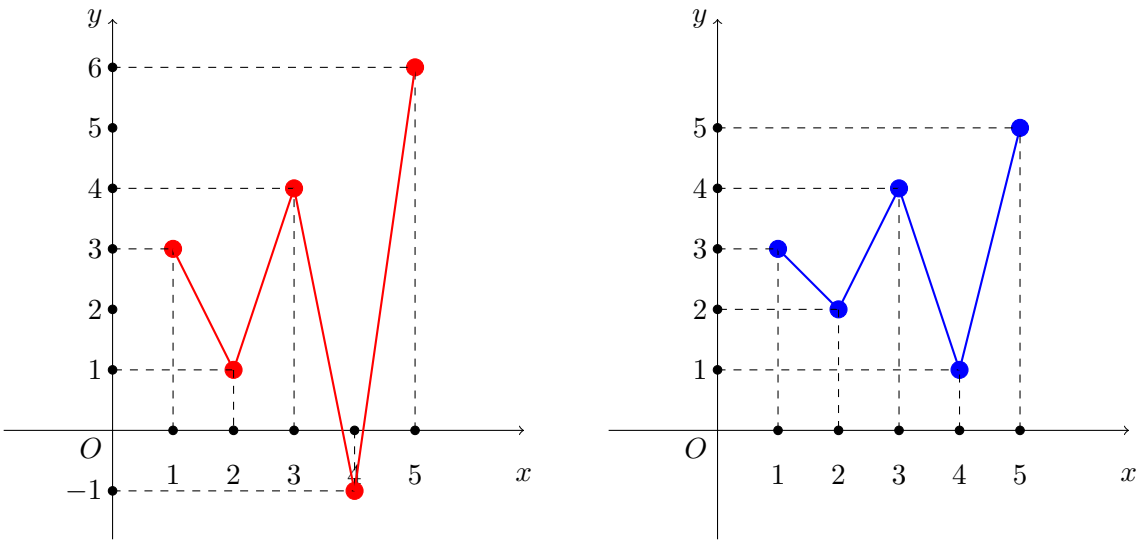

Figure 1.3: From the alternating sequence to the snake σ, as in Example 1.12.

Proposition 1.13. *Between any two consecutive local maxima (respectively minima) of a polynomial function $P : \mathbb{R} \to \mathbb{R}$ there exists a unique local minimum (respectively maximum) of P. In other words, the minima and maxima alternate.*

Proof.

• Part 1: Let x_1 and x_2 be two consecutive local maxima of P, i.e. there exists no other real number $x \in]x_1, x_2[$ such that x is a local maximum of P. Since P is continuous, one can apply the Extreme values theorem (due to Weierstrass) on the closed interval $[x_1, x_2]$. Thus there exists $m \in [x_1, x_2]$ such that $f(m) \leq f(x)$, for any $x \in [x_1, x_2]$. In other words, P has a local minimum on any interval delimited by two consecutive local maxima of P.

• Part 2: For two consecutive local minima, the proof is similar.

• Part 3: Let us now prove that the local minimum between any two consecutive local maxima is unique. We argue by contradiction. If there existed two local minima m_1 and m_2 between the two consecutive local maxima x_1 and x_2, then by Part 2, we have a local maximum between m_1 and m_2, which contradicts the fact that x_1 and x_2 are consecutive local maxima.

• Part 4: Similarly we prove that the local maximum between any two consecutive local minima is unique. □

Definition 1.14. [Lan03, page 64] Let us fix $n \geq 1$. We say that a polynomial $P : \mathbb{R} \to \mathbb{R}$ is an n-**Morse polynomial** if it satisfies the following conditions:

(a) $\deg P = n$;

(b) P is monic, i.e. the leading coefficient of P is equal to 1;

(c) its critical points (i.e. the values $x_i \in \mathbb{C}$ such that $P'(x_i) = 0$) are distinct (i.e. simple) and real;

(d) its critical values (i.e. the values $P(x_i)$, where x_i is a critical point) are all distinct.

The following Definition 1.15 is inspired from [KS02].

Definition 1.15. We say that a polynomial is **a hyperbolic polynomial** if all its roots are real and distinct.

Proposition 1.16. *The derivative of an n-Morse polynomial is a hyperbolic polynomial.*

Notation 1.17. *Let $P : \mathbb{R} \to \mathbb{R}$ be an n-Morse polynomial. Let us denote by $[\eta_1, \eta_2, \eta_3, \ldots, \eta_{n-1}]$ the sequence of the critical values of P, ordered according to the order of the corresponding critical points, seen as elements of $\mathbb{R}$ endowed with the usual total order.*

Corollary 1.18. *The sequence $[\eta_1, \eta_2, \eta_3, \ldots, \eta_{n-1}]$ is an alternating sequence. Namely this is an ω-up-down sequence since P is monic by Definition 1.14*

Proof. This is a Corollary of Proposition 1.13. □

The following definition is similar to the one given in [Lan03, pages 66-67].

Definition 1.19. Let $P : \mathbb{R} \to \mathbb{R}$ be an n-Morse polynomial.

The $(n-1)$-snake associated to the alternating sequence of the critical values of P (see Definition 1.10) is called **the snake associated to the polynomial** P.

Example 1.20. Let us consider the polynomial $Q : \mathbb{R} \to \mathbb{R}$, $Q(x) := (x-1)(3x-2)$. By integration, we obtain the polynomial $P : \mathbb{R} \to \mathbb{R}$,

$$P(x) := \int_0^x Q(t)\mathrm{d}t,$$

namely $P : \mathbb{R} \to \mathbb{R}$, $P(x) = x^3 - \frac{5}{2}x^2 + 2x$. Thus P has two critical points ($x_1 = \frac{2}{3}$, $x_2 = 1$) and their corresponding critical values $\eta_1 := P(\frac{2}{3}) = \frac{14}{27}$ and $\eta_2 := P(1) = \frac{1}{2}$ form the following alternating sequence: $[\frac{14}{27}, \frac{1}{2}]$. By Definition 1.10 we obtain the snake associated to P:

$$\sigma := \begin{pmatrix} 1 & 2 \\ 2 & 1 \end{pmatrix}.$$

Let us see a slightly more complicated example.

Example 1.21. Let us consider the polynomial $Q : \mathbb{R} \to \mathbb{R}$, $Q(x) := (5x-5)(x-2)(x-4)(x-7)$. By integration, we obtain the polynomial $P : \mathbb{R} \to \mathbb{R}$,

$$P(x) := \int_0^x Q(t)\mathrm{d}t,$$

namely $P(x) = x^5 - \frac{35}{2}x^4 + 105x^3 - 265x^2 + 280x$. Thus P has four critical points and the following critical values: $\eta_1 := P(1) = 103.5$, $\eta_2 := P(2) = 92$, $\eta_3 := P(4) = 144$ and $\eta_4 := P(7) = -220.5$ The alternating sequence of the critical values is $[20.7, 18.4, 28.8, -44.1]$. The snake associated to P is $\sigma := \begin{pmatrix} 1 & 2 & 3 & 4 \\ 3 & 2 & 4 & 1 \end{pmatrix}$ and it is shown in Figure 1.4.

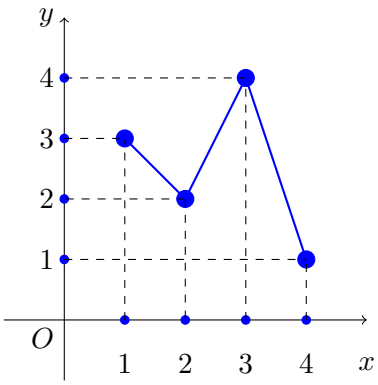

Figure 1.4: Snake σ from Example 1.21.

REMARK 1.22. Since P is monic, the last critical value is a local minimum both in the case where P has an even degree n, and in the case where P has an odd degree. Nonetheless, if we would work also with non-monic polynomials, for instance with the leading term being $-x^n$, the last critical value could be a local maximum.

In conclusion: if one considers an $n-$Morse polynomial function $P : \mathbb{R} \to \mathbb{R}$, then one can associate to it both an alternating sequence and a snake.

Conversely, two questions appear, both regarding the existence of polynomials with constraints:

QUESTION 1.23. Given an ω-up-down sequence $A := [\eta_1, \ldots, \eta_{n-1}]$, does there exist an $n-$Morse polynomial that realises the alternating sequence?

Question 1.23 will be treated in Subsection 1.3.2. As a subquestion, we have:

QUESTION 1.24. Given an $(n-1)$-snake σ, which has the property that $\sigma(n-2) > \sigma(n-1)$, does there exist an $n-$Morse polynomial that realises σ?

By [Arn92], the answer to Question 1.24 is affirmative. For instance, see Figure 1.5 for all the $1, 2, 3, 4$-snakes: they are realised by polynomials. The purpose of this chapter is to give a **constructive answer** to Question 1.24, in a special case, namely in the case of **separable** snakes (which will be introduced later in Definition 1.128).

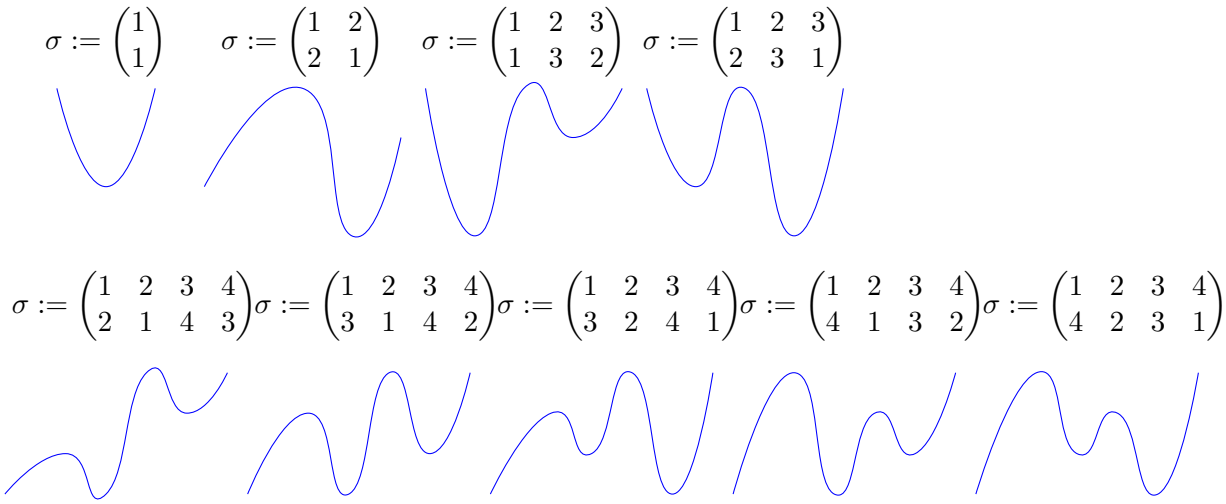

Figure 1.5: Examples of $n-$Morse polynomials of degrees $n = 2, 3, 4$ and 5 respectively that realise the given $(n-1)$-snakes σ (see [Lan03, page 67], [Arn00, Leçon 3, page 59]).

1.3 Proofs of the existence, which are not constructive

1.3.1 Arnold's snakes theorem

The answer to Question 1.24 is given in Theorem 1.25, proved by Arnold; he only takes into account the relative position of the critical values, given by the snake. He does not consider alternating sequences (i.e. the exact extreme values); however, Arnold only proved **the existence** of monic Morse polynomials which realise any given snake. We shall present our **constructive** proof in Section 1.8, for the case of **separable** snakes (see Definition 1.128).

Theorem 1.25. *[Arn92, Theorem 29, page 37] The number of $n-$snakes which have the property that $\sigma(n-1) > \sigma(n)$ is equal to the number of topologically inequivalent Morse polynomials of one variable with n critical values that behave like x^{n+1} at infinity.*

Remark 1.26. For the proof and for more information on the enumeration of snakes, see [Lan03, Chapter 5, page 59], [Arn92], [Arn00]. In fact, the number of $n-$snakes which have the property that $\sigma(n-1) > \sigma(n)$ is equal to the number A_n of André (see Remark 1.4).

1.3.2 Proof of existence by Davis

In the sequel, we are going to prove the existence of a polynomial with prescribed critical values, which gives an answer to Question 1.23. More precisely, we add details to the initial solution given in 1956 by Davis in [Dav57]. Note that we are going to use most of Davis' notations. Nevertheless, Davis' approach was not constructive. This fact motivated us in our research to find explicitly such a polynomial, as the reader shall see in the following sections.

In [Dav57], Davis stated the following problem:

> *"For a real polynomial $P(x)$ of degree n, denote the zeros of $P'(x)$ (multiplicity counted) by ξ_i, $i = 1, \ldots, n-1$. Assume all ξ_i are real and let $\xi_1 \leq \xi_2 \leq \ldots \leq \xi_{n-1}$. Now to what extent are the numbers $P(\xi_i)$ arbitrary? More precisely, give necessary and sufficient conditions on an $(n-1)$-tuple of real numbers $\eta_1, \ldots, \eta_{n-1}$ in order that there exists a polynomial P such that $P'(\xi_i) = 0$, $P(\xi_i) = \eta_i$, $i = 1, \ldots, n-1$."*

The solution proposed by Davis was that the numbers $(-1)^i(\eta_i - \eta_{i-1})$, $i = 2, \ldots, n-1$ must be either all non negative or all non positive. Let us choose without loss of generality the case where the numbers $(-1)^i(\eta_i - \eta_{i-1})$, $i = 2, \ldots, n-1$ are all non negative.

Note that the derivative of $P(x)$ can have multiple roots, thus this is why η_i, $i = 1, \ldots, n-1$ form a **weakly** alternating sequence of real numbers (see Definition 1.3).

Before we describe in more detail the solution proposed by Davis, let us present two lemmas proven by Jan Mycielski in [Myc70].

Lemma 1.27. *[Myc70] Let us consider two subsets A and B of a topological space X. If $A \subset B$ and A is dense in X and connected, then B is dense in X and connected.*

Proof. Let us suppose by contraposition that B is not connected, hence by definition there exist two disjoint open sets U_1 and U_2 of X, such that $B = (B \cap U_1) \cup (B \cap U_2)$, where $B \cap U_1 \neq \emptyset$ and $B \cap U_2 \neq \emptyset$. Since $A \subset B$, one has $A = (A \cap U_1) \cup (A \cap U_2)$. One obtains a contradiction: since A is dense, $A \cap U_i \neq \emptyset$, $i = 1, 2$, thus A is not connected. □

Lemma 1.28. *[Myc70] Let f be a continuous mapping of a compact Hausdorff space X into a space Y and $O \subset X$ be a nonempty set such that $f(O)$ is open and the set $Y \setminus f(X \setminus O)$ is connected and dense in Y. Then f maps X onto Y.*

For the proof, see [Myc70].

Definition 1.29. A **weakly-Morse polynomial** is a real one variable polynomial whose derivative has only real roots.

REMARK 1.30. The difference between an n-Morse polynomial and a weakly-Morse polynomial is the following: the weakly-Morse polynomials can have derivatives with multiple roots, while the roots of the derivative of an n-Morse polynomial are simple.

Theorem 1.31. *[Dav57] Given a weakly alternating sequence of n real numbers, there exists a weakly-Morse polynomial of degree $n+1$ whose sequence of critical values is the given sequence.*

The proof consists, briefly speaking, of the following three steps:

(a) if we choose a real positive number $A > 0$, one can write

$$P(x) = A \int_0^x \prod_{i=1}^{n-1} (t - \xi_i) \mathrm{d}t. \tag{1.1}$$

For $i = 1, \ldots, n$, we denote by

$$\delta_i := A(\xi_i - \xi_{i-1});$$

(b) we introduce the real numbers (see Figure 1.6)

$$\phi_i := (-1)^{i-1}(\eta_i - \eta_{i-1}) = (-1)^{i-1}(P(\xi_i) - P(\xi_{i-1})),$$

$i = 1, \ldots, n$ where $\eta_i := P(\xi_i)$, in order to define the continuous mapping

$$\phi : (\mathbb{R}_+)^n \to (\mathbb{R}_+)^n, \ \phi(\delta_1, \ldots, \delta_n) = (\phi_1, \ldots, \phi_n);$$

(c) we prove that ϕ is a local diffeomorphism in the interior of $(\mathbb{R}_+)^n$;

(d) we prove that the map $\phi : (\mathbb{R}_+)^n \setminus \{0\} \to (\mathbb{R}_+)^n \setminus \{0\}$ is surjective.

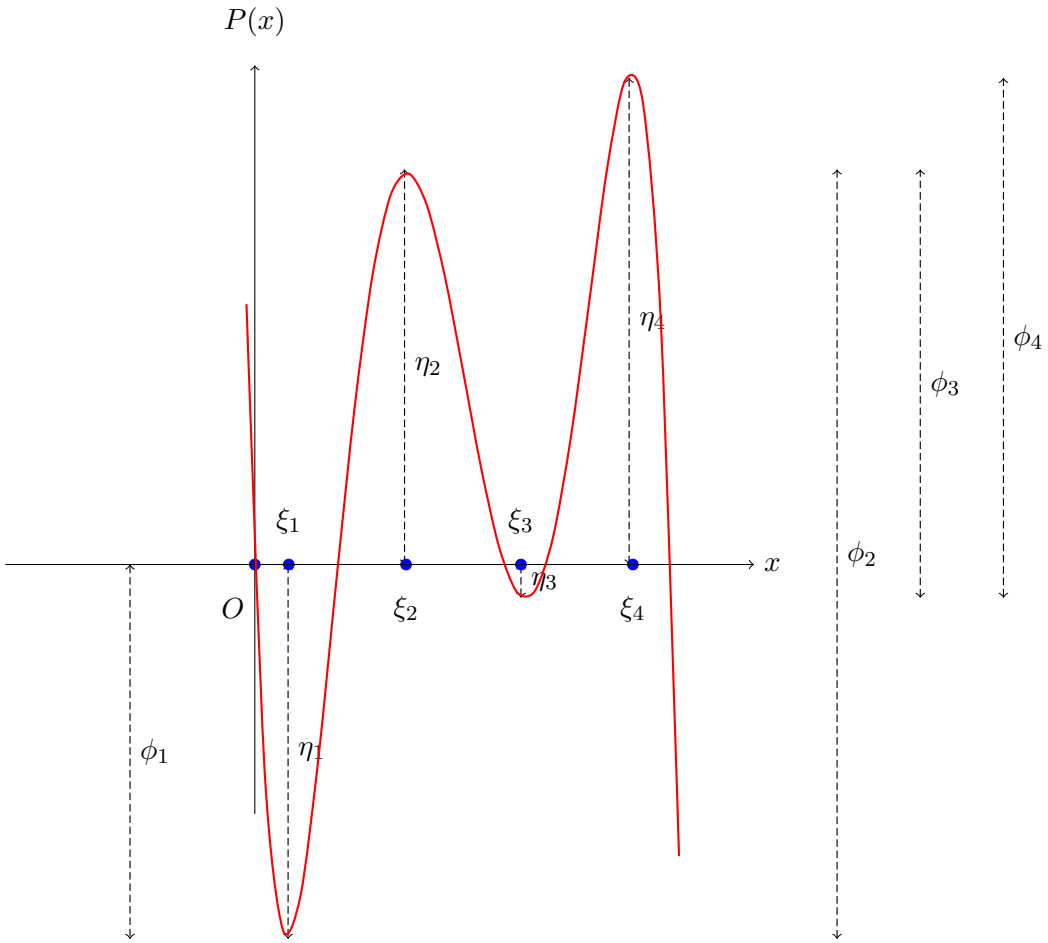

Figure 1.6: The values η_i, ϕ_i, ξ_i.

Proof. The following proof is due to Davis (see [Dav57]). We shall present it in more detail, from our point of view. Note that we are going to use most of Davis' notations.

Let us suppose that $P(0) = 0$. This may be achieved by replacing $P(x)$ by a polynomial of the form $P(x - \alpha) + \beta$, where $\alpha, \beta \in \mathbb{R}$.

If we fix the extremities $\xi_0 := 0$ and $\xi_n := 1$, we have

$$\xi_0 = 0 \leq \xi_1 \leq \ldots \leq \xi_{n-1} \leq 1 = \xi_n.$$

Choosing a real positive number $A > 0$, one can write

$$P(x) = A \int_0^x \prod_{i=1}^{n-1} (t - \xi_i) \mathrm{d}t. \tag{1.2}$$

Note that ξ_0 and ξ_n are not roots of P'.

For $i = 1, \ldots, n$, if we denote by

$$\delta_i := A(\xi_i - \xi_{i-1}),$$

then $\sum_{i=1}^n \delta_i = A$.

Denote by $\eta_i := P(\xi_i)$.

We introduce the real numbers

$$\phi_i := (-1)^{i-1}(\eta_i - \eta_{i-1}) = (-1)^{i-1}(P(\xi_i) - P(\xi_{i-1})), \tag{1.3}$$

$i = 1, \ldots, n$. One can define the continuous mapping

$$\phi : (\mathbb{R}_+)^n \to (\mathbb{R}_+)^n, \phi(\delta_1, \ldots, \delta_n) = (\phi_1, \ldots, \phi_n).$$

One should remark that $\xi_1, \ldots, \xi_{n-1}, A$ are continuous functions of $\delta_1, \ldots, \delta_n$ and that the functions ϕ_i, $i = 1, \ldots, n$ are continuous functions of $\xi_1, \ldots, \xi_{n-1}, A$. Moreover, there is a bijective continuous map

$$\psi_1 : \mathbb{R}^n \to \mathbb{R}^n, \ \psi_1(\xi_1, \ldots, \xi_{n-1}, A) = (\delta_1, \ldots, \delta_n).$$

The map ψ_2 is given by the above Equation 1.3. Note that the polynomial $P(x)$ depends also on the real positive number A.

Therefore, we prefer expressing ϕ in function of the variables δ_i, and not in terms of the variables ξ_i and A. More precisely, we have $\phi = \psi_2 \circ \psi_1^{-1}$, thus the diagram below is commutative:

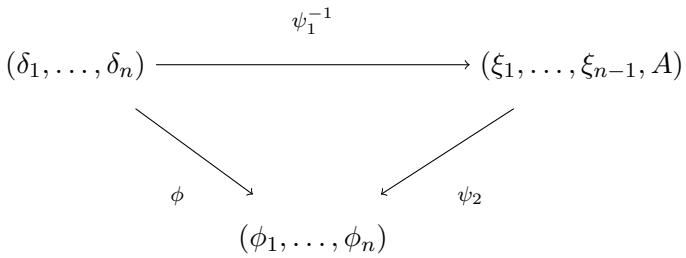

By Rolle's theorem, applied to two consecutive critical points of the polynomial P, one has the equivalence $\phi_i = 0 \Leftrightarrow \xi_i = \xi_{i-1} \Leftrightarrow \delta_i = 0$, hence the boundary of $(\mathbb{R}_+)^n$ is mapped into the boundary of $(\mathbb{R}_+)^n$ and the interior into the interior.

Let us define a polynomial Q such that

$$Q(x) := A \int_0^x \prod_{i=1}^{n-1} (t - \lambda\xi_i) \mathrm{d}t.$$

In addition, let us introduce the real numbers $\tilde{\phi}_i := (-1)^{i-1}(Q(\lambda\xi_i) - Q(\lambda\xi_{i-1}))$, $i = 1, \ldots, n$. Then

$$Q(\lambda x) = A \int_0^{\lambda x} \prod_{i=1}^{n-1} (t - \lambda\xi_i) \mathrm{d}t = A \int_0^x \prod_{i=1}^{n-1} (\lambda u - \lambda\xi_i) \lambda \mathrm{d}u = A\lambda^n \int_0^x \prod_{i=1}^{n-1} (u - \xi_i) \mathrm{d}u = \lambda^n P(x).$$

Hence

$$Q(\lambda\xi_{i+1}) - Q(\lambda\xi_i) = \lambda^n (P(\xi_{i+1}) - P(\xi_i))$$

and one obtains $\tilde{\phi}_i = \lambda^n \phi_i$. This can be written shortly as follows:

$$\phi(\lambda\delta_1, \ldots, \lambda\delta_n) = (\lambda^n\phi_1, \ldots, \lambda^n\phi_n),$$

which means that ϕ maps any ray through the origin onto some ray through the origin.

We are going to prove that ϕ is a local diffeomorphism in the interior of $(\mathbb{R}_+)^n$ and that ϕ is surjective on $(\mathbb{R}_+)^n \setminus \{0\}$.

Let us first prove that ϕ is a local diffeomorphism in the interior of $(\mathbb{R}_+)^n$. It is sufficient to prove that ψ_1^{-1} and ψ_2 are local diffeomorphisms.

In what follows, we shall denote by $\mathrm{J}(F)$ the Jacobian matrix of a map F. By applying the chain rule to $\psi_2 \circ \psi_1^{-1}$, one gets:

$$\det \mathrm{J}(\phi) = \det \mathrm{J}(\psi_2 \circ \psi_1^{-1}) = \det \mathrm{J}_{\psi_1^{-1}}(\psi_2) \det \mathrm{J}(\psi_1^{-1}).$$

Since

$$\det \mathrm{J}(\psi_1^{-1}) = \det \begin{bmatrix} \frac{\partial \delta_1}{\partial \xi_1} & \frac{\partial \delta_1}{\partial \xi_2} & \cdots & \frac{\partial \delta_1}{\partial \xi_{n-1}} & \frac{\partial \delta_1}{\partial A} \\ \frac{\partial \delta_2}{\partial \xi_1} & \frac{\partial \delta_2}{\partial \xi_2} & \cdots & \frac{\partial \delta_2}{\partial \xi_{n-1}} & \frac{\partial \delta_2}{\partial A} \\ \vdots & \vdots & \ddots & \vdots & \vdots \\ \frac{\partial \delta_n}{\partial \xi_1} & \frac{\partial \delta_n}{\partial \xi_2} & \cdots & \frac{\partial \delta_n}{\partial \xi_{n-1}} & \frac{\partial \delta_n}{\partial A}. \end{bmatrix},$$

after computations, one gets $\det \mathrm{J}(\psi_1) = A^{n-1} \neq 0$. Clearly ψ_1^{-1} is a local diffeomorphism, since

$$\det \mathrm{J}(\psi_1^{-1}) = \frac{1}{\det \mathrm{J}(\psi_1)} = \frac{1}{A^{n-1}} \neq 0.$$

We shall prove in the following that ψ_2 is also a local diffeomorphism. Let us denote by $a_{ij} := \frac{\partial \phi_i}{\partial \xi_j}$, for $i, j = 1, \ldots, n-1$ and $a_{in} := \frac{\partial \phi_i}{\partial A}$.

Let us recall below the classic Leibniz rule for differentiating under an integral. Two different proofs can be found for instance in [Fla73] and [Woo26, page 142].

$$\frac{\mathrm{d}}{\mathrm{d}x}\left(\int_{a(x)}^{b(x)} f(x,t)\mathrm{d}t \right) = \int_{a(x)}^{b(x)} \frac{\partial f(x,t)}{\partial x}\mathrm{d}t + f(b(x),x)b'(x) - f(a(x),x)a'(x).$$

Since we need $a_{ij} := \frac{\partial \phi_i}{\partial \xi_j}$, let us first compute $\frac{\partial P(\xi_{i_0})}{\partial \xi_j}$.

If $j \neq i_0$, then

$$\frac{\partial P(\xi_{i_0})}{\partial \xi_j} = A \int_0^{\xi_{i_0}} \frac{\partial}{\partial \xi_j} \prod_i (t - \xi_i)\mathrm{d}t.$$

If $j = i_0$, then

$$\frac{\partial P(\xi_{i_0})}{\partial \xi_{i_0}} = A \int_0^{\xi_{i_0}} \frac{\partial}{\partial \xi_{i_0}} \prod_i (t - \xi_i)\mathrm{d}t + (\xi_{i_0})' \prod_i (\xi_{i_0} - \xi_i) = A \int_0^{\xi_{i_0}} \frac{\partial}{\partial \xi_{i_0}} \prod_i (t - \xi_i)\mathrm{d}t.$$

One has $\frac{\partial}{\partial \xi_j} \prod_k (\xi_k - t)\mathrm{d}t = \prod_{k \neq j} (\xi_k - t) = \frac{P'(t)}{A(\xi_j - t)}$, hence

$$a_{ij} = (-1)^{i-1} \frac{\partial P(\xi_i)}{\partial \xi_j} - \frac{\partial P(\xi_{i-1})}{\partial \xi_j} = (-1)^{i-1} \int_{\xi_{i-1}}^{\xi_i} \frac{P'(t)}{A(\xi_j - t)}\mathrm{d}t.$$

In addition, one has

$$a_{in} = (-1)^{i-1} \frac{\partial P(\xi_i)}{\partial A} - \frac{\partial P(\xi_{i-1})}{\partial A} = \int_0^{\xi_i} \frac{P'(t)}{A}\mathrm{d}t - \int_0^{\xi_{i-1}} \frac{P'(t)}{A}\mathrm{d}t = \int_{\xi_{i-1}}^{\xi_i} \frac{P'(t)}{A}\mathrm{d}t.$$

We argue by contradiction. If we suppose that $\det(a_{ij}) = 0$, then there exist numbers $c_1, \ldots, c_n \in \mathbb{R}^*$ such that $\sum_{j=1}^n c_j a_{ij} = 0$, which is equivalent to

$$\sum_{j=1}^{n-1} \frac{c_j}{A} \int_{\xi_{i-1}}^{\xi_i} \frac{P'(t)}{\xi_j - t}\mathrm{d}t + \frac{c_n}{A} \int_{\xi_{i-1}}^{\xi_i} P'(t)\mathrm{d}t = 0 \Leftrightarrow$$

$$\int_{\xi_{i-1}}^{\xi_i} \left(\sum_{j=1}^{n-1} \frac{c_j}{A} \frac{P'(t)}{\xi_j - t} + \frac{c_n}{A} P'(t) \right) \mathrm{d}t = 0.$$

If we denote by $F(t) := \sum_{j=1}^{n-1} \frac{c_j}{A} \frac{P'(t)}{\xi_j - t} + \frac{c_n}{A} P'(t)$, then the above equality implies that

$$\int_{\xi_{i-1}}^{\xi_i} F(t)\mathrm{d}t = 0. \tag{1.4}$$

In addition, F is a polynomial of degree less or equal to $n-1$.

If one denotes by $g(x) := \int_0^x F(t)\mathrm{d}t$, then $g(0) = 0$; since $\xi_0 = 0$, $g(\xi_1) = 0$, by relation (1.4), $g(\xi_2) = \int_0^{\xi_2} F(t)\mathrm{d}t = \int_0^{\xi_1} F(t)\mathrm{d}t + \int_{\xi_i}^{\xi_2} F(t)\mathrm{d}t = 0, \ldots, g(\xi_n) = 0$, hence g is a polynomial with $\deg g \leq n$ and with at least $n+1$ roots. Clearly, $F \equiv 0$ and

$$\sum_{j=1}^{n-1} \frac{c_j}{A} \frac{P'(t)}{\xi_j - t} + \frac{c_n}{A} P'(t) = 0,$$

for any $t \in \mathbb{R}$. Since in the interior of $(\mathbb{R}_+)^n$ the polynomials $\frac{P'(t)}{\xi_j - t}$, $j = 1, \ldots, n-1$ and $P'(t)$ are linearly independent, one obtains $c_j = 0$, for any $j = 1, \ldots, n$. Thus we obtained a contradiction with $c_j \in \mathbb{R}^*$, $j = 1, \ldots, n$, which proves that the columns of the (a_{ij}) matrix are linearly independent. More precisely, $\det(a_{ij}) \neq 0$, thus ψ_2 is a local diffeomorphism in the interior of $(\mathbb{R}_+)^n$.

In conclusion, ϕ is a local diffeomorphism in the interior of $(\mathbb{R}_+)^n$.

In the following we will prove that $\phi : (\mathbb{R}_+)^n \setminus \{0\} \to (\mathbb{R}_+)^n \setminus \{0\}$ is surjective by applying Lemma 1.28 to a continuous function $\overline{\phi}$.

First, let us denote by $(\mathbb{R}_+^*)^n$ the interior of $(\mathbb{R}_+)^n$. We have proved that ϕ is a local diffeomorphism in the interior of $(\mathbb{R}_+)^n$, thus ϕ is an open map, hence $\phi((\mathbb{R}_+^*)^n)$ is an open set in $(\mathbb{R}_+)^n$.

Secondly, let us compactify the space, by considering the projective homogeneous coordinates with the classical notation $[x_1 : x_2 : \ldots : x_n]$. Let us denote by

$$\mathbb{RP}_+^{n-1} := \{[x_1 : \ldots : x_n] \mid x_i \geq 0, \forall i\}.$$

For $[\delta_1 : \delta_2 : \ldots : \delta_n] \in \mathbb{RP}_+^{n-1}$ and $[\phi_1 : \phi_2 : \ldots : \phi_n] \in \mathbb{RP}_+^{n-1}$, define the map

$$\overline{\phi} : \mathbb{RP}_+^{n-1} \to \mathbb{RP}_+^{n-1}, \overline{\phi}([\delta_1 : \delta_2 : \ldots : \delta_n]) := [\phi_1 : \phi_2 : \ldots : \phi_n].$$

Let us prove that $\overline{\phi}$ is well-defined. If one takes $(\delta_1, \delta_2, \ldots, \delta_n) \in \mathbb{RP}_+^{n-1}$, then

$$\overline{\phi}[\lambda\delta_1 : \lambda\delta_2 : \ldots : \lambda\delta_n] = [\lambda^n\phi_1 : \ldots : \lambda^n\phi_n] = [\phi_1 : \ldots : \phi_n] = \overline{\phi}[\delta_1 : \ldots : \delta_n],$$

hence $\overline{\phi}$ is well-defined.

After a choice of representatives, one can identify $\mathbb{RP}_+^{n-1}$ with $\mathbb{R}_+^n \cap \mathbb{S}_1^{n-1}$, where $\mathbb{S}_1^{n-1} := \{x \in \mathbb{R}^n \mid \|x\| = 1\}$ is the unit $(n-1)$-sphere. Thus $\mathbb{RP}_+^{n-1}$ is compact, being homeomorphic to the intersection between a closed set and a compact set.

Apply in the sequel Lemma 1.28 to the continuous function $\overline{\phi}$.

Let us denote by $\mathbb{S}_+^{n-1} := \mathbb{S}_1^{n-1} \cap \{(x_1, \ldots, x_n) \mid x_i \geq 0\}$ and by $O := \operatorname{Int} \mathbb{S}_+^{n-1}$, thus

$$O = \mathbb{S}_1^{n-1} \cap \{(x_1, \ldots, x_n) \mid x_i > 0\}.$$

By the induced topology, $\overline{\phi}(O)$ is an open set of $\mathbb{S}_+^{n-1}$. The nonempty set O is dense and connected in $\mathbb{S}_+^{n-1}$. In addition, we have $O \subset \mathbb{S}_+^{n-1} \setminus \overline{\phi}(\partial O) = \mathbb{S}_+^{n-1} \setminus \overline{\phi}(\mathbb{S}_+^{n-1} \setminus O)$. Thus by Lemma 1.27, we conclude that the set $\mathbb{S}_+^{n-1} \setminus \overline{\phi}(\mathbb{S}_+^{n-1} \setminus O)$ is dense and connected.

To conclude, we proved that all the hypotheses of Lemma 1.28 are satisfied hence $\overline{\phi}$ is surjective. Hence ϕ is surjective and thus the proof of the existence of a polynomial associated to $(\phi_1, \ldots, \phi_n)$ is completed.

□

REMARK 1.32. A similar proof to the one of Davis' can be found in [Dou97, page 17], where Douady gave a proof of existence for polynomials of degree 4 and a sketch of the proof for the general case. For more references, see [Myc70, page 853].

1.4 Basic notions about graphs and trees

1.4.1 Standard vocabulary for graphs and trees

This subsection is meant to present briefly **standard terminology** for graphs and trees. Whoever is already familiar with these notions, is invited to go to Subsection 1.4.2.

Intuitively, a graph represents a collection of vertices and of edges such that each edge connects two vertices. For a detailed description of graphs and for the basic terminology, the reader is invited to refer to [Gos09], which represents the main source for the standard notions we introduce in what follows. Other useful sources are [PP01], [Die10], [Bol98], [Tut84], [BM08], [Tru93].

Definition 1.33. [Gos09, page 592] A **graph** $G = (V, E, \varphi)$ consists of a nonempty finite set of **vertices** V, a finite set of **edges** E and an incidence function φ that maps edges to unordered pairs of vertices. If the two vertices in the unordered pair are the same vertex, then the edge is called a **loop**.

Definition 1.34. [Die10] The **valency** of a vertex v is the number of edges of v.

Definition 1.35. [Gos09, pages 600-601] A nonempty sequence of alternating vertices and edges of the form

$$(a_1, e_1, a_2, e_2, \ldots, e_{n-1}, a_n),$$

with $n \geq 1$ and the edge e_i connecting the vertices a_i et a_{i+1} is called a **walk**.

The **length** of a walk is the number of its edges.

A **trail** is a walk with no repeated edges.

A **path** is a walk with no repeated vertices.

A walk is **closed** if it has length of at least one and its endpoints are the same vertex.

A **circuit** is a closed trail.

A **cycle** is a circuit in which the endpoints are the only repeated vertices.

Definition 1.36. [Gos09, page 601] A graph $G = (V, E, \varphi)$ is **connected** if it has only one vertex or if there is a walk in G between every pair of distinct vertices.

In the following and more restrictive definition, one can observe that loops and multiple edges between two vertices are not allowed to appear in the well-known notion of simple graph.

Definition 1.37. [Gos09, page 592] A **simple graph** $G = (V, E, \varphi)$ consists of a nonempty finite set of vertices V, a finite set of edges E and an injective incidence function φ that maps edges to unordered pairs of distinct vertices.

When we name a walk of a simple graph, we shall only list its vertices (it is not necessary to include the edges, since the reader can deduce them from the notation).

Definition 1.38. [Gos09, page 602] Two distinct vertices u and v are **adjacent** if there exists an edge e such that $\varphi(e) = \{u, v\}$.

Example 1.39. In Figure 1.7 (inspired from [Gos09, Example 10.8, page 601]), the graph contains several walks. For instance, the walk $abdedc$ has length 5. Moreover, $abdca$ is a closed walk. The walk $acdfg$ is both a trail and a path. An example of cycle is hh, while $dbhhed$ is a circuit. Finally, $hegfdeh$ is a trail which is neither a path, nor a circuit.

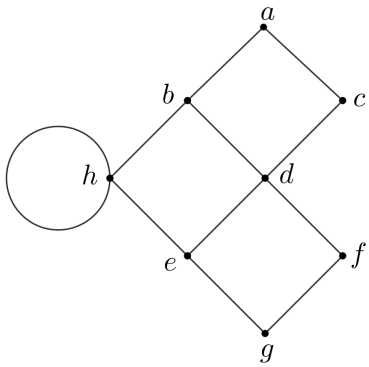

Figure 1.7: Walks, trails, paths, circuit, cycles.

We will be particularly interested in the following class of simple graphs.

Definition 1.40. [Gos09, page 673, Chapter 11] **A tree** is a connected graph without cycles. A **rooted tree** is a tree endowed with a base vertex, called its **root**.

Remark 1.41. As a consequence of Definition 1.40, trees have no loops, nor multiple edges.

Theorem 1.42. *[Gos09, page 668] A connected simple graph is a tree if and only if it contains a unique path between any two vertices.*

Theorem 1.42 can be seen as a characterisation of trees. Its proof is given in [Gos09, page 668].

Definition 1.43. [Ser80, Section 2.2, page 18] A **geodesic** between two vertices of a tree is the shortest path between the two vertices.

Remark 1.44. In this section, our convention is to draw the root on the top of the tree.

Example 1.45. A geodesic is shown in Figure 1.8 below.

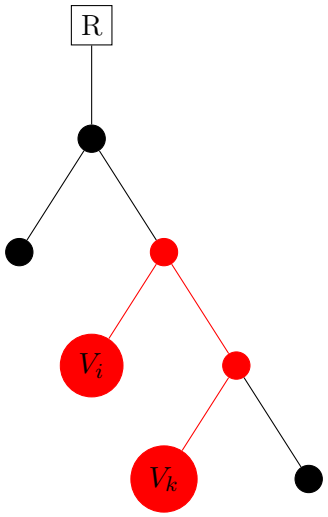

Figure 1.8: Geodesic in a tree, between the vertices V_i and V_k.

Definition 1.46. [Gos09, page 669]

(a) In a rooted tree, the length (i.e. the number of edges) of the geodesic from the root to a vertex is called the **level** of the vertex. The root is at level zero.

(b) A vertex p of a rooted tree is called the **parent** of a vertex c if p and c are adjacent and the level of c is one plus the level of p. We say then also that c is a **child** of p. We call **ancestor** of a vertex c every vertex on the path from c to the root (excluding c but including the root). The vertex c is said to be a **descendant** of each of its ancestors. Two vertices are called **siblings** if they have the same parent.

(c) In a rooted tree, a vertex is called a **leaf** if it has no children. A vertex that is not a leaf, i.e. it has children, is said to be an **internal vertex**.

(d) Let v be a vertex of the rooted tree $\mathcal{T}$. The **subtree of $\mathcal{T}$ rooted at** v is the tree consisting of all the descendants of v in $\mathcal{T}$, including v itself.

1.4.2 Non-standard vocabulary for trees

Here we present some non-standard terminology that we need in this thesis.

Definition 1.47. A **real oriented plane** is a topological surface which is oriented and homeomorphic to $\mathbb{R}^2$.

Remark 1.48. The following definition is inspired from [Tru93, Section 3] and [Gos09, page 624]. Note the difference between the notion of planar tree (can be embedded in a real plane) and plane tree (it is embedded in a real plane).

Definition 1.49. A **plane tree** is a tree which is embedded in a real oriented plane without edge crossings.

Remark 1.50. One can also give the following abstract characterisation of plane trees: plane trees are abstract ordered trees, in the sense that each vertex has a cyclic order of the edges adjacent to it (see [Knu05, page 308]). Any embedding of a rooted tree in an oriented plane gives the order of children for each vertex: from left to right, for instance (see [Wi]). Note that, to give an abstract order on a rooted tree is the same as cyclically ordering the set of children of the root and totally ordering the set of children of any other vertex.

Example 1.51. Two different embeddings of the same abstract rooted tree in the real plane are shown in Figure 1.9.

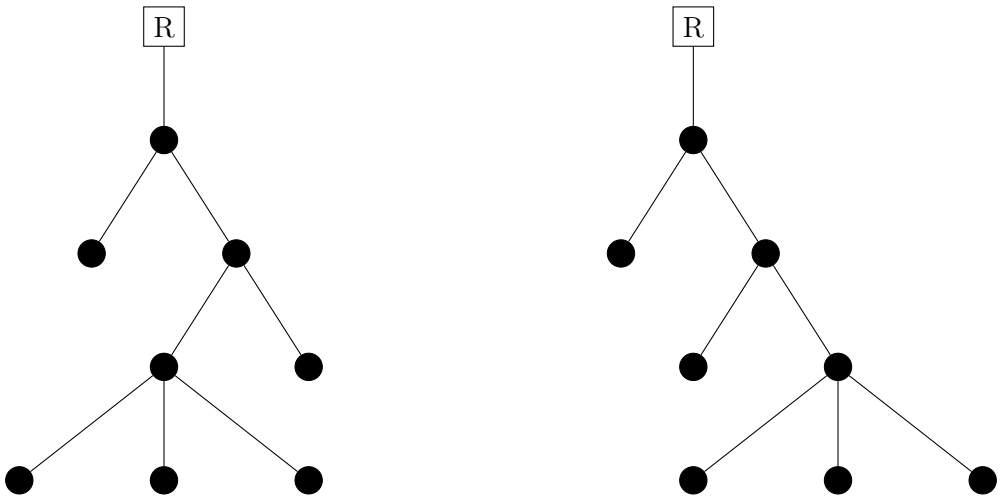

Figure 1.9: Two different embeddings of the same abstract rooted tree.

Definition 1.52. [AF08, page 410] Let $\mathcal{T}_1$ and $\mathcal{T}_2$ be two different embeddings of the same tree in a real oriented plane $\mathcal{P}$. We say that the two embeddings are **equivalent** if there exists an orientation preserving homeomorphism ϕ from $\mathcal{P}$ to $\mathcal{P}$ such that $\phi(\mathcal{T}_1) = \mathcal{T}_2$ and the image of the root of $\mathcal{T}_1$ is the root of $\mathcal{T}_2$.

Definition 1.53. [Gos09, page 670] A **binary tree** is a rooted tree in which every vertex has at most two children.

The following definition is inspired from [Sta12, page 24], [Sta10, page 7].

Definition 1.54. A plane binary tree is called **complete** if the root and the internal vertices have each exactly two children.

Example 1.55. In Figure 1.10 we present a plane binary tree which is not complete, while in Figure 1.11 a complete binary tree is shown.

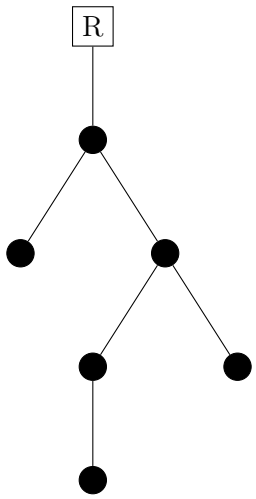

Figure 1.10: A plane binary tree which is not complete.

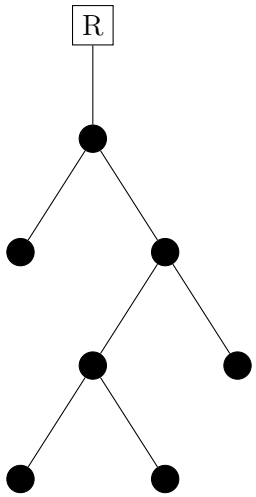

Figure 1.11: A plane complete binary tree.

REMARK 1.56. We provide below a recursive definition of the set of complete plane binary trees (inspired from [Knu05, page 308]). We need two steps in order to define it. The first step is the basic one: we specify an initial collection of elements of the set. The second step is the recursive one: we give a rule to form new elements from those already known to be in the set.

The advantage of using the recursion for this definition lies in the fact that we shall need a structural induction (see [Sha]) for the proof of Proposition 1.141. The set of **complete plane binary trees** is defined recursively as follows:

(a) the tree consisting of a single vertex is a complete plane binary tree whose root is itself.

(b) if $\mathcal{T}_1$ and $\mathcal{T}_2$ are disjoint complete plane binary trees whose roots are $\mathcal{R}_1$ and $\mathcal{R}_2$ respectively, let us denote by $\mathcal{T}$ the tree consisting of a root $\mathcal{R}$ with edges connecting $\mathcal{R}$ to the roots $\mathcal{R}_1$ and $\mathcal{R}_2$ such that $\mathcal{T}_1$ is the left subtree and $\mathcal{T}_2$ is the right subtree. Then $\mathcal{T}$ is also a complete plane binary tree.

EXAMPLE 1.57. In Figure 1.12, one can observe the recursive step in the construction of a complete plane binary tree: the new root is in red and it has as children the two given trees, in green and in blue.

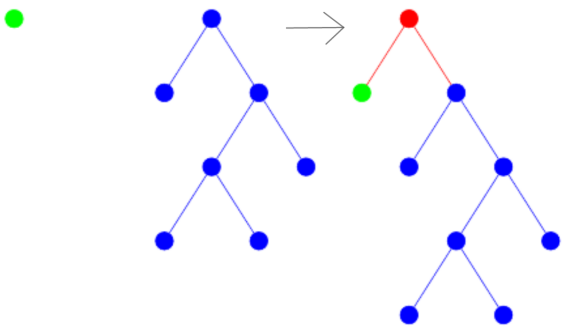

Figure 1.12: The recursive construction of a complete plane binary tree.

The following terminology of end-rooted tree is inspired from [GBGPPP18, Definition 3.6].

Definition 1.58. An **end-rooted rooted tree** is a rooted tree whose root has exactly one neighbour.

Example 1.59. In Figure 1.13, let us observe the root (R), the internal vertices (IV), the leaves (L), vertices that are parents (P), left children (LC), right children (RC) and in red a subtree of the initial tree.

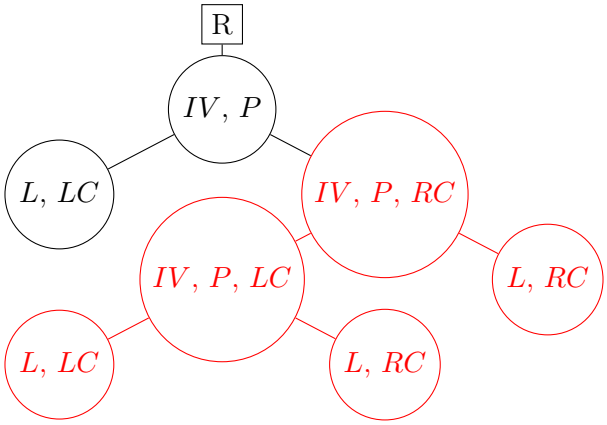

Figure 1.13: Vocabulary for the elements of an end-rooted complete plane binary tree.

Remark 1.60. The terminology of **left** child, respectively **right** child is motivated by our convention of drawing the root on the top of the tree.

1.5 Snake-trees

Definitions 1.61 and 1.63 are inspired from Stanley's survey [Sta10, page 7].

Definition 1.61. A rooted plane tree with m vertices is called **a decreasing tree** (respectively **an increasing tree**) if each vertex is decorated by a different number of $\{1, 2, \ldots, m\}$, such that any sequence of numbers formed by any geodesic starting from the root is a strictly decreasing sequence (respectively a strictly increasing sequence).

Example 1.62. A decreasing tree is shown in Figure 1.14 below.

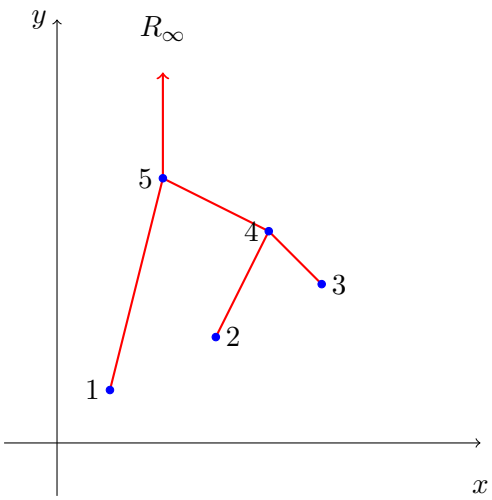

Figure 1.14: A decreasing tree.

In the sequel, we show that to any $(n-1)$-snake σ we can associate a complete binary decreasing tree, denoted by $\mathcal{T}(\sigma)$, using an idea from [Sta10].

Definition 1.63. Let us consider an $(n-1)$-snake

$$\sigma = \begin{pmatrix} 1 & 2 & \dots & n-1 \\ \sigma(1) & \sigma(2) & \dots & \sigma(n-1) \end{pmatrix}$$

such that $\sigma(n-2) > \sigma(n-1)$.

We call **snake-tree associated to** σ and we denote by $\mathcal{T}(\sigma)$, the end-rooted complete plane binary decreasing tree constructed recursively as follows:

(a) if σ is empty (i.e. $n \leq 1$) then set $\mathcal{T}(\sigma) = \emptyset$ and the algorithm stops;

(b) find the position j such that $\max\{\sigma(i) \mid i = 1, \dots, n-1\} = \sigma(j)$;

(c) create a vertex decorated with σ_j and having the coordinates $(j, \sigma(j))$; add an edge from it to the previous vertex added (if any);

(d) the alternating sequence associated to the given snake σ can now be uniquely decomposed in the form

$$\sigma = \begin{pmatrix} 1 & 2 & \dots & j-1 & j & j+1 & \dots & n-1 \\ \sigma(1) & \sigma(2) & \dots & \sigma(j-1) & \sigma(j) & \sigma(j+1) & \dots & \sigma(n-1) \end{pmatrix},$$

where we denote by α the alternating sequence situated to the left of the j-th position:

$$\alpha := \begin{pmatrix} 1 & 2 & \dots & j-1 \\ \sigma(1) & \sigma(2) & \dots & \sigma(j-1) \end{pmatrix}$$

and by β the alternating sequence situated to the right of the j-th position:

$$\beta := \begin{pmatrix} j+1 & j+2 & \dots & n-1 \\ \sigma(j+1) & \sigma(j+2) & \dots & \sigma(n-1) \end{pmatrix}$$

Apply recursively the above construction for the alternating sequences α and β.

In the end, fix a root denoted R_∞ and having the coordinates (j, n); note that when we draw the tree, we shall draw the root at the top.

This algorithm yields an inductive definition of the snake-tree. In the case of odd degree polynomials, at some point the left sequence is empty; by convention, the vertex added to $\mathcal{T}(\rho)$ will be decorated with $-\infty$ and the coordinates of this vertex will be $(0,0)$; in addition, the edge which connects the $-\infty$ vertex to the rest of the tree is symbolized by an arrow.

EXAMPLE 1.64. For the snake

$$\rho := \begin{pmatrix} 1 & 2 & 3 & 4 & 5 \\ 1 & 5 & 2 & 4 & 3 \end{pmatrix},$$

we find the biggest entry 5, and obtain the left sequence (1) and the right sequence $(2,4,3)$. By following the algorithm from Definition 1.63 and adding the nodes in the snake-tree $\mathcal{T}(\rho)$, we obtain:

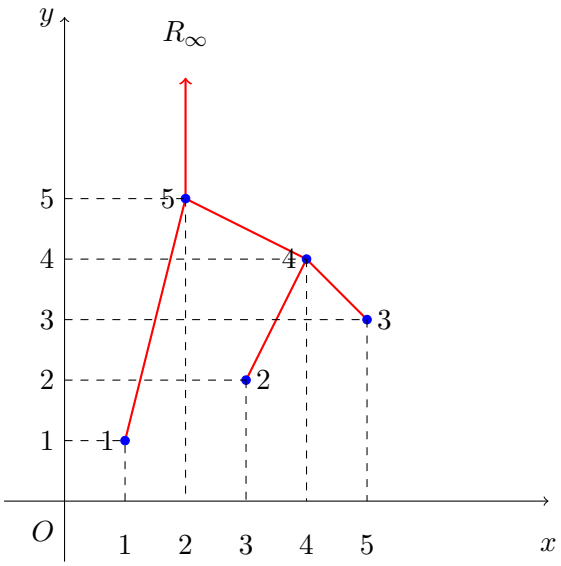

Figure 1.15: The snake-tree of a snake with odd number of entries.

EXAMPLE 1.65. For the snake $\sigma := (6,1,4,2,5,3)$, we find the biggest entry 6, and obtain the empty left sequence $\emptyset$ and the right sequence $(1,4,2,5,3)$. By following the algorithm from Definition 1.63 and adding the vertices in the snake-tree $\mathcal{T}(\sigma)$, we obtain:

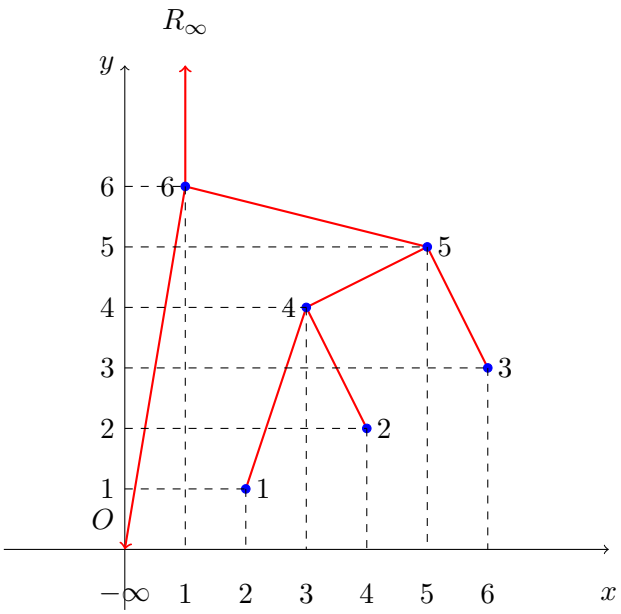

Figure 1.16: The snake-tree of a snake with even number of entries.

REMARK 1.66. The above mentioned construction gives us a tree with the following properties:

(a) it is rooted: the root is always connected by an edge to the highest vertex; by convention, we fix the y-coordinate of the root to be a real number bigger than n;

(b) it is binary: each time we separate in left and right, thus each vertex has at most two children;

(c) it is complete: by convention, if needed we add the vertex $-\infty$, such that each vertex has exactly two children;

(d) it is plane: as we prove in Lemma 1.67 below.

Lemma 1.67. *The snake-tree is embedded in the real plane.*

Proof. All the vertices of the snake-tree are distinct, since the snake is a permutation. By recursion, at each step of the construction (see Definition 1.63) we create a subtree to the left and a subtree to the right, each with descending edges, thus the open edges do not intersect. □

REMARK 1.68. The algorithm used in Definition 1.63 to construct the snake-tree is similar to the one described by Stanley in [Sta10, Section 3.1, page 7] and [Sta12, page 23].

Proposition 1.69. *There is a bijection between the set of snakes and the set of snake-trees.*

Proof. Let us show that the algorithm given in Definition 1.63 provided us a bijection $\mathcal{T}$.

• Let us first prove that $\mathcal{T}$ is injective. Consider two different n-snakes σ and τ. Therefore there exists $i \in 1, \ldots, n$ such that $\sigma(i) \neq \tau(i)$. Let us construct using the algorithm in Definition 1.63 the trees $\mathcal{T}(\sigma)$ and $\mathcal{T}(\tau)$. By construction, there exists a vertex $(i, \sigma(i))$ in $\mathcal{T}(\sigma)$ which is different than the vertex $(i, \tau(i))$ in $\mathcal{T}(\tau)$, thus $\mathcal{T}(\sigma) \neq \mathcal{T}(\tau)$.

• Let us prove the surjectivity. Let T be an end-rooted complete plane binary decreasing tree with n vertices (see Definition 1.61). Namely, each vertex v is labelled with a different number of $\{1, \ldots, n\}$, denoted by $p(v)$ such that any sequence of numbers read along a geodesic starting

from the root is a strictly decreasing sequence. We shall give a second label to each vertex, using the following depth-first inspired algorithm (see Figure 1.17).

BEGIN

-Let $N := 0$.

-Start visiting the vertices of the tree, from the root.

-If the vertex v visited is a leaf, then put $N := N + 1$ and $q(v) := N$, then go one step up and visit its parent.

-If the vertex v visited is an internal vertex, then

(a) if you have not labelled its left subtree, go visit its left child. Repeat the step until you find a leaf.

(b) if you have already labelled its left subtree, then put $N := N + 1$ and $q(v) := N$,then go visit its right child.

END

Therefore each vertex v of T has two labels, namely $p(v)$ and $q(v)$. Construct the snake as follows. For each vertex v, put $\sigma(q(v)) := p(v)$. Thus for each end-rooted complete plane binary decreasing tree T, there exists a snake σ such that T is the snake-tree of σ. Thus the function $\mathcal{T}$ is surjective.

In conclusion, $\mathcal{T}$ is a bijection. □

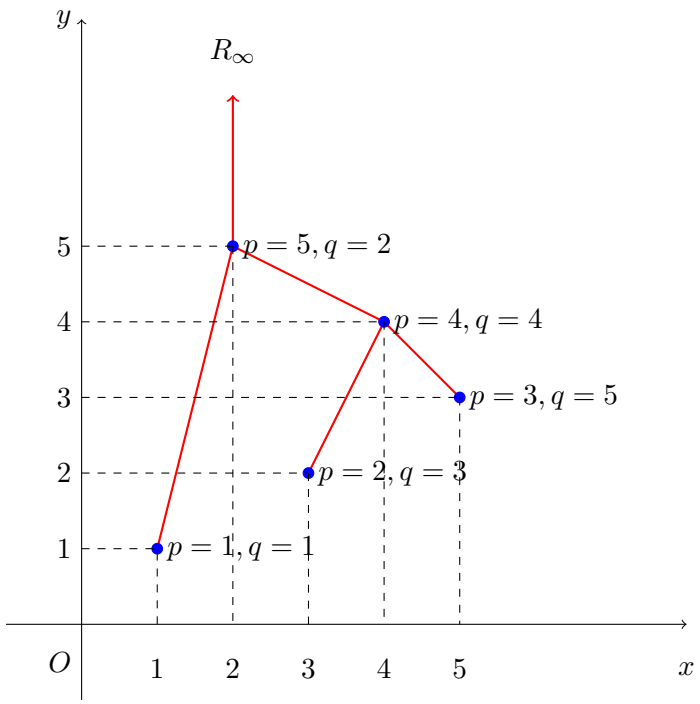

Figure 1.17: The second label $q(v)$ to each vertex v, following a depth-first type algorithm.

1.6 The Poincaré-Reeb tree of a one variable polynomial

REMARK 1.70. In the sequel we define the Poincaré-Reeb tree for one variable polynomials. In this chapter we will call it shortly the Poincaré-Reeb tree. However, in the next chapter we will introduce the Poincaré-Reeb tree for polynomials in two variables. We will call those also Poincaré-Reeb trees, if there is no confusion in the context.

Definition 1.71. [AB06, page 8] Let $P : \mathbb{R} \to \mathbb{R}$ be a one variable polynomial function. The **epigraph** of P is the following unbounded semialgebraic subset of $\mathbb{R}^2$, situated above or on the graph of P :

$$\text{epi}_P := \Big\{(x, y) \in \mathbb{R}^2 \mid y \geq P(x)\Big\} \subset \mathbb{R}^2.$$

Let $y : \mathbb{R}^2 \to \mathbb{R}$ be the second projection.

Definition 1.72. We say that two points in the real plane, say (x, y) and (x', y') are equivalent, denoted by $(x, y) \sim (x', y')$ if and only if they belong to the same connected component of a fibre of the restriction of y to epi_P.

Denote by $[(x, y)]$ the equivalence class of the point $(x, y) \in \mathbb{R}^2$.

We take the quotient space $\mathbb{R}^2/_\sim$ given by $\sim$, with the natural quotient topology. Denote by $q : \mathbb{R}^2 \to \mathbb{R}^2/_\sim$ the quotient map. The function y being constant on equivalence classes, it descends to the quotient, and this is what we call $\tilde{y}$. By [Wil70, Theorem 9.4], the function $\tilde{y} : \mathbb{R}^2/_\sim \to \mathbb{R}$ makes the diagram from Figure 1.18 commute and it is continuous.

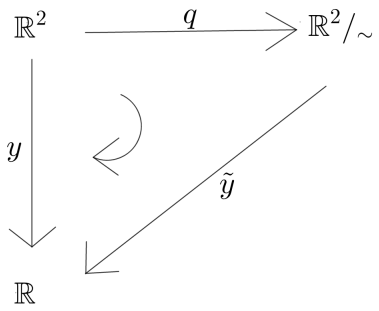

Figure 1.18: The quotient space $\mathbb{R}^2/_\sim$

Definition 1.73. The image of the epigraph of $P(x)$, by the quotient map q, namely

$$\mathcal{R} := q(\text{epi}_P)$$

is called **the Poincaré-Reeb tree of a one variable polynomial** P (see Figure 1.19).

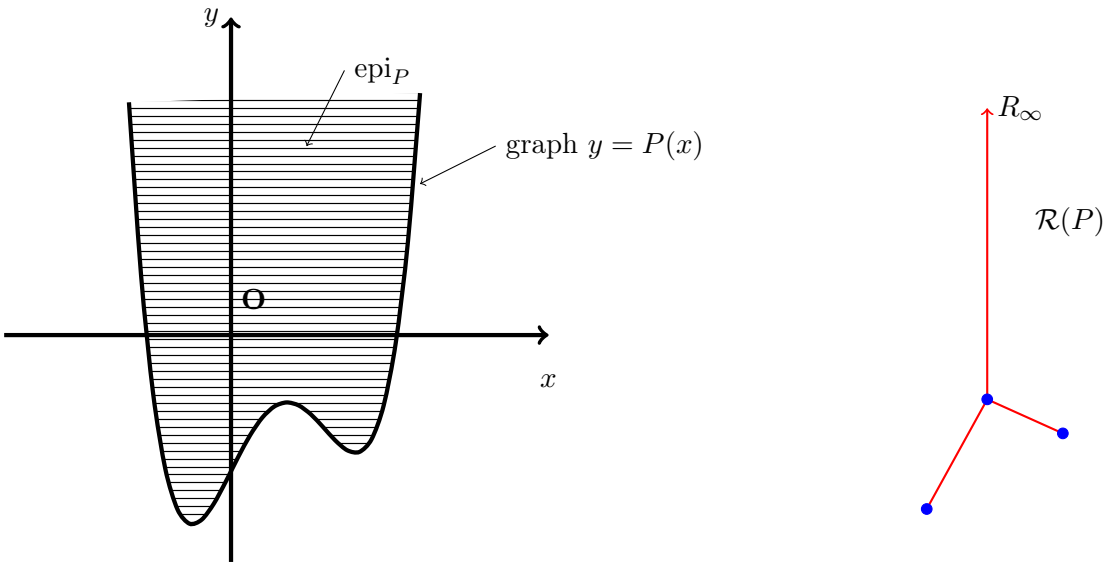

Figure 1.19: The epigraph and the Poincaré-Reeb tree $\mathcal{R}(P)$ of an n-Morse polynomial P when the degree n is even.

The Poincaré-Reeb tree is a tree embedded in the real plane. The vertices of this tree correspond to the critical points of the polynomial. We shall prove this in more detail and in a more general setting in Chapter 2 (see Subsection 2.4.1).

Proposition 1.74. *The Poincaré-Reeb tree of P, is a rooted plane tree such that the function $\tilde{y}$ is decreasing on each of the geodesics starting from the root.*

Remark 1.75. By convention, the root r is situated in the real plane, such that its $y-$coordinate approaches infinity. We shall always draw the root in the real plane, by choosing its $y-$coordinate bigger than all the critical values of $P(x)$.

Remark 1.76. In the sequel, we shall only study the Poincaré-Reeb tree of P, where P is an n-Morse polynomial (see Definition 1.14).

Remark 1.77. Both in the case of an odd degree polynomial P and in the case of an even degree polynomial P, we add to its Poincaré-Reeb tree a supplementary vertex denoted by R_∞ which is marked by an arrow and is called the **root**; this symbolises the fact that the edge should be infinite and corresponds to $\lim_{y\to+\infty} \pi^{-1}(y)$. In addition, since the Poincaré-Reeb tree of an odd degree polynomial P verifies $\lim_{x\to-\infty} P(x) = -\infty$ (because we only consider Morse polynomials (see Definition 1.14), which are monic by definition), we add a supplementary vertex to $\mathcal{R}(P)$, namely the vertex corresponding to $\lim_{y\to-\infty} \pi^{-1}(y)$; we mark it by an arrow to symbolise that the edge should be infinite (see Figure 1.20). In this way, the Poincaré-Reeb tree $\mathcal{R}$ is an end-rooted complete plane binary tree.

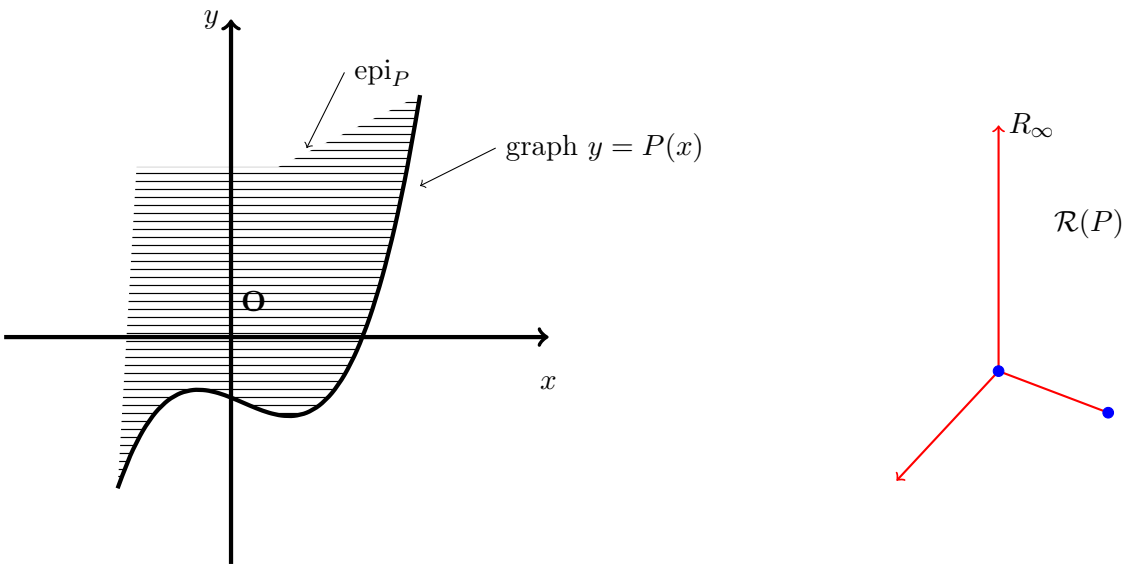

Figure 1.20: The epigraph and the Poincaré-Reeb tree $\mathcal{R}(P)$ of an n-Morse polynomial P when the degree n is odd.

Let us present a more complicated example in Figure 1.21 below.

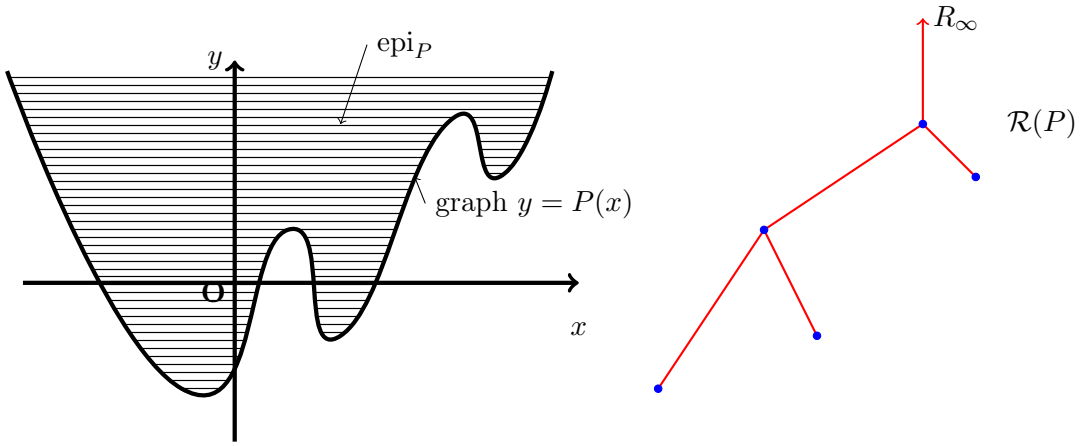

Figure 1.21: The epigraph and the Poincaré-Reeb tree $\mathcal{R}(P)$ of a 6-Morse polynomial.

Lemma 1.78. *The Poincaré-Reeb tree of an n-Morse polynomial is a tree whose vertices are in a total order relation given by the induced application $\tilde{y} := y$ (see Definition 1.73), such that this total order is strictly decreasing on any geodesic going from the root to the leaves.*

Proof. Recall from Definition 1.73 that $\tilde{y}$ denotes the quotient of y, defined on the plane in which lives the Poincaré-Reeb tree. Restrict it to this tree.

The order between the vertices is given by the values of $\tilde{y}$ on the vertices. Since the polynomial is n-Morse (see Definition 1.14), it has pairwise distinct critical values, thus it is a total order relation. □

Corollary 1.79. *The Poincaré-Reeb tree $\mathcal{R}(P)$ is a decreasing tree.*

Proposition 1.80. *Let us consider an n-Morse polynomial $P : \mathbb{R} \to \mathbb{R}$. If $\sigma(P)$ is the snake associated to P, $\mathcal{T}(\sigma(P))$ is its snake-tree and $\mathcal{R}(P)$ is the Poincaré-Reeb tree of P, then the*

snake-tree $\mathcal{T}(\sigma(P))$ *is isomorphic to the Poincaré-Reeb tree* $\mathcal{R}(P)$*:*

$$\mathcal{T}(\sigma(P)) \simeq \mathcal{R}(P).$$

Proof. By construction (see Definition 1.63) the snake tree is a decreasing tree. Similarly, by Corollary 1.79, the Poincaré-Reeb tree is a decreasing tree. In addition, the vertical total order between the vertices of the Poincaré-Reeb tree is the same as the one between the vertices of the snake-tree, since these orders are both given by the critical values of the n-Morse polynomial P. Similarly, the horizontal total orders are the same in both trees. □

In other words, we can identify (up to a tree isomorphism) the snake-tree of P and the Poincaré-Reeb tree of the epigraph of P.

Corollary 1.81. *There is a bijection between the set of snakes and the set of Poincaré-Reeb trees of one variable Morse polynomials, up to isomorphism.*

Proof. This follows from Proposition 1.80 and Proposition 1.69. □

In Figure 1.22 below, we can see a Poincaré-Reeb tree in one variable and its unique corresponding snake.

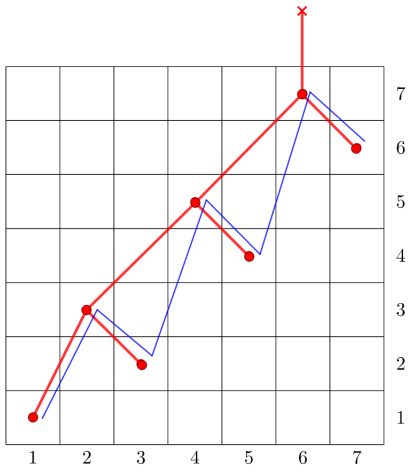

Figure 1.22: A Poincaré-Reeb tree in one variable and its corresponding snake.

1.7 The contact tree

QUESTION 1.82. Given a snake σ, is it possible to construct a Morse polynomial $Q : \mathbb{R} \to \mathbb{R}$ that realises σ?

While we know (see Theorem 1.25) that the existence of such a Morse polynomial is proven, the goal of this chapter is to give a *constructive* answer, for a special class of snakes, i.e. in the case of separable snakes. The contact tree, described in the next sections, plays a key role in our construction.

1.7.1 Notations

In this subsection we will set up notations and terminology.

Definition 1.83. Let $P \in \mathbb{R}[x]$ and $Q \in \mathbb{R}[x]$ be two polynomials. We say that **the polynomial P is smaller than the polynomial Q to the right**, denoted by $P \prec_+ Q$, if and only if one has $P(x) < Q(x)$ for any sufficiently small $0 < x \ll 1$, that is to say there exists $x_0 > 0$ such that for any $0 < x < x_0$, one has $P(x) < Q(x)$.

Let us consider the monic polynomial $P_x(y) \in \mathbb{R}[x][y]$, such that

$$P_x(y) := \prod_{i=1}^{m+1} (y - a_i(x)) \in \mathbb{R}[x][y], \tag{1.5}$$

where $m \in \mathbb{N}$, the roots $a_i(x) \in \mathbb{R}[x]$ for any $i = 1, \dots, m+1$ and

$$a_1(x) \prec_+ a_2(x) \prec_+ \dots \prec_+ a_{m+1}(x), \tag{1.6}$$

as one can see in Figure 1.23 below.

In what follows we denote by

$$\mathcal{A} := \{a_1(x), \dots, a_{m+1}(x)\} \tag{1.7}$$

the set of roots of $P_x(y)$.

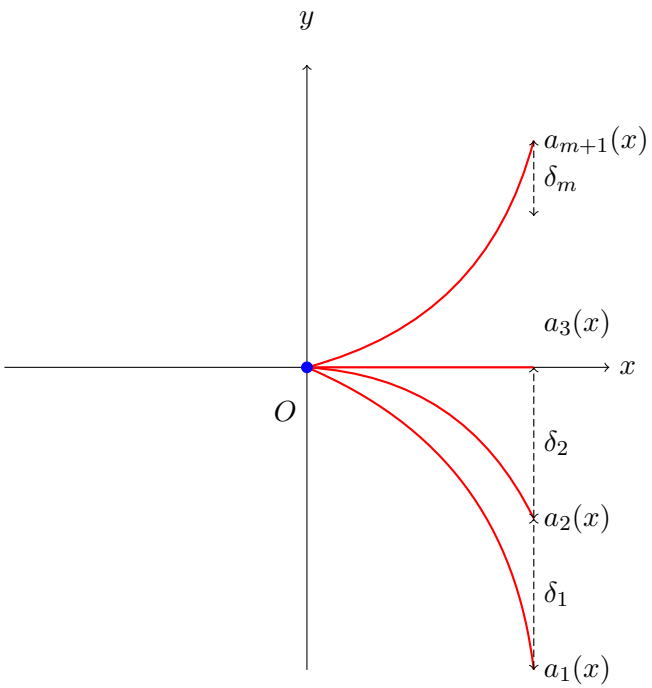

Figure 1.23: The roots of $P_x(y)$, ordered.

The following definition is well-known:

Definition 1.84. Let $a(x) = b_0 + b_1 x + b_2 x^2 + \dots$ be a polynomial. The **valuation** of a at 0, denoted by $\nu_x(a)$, is the smallest integer $k \geq 0$ such that $b_k \neq 0$. By convention, the valuation of the zero polynomial is ∞.

In the sequel, we will consider only polynomials a_i such that $\nu_x(a_i) \geq 1$, i.e. $a_i(0) = 0$, for any $i = 1, \dots, m+1$.

Definition 1.85. For any $i = 1, \dots, m$, the difference

$$\delta_i(x) := a_{i+1}(x) - a_i(x)$$

is called the **gap** between $a_{i+1}(x)$ and $a_i(x)$.

REMARK 1.86. Note that by the initial hypothesis (1.6), one has $0 \prec_+ \delta_i(x)$, for any $i = 1, \dots, m$.

Definition 1.87. For any $i = 1, \dots, m$, the number

$$\mathrm{S}_i(x) := \left| \int_{a_i(x)}^{a_{i+1}(x)} P_x(y)\mathrm{d}y \right|$$

is called **the i-th area**.

This section is intended to construct a polynomial P that realises a given configuration of areas S_i. More precisely, we want the following equivalence to hold for any $i \neq j$:

$$\delta_i \prec_+ \delta_j \Leftrightarrow \mathrm{S}_i \prec_+ \mathrm{S}_j,$$

as in Figure 1.24 below.

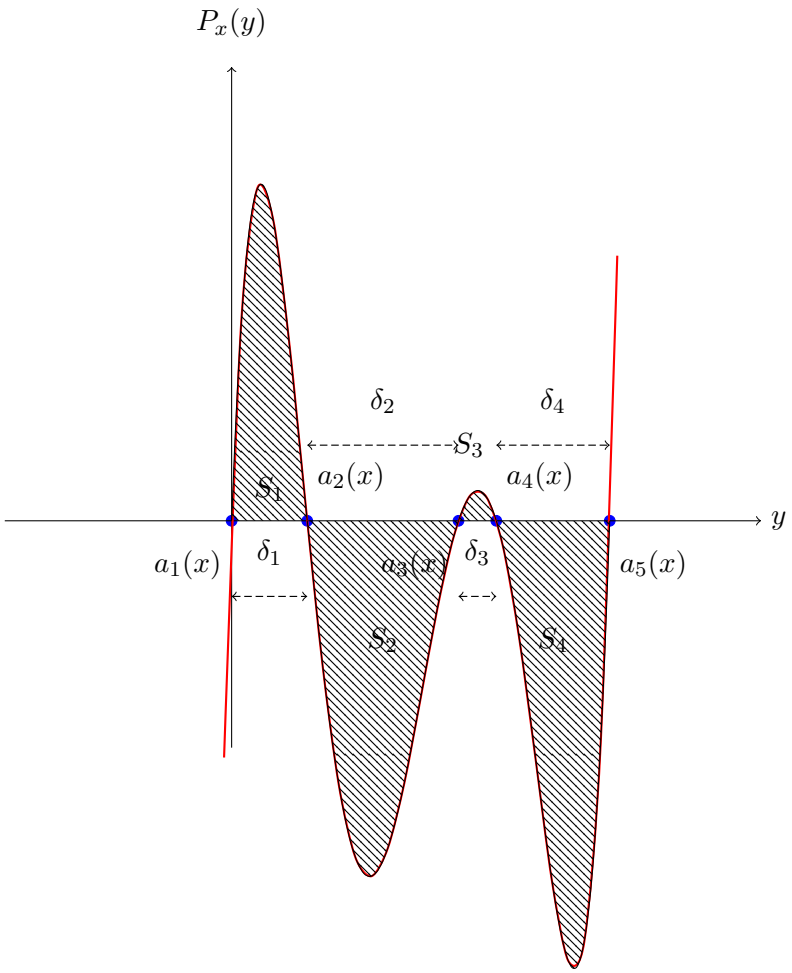

Figure 1.24: A given configuration of areas S_i.

Definition 1.88. Let us consider a sufficiently small $0 < x \ll 1$. From now on, e_i stands for the valuation of each δ_i, namely

$$e_i := \nu_x(\delta_i) \in \mathbb{N}.$$

1.7.2 Construction of the contact tree

In order to study the type of contact between the polynomials $a_i(x)$ (the roots of the polynomial $P_x(y)$) for a sufficiently small $x > 0$, we shall now define a combinatorial object, which takes the form of a tree with numerical information attached. In the sequel we give a constructive definition of this object called **the contact tree**.

REMARK 1.89. The notion of contact tree is inspired from **the Eggers-Wall tree** (see [GBGPPP18, Section 4.3], [Wal04, page 75, Section 4.2]). Our definition of the contact tree agrees with the one given by Ghys in [Ghy17, pages 27-28], [Ghy13] and with the one in [Kap93, Section 3, Definition 3.5, pages 131-132], where Kapranov called it **the Bruhat-Tits tree**.

Let us first start with some examples, making Definition 1.92 easier to understand.

EXAMPLE 1.90. Let us consider Figure 1.25 and let us study the contact tree of the following three polynomials in x:

$$a_1(x) := x^1 + x^2 + x^4 + x^5 + 2x^6 + \dots$$
$$a_2(x) := x^1 + x^2 + 2x^4 + x^5 + x^6 + \dots$$
$$a_3(x) := x^1 + x^2 + x^3 + 3x^4 + x^5 + \dots.$$

For sufficiently small $x > 0$, the three polynomials are ordered increasingly: $a_1(x) \prec_+ a_2(x) \prec_+ a_3(x)$. One obtains $\nu_x(a_2(x) - a_1(x)) = 4$ and $\nu_x(a_3(x) - a_2(x)) = 3$.

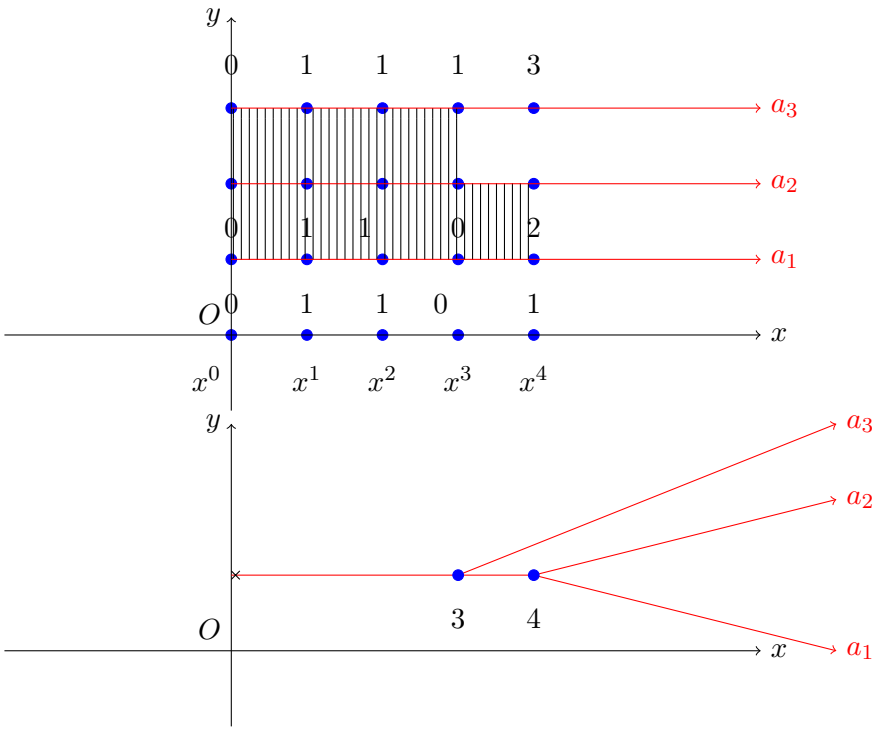

Figure 1.25: Example of the rooted, oriented, embedded contact tree of three polynomials in x: $a_1(x)$, $a_2(x)$ and $a_3(x)$ given in Example 1.90.

EXAMPLE 1.91. An example of the construction of the contact tree of two given polynomials

$$a_1 := m_0 x^0 + m_1 x^1 + \dots + m_k x^k + \dots$$

and

$$a_2 := n_0x^0 + n_1x^1 + \ldots + n_kx^k + \ldots,$$

where $m_i = n_i$, for $i = 1, \ldots, k-1$ and $m_k < n_k$ is shown in Figure 1.26 below. Let us observe that the relation $m_k < n_k$ gives the order of the two polynomials: $a_1 \prec_+ a_2$.

The construction consists of identifying the points of the real plane up to the point where the contact of the corresponding polynomials ends and the respective coefficients of the two polynomials are starting to differ.

More precisely, if we consider the xOy coordinate system in the real plane, then let each polynomial a_i, $i = 1, 2$ be represented by the semi-straight line $(y = i) \cap (x > 0)$ in the first quadrant $\mathbb{R}^2_+$. The line is called the a_i-axis.

The point of coordinate $(\ell, 0)$ on the Ox axis corresponds to the monomial x^ℓ. On each a_i-axis a point (ℓ, i) is decorated with the coefficient corresponding to the monomial x^ℓ, as it appears in the polynomials a_i.

In this example, the valuation $\nu_x(a_2(x) - a_1(x)) = k$. Let us now identify the points of the first quandrant situated between $a_2(x)$ and $a_1(x)$, up to the point $x = k$, where the two polynomials separate.

As one can see, the vertices of the tree are only the root, the bifurcation vertex and the two leaves. By construction, the contact tree is rooted, embedded in the real plane.

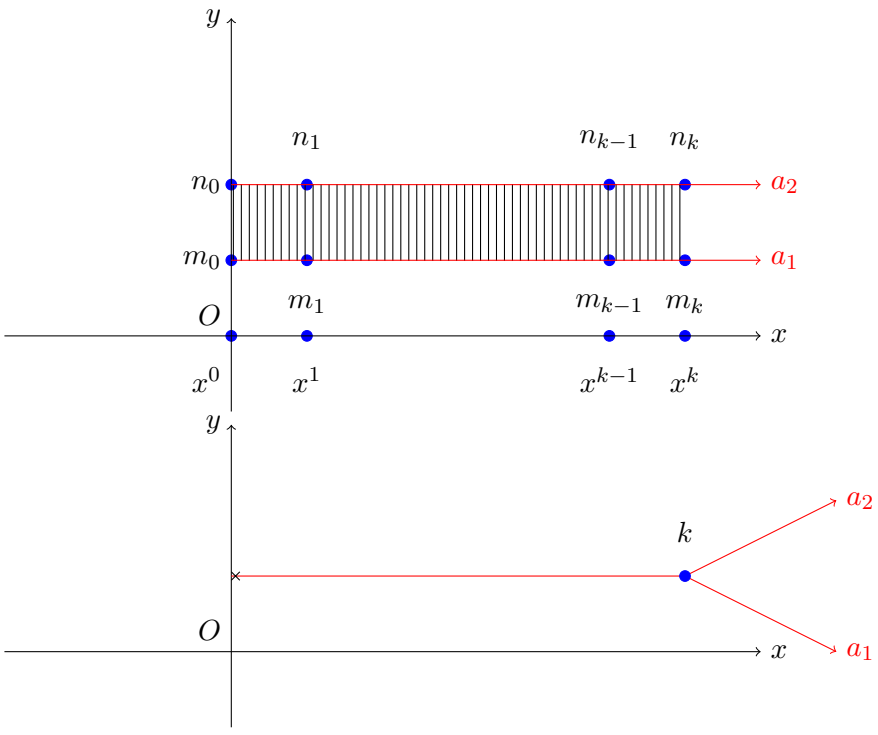

Figure 1.26: Construction of the contact tree of two polynomials.

Definition 1.92. Given the polynomials $a_i(x) \in \mathcal{A}$ (see notation 1.7) such that $a_i(0) = 0$, for any $i = 1, \ldots, m+1$, we construct **the contact tree** associated to all the polynomials in $\mathcal{A}$ as follows.

Let us consider the xOy coordinate system in the real plane. In the first quadrant $\mathbb{R}^2_+$, let each polynomial a_i be represented by the semi-straight line $(y = i) \cap (x > 0)$. We call it the a_i-axis. Recall that, by hypothesis, the polynomials are ordered: $a_1(x) \prec_+ a_2(x) \prec_+ \ldots \prec_+ a_{m+1}(x)$.

The point of coordinate $(k, 0)$ on the Ox axis corresponds to the monomial x^k. On each a_i-axis a point (k, i) is decorated with the coefficient corresponding to the monomial x^k, as it

appears in the polynomial a_i.

Note that for each $i = 1, \ldots, m$, the valuation $\nu_x(a_{i+1}(x) - a_i(x))$ measures the contact between the polynomials $a_{i+1}(x)$ and $a_i(x)$. In particular, it is the exponent of maximal contact between $a_{i+1}(x)$ and $a_i(x)$.

For each i let us identify the points of the first quadrant situated between $a_{i+1}(x)$ and $a_i(x)$, up to the point where the two polynomials separate. Formally, for each $i = 1, \ldots, m$ let us consider the equivalence relation: $(x_1, y_1) \sim (x_2, y_2) \Leftrightarrow x_1 = x_2$ and $x_1, x_2 \leq \nu_x(a_{i+1}(x) - a_i(x))$, for any two points (x_1, y_1) and (x_2, y_2) with $i \leq y_1, y_2 \leq i + 1$.

Now we are able to construct inductively the contact tree, by applying the equivalence relation described above, for all $i = 1, \ldots, m$. We denote by $\mathcal{CT}(\mathcal{A})$ the quotient given by this equivalence relation and let us call $\Lambda : \mathbb{R}^2_+ \to \mathcal{CT}(\mathcal{A})$ the quotient map. By construction, the quotient $\mathcal{CT}(\mathcal{A})$ is embedded in the real plane, since the orientation of the contact tree, both horizontally and vertically, is induced by the orientation of the real line $\mathbb{R}$, since the polynomials $a_i(x)$ are ordered increasingly as horizontal semi-straight lines with their ends on the Oy-axis, and the valuations of their corresponding monomials increase along the Ox-axis.

In addition, one has $\Lambda(0, 0) \equiv \Lambda(0, i)$, for any i. Therefore $\mathcal{CT}(\mathcal{A})$ is a tree, whose root is $\Lambda(0, 0)$.

We call **bifurcation vertices of the contact tree**, the vertices whose valency is greater or equal to 3. We preserve as numerical decoration only the values of the valuation function in its bifurcation vertices $\nu_x(a_{i+1}(x) - a_i(x))$, for any $i = 1, \ldots, m$. Namely, each bifurcation vertex of the contact tree is the point where the contact of the corresponding polynomials a_i and a_{i+1} ends and the respective coefficients of the two polynomials are starting to differ. For a bifurcation vertex v, we shall denote this by $\nu_x(v) := \nu_x(a_{i+1}(x) - a_i(x))$.

The vertices of the contact tree are: the bifurcation vertices, the leaves and the root.

The leaves, i.e. the extremities of the maximal geodesics going from the root, are decorated with arrows and are in a bijective correspondence with the polynomials $a_i \in \mathcal{A}$ of the given polynomial. In other words, each leaf of the tree is decorated with and denoted by its corresponding polynomial a_i. Let us denote the geodesic from the root to a_i by $\mathcal{G}_i$, for all i.

The decorating valuations associated to the bifurcation vertices are, by construction, increasing along any geodesic which starts from the root towards the leaves.

By construction, the contact tree is rooted, embedded in the real plane, which induces an orientation on its leaves: its leaves are totally ordered, and the order is given by the vertical order on the Oy-axis.

Some examples of contact trees can be seen in Figure 1.25, Figure 1.26 and Figure 1.28.

1.7.3 Properties of the contact tree

By construction, we saw that the contact tree is a rooted tree, embedded in the real plane, whose leaves are labelled by the polynomials a_i, for $i = 1, \ldots, m + 1$.

The property of being a tree gives the contact tree also the structure of a lower semi-lattice.

Furthermore we want to consider only the complete binary contact trees, in order to have a bijection between the bifurcation vertices of the complete binary contact tree and the pairs (a_{i+1}, a_i) for $i = 1, \ldots, m$.

Definition 1.93. [Vic89, page 13] A **partially ordered set** (called also **poset**) is a set endowed with a binary relation that is reflexive, transitive and antisymmetric.

Definition 1.94. [Vic89, page 14] Let us consider a partially ordered set S and a subset $A \subseteq S$. Take $b \in S$. We say that b is a **greatest lower bound** for the subset A, if the following conditions hold:

-the element b is a lower bound for A;

-any other lower bound c for A has the property: $c \leq b$.

Definition 1.95. [Vic89, page 38] A **lower semi-lattice** is a partially ordered set whose every finite subset has a greatest lower bound.

Definition 1.96. Let us consider two vertices V_1 and V_2 of a rooted tree $\mathcal{T}$. We denote by $\mathcal{G}_1$ the geodesic from the root of $\mathcal{T}$ to V_1 and by $\mathcal{G}_2$ the geodesic from the root of $\mathcal{T}$ to V_2. If $\mathcal{G}_1 \subseteq \mathcal{G}_2$, then we say that $V_1 \leq_{\mathcal{T}} V_2$. In other words, the smallest vertex is the one closer to the root on the geodesic $\mathcal{G}_2$.

If $V_1 \leq_{\mathcal{T}} V_2$ or $V_2 \leq_{\mathcal{T}} V_1$, then we say that V_1 and V_2 are **comparable vertices** of the tree $\mathcal{T}$. If neither of the two cases mentioned above is true, then one says that V_1 and V_2 are **not comparable**.

Proposition 1.97. *The contact tree is a lower semi-lattice.*

Proof. This follows directly from the fact that any rooted tree is a lower semi-lattice (see [Vic89; LG95] for more details). □

We are thus allowed to introduce the following definition:

Definition 1.98. We call the **meet** (or greatest lower bound) of any two distinct vertices v_i and $v_j \in \mathbb{R}[x]$, with $i \neq j$, denoted by $v_i \wedge v_j$ the vertex where the geodesic from the root to v_i and the geodesic from the root to v_j separate in the contact tree. Namely, $v_i \wedge v_j$ is the furthest vertex from the root and it is the most recent common ancestor of v_i and v_j. See Figure 1.27.

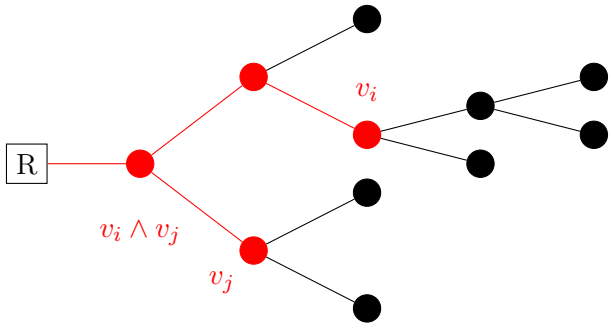

Figure 1.27: The vertex $v_i \wedge v_j$ where the geodesics of v_i and v_j separate.

Since the meet in any semilattice is associative as a binary operation (see [SS15, page 199]), one has $(a_i \wedge a_j) \wedge a_k = a_i \wedge (a_j \wedge a_k)$ and we usually skip the parentheses and use the simple notation $a_i \wedge a_j \wedge a_k$.

Remark 1.99. The important thing to note here is the fact that by Definition 1.98 and the notations introduced before, the meet of two consecutive polynomials $a_{i+1}(x)$ and $a_i(x) \in \mathcal{A}$ has the property

$$\nu_x(a_i \wedge a_{i+1}) = \nu_x(a_{i+1}(x) - a_i(x)) = \nu_x(\delta_i) = e_i.$$

Proposition 1.100. *The map $(a_i, a_{i+1}) \mapsto a_i \wedge a_{i+1}$ is a surjection from the set of pairs of consecutive leaves to the set of internal vertices of the contact tree.*

Proof. By construction of the contact tree, for each internal vertex v, called also bifurcation vertex, there is at least a pair of consecutive polynomials (a_i, a_{i+1}), such that the meet of a_i and a_{i+1} is v, where $i \in \{1, \ldots, m\}$. □

Corollary 1.101. *If the contact tree is an end-rooted complete binary plane tree then there is a bijection between the set of internal vertices of the contact tree and the set of the vertices $a_i \wedge a_{i+1}$, for $i = 1, \ldots, m$.*

REMARK 1.102. To be more precise, if the contact tree is complete binary, then there is a bijection between the set $\{a_i \wedge a_{i+1} \mid i = 1, \dots, m\}$ and the set of pairs $\{(a_i, a_{i+1}) \mid i = 1, \dots, m-1\}$: to each pair of consecutive polynomials it corresponds the unique vertex $a_i \wedge a_{i+1}$ and vice-versa. In this case, the contact tree is necessarily an end-rooted complete plane binary tree.

EXAMPLE 1.103. Let us give an example of a non binary contact tree:

$$\mathcal{CT}(0, x^1, x^1 + x^2, \frac{3}{2}x^1 + x^2, \frac{3}{2}x^1 + x^2 + x^3),$$

presented in Figure 1.28 below. Namely, given

$$a_1(x) = 0,$$

$$a_2(x) = x^1,$$

$$a_3(x) = x^1 + x^2,$$

$$a_4(x) = \frac{3}{2}x^1 + x^2,$$

$$a_5(x) = \frac{3}{2}x^1 + x^2 + x^3,$$

there exist two gaps δ_1 and δ_3, such that $e_1 = e_3 = 1$. In this situation the vertex $a_1 \wedge a_2$ coincides with the vertex $a_3 \wedge a_4$ and has valency 4.

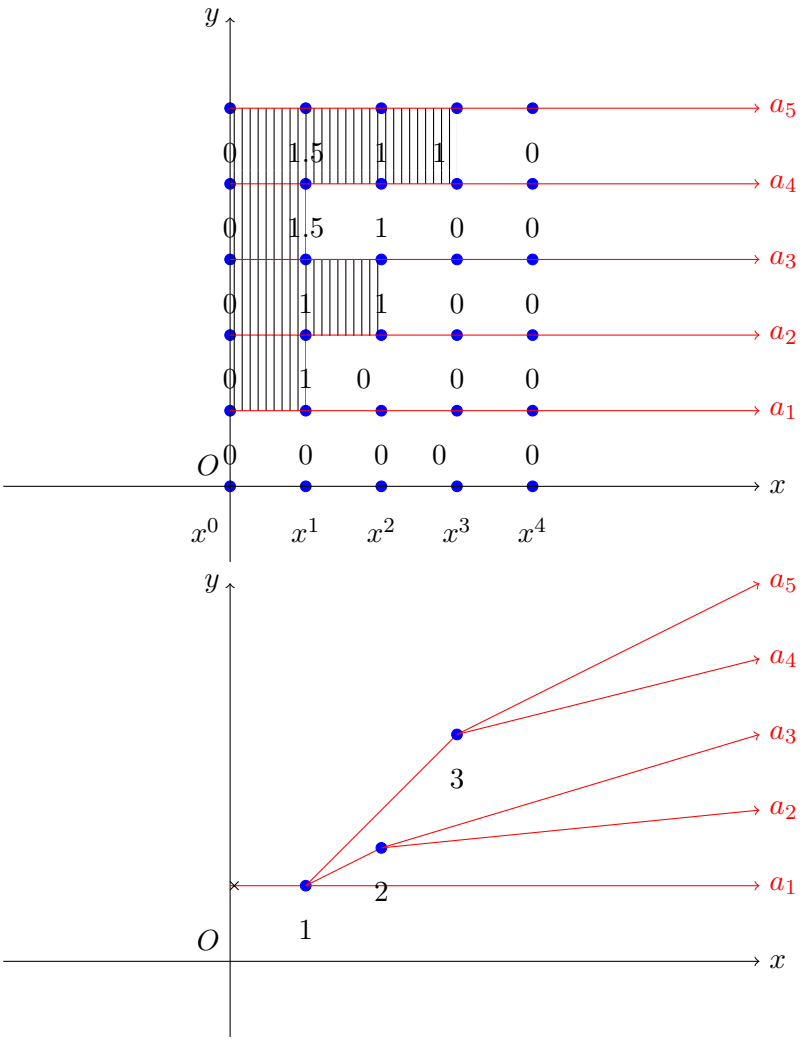

Figure 1.28: Example of a non binary contact tree, where the vertex $a_1 \wedge a_2$ is the same as the vertex $a_3 \wedge a_4$.

Lemma 1.104. *If three polynomials a_i, a_{i+1} and $a_{i+2} \in \mathcal{A}$ (see Subsection 1.7.1, notation 1.7), such that $a_i \prec_+ a_{i+1} \prec_+ a_{i+2}$ are consecutive roots of the polynomial $P \in \mathbb{R}[x][y]$, i.e. three consecutive leaves in the contact tree $\mathcal{CT}(\mathcal{A})$, then $a_i \wedge a_{i+1} \wedge a_{i+2}$ is either $a_i \wedge a_{i+1}$ or $a_{i+1} \wedge a_{i+2}$. In particular, one has:*

$$\nu_x(a_i \wedge a_{i+1} \wedge a_{i+2}) = \min\ (\nu_x(a_i \wedge a_{i+1}), \nu_x(a_{i+1} \wedge a_{i+2})).$$

Example 1.105. An example where $a_i \wedge a_{i+1} \wedge a_{i+2} \equiv a_{i+1} \wedge a_{i+2}$ is presented in Figure 1.29.

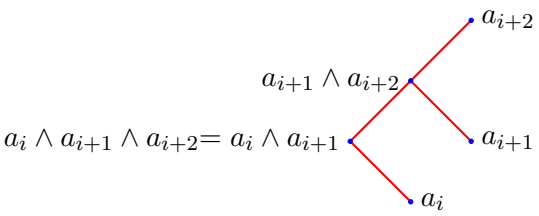

Figure 1.29: Example of $a_i \wedge a_{i+1} \wedge a_{i+2} \equiv a_{i+1} \wedge a_{i+2}$.

Proof. Recall that the meet in any semilattice is associative (see [SS15, page 199]) as a binary operation, that is to say $(a_i \wedge a_{i+1}) \wedge a_{i+2} = a_i \wedge (a_{i+1} \wedge a_{i+2}) = a_i \wedge a_{i+1} \wedge a_{i+2}$. In addition, by definition of the meet $\wedge$, one has both

$$\nu_x(a_i \wedge a_{i+1} \wedge a_{i+2}) = \nu_x((a_i \wedge a_{i+1}) \wedge a_{i+2}) \leq \nu_x(a_i \wedge a_{i+1}) \tag{1.8}$$

and

$$\nu_x(a_i \wedge a_{i+1} \wedge a_{i+2}) = \nu_x(a_i \wedge (a_{i+1} \wedge a_{i+2})) \leq \nu_x(a_{i+1} \wedge a_{i+2}). \tag{1.9}$$

However, there are only the following three possibilities as one can see in Figure 1.30 below.

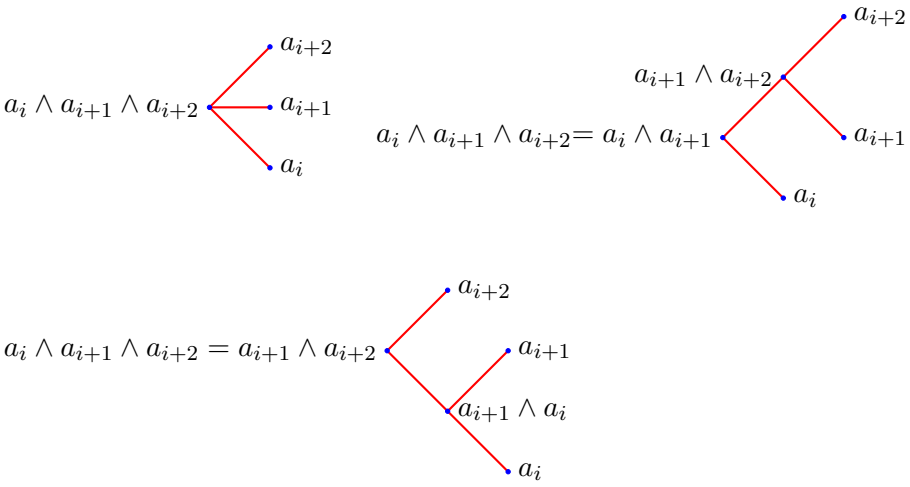

Figure 1.30: The only three possible configurations of $a_i \wedge a_{i+1} \wedge a_{i+2}$.

The conclusion is true for all the three situations above, except for the one presented in Figure 1.31 below. The case in Figure 1.31 could be considered in terms of graphs, but it is impossible in terms of trees, because it creates a cycle inside the contact tree, which is not permitted by definition (see Definition 1.40). This concludes the proof.

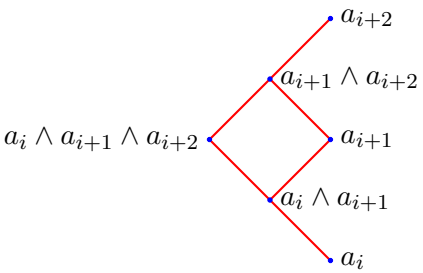

Figure 1.31: Impossible configuration for $a_i \wedge a_{i+1} \wedge a_{i+2}$.

□

Corollary 1.106. *If the polynomials a_i, a_{i+1} and $a_{i+2} \in \mathcal{A}$, $a_i \prec_+ a_{i+1} \prec_+ a_{i+2}$ are consecutive roots of the polynomial $P_x(y) \in \mathbb{R}[x][y]$, i.e. three consecutive leaves in the contact tree $\mathcal{CT}(\mathcal{A})$, then one has the following equality: $a_i \wedge a_{i+1} \wedge a_{i+2} = a_i \wedge a_{i+2}$.*

Corollary 1.107. *Let us consider an arbitrary number of consecutive roots of the polynomial $P \in \mathbb{R}[x][y]$, denoted by $a_i, a_{i+1}, \ldots, a_j$, $j > i$,. Therefore, $a_i, a_{i+1}, \ldots, a_j$ are consecutive leaves of the contact tree $\mathcal{CT}(\{a_1, a_2, \ldots, a_{m+1}\})$. Then one has the following equality:*

$$\nu_x(a_i \wedge a_{i+1} \wedge \ldots \wedge a_j) = \min\left(\nu_x(a_i \wedge a_{i+1}), \nu_x(a_{i+1} \wedge a_{i+2}), \ldots, \nu_x(a_{j-1} \wedge a_j)\right).$$

Moreover, one also has the following equality:

$$a_i \wedge a_{i+1} \wedge \ldots \wedge a_j = a_i \wedge a_j.$$

Example 1.108. An example of the conclusions presented in Corollary 1.107 can be seen in Figure 1.32.

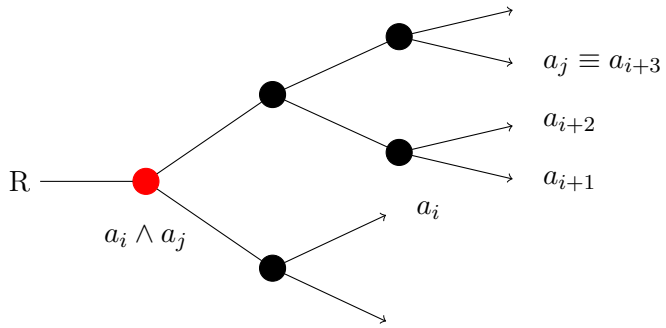

Figure 1.32: The maximal contact between several consecutive roots.

Proof. For the proof of Corollary 1.107, let us proceed by induction on the number, say $n-1$, of the leaves $a_i, a_{i+1}, \ldots, a_j$. Denote by $\mathcal{P}(k)$ the proposition "if $a_i, a_{i+1}, \ldots, a_j$ are k consecutive leaves in the contact tree $\mathcal{CT}(\mathcal{A})$, then $\nu_x(a_i \wedge a_{i+1} \wedge \ldots \wedge a_j) = \min\left(\nu_x(a_i \wedge a_{i+1}), \nu_x(a_{i+1} \wedge a_{i+2}), \ldots, \nu_x(a_{j-1} \wedge a_j)\right)$."

By Corollary 1.106, the proposition $\mathcal{P}(3)$ is true.

Let us prove that if $\mathcal{P}(n-1)$ is true then $\mathcal{P}(n)$ is also true. There are two situations, as the reader can observe in Figure 1.33 and Figure 1.34 below:

(a) either $a_i \wedge \ldots \wedge a_j \leq_{\mathcal{CT}} a_j \wedge a_{j+1}$ and then by the hypothesis $\mathcal{P}(n-1)$ we have $\mathcal{P}(n)$ is also true;

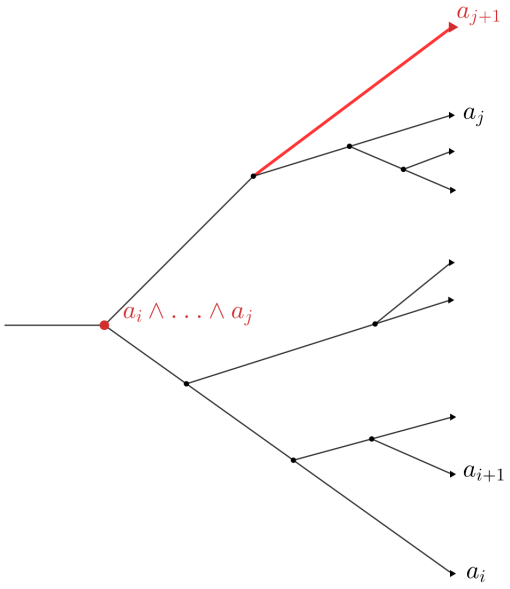

Figure 1.33: Recursive step case (a).

(b) or $a_i \wedge \ldots \wedge a_j >_{\mathcal{CT}} a_j \wedge a_{j+1}$; in this case, $\nu_x(a_i \wedge a_{i+1} \wedge \ldots \wedge a_j \wedge a_{j+1}) = \nu_x(a_j \wedge a_{j+1})$. Since $a_i \wedge \ldots \wedge a_j >_{\mathcal{CT}} a_j \wedge a_{j+1}$, we have $\nu_x(a_j \wedge a_{j+1}) = \min(\nu_x(a_i \wedge a_{i+1}), \nu_x(a_{i+1} \wedge a_{i+2}), \ldots, \nu_x(a_{j-1} \wedge a_j))$ and the induction step is finished.

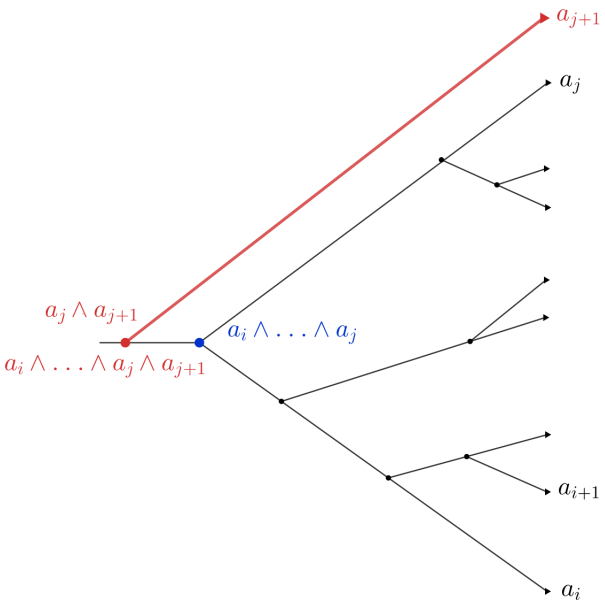

Figure 1.34: Recursive step case (b).

□

1.7.4 Computing the valuations of the areas S_i

In the sequel, we fix i and we compute $\nu_x(\mathrm{S}_i(x))$, in terms of the contact tree and of the valuations $e_j := \nu_x(\delta_j(x))$, for $j = 1, \dots, m$.

The reader should remember the notations we introduced in Section 1.7. The roots of the polynomial

$$P_x(y) := \prod_{i=1}^{m+1} (y - a_i(x)) \in \mathbb{R}[x][y]$$

(see equation 1.5), namely $a_i(x) \in \mathcal{A}$ verify equation 1.6:

$$a_1(x) \prec_+ a_2(x) \prec_+ \dots \prec_+ a_{m+1}(x).$$

For any $i = 1, \dots, m+1$, one has

$$\delta_i(x) := a_{i+1}(x) - a_i(x),$$

$$\nu_x(\delta_i(x)) := e_i$$

and the area

$$\mathrm{S}_i(x) := \left| \int_{a_i(x)}^{a_{i+1}(x)} P_x(y) \mathrm{d}y \right|.$$

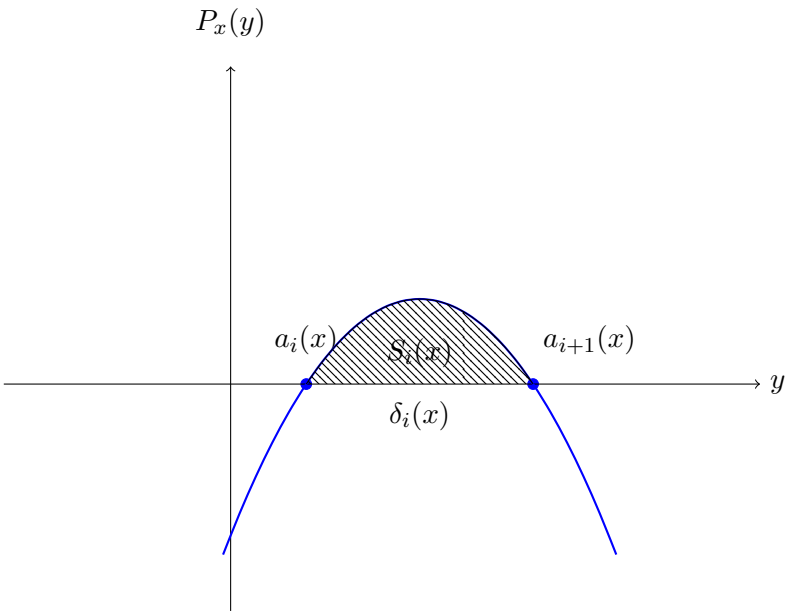

Figure 1.35: Area S_i, corresponding to $\delta_i = a_{i+1} - a_i$.

Proposition 1.109. *Let us consider the geodesic $\mathcal{G}_i$, from the root to a_i. One has the formula:*

$$\nu_x(\mathrm{S}_i) = e_i + \sum_{\{G \in \mathcal{G}_i | G \leq_{\mathcal{CT}} a_i \wedge a_{i+1}\}} c_G(i) \nu_x(G), \tag{1.10}$$

where the coefficient $c_G(i) \in \mathbb{N}$ represents the number of leaves of the contact tree $\mathcal{CT}(\mathcal{A})$, whose most recent ancestor belonging to $\mathcal{G}_i$ is G. We shall further write $c_G(i) := c_G$ if i is clear from the context.

Before proceeding to the proof of Proposition 1.109, we strongly recommend the lecture of Example 1.110 below.

EXAMPLE 1.110. Let us consider the following given roots of the polynomial $P_x(y)$:

$a_1(x) = 0$,
$a_2(x) = x^4$,
$a_3(x) = x^3 + x^4$,
$a_4(x) = x^2 + x^3 + x^4$,
$a_5(x) = x^1 + x^2 + x^3 + x^4$.

Therefore, we obtain:

$\delta_1 := a_2(x) - a_1(x) = x^4$, $e_1 := \nu_x(\delta_1) = 4$,
$\delta_2 := a_3(x) - a_2(x) = x^3$, $e_2 := \nu_x(\delta_2) = 3$,
$\delta_3 := a_4(x) - a_3(x) = x^2$, $e_3 := \nu_x(\delta_3) = 2$,
$\delta_4 := a_5(x) - a_4(x) = x^1$, $e_4 := \nu_x(\delta_4) = 1$.

We want to compute the valuation of the following area $S_3(x) := \left| \int_{a_3(x)}^{a_4(x)} P_x(y)\mathrm{d}y \right|$.

We may write $S_3(x) = \int_{a_3(x)}^{a_4(x)} (y - a_1(x))(y - a_2(x))(y - a_3(x))(a_4(x) - y)(a_5(x) - y)\mathrm{d}y$.

Let us now make the following change of variable: $y := a_3(x) + s\delta_3(x)$, where $s \in [0, 1]$. We obtain :

$S_3(x) = \int_0^1 (\delta_1(x)+\delta_2(x)+s\delta_3(x))(\delta_2(x)+s\delta_3(x))s\delta_3(x)(1-s)\delta_3(x)(\delta_4(x)+(1-s)\delta_3(x))\delta_3(x)\mathrm{d}s =$
$= \delta_1(x)\delta_2(x)\delta_3(x)^3\delta_4(x) \int_0^1 s(1-s)\mathrm{d}s+$
$+\delta_1(x)\delta_2(x)\delta_3(x)^4 \int_0^1 s(1-s)^2\mathrm{d}s+$
$+\delta_1(x)\delta_3(x)^4\delta_4(x) \int_0^1 s^2(1-s)\mathrm{d}s+$
$+\delta_1(x)\delta_3(x)^5 \int_0^1 s^2(1-s)^2\mathrm{d}s+$
$+\delta_2(x)^2\delta_3(x)^3\delta_4(x) \int_0^1 s(1-s)\mathrm{d}s+$
$+\delta_2(x)^2\delta_3(x)^4 \int_0^1 s(1-s)^2\mathrm{d}s+$
$+\delta_2(x)\delta_3(x)^4\delta_4(x) \int_0^1 2s^2(1-s)\mathrm{d}s+$
$+\delta_2(x)\delta_3(x)^5 \int_0^1 2s^2(1-s)\mathrm{d}s+$
$+\delta_3(x)^5\delta_4(x) \int_0^1 s^3(1-s)\mathrm{d}s+$
$+\delta_3(x)^6 \int_0^1 s^3(1-s)\mathrm{d}s.$

Now, $\nu_x(S_3(x)) = \min\{\nu_x(\delta_1(x)\delta_2(x)\delta_3(x)^3\delta_4(x)), \nu_x(\delta_1(x)\delta_2(x)\delta_3(x)^4), \nu_x(\delta_1(x)\delta_3(x)^4\delta_4(x)),$
$\nu_x(\delta_1(x)\delta_3(x)^5), \nu_x(\delta_2(x)^2\delta_3(x)^3\delta_4(x)), \nu_x(\delta_2(x)^2\delta_3(x)^4),$
$\nu_x(\delta_2(x)\delta_3(x)^4\delta_4(x)), \nu_x(\delta_2(x)\delta_3(x)^5), \nu_x(\delta_3(x)^5\delta_4(x)), \nu_x(\delta_3(x)^6)\} =$
$= \nu_x(\delta_3(x)^5\delta_4(x)) = 5e_3 + e_4 = \mathbf{11}$.

Let us now interpret the result obtained above, this time with respect to the contact tree. Denote by $\mathcal{G}_i$, the geodesic from the root to a_i. We shall prove that:

$\nu_x(\mathrm{S}_3) = e_3 + \sum_{\{G \in \mathcal{G}_3 | G \leq_{\mathcal{CT}} a_3 \wedge a_4\}} c_G(3)\nu_x(G)$,

where the coefficient $c_G(3) \in \mathbb{N}$ represents the number of leaves of the contact tree $\mathcal{CT}(\mathcal{A})$, whose most recent ancestor belonging to $\mathcal{G}_3$ is G.

In this example, $a_3 \wedge a_4 \equiv G_2$ and we can check if the formula 1.10 gives us the same result, namely $\nu_x(S_3(x)) = 11$: the vertices on the geodesic $\mathcal{G}_3$ which are $\leq_{\mathcal{CT}} G_2$ are G_1 and G_2. We have $c_{G_1}(3) = 1$ representing the number of leaves of the contact tree $\mathcal{CT}(\mathcal{A})$, whose most recent ancestor belonging to $\mathcal{G}_3$ is G_1. Also, $c_{G_2}(3) = 4$ representing the number of leaves of the contact tree $\mathcal{CT}(\mathcal{A})$, whose most recent ancestor belonging to $\mathcal{G}_3$ is G_2.

Thus $\nu_x(\mathrm{S}_3) = e_3 + c_{G_1}(3)\nu_x(G_1) + c_{G_2}(3)\nu_x(G_2) = 2 + 1 \times 1 + 4 \times 2 = 11$. The verification is completed.

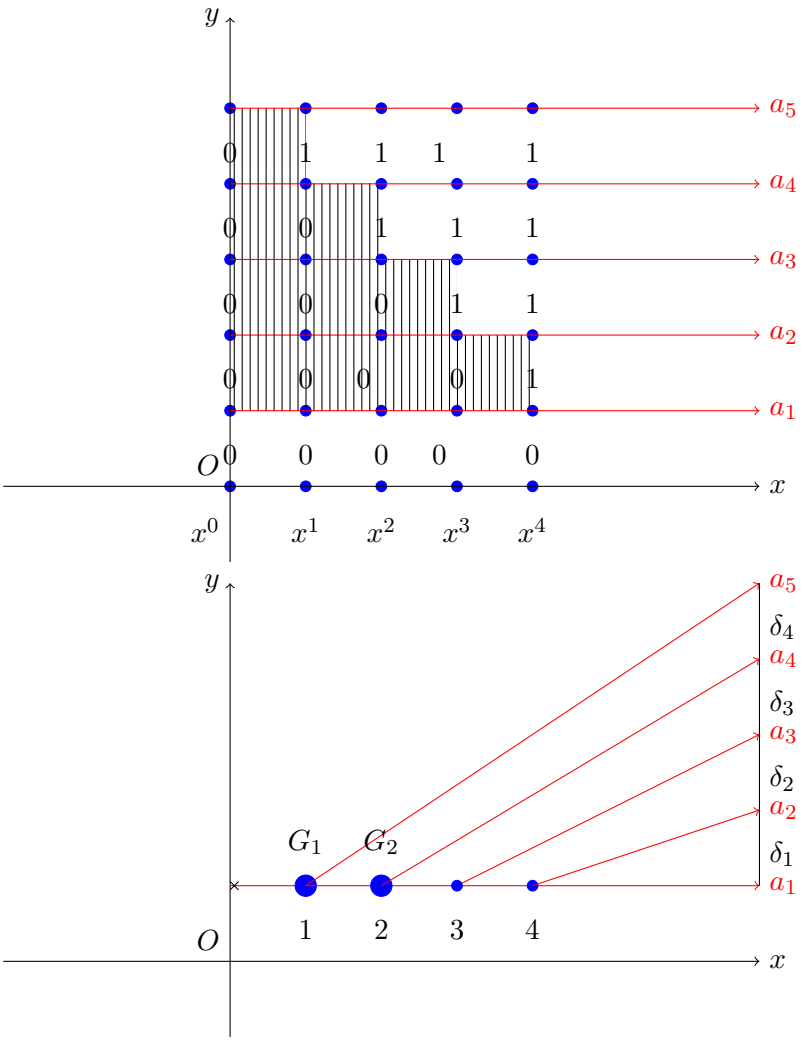

Figure 1.36: How to read the valuation of $\mathrm{S}_3(x)$ on the contact tree of the roots $a_i(x) \in \mathcal{A}$.

Proof. Let us prove Proposition 1.109. We have (recall equation 1.5)

$$\mathrm{S}_i(x) := \left| \int_{a_i(x)}^{a_{i+1}(x)} P_x(y)\mathrm{d}y \right| = \left| \int_{a_i(x)}^{a_{i+1}(x)} (y - a_1(x))(y - a_2(x)) \cdots (y - a_{m+1}(x))\mathrm{d}y \right|.$$

Let us observe that $y \geq a_k(x)$, for any $k \leq i$ and that $y \leq a_k(x)$ for any $k \geq i+1$, thus by taking the absolute value we have

$$\mathrm{S}_i(x) = \int_{a_i(x)}^{a_{i+1}(x)} (y-a_1(x))(y-a_2(x)) \cdots (y-a_i(x))(a_{i+1}(x)-y)(a_{i+2}(x)-y) \cdots (a_{m+1}(x)-y)\mathrm{d}y.$$

Now let us make the change of variables given by $y = a_i(x) + s\delta_i(x)$, where $s \in [0,1]$, as in Figure 1.37 below.

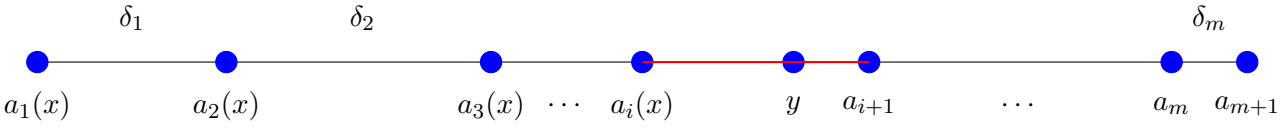

Figure 1.37: Change of variable $y = a_i(x) + s\delta_i(x)$

Thus we obtain

$$\mathrm{S}_i(x) = \int_0^1 (\delta_1(x) + \delta_2(x) + \cdots + \delta_{i-1}(x) + s\delta_i(x))(\delta_2(x) + \cdots + \delta_{i-1}(x) + s\delta_i(x)) \cdots$$

$$\cdots (0+s\delta_i(x))((1-s)\delta_i(x))((1-s)\delta_i(x)+\delta_{i+1}(x)) \cdots ((1-s)\delta_i(x)+\delta_{i+1}(x)+\cdots+\delta_m(x))(\delta_i(x)\mathrm{d}s).$$

Let us study the valuation in x of one of the parenthesis, say $\nu := \nu_x((1-s)\delta_i(x) + \delta_{i+1}(x) + \cdots + \delta_j(x))$. The other parenthesis can all be treated similarly. The key observation is the fact that by integrating in s one does not change the valuation in x.

Since $a_1 \prec_+ a_2 \prec_+ \ldots \prec_+ a_{m+1}$, one has $\delta_i(x) > 0$, for any $0 < x \ll 1$ and for any $i = 1, \ldots, m$. Thus we need to compute the valuation of a sum of positive terms. Therefore the valuation will be equal to the minimum of the valuations of the terms in the chosen parenthesis, namely: $\nu = \min(\nu_x(\delta_i), \nu_x(\delta_{i+1}), \ldots, \nu_x(\delta_j))$. By Remark 1.99 we get $\nu = \min(\nu_x(a_i \wedge a_{i+1}), \nu_x(a_{i+1} \wedge a_{i+2}), \ldots, \nu_x(a_j \wedge a_{j+1}))$. Now we apply Corollary 1.107 and we obtain $\nu = \nu_x(a_i \wedge a_{i+1} \wedge \ldots \wedge a_{j+1})$. There are two consequences of this fact, as follows:

(a) $\nu \leq \nu_x(a_i \wedge a_{i+1}) = e_i$;

(b) by Corollary 1.107, $\nu = \nu_x(a_i \wedge a_{j+1})$, namely the valuation of the vertex G where the geodesic of a_i and the geodesic of a_{j+1} separate in the contact tree. Thus the vertex G is on the geodesic $\mathcal{G}_i$.

In conclusion, to each leaf a_j, $j = 1, \ldots, m+1$, it corresponds a parenthesis in the expression of S_i as above. As we have just seen, the parenthesis corresponds to exactly one vertex G situated on the geodesic $\mathcal{G}_i$ such that $G \leq_{\mathcal{CT}} a_i \wedge a_{i+1}$.

Let us count differently, namely for each vertex G laying on the geodesic $\mathcal{G}_i$, with $G \leq_{\mathcal{CT}} a_i \wedge a_{i+1}$, we count the number of leaves of $\mathcal{CT}$ whose most recent ancestor belonging to $\mathcal{G}_i$ is G. Denote this number by c_G. Note that we only consider the vertices $G \leq_{\mathcal{CT}} a_i \wedge a_{i+1}$ since we proved above that for each parenthesis we have $\nu \leq \nu_x(a_i \wedge a_{i+1}) = e_i$. Let us observe that when we make the change of variable, another factor δ_i appeared in the product. The valuation $e_i = \nu_x(\delta_i)$ has to be taken into consideration when we sum all the terms. In conclusion,

$$\nu_x(\mathrm{S}_i) = e_i + \sum_{\{G \in \mathcal{G}_i | G \leq_{\mathcal{CT}} a_i \wedge a_{i+1}\}} c_G \nu_x(G).$$

□

Below we give some more examples.

EXAMPLE 1.111. Given the roots $a_1(x) = 0$, $a_2(x) = x^6$, $a_3(x) = x + x^6$, $a_4(x) = x + x^2 + x^6$, $a_5(x) = x + x^2 + x^3 + x^6$, $a_6(x) = x + x^2 + x^3 + x^4 + x^6$, $a_7(x) = x + x^2 + x^3 + x^4 + x^5 + x^6$, let us compute $\nu_x(\mathrm{S}_i(x))$, for $i = 4$.

We have $\delta_1 = x^6$, $e_1 = 6$, $\delta_2 = x$, $e_2 = 1$, $\delta_3 = x^2$, $e_3 = 2$, $\delta_4 = x^3$, $e_4 = 3$, $\delta_5 = x^4$, $e_5 = 4$, $\delta_6 = x^5$, $e_6 = 5$.

Let us consider three steps: first we compute the valuation by integration; second we compute the valuation by using formula 1.10; in the end, the third step is to check if the two results coincide.

• *Step 1: integration*
We have

$$\mathrm{S}_4(x) = \int_0^1 (\delta_1+\delta_2+\delta_3+s\delta_4)(\delta_2+\delta_3+s\delta_4)(\delta_3+s\delta_4)s\delta_4(1-s)\delta_4((1-s)\delta_4+\delta_5)((1-s)\delta_4+\delta_5+\delta_6)(\delta_4 \mathrm{d}s) =$$

$$= \int_0^1 (x^6+x^1+x^2+sx^3)(x^1+x^2+sx^3)(x^2+sx^3)sx^3(1-s)x^3((1-s)x^3+x^4)((1-s)x^3+x^4+x^5)(x^3 \mathrm{d}s).$$

We obtain $\nu_x(\mathrm{S}_4(x)) = \nu_x(\int_0^1 x^1x^1x^2sx^3(1-s)x^3(1-s)x^3(1-s)x^3(x^3\mathrm{d}s))$, hence
$\nu_x(\mathrm{S}_4(x)) = 2\nu_x(x^1) + 1\nu_x(x^2) + 4\nu_x(x^3) + \nu_x(x^3) = 2e_2 + 1e_3 + 4e_4 + e_4 = 19.$

• *Step 2: formula and contact tree*
Let us see this better in Figure 1.38, where we compute the coefficients c_k in the formula for the valuation of S_4.

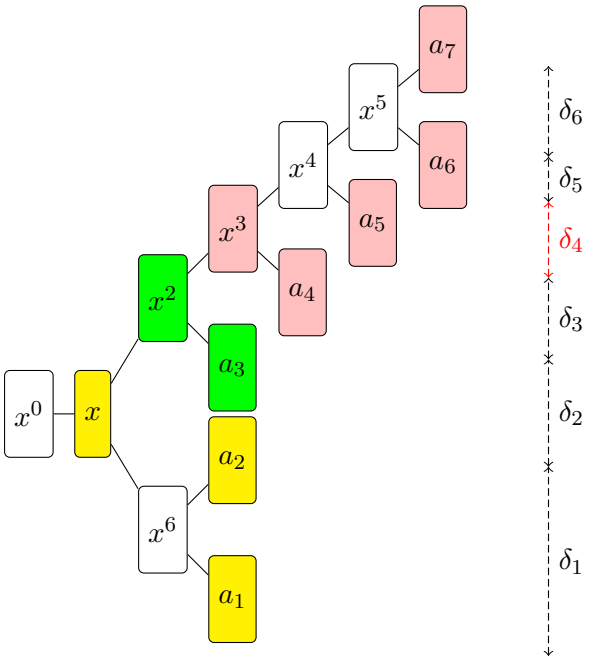

Figure 1.38: How to compute the coefficients c_k in the formula for the valuation of S_4, by counting the leaves whose most recent common ancestor is each of the vertices on the geodesic to $a_4 \wedge a_5$.

The vertex $a_4 \wedge a_5$ corresponds to δ_4. Here $a_1 \wedge a_2 \notin \mathcal{G}_4$, so e_1 does not appear in the sum. For each G on the geodesic $\mathcal{G}_4$ with $G \leq_{\mathcal{CT}} a_4 \wedge a_5$, we count the number of leaves of $\mathcal{CT}$ whose most recent ancestor belonging to $\mathcal{G}_4$ is G. Thus $c_{a_2\wedge a_3} = 2$, $c_{a_3\wedge a_4} = 1$, $c_{a_4\wedge a_5} = 4$.
Thus $\nu_x(\mathrm{S}_4(x)) = 2 \times 1 + 1 \times 2 + 4 \times 3 + 3 = 19$.

• *Step 3: comparison of the two results*
Both methods give the same result: $\nu_x(\mathrm{S}_4(x)) = 19$.

Example 1.112. For the same roots as in Example 1.111, compute $\nu_x(\mathrm{S}_i(x))$, for $i = 3$. From the contact tree given in Figure 1.38, we have $c_{a_2\wedge a_3} = 2$, $c_{a_3\wedge a_4} = 5$, thus by the formula given in Proposition 1.109. $\nu_x(\mathrm{S}_3(x)) = 2\nu_x(x^1) + 5\nu_x(x^2) + \nu_x(x^2) = 2e_2 + 5e_3 + e_3 = 14$.

Corollary 1.113. *With the hypotheses and notations from Proposition 1.109, one can write*

$$\nu_x(\mathrm{S}_i) = e_i + \sum_{j=1}^{i} q_{ij} e_j,$$

where $q_{ij} \in \mathbb{N}$, $q_{ij} = \begin{cases} c_G(i), & \text{if } G \text{ is comparable to } a_i \wedge a_{i+1} \text{ and } G \in \mathcal{G}_i,\ G \leq_{\mathcal{CT}} a_i \wedge a_{i+1}; \\ 0 & \text{else.} \end{cases}$

The purpose of Corollary 1.113 is to be able to express $\nu_x(\mathrm{S}_i)$ in function of all the e_j, for $j = 1, i$, even if some of the e_j will have zero coefficient.

Also under the hypotheses and notations from Proposition 1.109, we conclude this subsection with a lemma and a corollary, which we will need later, in Subsection 1.8.2.

Lemma 1.114. *If $P_x(y)$ is a monic polynomial such that all its roots $a_i \in \mathcal{A}$, $i = 1, \ldots, m+1$ are distinct, then we have $\int_{a_i(x)}^{a_{i+1}(x)} P_x(t)\mathrm{d}t = (-1)^{m+1-i}\ \mathrm{S}_i$.*

Proof. Since $P_x(y)$ is a monic polynomial, we know that $\lim_{y\to\infty} P_x(y) = \infty$, thus the area $\int_{a_m(x)}^{a_{m+1}(x)} P_x(t)\mathrm{d}t = -\mathrm{S}_m$ (namely the corresponding area is always under the horizontal Oy-axis). By hypothesis, all the roots of $P_x(y)$ are distinct, thus the areas are alternatively above and under the Oy-axis drawn horizontally. One can conclude that a given area S_i is above Oy-axis if and only if $m+1-i$ is even and we have $\int_{a_i(x)}^{a_{i+1}(x)} P_x(t)\mathrm{d}t = (-1)^{m+1-i}\ \mathrm{S}_i$. □

Corollary 1.115. *If $\mathrm{S}_i := \int_{a_i(x)}^{a_{i+1}(x)} P_x(t)\mathrm{d}t$, then S_i is above Oy-axis if and only if $m+1-i$ is even.*

1.7.5 The inequalities between areas S_i, read on the contact tree

If one considers the contact tree $\mathcal{CT}$ and two comparable vertices v_k and v_ℓ, then we are interested if the order relation between the two vertices gives us an order between the corresponding areas S_k and S_ℓ.

Proposition 1.116. *Let $v_k := a_k \wedge a_{k+1}$ and $v_\ell := a_\ell \wedge a_{\ell+1}$ denote two comparable vertices of the contact tree $\mathcal{CT}$. If $v_k <_{\mathcal{CT}} v_\ell$, then we have the polynomial inequality $\mathrm{S}_k \succ_+ \mathrm{S}_\ell$.*

Before reading the proof of Proposition 1.116, we suggest to look at the following example.

Example 1.117. For the contact tree in Figure 1.39, we want to compare the coefficients which appear in the computation of $\nu_x(\mathrm{S}_3)$, i.e. $c_{a_i \wedge a_{i+1}}(3)$ with the coefficients which appear in the computation of $\nu_x(\mathrm{S}_7)$, i.e. $c_{a_i \wedge a_{i+1}}(7)$. We have the inclusion of geodesics $\mathcal{G}_3 \subset \mathcal{G}_7$.

Let us count the number of leaves that exit each vertex, for both geodesics. We find equality in the case of the common vertices:

$c_{a_1 \wedge a_2}(3) = c_{a_1 \wedge a_2}(7) = 1$,

$c_{a_2 \wedge a_3}(3) = c_{a_2 \wedge a_3}(7) = 1$.

Starting with the vertex $a_3 \wedge a_4$, which is the end on the first geodesic $\mathcal{G}_3$, we obtain different number of leaves which exit the two geodesics:

$c_{a_3 \wedge a_4}(3) = 6$ and $c_{a_3 \wedge a_4}(7) = 1$.

Moreover, since the vertices $a_4 \wedge a_5$, $a_5 \wedge a_6$, $a_6 \wedge a_7$ and $a_7 \wedge a_8$ are not on the geodesic $\mathcal{G}_3$, it follows that:

$c_{a_4 \wedge a_5}(3) = c_{a_5 \wedge a_6}(3) = c_{a_6 \wedge a_7}(3) = c_{a_7 \wedge a_8}(3) = 0$.

However, on the rest of the geodesic $\mathcal{G}_7$, i.e. on $\mathcal{G}_7 \setminus \mathcal{G}_3$ we have:

$c_{a_4 \wedge a_5}(7) = 1$, $c_{a_5 \wedge a_6}(7) = 1$;

Since $a_6 \wedge a_7 \notin \mathcal{G}_7$ we have $c_{a_6 \wedge a_7}(7) = 0$.

Finally, we have $c_{a_7 \wedge a_8} = 3$, wince there are three leaves that exit $\mathcal{G}_7$ at the vertex $a_7 \wedge a_8$.

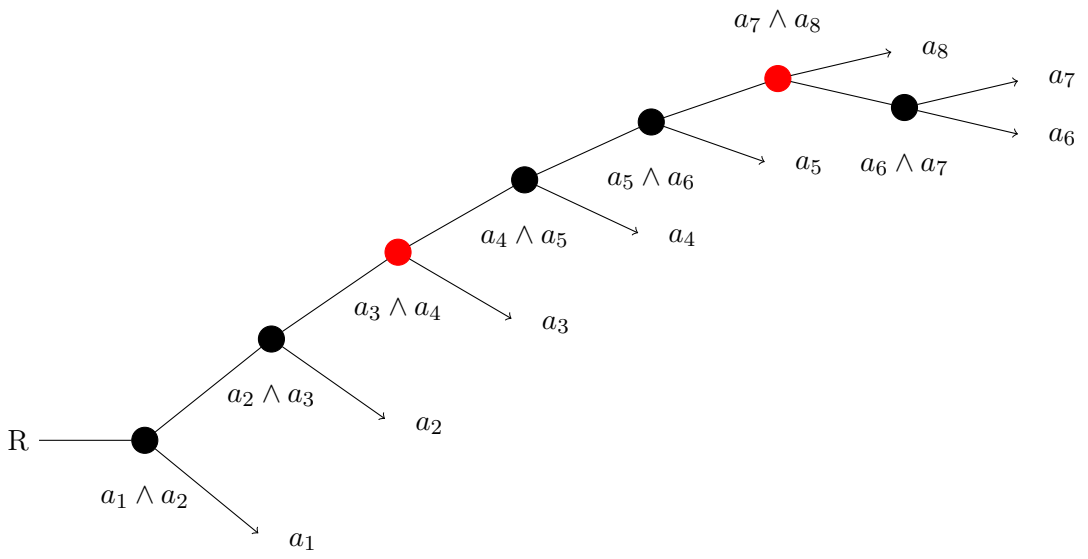

Figure 1.39: Computing the valuation of S_3 and of S_7.

Proof. Let us prove Proposition 1.116. Since $v_k <_{\mathcal{CT}} v_\ell$, by Definition 1.96 we know that $\mathcal{G}_k \subset \mathcal{G}_\ell$. The main idea is to compare the number of leaves on each vertex of the geodesic to v_ℓ. Namely, on the common geodesic $\mathcal{G}_k$, the number of leaves that exit the geodesic at a vertex different from v_k is the same both in the computation of $\nu_x(S_k)$ and in the computation of $\nu_x(S_\ell)$: for $\{G \in \mathcal{G}_\ell \mid G <_{\mathcal{CT}} a_{k-1} \wedge a_k\}$ we have $c_G(k) = c_G(\ell)$. Then, in the case of $\nu_x(S_k)$, the number of leaves that exit the geodesic at v_k (denoted by $c_{a_k \wedge a_{k+1}}(k)$) is the sum of all the leaves that exit the geodesic $\mathcal{G}_\ell$ computed for $\nu_x(S_\ell)$ i.e. $\sum_{\{G \in \mathcal{G}_\ell | a_k \wedge a_{k+1} \leq_{\mathcal{CT}} G \leq_{\mathcal{CT}} a_\ell \wedge a_{\ell+1}\}} c_G(\ell) = c_{a_k \wedge a_{k+1}}(k)$.

By Proposition 1.109, if we denote by $e_k := \nu_x(v_k)$ we have

$$\nu_x(\mathrm{S}_k) = e_k + \sum_{\{G \in \mathcal{G}_k | G \leq_{\mathcal{CT}} a_k \wedge a_{k+1}\}} c_G(k)\nu_x(G),$$

where the coefficient $c_G(k) \in \mathbb{N}$ represents the number of leaves of the contact tree $\mathcal{CT}(\mathcal{A})$, whose most recent ancestor belonging to $\mathcal{G}_k$ is G.

Similarly, if we denote by $e_\ell := \nu_x(v_\ell)$ we have

$$\nu_x(\mathrm{S}_\ell) = e_\ell + \sum_{\{G \in \mathcal{G}_\ell | G \leq_{\mathcal{CT}} a_\ell \wedge a_{\ell+1}\}} c_G(\ell)\nu_x(G),$$

where the coefficient $c_G(\ell) \in \mathbb{N}$ represents the number of leaves of the contact tree $\mathcal{CT}(\mathcal{A})$, whose most recent ancestor belonging to $\mathcal{G}_\ell$ is G.

By Definition 1.92, since on each geodesic the integers decorating the bifurcation vertices of $\mathcal{CT}(\mathcal{A})$ form a strictly increasing subsequence, we obtain that $e_k < e_\ell$.

Thus

$$\nu_x(\mathrm{S}_\ell) = e_\ell + \sum_{\{G \in \mathcal{G}_\ell | G \leq_{\mathcal{CT}} a_\ell \wedge a_{\ell+1}\}} c_G(\ell)\nu_x(G) >$$

$$> e_k + \sum_{\{G \in \mathcal{G}_\ell | G \leq_{\mathcal{CT}} a_{k-1} \wedge a_k\}} c_G(\ell)\nu_x(G) + \sum_{\{G \in \mathcal{G}_\ell | a_k \wedge a_{k+1} \leq_{\mathcal{CT}} G \leq_{\mathcal{CT}} a_\ell \wedge a_{\ell+1}\}} c_G(\ell)\nu_x(G).$$

Since for $\{G \in \mathcal{G}_\ell \mid G <_{\mathcal{CT}} a_{k-1} \wedge a_k\}$ we have $c_G(k) = c_G(\ell)$ and for $\{G \in \mathcal{G}_\ell \mid a_k \wedge a_{k+1} \leq_{\mathcal{CT}} G \leq_{\mathcal{CT}} a_\ell \wedge a_{\ell+1}\}$, we have $\nu_x(G) > e_k$, we obtain

$$\nu_x(\mathrm{S}_\ell) > e_k + \sum_{\{G \in \mathcal{G}_\ell | G <_{\mathcal{CT}} a_{k-1} \wedge a_k\}} c_G(k)\nu_x(G) + \sum_{\{G \in \mathcal{G}_\ell | a_k \wedge a_{k+1} \leq_{\mathcal{CT}} G \leq_{\mathcal{CT}} a_\ell \wedge a_{\ell+1}\}} c_G(\ell)e_k =$$

$$= e_k + \sum_{\{G\in\mathcal{G}_\ell | G<_{\mathcal{CT}} a_{k-1}\wedge a_k\}} c_G(k)\nu_x(G) + e_k \sum_{\{G\in\mathcal{G}_\ell | a_k\wedge a_{k+1}\leq_{\mathcal{CT}} G\leq_{\mathcal{CT}} a_\ell\wedge a_{\ell+1}\}} c_G(\ell).$$

Since $\sum_{\{G\in\mathcal{G}_\ell | a_k\wedge a_{k+1}\leq_{\mathcal{CT}} G\leq_{\mathcal{CT}} a_\ell\wedge a_{\ell+1}\}} c_G(\ell) = c_{a_k\wedge a_{k+1}}(k)$, we have

$$\nu_x(\mathrm{S}_\ell) > e_k + \sum_{\{G\in\mathcal{G}_\ell | G<_{\mathcal{CT}} a_{k-1}\wedge a_k\}} c_G(k)\nu_x(G) + e_k c_{a_k\wedge a_{k+1}}(k) =$$

$$= e_k + \sum_{\{G\in\mathcal{G}_k | G\leq_{\mathcal{CT}} a_k\wedge a_{k+1}\}} c_G(k)\nu_x(G) = \nu_x(\mathrm{S}_k).$$

□

Remark 1.118. By Definition 1.92 and by the initial hypothesis that $a_1 \prec_+ a_2 \prec_+ \ldots \prec_+ a_{m+1}$, if $V_k <_{\mathcal{CT}} V_\ell$, then one has $e_k < e_\ell$, which is equivalent to $\delta_k \succ_+ \delta_\ell$. By Proposition 1.116, $\mathrm{S}_k \succ_+ \mathrm{S}_\ell$. However, if V_ℓ and V_k are not comparable, then it may happen that either $\mathrm{S}_k \succ_+ \mathrm{S}_\ell$, or $\mathrm{S}_k \prec_+ \mathrm{S}_\ell$. See Example 1.119.

Example 1.119. Let us study the contact tree given in Figure 1.40 below and let us compute the valuations of S_7, S_1 and S_3 using Corollary 1.113. We get $\nu_x(\mathrm{S}_7) = 2\cdot 6 + 2\cdot 4 + 4 = 24$, $\nu_x(\mathrm{S}_1) = 2\cdot 8+1\cdot 6+3\cdot 3+2\cdot 2+8 = 43$ and $\nu_x(\mathrm{S}_3) = 2\cdot 2+3\cdot 6+3 = 25$. Here the vertices $a_7\wedge a_8$ and $a_3\wedge a_4$ are not comparable. We cannot apply Proposition 1.116. We have $e_3 = 3 < e_7 = 4$ thus $\delta_7 \prec_+ \delta_3$, i.e. $S_3 \prec_+ S_7$. On the other hand, for other two non comparable vertices $a_7\wedge a_8$ and $a_1\wedge a_2$ we have $e_7 = 4 < e_1 = 8$ thus $\delta_1 \prec_+ \delta_7$ but we obtain the opposite inequality, namely $S_1 \prec_+ S_7$.

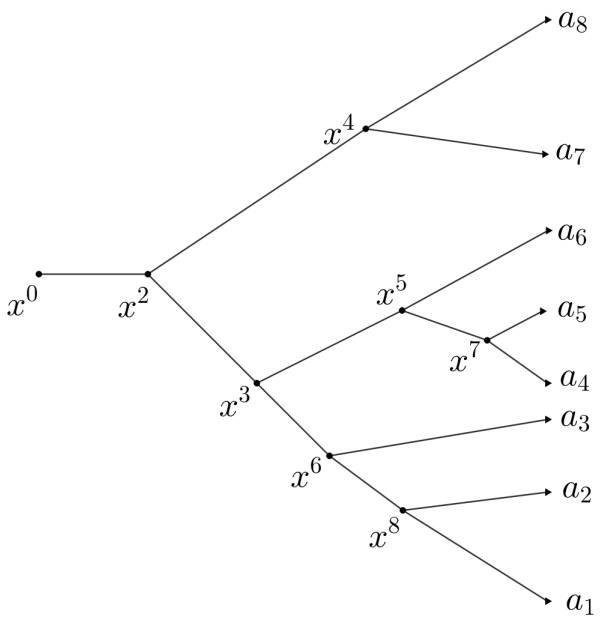

Figure 1.40: Illustration for Example 1.119.

Proposition 1.120. *Let us consider the contact tree $\mathcal{CT}(\mathcal{A})$ of the roots $a_i(x) \in \mathcal{A}$, $i = 1,\ldots,m+1$ of the polynomial $P_x(y)$. Let us suppose that the contact tree is complete binary. If $i < j$, then*

$$\nu_x\left(\pm\mathrm{S}_i \pm \mathrm{S}_{i+1} \pm \ldots \pm \mathrm{S}_{j-1}\right) = \nu_x(\mathrm{S}_k)\,,$$

where S_k denotes the unique area corresponding to the bifurcation vertex $a_i\wedge a_j$.

Proof. Let us take $\ell \in \{i, \dots, j-1\}$ such that $\ell \neq k$. We have $v_k <_{\mathcal{CT}} v_\ell$. By Proposition 1.116, we have $\nu_x(\mathrm{S}_\ell) > \nu_x(\mathrm{S}_k)$.

Now, since S_k has the minimal valuation in the sum $\pm\mathrm{S}_i \pm \mathrm{S}_{i+1} \pm \ldots \pm \mathrm{S}_{j-1}$ and since the contact tree is binary this valuation appears only once, we conclude that

$$\nu_x\left(\pm\mathrm{S}_i \pm \mathrm{S}_{i+1} \pm \cdots \pm \mathrm{S}_{j-1}\right) = \nu_x(\mathrm{S}_k).$$

□

1.7.6 Doubly asymptotic inequalities

QUESTION 1.121. How can we construct explicitly a polynomial such that for any $i \neq j$,

$$\delta_i \prec_+ \delta_j \Leftrightarrow \mathrm{S}_i \prec_+ \mathrm{S}_j?$$

ANSWER: By choosing the special valuations

$$e_i := p^{f_i},$$

with p sufficiently large and $f_i \in \mathbb{N}$.

It will be important in the sequel to keep in mind the following equivalences:

$$f_k < f_\ell \Leftrightarrow e_k < e_\ell \Leftrightarrow \delta_k \succ_+ \delta_\ell.$$

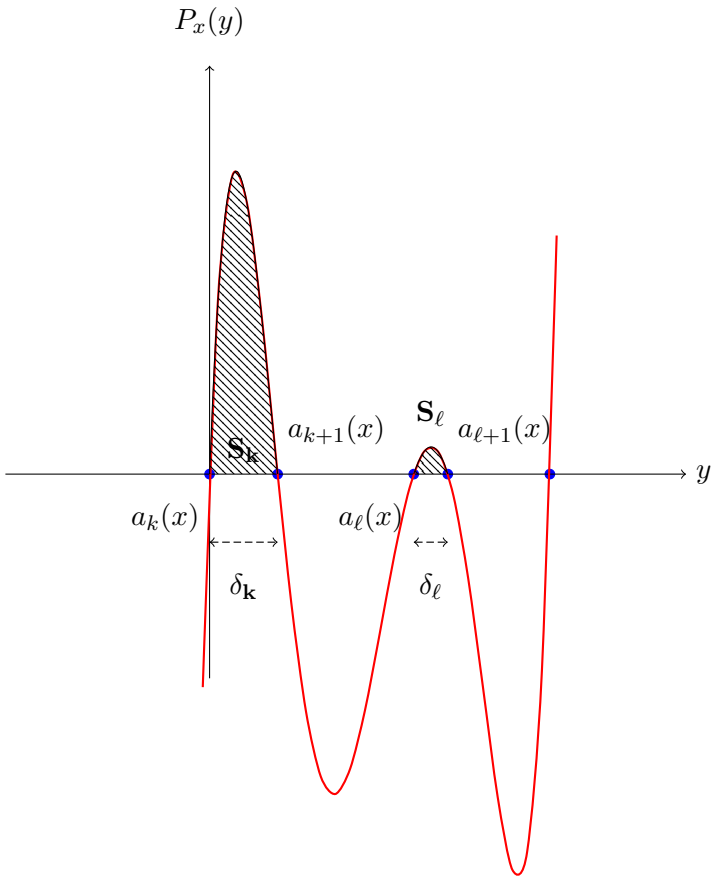

Figure 1.41: For any $k \neq l$, $\delta_k \succ_+ \delta_\ell$ implies $\mathrm{S}_k \succ_+ \mathrm{S}_\ell$.

EXAMPLE 1.122. We can consider for instance $\delta_i(x) := x^{p^{f_i}}$ and thus $a_1(x) = 0$, $a_2(x) = \delta_1 = x^{p^{f_1}}$, $a_3(x) = \delta_1 + \delta_2 = x^{p^{f_1}} + x^{p^{f_2}}$ etcetera, $a_{m+1}(x) = \delta_1 + \ldots + \delta_m = x^{p^{f_1}} + \ldots + x^{p^{f_m}}$. In this case, we shall be able to compare the areas two by two as follows (see Theorem 1.125): $\delta_k(x) > \delta_\ell(x) \Leftrightarrow \mathrm{S}_k(x) > \mathrm{S}_\ell(x), \forall k \neq l$.

PROBLEM 1.123. One can obtain any total order relation between all the valuations e_i, for $i = 1, \ldots, m$ which decorate the contact tree, by choosing the right family of polynomials which realise the tree as described in Definition 1.92. The problem is that a total order relation is not sufficient to determine the total order relation between the areas S_i, for $i = 1, \ldots, m$, as one saw in Example 1.119. This example provides a complete binary contact tree where there exist $e_7 > e_3$ but $\nu_x(\mathrm{S}_7) < \nu_x(\mathrm{S}_3)$, which is the opposite inequality compared to the one we want to obtain. Therefore, imposing the conditions that the contact tree is an end-rooted complete binary plane tree and that there is a total order relation between the vertices of the contact tree is not sufficient for the answer to Question 1.121.

IDEA 1.124. If we choose special valuations e_i, $i = 1, \ldots, m$, which depend on a parameter $p \gg 1, p \in \mathbb{N}$, we obtain the total order relation between the areas. In other words, if besides the total order relation of the valuations for a sufficiently small $x > 0$ we have $e_i \in \mathbb{Z}[p]$, monic polynomials with integer coefficients, $\deg(e_i) := f_i \geq 1$, such that $f_i \neq f_j$ for any $i \neq j$, we shall obtain the total order relation between the areas, as we prove in Theorem 1.125 below.

Theorem 1.125. *Let us consider two vertices V_ℓ and V_k in a contact tree which is an end-rooted complete binary plane tree. Recall that $e_i := \nu_x(\delta_i)$, for any $i = 1, \ldots, m$. Take $p \gg 1, p \in \mathbb{N}$ large enough and the natural numbers $f_i \in \mathbb{N}$ such that $f_i \neq f_j$ for $i \neq j$. If we choose $e_i := p^{f_i}$, then for any sufficiently small $0 < x \ll 1$, the following equivalence holds:*

$$\delta_k(x) > \delta_\ell(x) \Leftrightarrow \mathrm{S}_k(x) > \mathrm{S}_\ell(x), \forall k \neq l.$$

Proof. If V_ℓ and V_k are comparable, we are in the situation of Proposition 1.116.

Let us consider two vertices V_ℓ and V_k which are not comparable. By Corollary 1.113, one has $\nu_x(\mathrm{S}_k) = \sum_{j=1}^{k} q_{kj} e_j + e_k = \sum_{j=1}^{k} q_{kj} p^{f_j} + p^{f_k} = (q_{kk} + 1)p^{f_k} + \mathrm{L.O.T}_{p\to\infty}$ and $\nu_x(\mathrm{S}_\ell) = \sum_{j=1}^{l} q_{\ell j} e_j + e_\ell = \sum_{j=1}^{l} q_{\ell j} p^{f_j} + p^{f_\ell} = (q_{\ell\ell} + 1)p^{f_\ell} + \mathrm{L.O.T}_{p\to\infty}$. By hypothesis, $\delta_k > \delta_\ell$, namely $e_k < e_\ell$, which is equivalent to $p^{f_k} < p^{f_\ell}$. Thus for a sufficiently large $p \to \infty$, $(q_{kk} + 1)p^{f_k} < (q_{\ell\ell} + 1)p^{f_\ell}$. In conclusion, $\nu_x(\mathrm{S}_k) < \nu_x(\mathrm{S}_\ell)$, hence $\mathrm{S}_k \succ \mathrm{S}_\ell$.

□

1.8 A construction of all the separable Poincaré-Reeb trees in one variable

The aim of this section is to associate to every separable snake $\sigma : \{1, 2, \ldots, m+1\} \to \{1, 2, \ldots, m+1\}$ such that $\sigma(m) > \sigma(m+1)$, an explicit polynomial $Q_x(y) \in \mathbb{R}[x][y]$ such that for every sufficiently small $x > 0$, the univariate polynomial $Q_x(y)$ is $(m+2)$-Morse and realises the given snake (see Theorem 1.149).

1.8.1 Separable permutations

In this section, we consider a special set of snakes (see Definition 1.6), i.e. the snakes that are separable permutations.

Definition 1.126. [Kit11, page 57] Let $\pi : \{1, \ldots, m\} \to \{1, \ldots, m\}$ and $\sigma : \{1, \ldots, n\} \to \{1, \ldots, n\}$ be two permutations. Then their **direct sum** $\pi \oplus \sigma$ and their **skew sum** $\pi \ominus \sigma$ are defined as follows:

$$\pi \oplus \sigma(i) := \begin{cases} \pi(i), i = 1, \ldots, m; \\ \sigma(i-m) + m, i = m+1, \ldots, m+n. \end{cases}$$

$$\pi \ominus \sigma(i) := \begin{cases} \pi(i) + n, i = 1, \ldots, m; \\ \sigma(i - m), i = m + 1, \ldots, m + n. \end{cases}$$

EXAMPLE 1.127. Let us consider the following two permutations: $\pi := \begin{pmatrix} 1 & 2 & 3 & 4 & 5 & 6 \\ 4 & 6 & 5 & 3 & 1 & 2 \end{pmatrix}$ and $\sigma := \begin{pmatrix} 1 & 2 & 3 \\ 1 & 3 & 2 \end{pmatrix}$. Thus by Definition 1.126, we obtain:

$$\pi \oplus \sigma = \begin{pmatrix} 1 & 2 & 3 & 4 & 5 & 6 & 7 & 8 & 9 \\ 4 & 6 & 5 & 3 & 1 & 2 & 7 & 9 & 8 \end{pmatrix}$$

$$\pi \ominus \sigma = \begin{pmatrix} 1 & 2 & 3 & 4 & 5 & 6 & 7 & 8 & 9 \\ 7 & 9 & 8 & 6 & 4 & 5 & 1 & 3 & 2 \end{pmatrix}$$

A very useful visual matrix representation of the direct sum (respectively of the skew sum) of π and σ can be seen in Figure 1.42 (respectively in Figure 1.43) below (see [Kit11, page 4]).

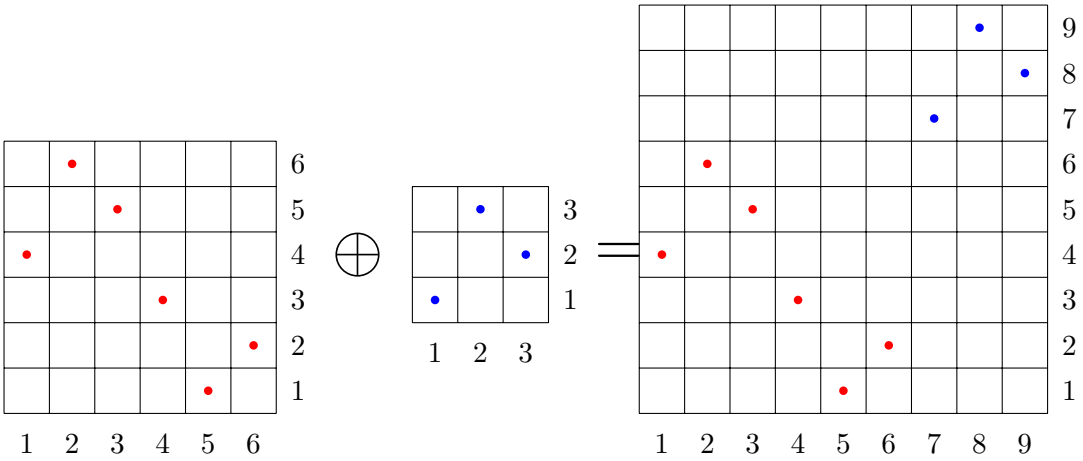

Figure 1.42: The direct sum $\pi \oplus \sigma$.

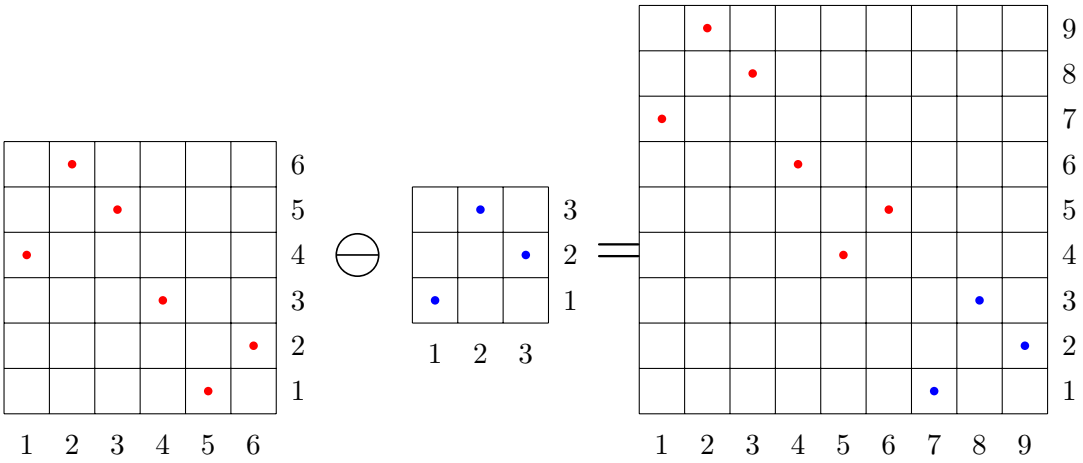

Figure 1.43: The skew sum $\pi \ominus \sigma$.

The notion of separable permutation was introduced in [BBL98].

Definition 1.128. [Kit11, page 57] A **separable permutation** is a permutation that is obtained by applying several times the $\oplus$ and $\ominus$ operations to the identity permutation of a single element, denoted by $\boxdot := \begin{pmatrix} 1 \\ 1 \end{pmatrix}$.

Definition 1.129. Given a separable permutation σ, **a decomposition of** σ consists of a sequence of operations $\oplus$ and $\ominus$ applied to the identity permutation $\boxdot := \begin{pmatrix} 1 \\ 1 \end{pmatrix}$, such that the result gives us σ.

Remark 1.130. The $\oplus$ operation is (individually) associative and the $\ominus$ operation is (individually) associative (see [AHP15, page 2]). Therefore, a separable permutation can have several decompositions.

For a new characterisation of the set of separable permutations, the reader should refer to Étienne Ghys's recent book [Ghy17, page 27].

The following definition of a binary separating tree associated to a separable permutation follows the one given in [BBL98, page 280].

The reader should remember Definition 1.58 of an end-rooted complete plane binary tree.

Definition 1.131. [Kit11, page 5] An **interval** is a non-empty sequence of contiguous integers.

Example 1.132. An example of interval is a permutation.

Definition 1.133. If σ is a separable permutation of $\{1, 2, \ldots, m+1\}$, then **a binary separating tree associated to the separable permutation** σ is a complete plane binary tree T such that:

(a) its root is at the top;

(b) its leaves are decorated with $\sigma(1)$, $\sigma(2)$,..., $\sigma(m+1)$ in this order from left to right;

(c) for every internal vertex v, the leaves (seen as a non-ordred set of numbers, for instance (2 3 1)) of the subtree of v form an interval, which we call **the interval of the node** v;

(d) let us denote by v_{left} and by v_{right} the left child and the right child of the node v, respectively; the internal vertices of T are decorated with $\oplus$ or $\ominus$ as follows:

-if all the numbers of the interval of v_{left} are smaller than all the numbers of the interval of v_{right}, then v is **a positive vertex** and is decorated with the $\oplus$ sign;

-if all the numbers of the interval of v_{left} are bigger than all the numbers of the interval of v_{right}, then v is **a negative vertex** and is decorated with the $\ominus$ sign.

To obtain the separating tree, one should follow step by step the decomposition in direct sums and skew sums of a separable permutation.

Remark 1.134. To a separable permutation one may associate several binary separating trees, as one could see for instance in Example 1.135. This is due to the associativity mentioned in Remark 1.130.

Example 1.135. An example of a separable permutation is $\sigma := \begin{pmatrix} 1 & 2 & 3 & 4 & 5 & 6 & 7 \\ 6 & 7 & 4 & 5 & 1 & 3 & 2 \end{pmatrix}$. The reader can observe in Figure 1.44 and in Figure 1.45 two possible ways in which σ can be decomposed by repeatedly applying the $\oplus$ and $\ominus$ operations. The algorithm gives us two binary separating trees of σ. The non-unicity of the decompositions of a separable permutation is due to the associativity of the operation $\oplus$ and of the associativity of the operation $\ominus$.

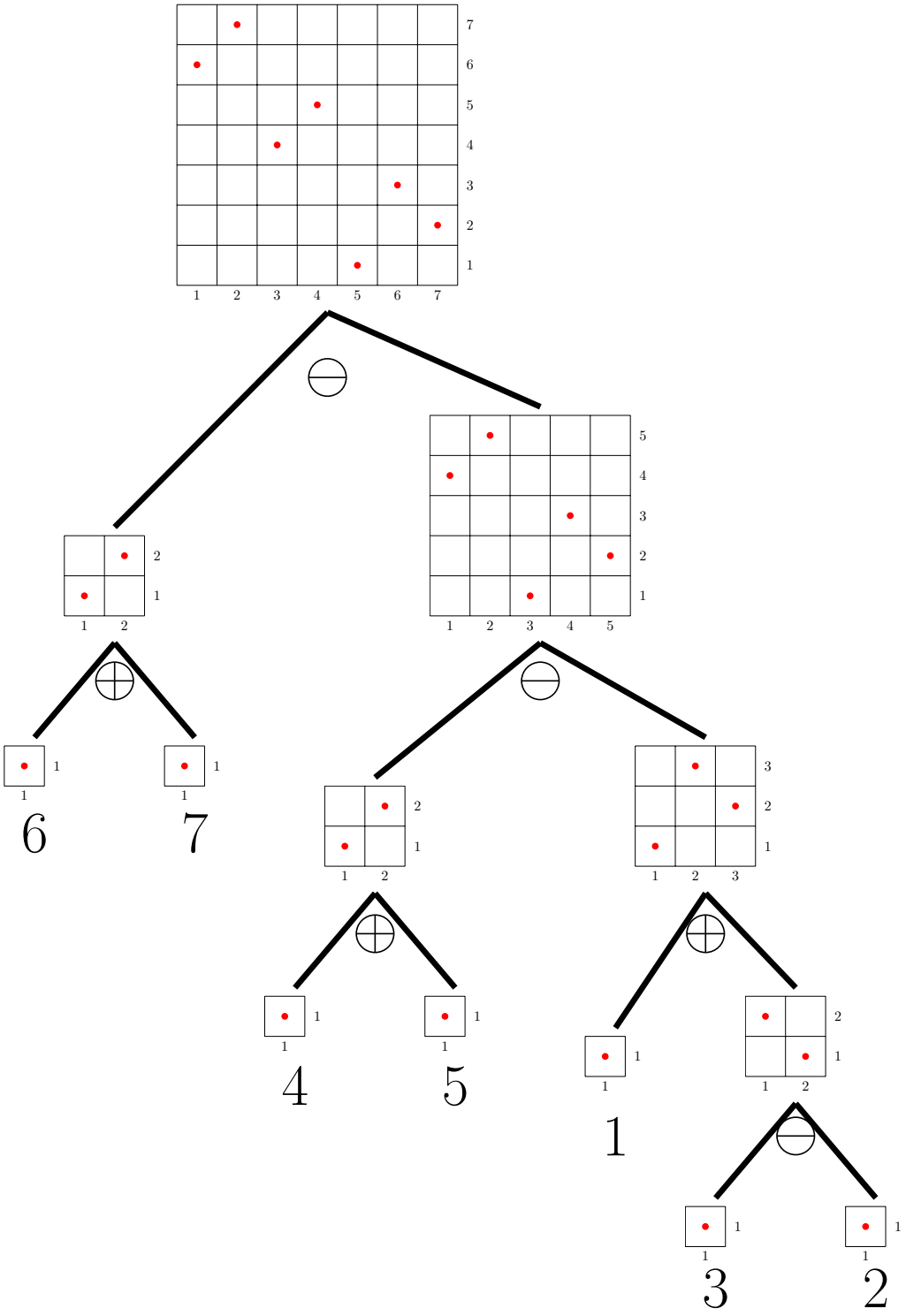

Figure 1.44: One possible decomposition: $\sigma = (\boxdot \oplus \boxdot) \ominus ((\boxdot \oplus \boxdot) \ominus (\boxdot \oplus (\boxdot \ominus \boxdot)))$.

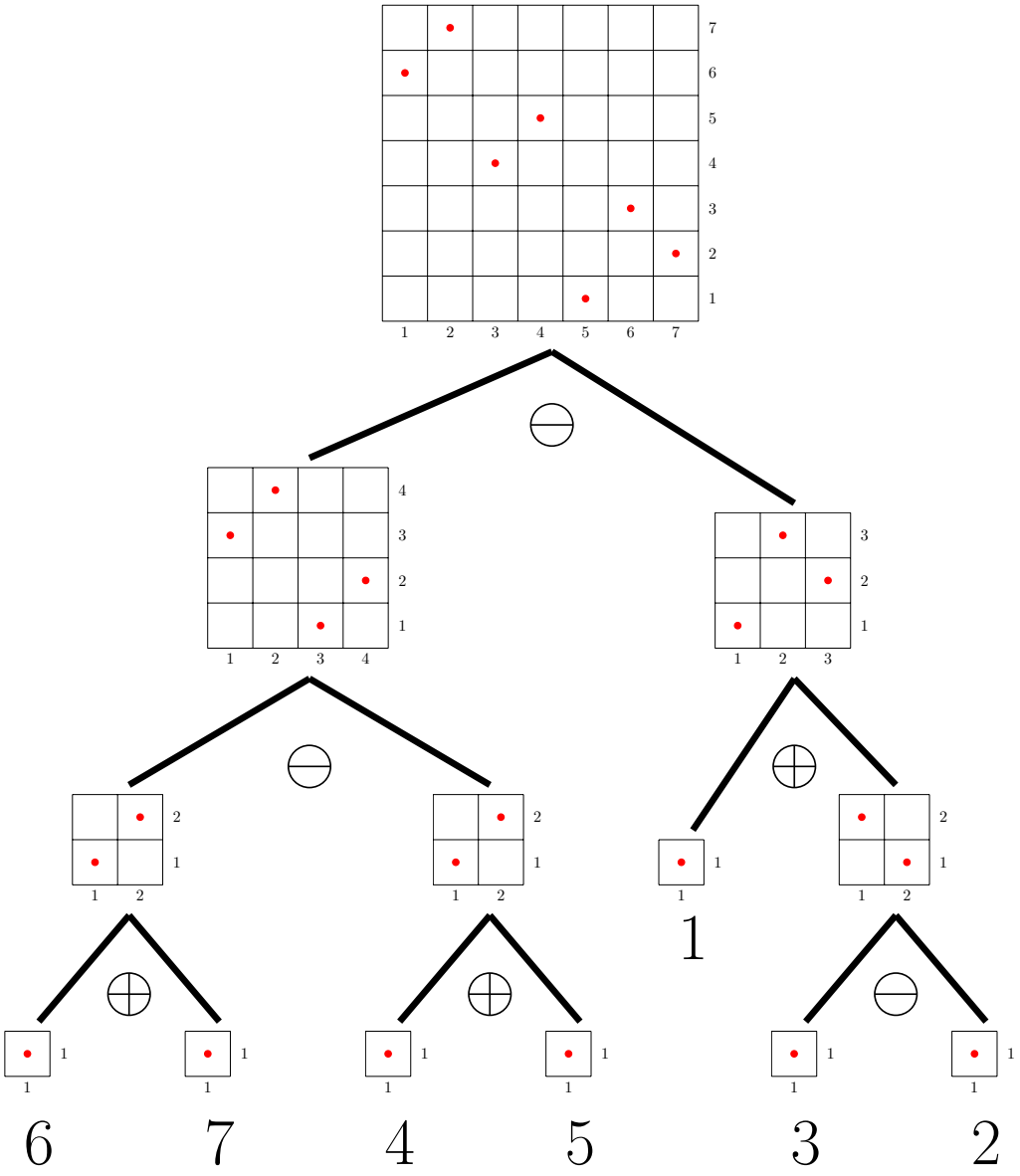

Figure 1.45: Another possible decomposition: $\sigma = ((\boxdot \oplus \boxdot) \ominus (\boxdot \oplus \boxdot)) \ominus (\boxdot \oplus (\boxdot \ominus \boxdot))$.

Remark 1.136. [BR06, page 3] If one also considers non-binary separating trees, then each separable permutation possesses a unique tree, obtained from any of its binary separating trees by contracting all edges between vertices decorated with the same sign (see Figure 1.46). This is due to the associativity properties of $\oplus$, respectively $\ominus$, operations. We shall not go into further details, since our interest are the binary trees associated to separable permutations. See [AHP15, page 4].

Example 1.137. Let us consider the same separable permutation $\sigma := \begin{pmatrix} 1 & 2 & 3 & 4 & 5 & 6 & 7 \\ 6 & 7 & 4 & 5 & 1 & 3 & 2 \end{pmatrix}$ from Example 1.135. Thanks to the associativity of the $\ominus$ operation, we can contract any of its two binary separating trees (see Figure 1.44 and Figure 1.45) in a non-binary tree. This is due to the fact that a parent node and its child have the same sign (here, $\ominus$). The contracted tree is shown in Figure 1.46 below.

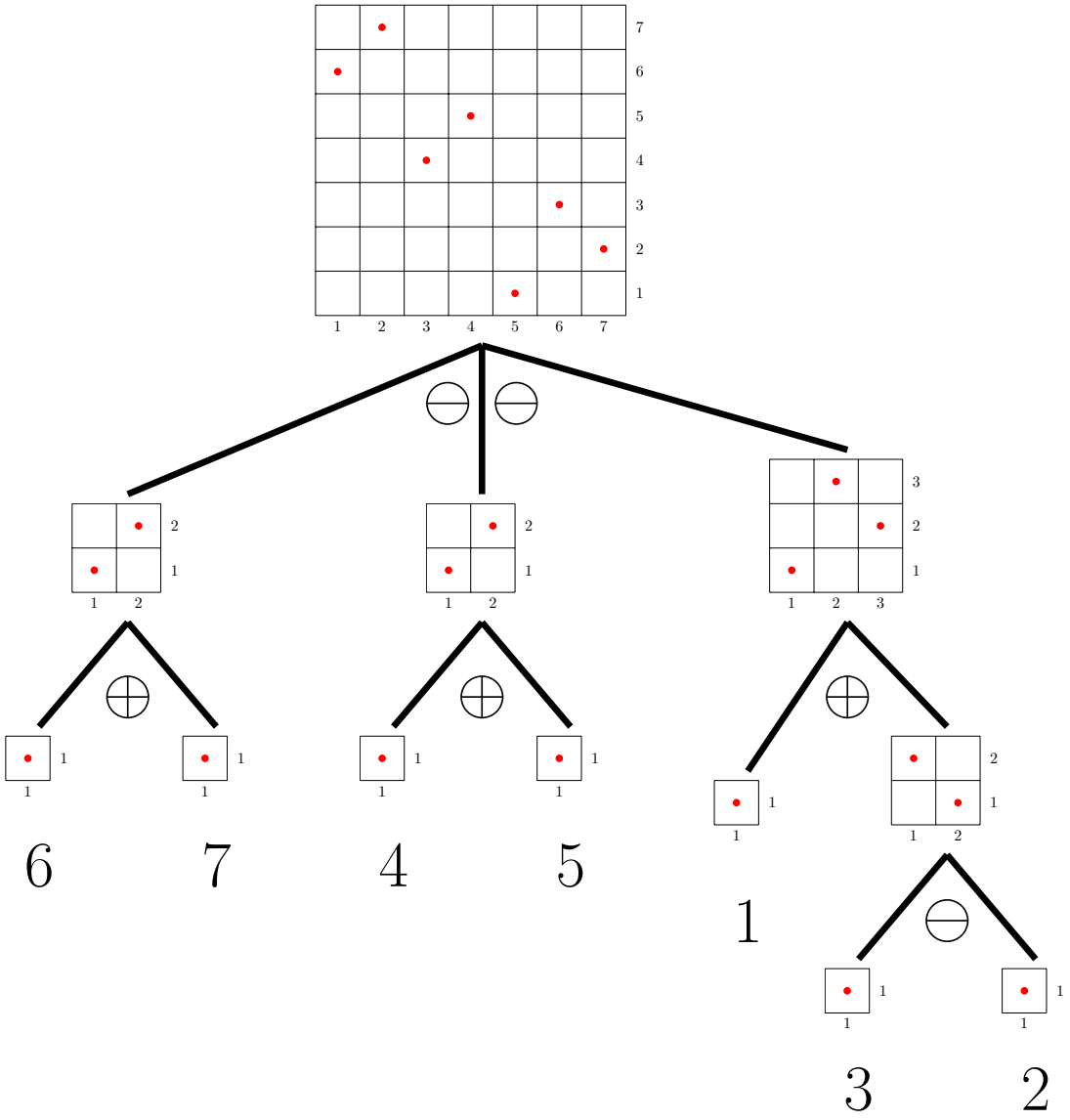

Figure 1.46: The associativity of $\ominus$ gives us the unique contracted tree associated to a separable permutation from any of its binary separating trees: $\sigma = (\boxdot \oplus \boxdot) \ominus (\boxdot \oplus \boxdot) \ominus (\boxdot \oplus (\boxdot \ominus \boxdot))$.

By Definition 1.128, the separable permutations have a recursive structure. We give now a recursive definition (see Remark in 1.56) of these binary decompositions that are obtained by applying several times the $\oplus$ and $\ominus$ operations.

Definition 1.138. The set of binary decompositions is defined recursively as follows:

(a) the trivial permutation $\boxdot := \begin{pmatrix} 1 \\ 1 \end{pmatrix}$ is itself a binary decomposition;

(b) if d_1 and d_2 are two binary decompositions, then the direct sum $d_1 \oplus d_2$ and the skew sum $d_1 \ominus d_2$ are both binary decompositions.

The above recursive definition will play an important role in establishing a bijection between the set of all the binary decompositions of a separable permutation σ and the set of all the binary separating trees associated to σ (recall the recursive Definition 1.54 and Definition 1.133), as the following Proposition 1.141 shows.

Notation 1.139. *If T_1 and T_2 are two complete binary plane trees, then by $T_1 \oplus T_2$ (respectively $T_1 \ominus T_2$) we denote the new complete binary plane tree obtained by creating a new vertex decorated with the sign $\oplus$ (respectively $\ominus$) such that its left subtree is T_1 and its right subtree is T_2.*

A reformulation of Definition 1.128 is the following:

Proposition 1.140. *[BBL98, page 280] A permutation σ is separable* if and only if *there exists a **binary** tree that is a separating tree associated to σ.*

Proposition 1.141. *There is a bijection between the set of all the binary decompositions of a separable permutation σ and the set of all the binary separating trees associated to σ.*

Proof. We give an inductive proof that follows the structure of the recursively defined sets (see Definition 1.54 and 1.138). The proof has two parts: (a), where we show that the proposition holds for all the minimal structures of the set, and (b) where we prove that if it holds for the immediate substructures of a certain structure $\mathcal{S}$ then it must hold for $\mathcal{S}$ too.

(a) First let us show by structural induction that to every binary decomposition one can associate a unique binary separating tree.

-to the trivial permutation one can associate uniquely the tree with one vertex;

-if d_1 and d_2 are two binary decompositions which have each a uniquely associated binary separating tree T_1 and T_2 respectively, then to $d_1 \oplus d_2$ (respectively $d_1 \ominus d_2$) we shall associate the unique binary separating tree $T_1 \oplus T_2$ (respectively $T_1 \ominus T_2$).

(b) A similar structural recursive proof can be given to show that to each binary separating tree one can associate a unique binary decomposition.

□

Remark 1.142. Given a complete binary plane tree such that all its vertices, except from the leaves are decorated with $\oplus$ or $\ominus$ sign, we can construct the unique separable permutation corresponding to it, by using Proposition 1.141 to obtain the decomposition of the permutation.

In other words, one can see any binary decomposition of a separable permutation σ as a complete plane binary tree which is in fact one of the binary separating trees of σ. In addition, if the binary decomposition has m signs, then the tree has m internal nodes and $m+1$ leaves.

Example 1.143. An example which illustrates the bijection from 1.141 is shown in Figure 1.44 and Figure 1.45.

We have now a Corollary of Proposition 1.140, as follows:

Corollary 1.144. *A permutation σ is separable* if and only if *σ has a **binary** separating decomposition.*

We conclude by emphasizing the fact that there is a bijective correspondence between the signs in a binary decomposition of σ and the internal vertices of the corresponding binary separating trees associated to σ. In addition, the internal vertices are not only decorated with the corresponding signs $\oplus$ or $\ominus$, but they also correspond to a certain matrix as one can see in the following definition.

Definition 1.145. Let us consider a separable permutation σ and one of its binary separating trees, say $T(\sigma)$. Let us suppose that $i < j$. We denote by $\sigma(i) \wedge \sigma(j)$ the internal vertex of $T(\sigma)$ where the geodesics from the root to the leaves $\sigma(i)$ and $\sigma(j)$ separate.

Definition 1.146. Let us consider a separable permutation σ. Let us denote by $\mathrm{mat}(\sigma(i) \wedge \sigma(j))$ the minimal submatrix of σ that contains $\sigma(i)$ and $\sigma(j)$.

In order to understand better the notion of minimal submatrix of a permutation, the reader is invited to read Example 1.147.

EXAMPLE 1.147. If $\sigma := \begin{pmatrix} 1 & 2 & 3 & 4 & 5 & 6 & 7 \\ 6 & 7 & 4 & 5 & 1 & 3 & 2 \end{pmatrix}$, let us illustrate in Figure 1.47 the matrix $\mathrm{mat}(\sigma(1) \wedge \sigma(4)) = \begin{pmatrix} 1 & 2 & 3 & 4 \\ 3 & 4 & 1 & 2 \end{pmatrix}$ which is the minimal submatrix of σ that contains $\sigma(1) = 6$ and $\sigma(4) = 5$. In addition, we show $\mathrm{sign}(\sigma(1) \wedge \sigma(4)) = \ominus$. Let us remark that $\sigma(1) > \sigma(4)$, i.e. $6 > 5$.

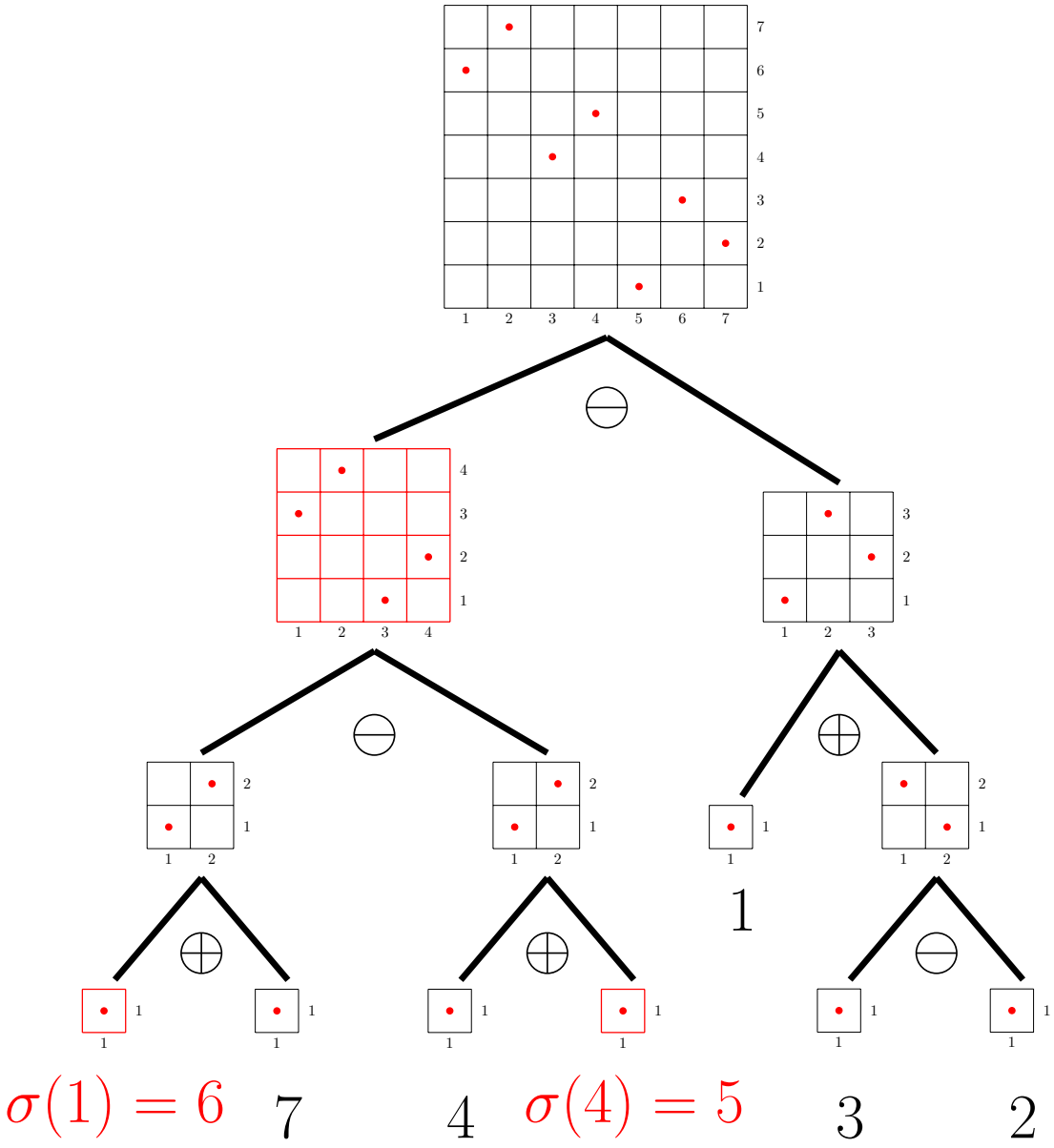

Figure 1.47: The matrix (in red) of $\sigma(1) \wedge \sigma(4)$ (in red) and the sign $\ominus$ of its corresponding vertex in the separating tree of σ.

Proposition 1.148. *Let us consider a separable permutation σ and one of its binary separating trees, say $T(\sigma)$. Let us suppose that $i < j$. If one denotes by $\sigma(i) \wedge \sigma(j)$ the internal vertex of $T(\sigma)$ where the geodesics from the root to the leaves $\sigma(i)$ and $\sigma(j)$ separate, then*

$$\sigma(i) < \sigma(j) \Leftrightarrow \mathrm{sign}(\sigma(i) \wedge \sigma(j)) = \oplus$$

and

$$\sigma(i) > \sigma(j) \Leftrightarrow \text{sign}(\sigma(i) \wedge \sigma(j)) = \ominus.$$

Proof. We have $\text{sign}(\sigma(i) \wedge \sigma(j)) = \oplus$ (respectively $\text{sign}(\sigma(i) \wedge \sigma(j)) = \ominus$) if and only if we can decompose the submatrix $\text{mat}(\sigma(i) \wedge \sigma(j)) = m_1 \oplus m_2$ (respectively $\text{mat}(\sigma(i) \wedge \sigma(j)) = m_1 \ominus m_2$) such that m_1 contains $\sigma(i)$ and m_2 contains $\sigma(j)$. Now by Definition 1.126, $\text{mat}(\sigma(i) \wedge \sigma(j)) = m_1 \oplus m_2$ if and only if $\sigma(i) < \sigma(j)$ (respectively $\text{mat}(\sigma(i) \wedge \sigma(j)) = m_1 \ominus m_2$ if and only if $\sigma(i) > \sigma(j)$). □

1.8.2 Realising a given separable snake

The fact that Davis', Arnold's and Douady's approaches (see Section 1.3) were not constructive motivated us to write this section, which is dedicated to our new and constructive proof of the existence of a polynomial with preassigned critical values configuration (i.e. which should be associated to a given snake). More precisely, we present here an origina result that, in comparison with the one in Section 1.3.1, is constructive: Theorem 1.149.

Theorem 1.149. *Consider $m \in \mathbb{N}$ and fix a separable $(m+1)$-snake $\sigma : \{1, 2, \dots, m+1\} \to \{1, 2, \dots, m+1\}$ such that $\sigma(m) > \sigma(m+1)$. Then we construct a polynomial $Q_x(y) \in \mathbb{R}[x][y]$,*

$$Q_x(y) := \int_0^y \prod_{i=1}^{n} (t - a_i(x)) \mathrm{d}t,$$

which is $(m+2)$-Morse (see Definition 1.14) such that, for sufficiently small $x > 0$, the snake associated to $Q_x(y)$ is σ, by choosing the polynomials $a_i(x) \in \mathbb{R}[x]$ such that their contact tree is one of the binary separating trees of σ.

Remark 1.150. Notice that we do not give a precise value $x_0 > 0$ sufficiently small such that the above theorem holds for all $0 < x \leq x_0$.

Before the proof of Theorem 1.149, let us prove some useful lemmas.

Lemma 1.151. *Let $\sigma : \{1, 2, \dots, m+1\} \to \{1, 2, \dots, m+1\}$ be a separable permutation. A binary decomposition of σ has alternating signs $\oplus$ and $\ominus$ if and only if σ is an $(m+1)$-snake (see Definition 1.6).*

Proof. By Definition 1.126 and Definition 1.128, if there are two signs $\oplus$ (respectively two signs $\ominus$) that appear consecutively in the binary decomposition, then σ is not a snake. Reversely, if σ is not a snake, then it has three leaves such that $\sigma(i) < \sigma(i+1) < \sigma(i+2)$ (respectively $\sigma(i) > \sigma(i+1) > \sigma(i+2)$) and this implies two signs $\oplus$ (respectively two signs $\ominus$) that appear consecutively in the binary decomposition. □

Corollary 1.152. *Let $\sigma : \{1, 2, \dots, m+1\} \to \{1, 2, \dots, m+1\}$ be a separable snake such that $\sigma(m) > \sigma(m+1)$. Then any binary decomposition of σ has alternating signs $\oplus$ and $\ominus$ such that the rightmost sign is $\ominus$.*

Lemma 1.153. *Let K_+ be an end-rooted complete plane binary tree, which has $m+1$ leaves. Then there exist $m+1$ polynomials with real coefficients $a_i(x) \in \mathbb{R}[x]$, for $i = 1, \dots, m+1$, such that $a_i(0) = 0$ for $i = 1, \dots, m+1$ and $K_+ = \mathcal{CT}(a_1(x), \dots, a_{m+1}(x))$, where $\mathcal{CT}(a_1(x), \dots, a_{m+1}(x))$ represents the contact tree of the polynomials a_i, introduced in Section 1.7.*

The result of Lemma 1.153 is already mentioned in [Ghy17, page 29]. Let us give a proof.

Proof. We shall construct the polynomials $a_i(x) \in \mathbb{R}[x]$ as follows: we decorate each internal vertex, i.e. bifurcation vertex, with a positive integer number such that the sequence of integer numbers is strictly increasing on each geodesic from the root towards any leaf. The root is decorated with 0. In other words: by taking into account the fact that on each geodesic going from the root the valuations of the monomials in x are increasing, we can assign to each vertex a valuation, say $\nu(v) := p \in \mathbb{N}$ (the root is assigned the 0 valuation); since K_+ is an end-rooted complete binary tree by hypothesis, each internal vertex v of K_+ has exactly two children. Each of the two children of v is connected to v by an edge. Since K_+ is embedded in the real plane, one can decide which is the first child and which is the second child of v, by the induced orientation of $\mathbb{R}^2$. Now let us label the edge connecting v to its first child with the coefficient $c_{first}(v) := 0$ (obtaining thus the monomial $0 \times x^p$). Similarly, let us label the edge connecting v to its second child with the coefficient $c_{second}(v) := 1$ (obtaining thus the monomial $1 \times x^p$). The unique edge starting from the root will have coefficient 0. Now for each leaf $a_i(x)$ we add the monomials on the geodesic $\mathcal{G}_i$ from the root to $a_i(x)$, thus obtaining $a_i(x) = \sum_{v \in \mathcal{G}_i} c_*(v) x^{\nu(v)}$, where $*$ is either *first* or *second*, depending on the geodesic we are following.

□

Remark 1.154. The condition $a_i(0) = 0$ for $i = 1, \ldots, m+1$ is realisable since by hypothesis the tree K_+ is an **end-rooted** complete plane binary tree.

Example 1.155. Given the end-rooted complete plane binary tree K_+ with 5 leaves like in Figure 1.48, one constructs the following polynomials $a_i(x)$, $i = 1, \ldots, 5$ such that $\mathcal{CT}(\{a_1(x), \ldots, a_5(x)\}) = K_+$. We shall procede by following the proof of Lemma 1.153. Namely, let us explain the construction of the leaf $a_1(x)$. On the geodesic $\mathcal{G}_1$ there are two bifurcation vertices, say v_1 and v_2. Let us say that we choose $\nu(v_1) = 2$ and $\nu(v_2) = 3$. Following the rule, we have $a_1(x) = c_{first}(v_1)x^{\nu(v_1)} + c_{first}(v_2)x^{\nu(v_2)} = 0x^2 + 0x^3 = 0$. Similarly, we construct $a_2(x) = 0x^2 + 1x^3 = x^3$, $a_3(x) = 1x^2 + 0x^5 = x^2$, $a_4(x) = 1x^2 + 1x^5 + 0x^6 = x^2 + x^5$ and $a_5(x) = 1x^2 + 1x^5 + 1x^6 = x^2 + x^5 + x^6$.

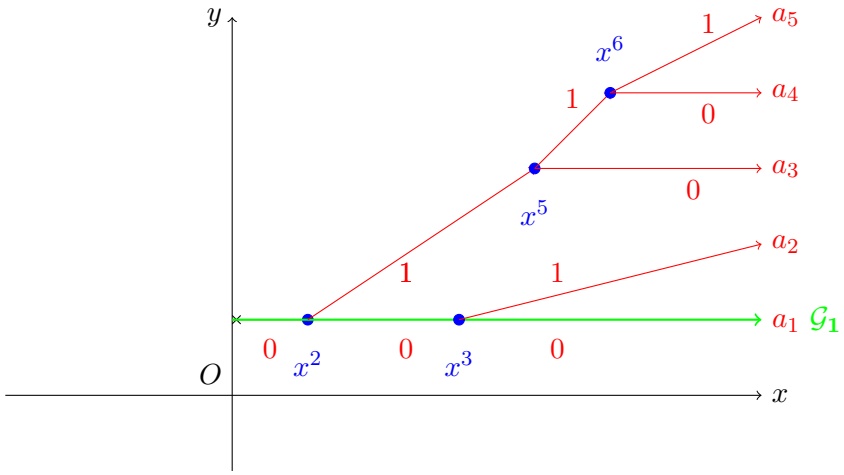

Figure 1.48: The polynomials realising a given end-rooted complete plane binary tree K_+ as their contact tree.

Proof. Let us prove now Theorem 1.149.

There are several steps. First, given a separable $(m+1)$-snake $\sigma : \{1, 2, \ldots, m+1\} \to \{1, 2, \ldots, m+1\}$ such that $\sigma(m) > \sigma(m+1)$, we construct one of its **binary** decomposition trees, denoted by K_+. By Definition 1.133, the leaves of K_+ are in a bijective relation with $\{\sigma(1), \ldots, \sigma(m+1)\}$. By Lemma 1.153 we can choose real polynomials $a_1(x), \ldots, a_{m+1}(x)$ such that (after adding an extra root to K_+, thus transforming it into an **end-rooted** binary

complete tree) we have $K_+ = \mathcal{CT}(a_1(x), \ldots, a_{m+1}(x))$. By the construction of the contact tree, the polynomials are in bijective correspondence with the leaves of the contact tree. In this proof, by abuse of language, if a leaf corresponds to the label $\sigma(i)$ we will sometimes label it with $a_i(x)$, for any $i \in \{1, \ldots, m+1\}$. Since K_+ is an embedded tree which represents both a contact tree and a binary separating tree of σ, this double labelling of the leaves will enable us to identify in the tree the vertices as follows: $a_i \wedge a_j \equiv \sigma(i) \wedge \sigma(j)$. Furthermore, we define the one real variable polynomials $P_x(y), Q_x(y) \in \mathbb{R}[x][y]$, $P_x(y) := \prod_{i=1}^{m+1} \big(y - a_i(x)\big)$ and then $Q_x(y) := (m+2) \int_0^y P_x(t)\mathrm{d}t$. Denote by c_i the critical values of $Q_x(y)$. Finally, we prove that for a sufficiently small $x > 0$, this construction gives us the desired equivalence $c_i > c_j$ if and only if $\sigma(i) > \sigma(j)$.

By hypothesis, σ is separable, thus by Proposition 1.140 σ has at least one binary decomposition. By Proposition 1.141, the binary decomposition corresponds to a binary separating tree. Let us denote this tree by K_+. Now, we have obtained K_+, a binary complete tree. In addition, since σ is also an $(m+1)$-snake $\sigma : \{1, 2, \ldots, m+1\} \to \{1, 2, \ldots, m+1\}$ such that $\sigma(m) > \sigma(m+1)$, by Lemma 1.151 and by Corollary 1.152 we know that the signs of the internal vertices of K_+ alternate and that the rightmost internal vertex is decorated with the $\ominus$ sign.

After adding an extra root to K_+, thus transforming it into an **end-rooted** binary complete tree, let us now apply Lemma 1.153 and construct the polynomials $a_i(x) \in \mathbb{R}[x]$ such that $K_+ = \mathcal{CT}(a_1(x), \ldots, a_{m+1}(x))$.

Let us now define the unitary polynomial $P_x(y) \in \mathbb{R}[x][y]$, of degree $m+1$ in the variable y such that $P_x(y)$ has as simple real distinct roots the polynomials $a_i(x)$ constructed above:

$$P_x(y) := \prod_{i=1}^{m+1} \big(y - a_i(x)\big).$$

Denote by

$$\mathrm{S}_i(x) := \left| \int_{a_i(x)}^{a_{i+1}(x)} P_x(y)\mathrm{d}y \right|.$$

By Corollary 1.115, we have that the area S_m is situated below the Ox-axis and then the positions of the areas alternate above and below. In other words, we say that an area S_i is situated below (respectively above) the Ox-axis when the integral $\int_{a_i(x)}^{a_{i+1}(x)} P_x(y)\mathrm{d}y$ is negative (respectively positive), thus we associate the minus (respectively plus) sign to the area S_i.

Similarly, the reader should remember that the signs of a binary decomposition of the separable snake σ are alternating and ending with $\ominus$. Therefore we obtain

$$\mathrm{sign}(\sigma(i) \wedge \sigma(i+1)) = \ominus \Leftrightarrow \int_{a_i(x)}^{a_{i+1}(x)} P_x(y)\mathrm{d}y < 0$$

and

$$\mathrm{sign}(\sigma(i) \wedge \sigma(i+1)) = \oplus \Leftrightarrow \int_{a_i(x)}^{a_{i+1}(x)} P_x(y)\mathrm{d}y > 0.$$

Furthermore, we denote by

$$Q_x(y) := (m+2) \int_0^y P_x(t)\mathrm{d}t,$$

the unitary polynomial in $\mathbb{R}[x][y]$ such that $\frac{\partial Q_x(y)}{\partial y} = (m+2)P_x(y)$, $Q_x(0) = 0$. Therefore, the critical points of $Q_x(y)$ are the roots of $P_x(y)$, i.e. the polynomials $a_i(x)$, for $i = 1, \ldots, m+1$. The critical values of $Q_x(y)$ are thus

$$c_i := Q_x(a_i(x)),$$

for $i = 1, \ldots, m+1$.

Now by using Corollary 1.115, let us compute the difference between two arbitrary critical values of $Q_x(y)$, say

$$c_j - c_i = Q_x(a_j(x)) - Q_x(a_i(x)) = (m+2)\int_{a_i(x)}^{a_j(x)} P_x(t)\mathrm{d}t = (m+2)((-1)^{m+1-i}\mathrm{S}_i + \ldots + (-1)^{m+1-j}\mathrm{S}_j).$$

For a better understanding, the reader should study Figure 1.49 below.

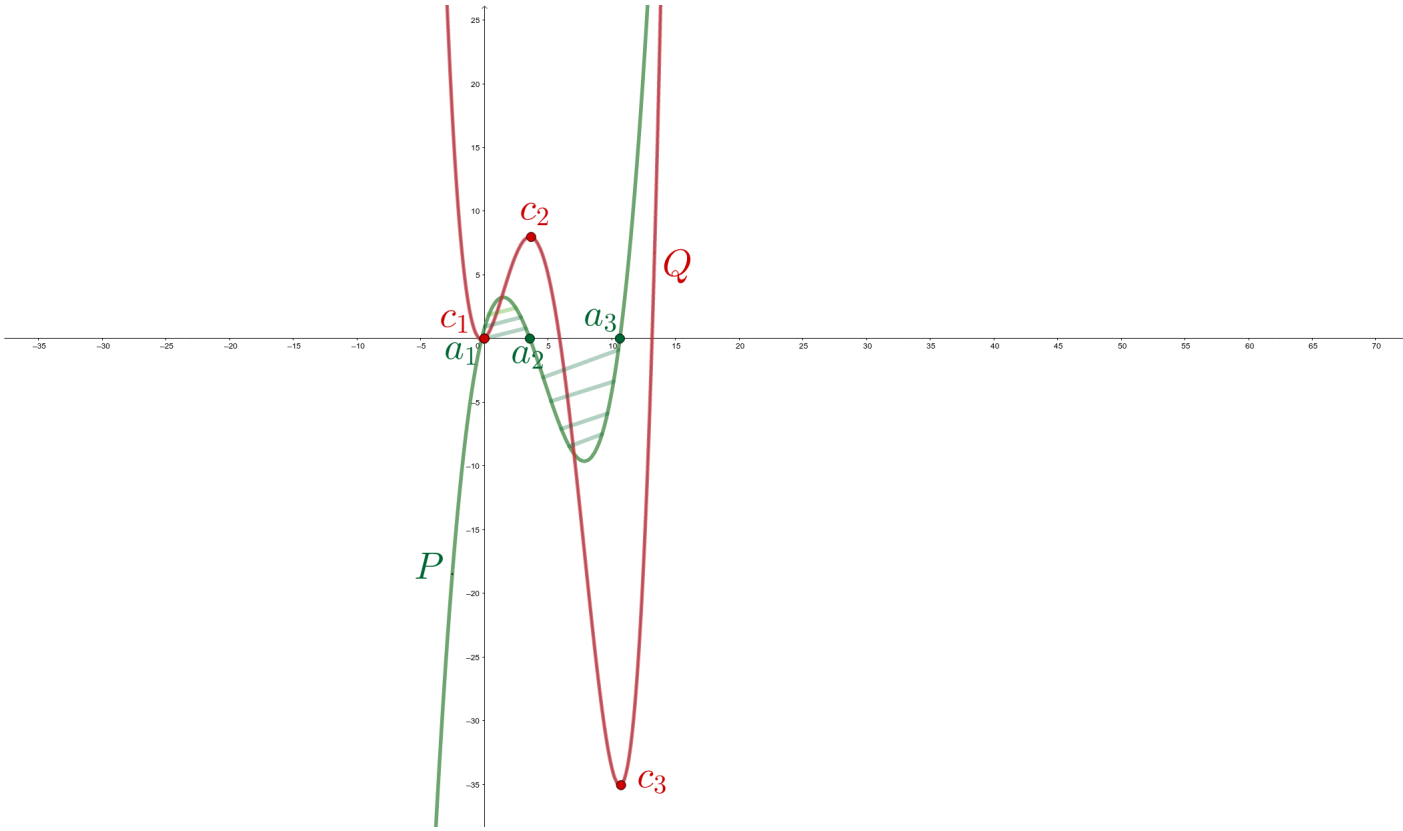

Figure 1.49: Comparing the critical values of the polynomial $Q_x(y)$, in terms of the areas S_i.

By Proposition 1.120, if $i < j$, then

$$\nu_x\left(\pm\mathrm{S}_i \pm \mathrm{S}_{i+1} \pm \ldots \pm \mathrm{S}_{j-1}\right) = \nu_x(\mathrm{S}_k),$$

where S_k denotes the unique area corresponding to the bifurcation vertex $a_i \wedge a_j$. Thus $c_j - c_i > 0$ if and only if the area S_k is situated above the Ox-axis, namely if and only if $\mathrm{sign}(\sigma(i) \wedge \sigma(j)) = \oplus$, which by Proposition 1.148 is equivalent to $\sigma(j) > \sigma(i)$.

The proof is complete: we constructed a polynomial $Q_x(y) \in \mathbb{R}[x][y]$ such that for a sufficiently small $x > 0$ the critical values of $Q_x(y)$ verify $c_j > c_i \Leftrightarrow \sigma(j) > \sigma(i)$, where σ is the given separable snake.

□

Example 1.156. Given the separable snake $\sigma := \begin{pmatrix} 1 & 2 & 3 & 4 & 5 \\ 4 & 5 & 1 & 3 & 2 \end{pmatrix}$, let us construct the real one variable 6-Morse polynomial $Q_x(y) \in \mathbb{R}[x][y]$ such that its associated snake is σ.

First step: obtain a binary separating tree of σ, denoted by K_+, and its associated binary decomposition (see Figure 1.50 below).

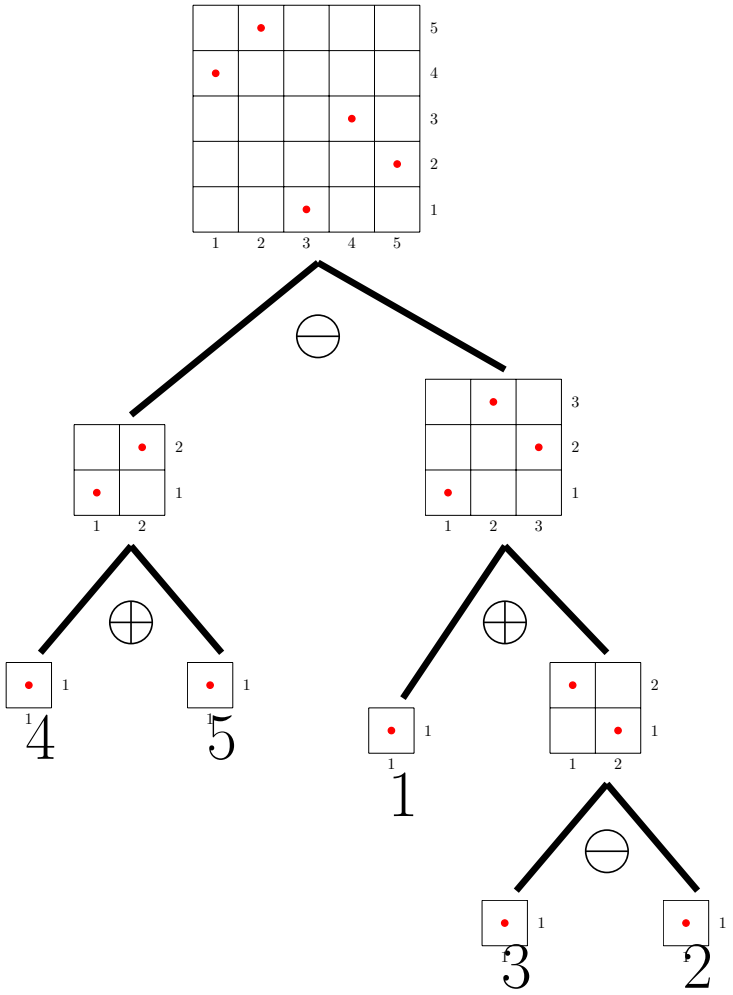

Figure 1.50: A binary separating tree of $\sigma = (\boxdot \oplus \boxdot) \ominus (\boxdot \oplus (\boxdot \ominus \boxdot))$.

Second step: construct the polynomials $a_i(x)$, for $i = 1, \ldots, 5$ such that $\mathcal{CT}(a_1(x), \ldots, a_5(x))$ is the separating tree K_+ of σ. This has already been done for this tree, in Example 1.155 (see Figure 1.51): $a_1(x) = 0$, $a_2(x) = x^3$, $a_3(x) = x^2$, $a_4(x) = x^2 + x^5$ and $a_5(x) = x^2 + x^5 + x^6$. For a better vision we just rotate the embedded separating tree $\pi/2$ counterclockwise, to obtain the tree in Figure 1.51:

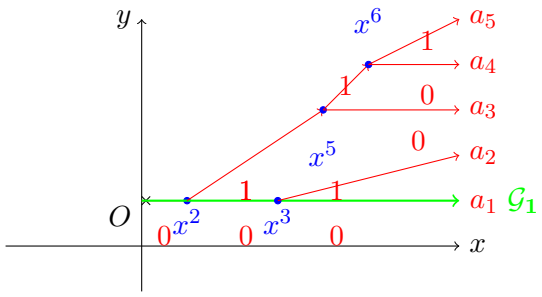

Figure 1.51: The polynomials realising a given end-rooted complete plane binary tree K_+ as their contact tree.

Now, for a sufficiently small $x > 0$, define $P_x(y) \in \mathbb{R}[x][y]$, $P_x(y) := \prod_{i=1}^{5}(y - a_i(x))$ (see Figure 1.52), then $Q_x(y) := 6\int_0^y P_x(t)\mathrm{d}t$ (see Figure 1.53). The critical points of $Q_x(y)$ are the roots of $P_x(y)$. Let us denote by $c_i := Q_x(a_i(x))$ the i-th critical value of $Q_x(y)$.

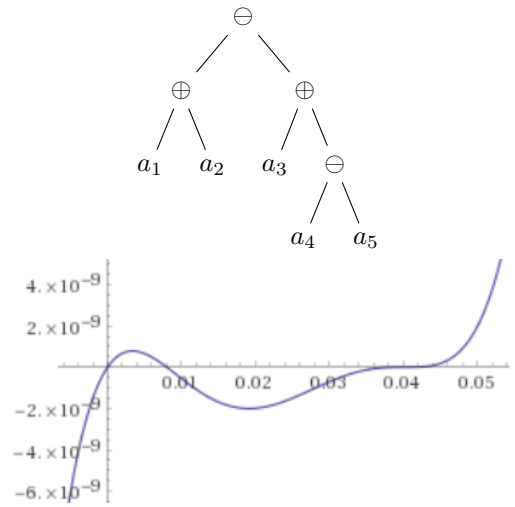

Figure 1.52: The graph of $P_x(y)$ for $x > 0$ small enough: the 5 roots of the polynomial $P_x(y)$ are in bijective correspondance with the leaves of the separating tree of the given separable snake σ; the sign of the internal vertices of the tree are in bijective corespondance with the position of the areas S_i ($\oplus$ for an area above Ox, respectively $\ominus$ for an area below Ox).

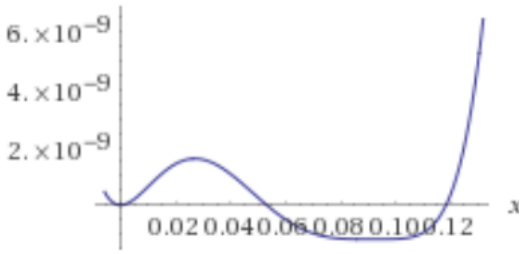

Figure 1.53: The graph of $Q_x(y)$ for $x > 0$ small enough: the snake associated to $Q_x(y)$ is σ.

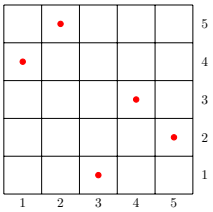

Figure 1.54: The matrix of the separable snake σ.

Remark 1.157. Note that separability of the snakes is due to the hypothesis we impose on the contact trees: they are complete and binary. See Example 1.158, where a non-binary contact tree provides a nonseparable snake.

Example 1.158. In Figure 1.55 we show the snake of the polynomial $Q_x(y) := \int_0^y P_x(t)\mathrm{d}t$, where $P_x(y) = y(y-3x)(y-5x)(y-8x)(y-10x)$. Namely, the snake is $\sigma := \begin{pmatrix} 1 & 2 & 3 & 4 & 5 \\ 1 & 4 & 2 & 5 & 3 \end{pmatrix}$ which is clearly nonseparable, by Lemma [Ghy17, page 14], since there are no two consecutive integers whose images through σ are consecutive.

Note that here the contact tree is not binary.

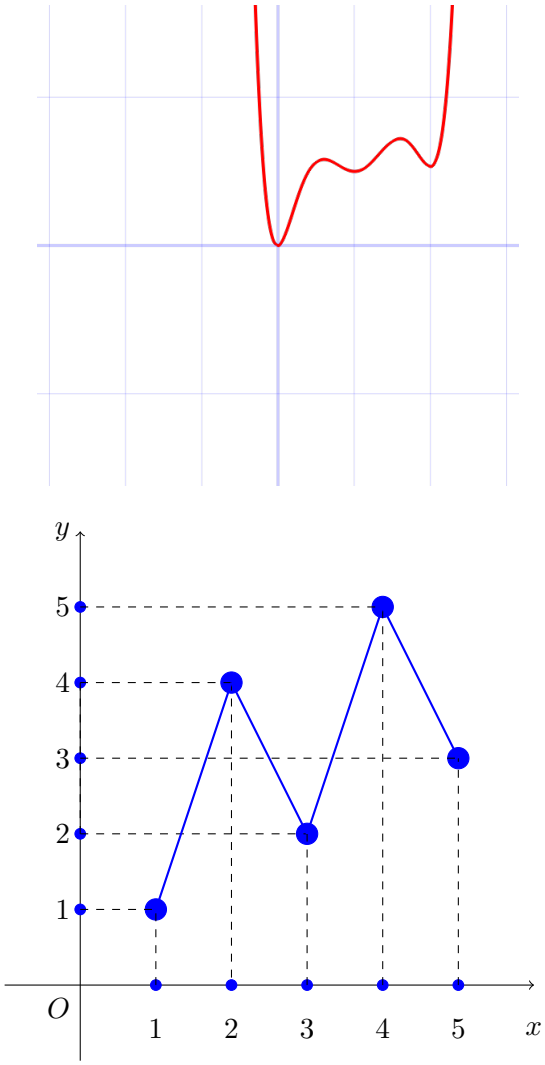

Figure 1.55: Nonseparable snake σ of the polynomial $Q_x(y)$.

1.8.3 The property of the trees associated to separable snakes

In this subsection we will study the separable permutations using their characterisation in terms of avoiding sub-permutations.

Definition 1.159. [Ghy17] The permutations $\begin{pmatrix} 1 & 2 & 3 & 4 \\ 2 & 4 & 1 & 3 \end{pmatrix}$ and $\begin{pmatrix} 1 & 2 & 3 & 4 \\ 3 & 1 & 4 & 2 \end{pmatrix}$ are called **Kontsevich's permutations.**

Definition 1.160. [Ghy17, page 17] A permutation π **contains** one of the Kontsevich's permutations if there are four indices $1 \leq i_1 < i_2 < i_3 < i_4$ such that either $\pi(i_2) < \pi(i_4) < \pi(i_1) < \pi(i_3)$ or $\pi(i_3) < \pi(i_1) < \pi(i_4) < \pi(i_2)$.

A separable permutation is a permutation that does not "contain" (see for instance [Ghy17, page 13]) either of the next two "forbidden" sub-permutations:

$$\begin{pmatrix} 1 & 2 & 3 & 4 \\ 2 & 4 & 1 & 3 \end{pmatrix}$$

or

$$\begin{pmatrix} 1 & 2 & 3 & 4 \\ 3 & 1 & 4 & 2 \end{pmatrix}.$$

An example of a permutation that is not separable is

$$\eta := \begin{pmatrix} 1 & 2 & 3 & 4 & 5 & 6 & 7 & 8 \\ 2 & 3 & 6 & 8 & 1 & 7 & 5 & 4 \end{pmatrix},$$

since it "contains" (see [Ghy17, page 18]) the sub-permutation $\begin{pmatrix} 1 & 2 & 3 & 4 \\ 3 & 1 & 4 & 2 \end{pmatrix}$. Namely, there exist four indices $i_1 := 2$, $i_2 := 3$, $i_3 := 5$, $i_4 := 8$ such that: $i_1 < i_2 < i_3 < i_4$, while we have (see Figure 27): $\eta(i_3) \ll \eta(i_1) \ll \eta(i_4) \ll \eta(i_2)$.

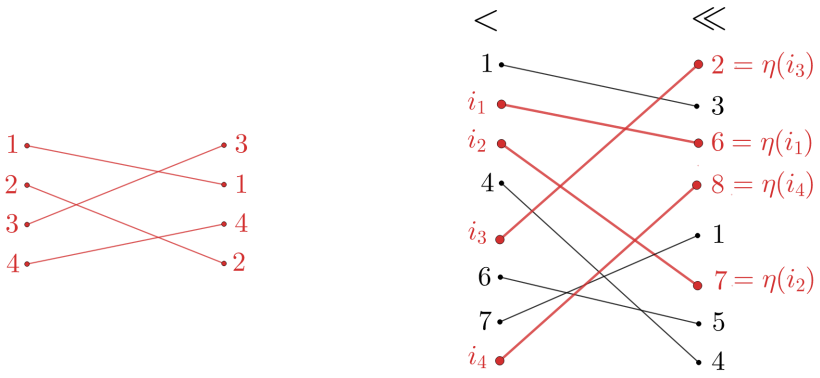

Figure 1.56: The nonseparable permutation η "contains" one of the two "forbidden" permutations.

As before, an alternative representation of the permutation η, through its graph, is drawn in Figure 1.57, where we mark a dot for each pair $(i, \eta(i))$. The forbidden sub-permutation is marked by blue triangles.

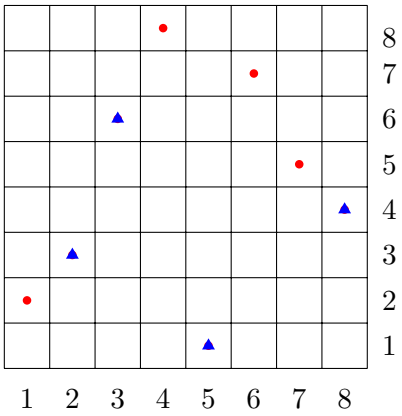

Figure 1.57: The nonseparable permutation η. The "forbidden" sub-permutation is marked by triangles.

Definition 1.161. Let T be an end-rooted complete plane binary tree. Let us denote by $\mathcal{V}^*$ the set of all its vertices, except the root, i.e. all its internal nodes and leaves. We denote by $a \wedge b$ the bifurcation vertex of the geodesics from the root to the leaves a and b. Then the **natural order** relation on $\mathcal{V}^*$ is obtained in two steps:

(a) first read the leaves in the order induced by the real plane;

(b) between each pair of consecutive leaves (a, b), intercalate the internal bifurcation vertex $a \wedge b$.

If V_1 and $V_2 \in \mathcal{V}^*$, then the notation we shall use for the natural order is $V_1 <_{nat} V_2$.

REMARK 1.162. Since by hypothesis the tree T is complete binary, we have a bijection from the set of pairs of consecutive leaves of T to the set of internal vertices of T. Therefore the order from Definition 1.161 is a total order relation on $\mathcal{V}^*$.

EXAMPLE 1.163. In Figure 1.58 there is an example of the natural order of an end-rooted complete plane binary tree with four leaves and three internal vertices:

$$V_1 <_{nat} V_2 <_{nat} V_3 <_{nat} V_4 <_{nat} V_5 <_{nat} V_6 <_{nat} V_7.$$

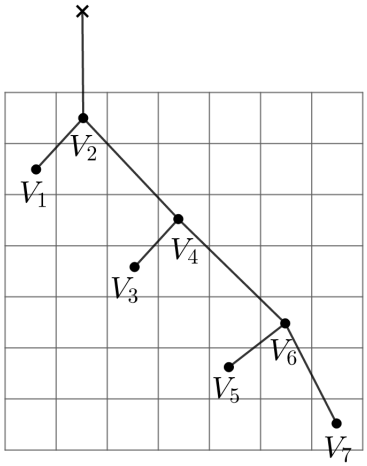

Figure 1.58: Example of the natural order of an end-rooted complete plane binary tree.

Definition 1.164. Let T be an end-rooted complete plane binary tree that is also a snake-tree (see Definition 1.63). The planarity allows us to define the **vertical order** on the set of vertices $\mathcal{V}^*$, which is the order induced by the coordinates of the real plane, as follows: if V_i and $V_j \in \mathcal{V}^*$, then we say that $V_i <_{vert} V_j$ if V_i is below V_j.

REMARK 1.165. The order from Definition 1.164 is a total order relation on $\mathcal{V}^*$.

Definition 1.166. Let T be an end-rooted complete plane binary tree that is a snake-tree enriched with its natural order on the set of vertices $\mathcal{V}^*$, denoted by $<_{nat}$ and with the vertical order on the set of vertices $\mathcal{V}^*$, denoted by $<_{vert}$. We say that T is a **separable tree** if there do not exist four vertices

$$V_{i_1} <_{nat} V_{i_2} <_{nat} V_{i_3} <_{nat} V_{i_4}$$

such that either

$$V_{i_2} <_{vert} V_{i_4} <_{vert} V_{i_1} <_{vert} V_{i_3}$$

or

$$V_{i_3} <_{vert} V_{i_1} <_{vert} V_{i_4} <_{vert} V_{i_2}$$

.

EXAMPLE 1.167. In Figure 1.59 we show an example of a separable tree, while Figure 1.60 presents a nonseparable tree.

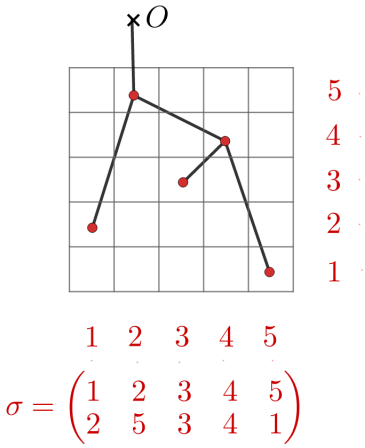

Figure 1.59: Separable tree.

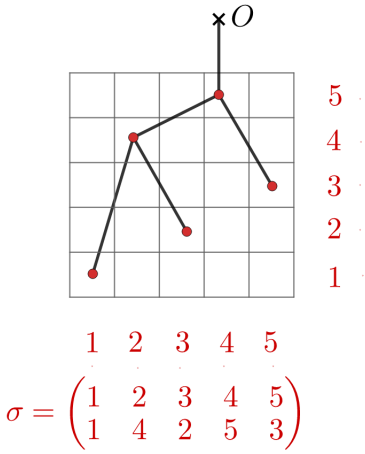

Figure 1.60: Nonseparable tree.

Lemma 1.168. *Let us fix a separable $(m+1)$-snake $\sigma : \{1, 2, \ldots, m+1\} \to \{1, 2, \ldots, m+1\}$ such that $\sigma(m) > \sigma(m+1)$, where m is even. Then the snake-tree associated to σ (see Definition 1.63) is a separable tree.*

Proof. By Definition 1.63 and by Remark 1.66, the tree associated to σ is an end-rooted complete plane binary tree. The only thing left to prove is that there do not exist four vertices

$$V_{i_1} <_{nat} V_{i_2} <_{nat} V_{i_3} <_{nat} V_{i_4}$$

such that either

$$V_{i_2} <_{vert} V_{i_4} <_{vert} V_{i_1} <_{vert} V_{i_3}$$

or

$$V_{i_3} <_{vert} V_{i_1} <_{vert} V_{i_4} <_{vert} V_{i_2}.$$

This follows immediately since a permutation is separable if and only if it does not contain $\begin{pmatrix} 1 & 2 & 3 & 4 \\ 2 & 4 & 1 & 3 \end{pmatrix}$ or $\begin{pmatrix} 1 & 2 & 3 & 4 \\ 3 & 1 & 4 & 2 \end{pmatrix}$. □

Corollary 1.169. *Given a separable tree T, we can construct a one variable polynomial $Q_x(y) \in \mathbb{R}[x][y]$ such that the Poincaré-Reeb tree of its epigraph is T.*

Proof. This follows now directly from Theorem 1.149 and by Lemma 1.168 . □

[This page intentionally left blank]

Chapter 2

The Poincaré-Reeb tree of a bivariate polynomial function

Contents

We dedicate this chapter to the answer of the following question:

QUESTION 2.1. What combinatorial object can encode the shape by measuring the non-convexity of a compact and smooth connected component of a real algebraic plane curve? What are the characteristics of this object - both in a general setting and in the asymptotic one, that is, for sufficiently small levels of a bivariate polynomial in a neighbourhood of a strict local minimum?

ANSWER: We shall construct an object called the Poincaré-Reeb graph, which is a plane tree.

2.1 Notations and hypotheses

In this chapter, the expressions "sufficiently small ε" or "small enough ε" mean: "there exists $\varepsilon_0 > 0$ such that, for any $0 < \varepsilon < \varepsilon_0$, one has ...". We will often denote this by $0 < \varepsilon \ll 1$.

We will consider a polynomial function $f : \mathbb{R}^2 \to \mathbb{R}$ in two variables with $f(0,0) = 0$. Let us **fix a neighbourhood** V of $(0,0)$ such that:

- the point $(0,0)$ is **the only strict local minimum** of f in V;
- we have $V \cap (f = 0) = \{(0,0)\}$.

Definition 2.2. Let us consider a polynomial function $f : \mathbb{R}^2 \to \mathbb{R}$ that vanishes at the origin O, exhibiting a strict local minimum at this point. For $\varepsilon > 0$, consider the set $f^{-1}([0,\varepsilon])$ and denote **its connected component that contains the origin** by $\mathcal{D}_\varepsilon$. Denote by $\mathcal{C}_\varepsilon := \mathcal{D}_\varepsilon \setminus \operatorname{Int} \mathcal{D}_\varepsilon$.

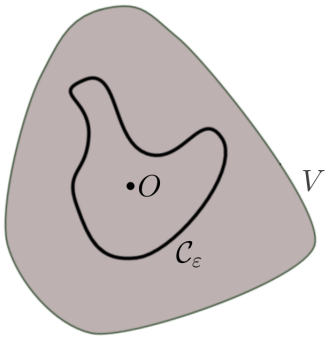

Figure 2.1: The curve $\mathcal{C}_\varepsilon$.

Later on (see Lemma 2.42), we shall prove that for $\varepsilon > 0$ sufficiently small $\mathcal{C}_\varepsilon$ is diffeomorphic to a circle and that $\mathcal{D}_\varepsilon$ is diffeomorphic to a disk, completely included in V.

EXAMPLE 2.3. The surface $\text{graph}(f) := \{(x, y, z) \in \mathbb{R}^3 \mid z = f(x, y)\}$ of the cubic $f(x, y) := y^2 - x^3 + x^2$ is shown in Figure 2.2 (see for instance [Wal78, page 57, Figure 2.2]).

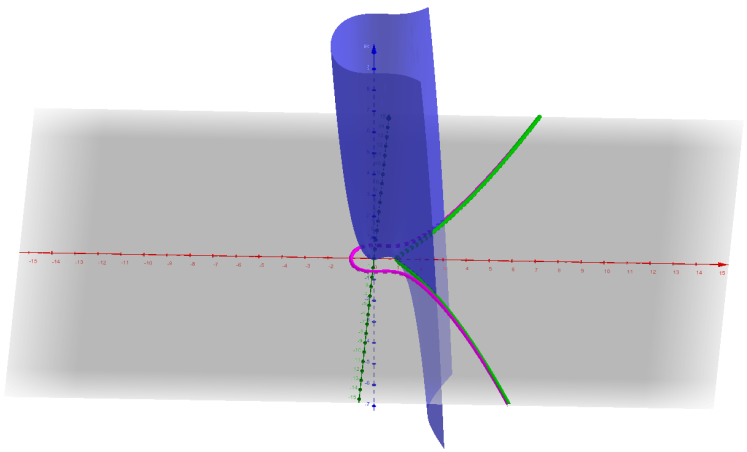

Figure 2.2: The graph of the cubic $f(x, y) := y^2 - x^3 + x^2$.

We did not choose yet a sufficiently small neighbourhood V of the origin. An illustration of such a neighbourhood V that satisfies the hypotheses from Section 2.1 is shown in Figure 2.3 below. The zero locus of f has two connected components: a point and a curve. We take V small enough such that it does not intersect the curve, that is the connected component far from the origin.

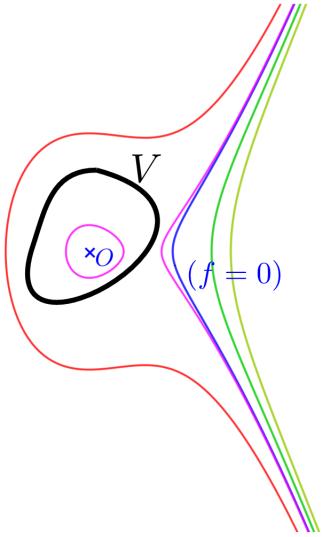

Figure 2.3: Choose a small enough neighbourhood V of the origin such that the point $(0,0)$ is the only strict local minimum of f in V and $V \cap (f=0) = \{(0,0)\}$.

Examples of functions f as in Section 2.1 are shown in Figure 2.4, Figure 2.6, Figure 2.8b.

In order to define what we will consider to be a good neighbourhood V of $O(0,0)$ to work in, let us first give the following classical definition of a singularity of a polynomial map.

For the following definition see for instance [Mil68, page 10]:

Definition 2.4. Let $\varphi : \mathbb{R}^n \to \mathbb{R}^p$, with $n, p \in \mathbb{N}^*$, $n \geq p$, be a polynomial map.

Let $\rho := \max\{\text{rank Jac}(\varphi)(x) \mid x \in \mathbb{R}^n\}$ be the maximal rank of φ, where $\text{Jac}(\varphi)(x)$ is the Jacobian matrix of φ, evaluated at x.

Then the set of **singular points** (called also **critical points**) of φ is by definition

$$\text{Sing}(\varphi) := \{x \in \mathbb{R}^n \mid \text{rank Jac}(\varphi)(x) < \rho\}.$$

The image of a singular point under φ is called a **singular value** of φ.

A point $x \in \mathbb{R}^n$ is called **regular** of φ if it is not singular.

Example 2.5. Let $f : \mathbb{R}^2 \to \mathbb{R}$ be a polynomial function. Then by Definition 2.4, the set of singular points of f is $\text{Sing} f = \left\{(x,y) \in \mathbb{R}^2 \;\middle|\; \frac{\partial f}{\partial x}(x,y) = \frac{\partial f}{\partial y}(x,y) = 0\right\}$.

See some examples of singular points of curves in [Wal78, page 57].

2.2 Morse extrema and convex level sets

The classical well-known statement that follows is meant to present equivalent characterisations of convex functions (see, for instance, [Rek+83, pages 640-650]).

Theorem 2.6. *Let us consider a convex set $C \subset \mathbb{R}^2$ and a $\mathcal{C}^2$ function $f : C \to \mathbb{R}$. The following properties are equivalent:*

(1) for any two points x, $y \in C$, for any $t \in [0,1]$, we have

$$f\left(tx + (1-t)y\right) \leq tf(x) + (1-t)f(y);$$

(2) the set $\text{epi}(f) := \{(x,y,z) \in \mathbb{R}^3 \mid z \geq f(x,y)\}$ is convex;

(3) the Hessian matrix of f, denoted by $\text{Hess}_f(x,y)$, is everywhere positive definite or positive semidefinite.

Definition 2.7. A $\mathcal{C}^2$ function $f : \mathbb{R}^2 \to \mathbb{R}$ is **convex** if f verifies one of the properties from Theorem 2.6.

The main purpose of this section is to prove that topological disks bounded by the level curves of f **in a small enough neighbourhood** (see Definition 2.2) of a non-degenerated critical point (i.e. Morse critical point) are convex sets.

Theorem 2.8. *Let $f : \mathbb{R}^2 \to \mathbb{R}$ be a polynomial function of the form $f(x, y) = ax^2 + by^2 + h(x, y)$, where $a, b \in \mathbb{R}$, $a > 0$, $b > 0$, $f(0, 0) = 0$ and $h : \mathbb{R}^2 \to \mathbb{R}$ is a polynomial function of degree of each monomial at least 3. Then for a sufficiently small $\varepsilon > 0$, $\mathcal{D}_\varepsilon$ is a convex set in a small enough neighbourhood of the origin.*

Let us now present the proof of Theorem 2.8.

Proof. Note that we are situated in a small enough neighbourhood of the origin. We have $a > 0$, $b > 0$, $\lim_{(x,y)\to(0,0)} \det H_f(x, y) = ab > 0$, for any (x, y) in a small enough neighbourhood of $(0, 0)$. Thus the Hessian matrix is positive definite and we conclude that f is a convex function, since we are in dimension 2 and by Sylvester criterion if a symmetric matrix has all diagonal elements and all the leading principal determinants positive, then the matrix is a positive definite matrix (see [Gil91, page 45], or [Rek+83]). Recall the fact that positive definite forms form an open set in the space of all forms. Since the function f is $\mathcal{C}^2$, its Hessian form varies continuously.

Therefore, the epigraph of f restricted to a convex domain is a convex set. Let us consider $\varepsilon > 0$, sufficiently small. Since $\tilde{\mathcal{D}}_\varepsilon := \text{epi}(f) \cap (z = \varepsilon)$, we obtain that $\tilde{\mathcal{D}}_\varepsilon$ is a convex set, since it is the intersection of two convex sets. Thus, the projection of $\tilde{\mathcal{D}}_\varepsilon$ on the plane xOy is also convex, in fact it is equal to $\mathcal{D}_\varepsilon$.

Let us sketch a second proof. Since $\lim_{x,y\to(0,0)} \det H_f(x, y) = ab \neq 0$, for any (x, y) in a small enough neighbourhood of $(0, 0)$, the Hessian curve of f given by $\{(x, y) \in \mathbb{R}^2 \mid \det H_f(x, y) = 0\}$, is empty. Thus (see [Wal04, page 71]) for a sufficiently small $\varepsilon > 0$, the level curve $\mathcal{C}_\varepsilon$ has no inflexion points, hence it is convex.

□

Example 2.9. The circular paraboloid $z = x^2 + y^2$ (see in Figure 2.4 below): $\mathcal{C}_\varepsilon$ are circles.

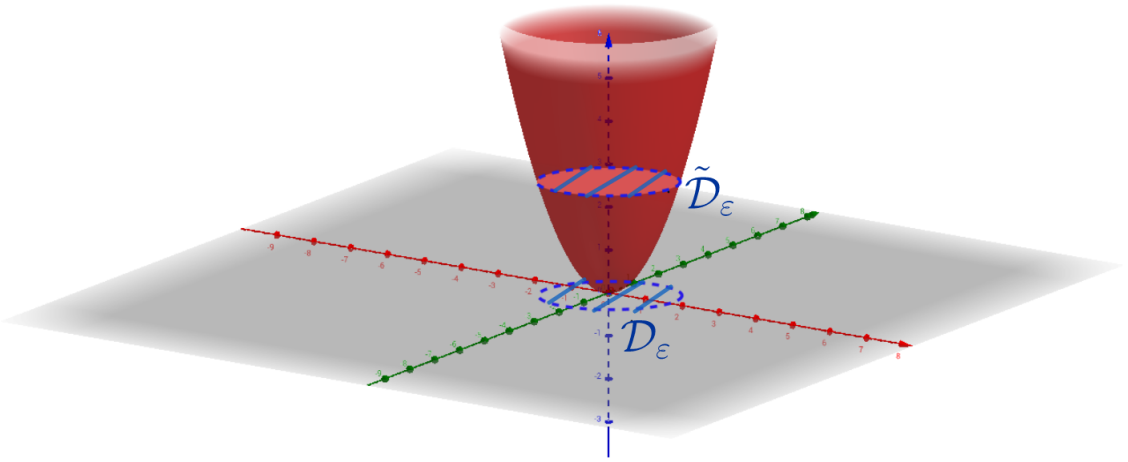

Figure 2.4: A non-degenerated (namely, Morse) critical point: we obtain convex disks.

2.3 The example of Coste and our generalisations

The starting point of this research is the following question posed in June 2004 by E. Giroux to P. Popescu-Pampu:

QUESTION. Are the small enough level curves of f near strict local minima always boundaries of convex disks (even for non-Morse singularities)?

ANSWER: The answer to this question is negative, as the following counterexample by M. Coste shows: $f(x,y) := x^2 + (y^2 - x)^2$.

EXAMPLE 2.10. We begin with the counterexample found by Coste:

$$f(x,y) := x^2 + (y^2 - x)^2.$$

The reader is invited to look at Figure 2.5b for the family of its level sets whose shape is like a banana. Figure 2.6 illustrates the graph of f and Figure 2.5a a single level $(f(x,y) = 0.1)$. The idea used by Coste was that instead of taking the sum of squares of functions defining transverse curves like in $x^2 + y^2$ (i.e. the lines defined by $x = 0$ and $y = 0$ are transverse), to take the sum of squares of x and $y^2 - x$, which define two curves that are tangent at the origin.

The previous function was mentioned also in [JK11], [Bol80].

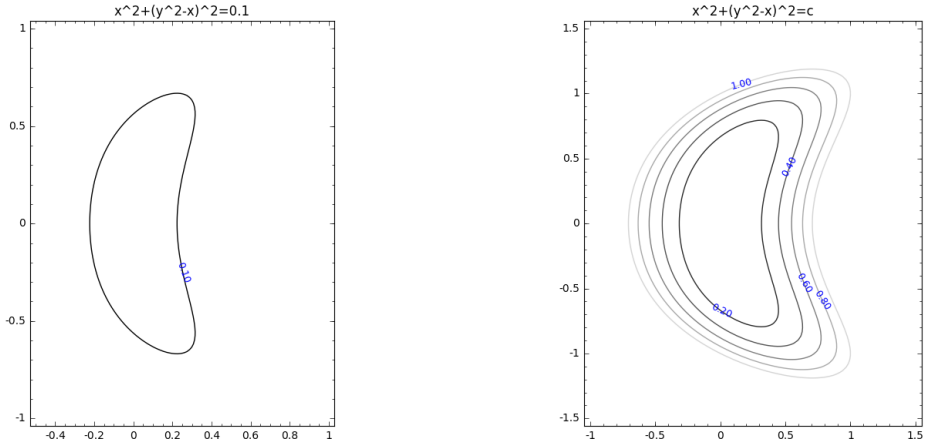

(a) The level curve $(f(x,y) = 0.1)$ in $\mathbb{R}^2$, where the function $f(x,y) := x^2 + (y^2 - x)^2$.

(b) A family of level curves in $\mathbb{R}^2$ of $f(x,y) := x^2 + (y^2 - x)^2$.

Figure 2.5: The counterexample provided by Coste.

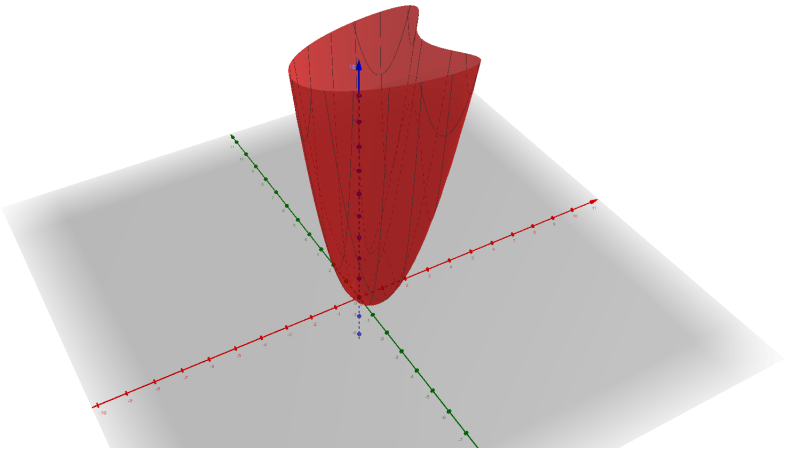

Figure 2.6: The graph of Coste's example in $\mathbb{R}^3$.

Proposition 2.11. *The topological disks $\mathcal{D}_\varepsilon$ from Example 2.10 are never convex for $\varepsilon > 0$.*

Proof. Indeed, if we denote by $M_\varepsilon := \mathcal{C}_\varepsilon \cap \{x > 0 \mid y = 0\}$, by $P_\varepsilon := \mathcal{C}_\varepsilon \cap \{y > 0 \mid y^2 - x = 0\}$ and by $N_\varepsilon := \mathcal{C}_\varepsilon \cap \{y < 0 \mid y^2 - x = 0\}$, then we get $x_{M_\varepsilon} = \sqrt{\frac{\varepsilon}{2}}$, $y_{M_\varepsilon} = 0$, $x_{P_\varepsilon} = \sqrt{\varepsilon}$, $y_{P_\varepsilon} = \sqrt[4]{\varepsilon}$, and $x_{N_\varepsilon} = \sqrt{\varepsilon}$, $y_{N_\varepsilon} = -\sqrt[4]{\varepsilon}$ (see Figure 2.7).

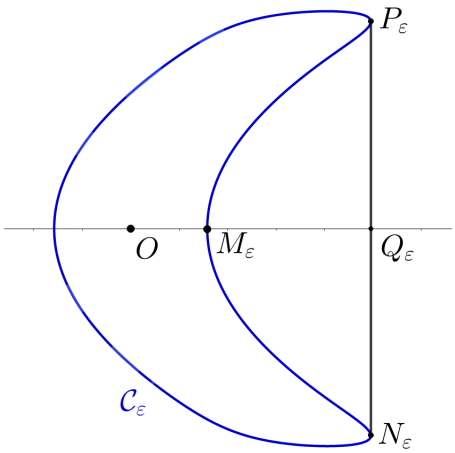

Figure 2.7: Coste's example is non-convex.

Denote by Q_ε the midpoint of $[N_\varepsilon P_\varepsilon]$. Then $x_{Q_\varepsilon} = \sqrt{\varepsilon} > x_{M_\varepsilon}$. Since $y_{M_\varepsilon} = y_{Q_\varepsilon} = 0$ and there is no other point to the right of M_ε, we conclude that $Q_\varepsilon \notin \mathcal{D}_\varepsilon$. Hence there exist the points $N_\varepsilon \in \mathcal{D}_\varepsilon$ and $P_\varepsilon \in \mathcal{D}_\varepsilon$ such that the segment $[N_\varepsilon P_\varepsilon]$ is not included in $\mathcal{D}_\varepsilon$. In conclusion, we proved that there exists at least a point outside the disk $\mathcal{D}_\varepsilon$ on the segment $[N_\varepsilon P_\varepsilon]$. □

In the sequel we give some new examples of functions $f : \mathbb{R}^2 \to \mathbb{R}$ with a strict local minimum at the origin $(0, 0)$, whose level sets $(f(x, y) = \varepsilon)$ are all boundaries of non-convex disks for a sufficiently small $0 < \varepsilon \ll 1$. The shape of these level curves $\mathcal{C}_\varepsilon$ stabilises for sufficiently small $\varepsilon > 0$, as we shall prove in this chapter.

EXAMPLE 2.12. Let us take the following polynomial:

$$f(x,y) := x^{16} + (y^2+x)^2(y^2-x)^2.$$

Its level curves have the shape of a bone, as one can see in Figure 2.8a. For a family of level curves of f, see Figure 2.8b.

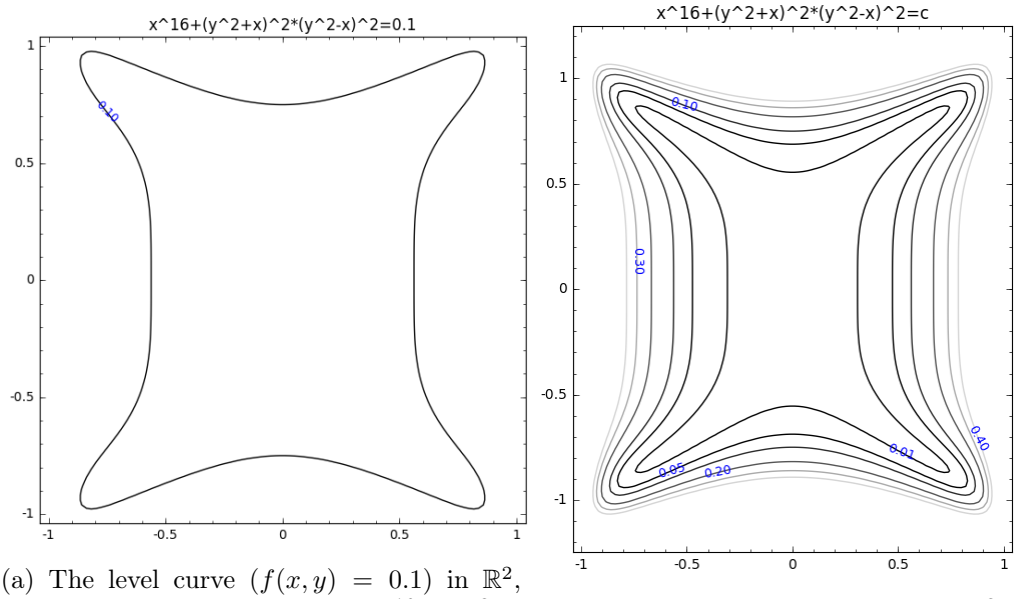

(a) The level curve $(f(x,y) = 0.1)$ in $\mathbb{R}^2$, where the function $f(x,y) := x^{16} + (y^2 + x)^2(y^2 - x)^2$

(b) A family of level curves in $\mathbb{R}^2$ of $f(x,y) := x^{16} + (y^2+x)^2(y^2-x)^2$.

Figure 2.8: A variation of Coste's counterexample.

EXAMPLE 2.13. Let us consider the following polynomial:

$$f(x,y) := x^6 + (y^4 + y^2 - x)^2(y^2 - x)^2.$$

The shape of its level curves is shown in Figure 2.9.

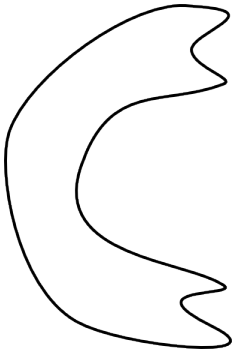

Figure 2.9: The sketch of the double banana shape of a level curve $(f = \varepsilon)$, for $f(x,y) := x^6 + (y^4 + y^2 - x)^2(y^2 - x)^2$.

2.3.1 Star domains

We have seen in Proposition 2.11 that the set $\mathcal{D}_\varepsilon$ is not always convex. Question: is $\mathcal{D}_\varepsilon$ always a star-domain? We shall prove in the following that the answer is negative.

The following definition is well-known:

Definition 2.14. [AB06, page 168] A set S in the Euclidean space $\mathbb{R}^n$ is called a **star domain with respect to** $x_0 \in S$ if for all $x \in S$, the line segment from x_0 to x is in S.

Proposition 2.15. *The polynomial function* $f : \mathbb{R}^2 \to \mathbb{R}$

$$f(x, y) := x^{2p} + (y^2 - x)^2$$

for $p \geq 3$*, has the following properties:* O *is a strict local minimum and for sufficiently small* $\varepsilon > 0$*, the set* $\mathcal{D}_\varepsilon := f^{-1}([0, \varepsilon])$ *is not a star domain with respect to any point* $P \in \mathcal{D}_\varepsilon$*.*

Before the proof, let us first present the following Lemma:

Lemma 2.16. *If a set* $\mathcal{D} \subset \mathbb{R}^2$ *is a star domain with respect to a point and if* $\mathcal{D}$ *admits a symmetry axis, say* Δ *(see Figure 2.10), then there exists a point* $P \in \mathcal{D} \cap \Delta$ *such that* $\mathcal{D}$ *is a star domain with respect to* P*.*

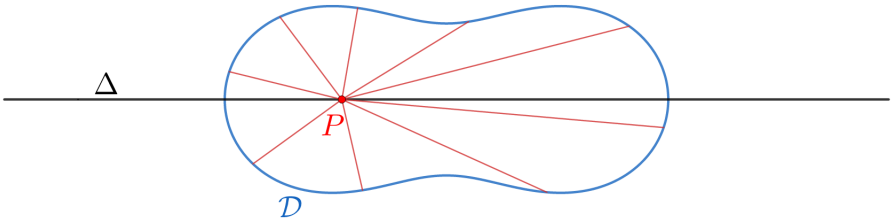

Figure 2.10: A star domain $\mathcal{D}$ with a symmetry axis Δ.

Proof. By hypothesis, the given set $\mathcal{D} \subset \mathbb{R}^2$ is a star domain with respect to a point. Denote this point by P_1. If $P_1 \in \Delta$, there is nothing to prove. Let us consider $P_1 \notin \Delta$, as pictured in Figure 2.11.

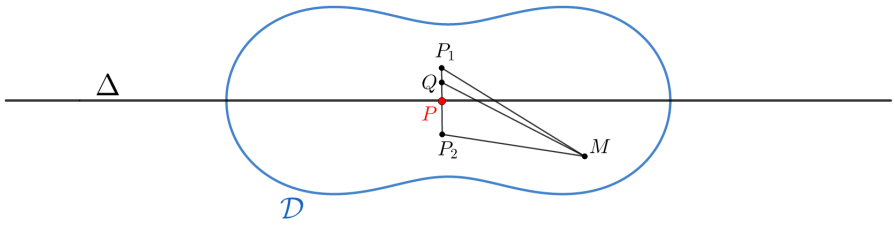

Figure 2.11: There exists $P \in \mathcal{D} \cap \Delta$ such that $\mathcal{D}$ is a star domain with respect to P.

By hypothesis, Δ is a symmetry axis for $\mathcal{D}$. Let us denote by $P_2 \in \mathcal{D}$ the symmetric of P_1 with respect to Δ. Denote by P the midpoint of the segment $[P_1P_2]$. Hence, $P \in \Delta$ and by symmetry, $\mathcal{D}$ is a star domain also with respect to P_2. Let us now prove that $\mathcal{D}$ is a star domain with respect to any point $Q \in [P_1P_2]$, hence $\mathcal{D}$ is a star domain with respect to the point P.

Let $M \in \mathcal{D}$. Since $\mathcal{D}$ is a star domain with respect to both P_1 and P_2, we have that $[MP_1]$, $[MP_2]$ and $[P_1P_2]$ are included in $\mathcal{D}$. Thus, both the triangle $\triangle MP_1P_2$ and its interior are

included in $\mathcal{D}$, since the interior is the union of $]P_1X[$, for all $X \in]P_2M[$. In particular, for any point $Q \in [P_1P_2]$, we obtain $[QM] \subset \mathcal{D}$. Namely, $\mathcal{D}$ is a star domain with respect to any point $Q \in [P_1P_2]$. In conclusion, $\mathcal{D}$ is a star domain with respect to P. □

In the following let us present the proof of Proposition 2.15.

Proof. By Lemma 2.16, it is sufficient to prove that $\mathcal{D}_\varepsilon$ is not a star domain with respect to any point $B(x_B, 0)$ on $(y = 0) \cap \mathcal{D}_\varepsilon$, such that $f(B) \leq \varepsilon$, because the line $\Delta := (y = 0)$ is a symmetry axis for $\mathcal{D}_\varepsilon$.

Take the point

$$A_\varepsilon \left(\varepsilon^{\frac{1}{2p}}, \varepsilon^{\frac{1}{4p}}\right) \in (y^2 - x = 0) \cap (f = \varepsilon).$$

Then the midpoint of the segment $[BA_\varepsilon]$ (see Figure 2.12 below) is the point

$$M_\varepsilon \left(\frac{\varepsilon^{\frac{1}{2p}} + x_B}{2}, \frac{\varepsilon^{\frac{1}{4p}}}{2}\right).$$

We will prove that $M_\varepsilon \notin \mathcal{D}_\varepsilon$.

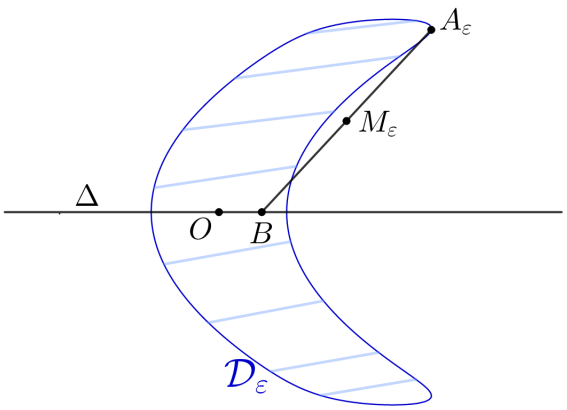

Figure 2.12: Example of a non-star domain.

□

Since $f(B) \leq \varepsilon$, we have $x_B^{2p} + x_B^2 \leq \varepsilon$. For sufficiently small $\varepsilon > 0$, we have x_B sufficiently small, thus $x_B^{2p} < x_B^2$. Hence $|x_B| < \sqrt{\varepsilon}$.

We have $f(M_\varepsilon) - \varepsilon > (\frac{1}{4}\varepsilon^{\frac{1}{2p}} - \frac{1}{2}(\varepsilon^{\frac{1}{2p}} + x_B))^2 - \varepsilon = \frac{1}{16}\varepsilon^{\frac{1}{p}} + \frac{1}{2}\varepsilon^{\frac{1}{2p}}x_B + \frac{1}{4}x_B^2 - \varepsilon$.

There are two cases to consider. First, if $x_B \geq 0$, then we have $f(M_\varepsilon) - \varepsilon \geq \frac{1}{16}\varepsilon^{\frac{1}{p}} - \varepsilon > 0$ for a sufficiently small $\varepsilon > 0$. Secondly, if $x_B < 0$, then $f(M_\varepsilon) - \varepsilon \geq \frac{1}{16}\varepsilon^{\frac{1}{p}} + \frac{1}{2}\varepsilon^{\frac{1}{2p}}x_B - \varepsilon$. Since $|x_B| \leq \sqrt{\varepsilon}$ and $\varepsilon^{\frac{1}{2p}} < 1$, we obtain $|x_B|\varepsilon^{\frac{1}{2p}} \leq \sqrt{\varepsilon}$. Thus, $f(M_\varepsilon) - \varepsilon \geq \frac{1}{16}\varepsilon^{\frac{1}{p}} - \frac{1}{2}\sqrt{\varepsilon} - \varepsilon > 0$ for a sufficiently small $\varepsilon > 0$ and for $p \geq 3$. In both cases, we get $f(M_\varepsilon) > \varepsilon$, hence $M \notin \mathcal{D}_\varepsilon$ and thus the segment $[BA_\varepsilon]$ is not included in $\mathcal{D}_\varepsilon$, even though $A_\varepsilon, B \in \mathcal{D}_\varepsilon$. In other words, $\mathcal{D}_\varepsilon$ is not a star domain with respect to any $B \in \mathcal{D}_\varepsilon \cap \Delta$.

2.4 The Poincaré-Reeb tree

2.4.1 The Poincaré-Reeb construction

The main purpose of this section is to introduce a new combinatorial object for studying the departure from convexity of a smooth and compact connected component of a real algebraic curve in $\mathbb{R}^2$. Our purpose is to define the Poincaré-Reeb graph, associated to the given curve and to a direction of projection x. It is adapted from the classical construction introduced by H. Poincaré (see [Poi10, 1904, Fifth supplement, page 221]), which was rediscovered by G. Reeb (in [Ree46]). Both used it as a tool in Morse theory (see [Mat02]). Namely, given a Morse function on a closed manifold, they associated it a graph as a quotient of the manifold by the equivalence relation whose classes are the connected components of the levels of the function. We will perform an analogous construction for a special type of manifold with boundary.

• Let us consider a smooth and compact connected component of a real algebraic curve in $\mathbb{R}^2$, denoted by $\mathcal{C}$. Let $\mathcal{D}$ denote the topological disk bounded by $\mathcal{C}$ (see Figure 2.13 below). Moreover, let us define the projection $\Pi : \mathbb{R}^2 \to \mathbb{R}$, $\Pi(x, y) := x$.

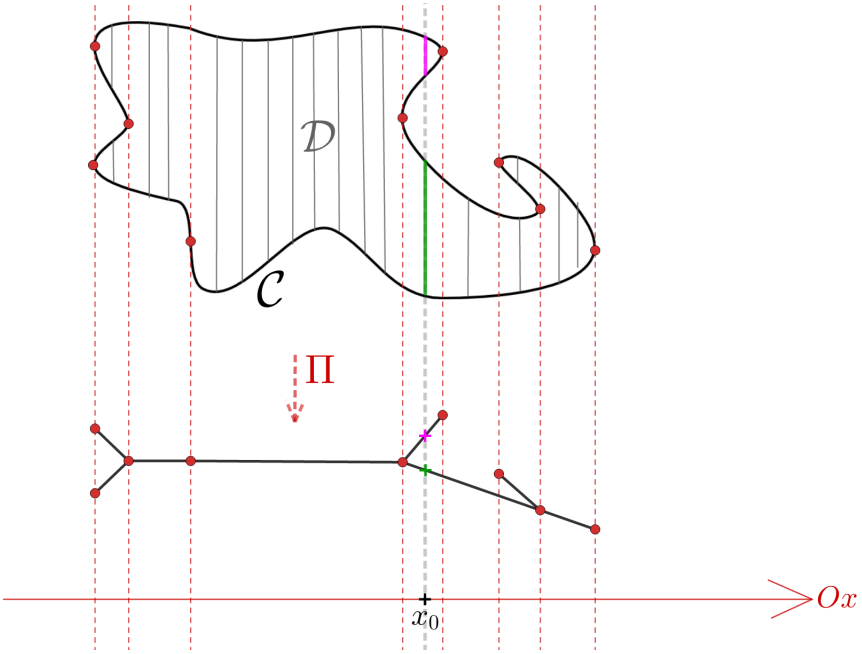

Figure 2.13: A Poincaré-Reeb graph of a smooth and compact connected component of a real algebraic curve $\mathcal{C}$.

Definition 2.17. For each $x \in \mathbb{R}$, $\Pi^{-1}(x) \cap \mathcal{D}$ is a finite union of connected vertical segments. Let us define the **equivalence relation** $\sim$ as follows: if (x, y) and (x, y') are two points in the real plane $\mathbb{R}^2$ then $(x, y) \sim (x, y')$ if and only if they belong to the same vertical connected component of the fibre $\Pi^{-1}(x) \cap \mathcal{D}$.

Given the above equivalence relation, let us consider the canonical quotient map

$$q : \mathbb{R}^2 \to \mathbb{R}^2/\sim .$$

Denote by $P := \mathbb{R}^2$ and by $\tilde{P} := \mathbb{R}^2/\sim$. The coordinates in $\tilde{P}$ are $(\tilde{x}, \tilde{y})$, with $\tilde{x} = x$.

The function Π descends to the quotient in a function $\tilde{\Pi} : \tilde{P} \to \mathbb{R}$, $\tilde{\Pi}(x, \tilde{y}) := x$. The function $\tilde{\Pi}$ is continuous, since Π is continuous.

We have the following commutative diagram (see Figure 2.14):

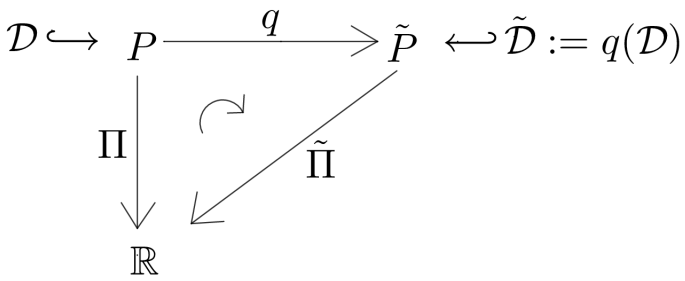

Figure 2.14: The diagram is commutative: $\Pi = \tilde{\Pi} \circ q$.

• Our next aim is to prove that $\tilde{P}$ is homeomorphic to $\mathbb{R}^2$. The first step will be to show that $\tilde{P}$, endowed with the function $\tilde{\Pi}$ is a fibre bundle, i.e. that satisfies a local triviality. We will prove that it is locally a cartesian product of two sub-spaces. Furthermore, we shall prove that the local trivialisation of the fibre bundle $\tilde{P}$ implies that $\tilde{P}$ is a trivial fibre bundle, i.e. it is not just locally a product of two spaces, but globally.

Proposition 2.18. *The topological space $\tilde{P}$ endowed with the function $\tilde{\Pi}$ is a fibre bundle.*

Proof. By the definition of the fibre bundle (see for instance [Frè13, page 51]), what we need to prove is that there exists a local trivialisation of $\tilde{P}$. Let us consider a point $x_0 \in \mathbb{R}$ in the base space, that is the Ox-axis. Take an open neighbourhood of x_0, called $U \subset \mathbb{R}$. We want to show that the set $\tilde{\Pi}^{-1}(U)$ is homeomorphic to $U \times \mathbf{R}$, here by $\mathbf{R}$ we mean a space that is homeomorphic to the real line $\mathbb{R}$. To this end, we have the following two arguments:

1. If on a vertical line we contract a finite number of segments into points (by the quotient map q described above), we obtain a topological space that is homeomorphic to $\mathbb{R}$. Denote this space by $\mathbf{R}$.

2. The set $\mathcal{D} \cap \Pi^{-1}(x_0)$ is a finite union of intervals (some of them empty intervals), whose extremities depend continuously on x (see Figure 2.15), except when x_0 is a critical point.

Hence we have the local triviality: $\tilde{\Pi}^{-1}(U)$ is homeomorphic to $U \times \mathbf{R}$. Thus the image $\tilde{P}$ of the plane P, by the quotient map q, is a fibre bundle.

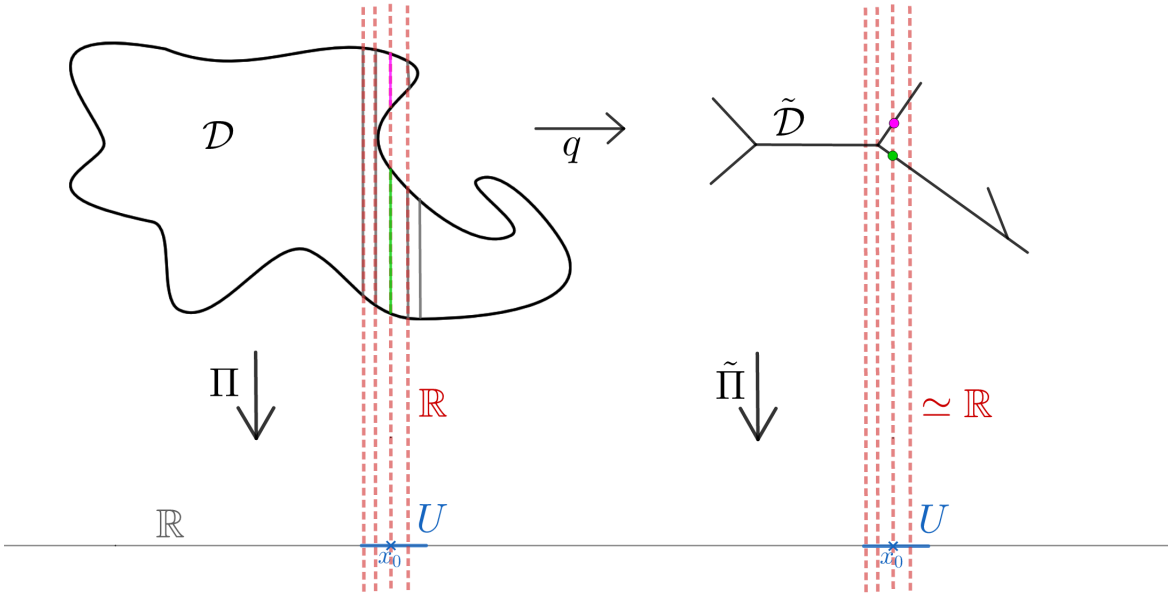

Figure 2.15: The extremities of the intervals in $\mathcal{D} \cap \Pi^{-1}(x_0)$ depend continously on x. After the quotient, we obtain vertical lines homeomorphic to $\mathbb{R}$.

□

Proposition 2.19. *The topological space $\tilde{P}$ endowed with the function $\tilde{\Pi}$ is a **trivial** fibre bundle.*

Proof. The base space of the fibre bundle $\tilde{P}$ is the Ox-axis, namely $\mathbb{R}$, and $\mathbb{R}$ is contractible to a point. Thus we conclude that $\tilde{P}$ is a trivial fibre bundle, since by [Osb82, Proposition 3.5, page 75] a fibre bundle over a base space that is contractible to a point is trivial. To be more precise, we have $\tilde{P}$ homeomorphic to $\mathbb{R}^2$. □

Corollary 2.20. *The topological subspace $\tilde{\mathcal{D}} := q(\mathcal{D})$ is embedded in a real plane (see Definition 1.47).*

Theorem 2.21. *The topological subspace $\tilde{\mathcal{D}}$ is connected.*

Proof. The image of a connected space by a continuous function is connected. Since $\tilde{\mathcal{D}} := q(\mathcal{D})$, the topological disk $\mathcal{D}$ is connected and the quotient map q is continuous, the proof is complete. □

Theorem 2.22. *The topological subspace $\tilde{\mathcal{D}}$ is a one-dimensional subspace of $\tilde{P}$. In each of the regular points of $\tilde{\mathcal{D}}$, we have $\tilde{\mathcal{D}}$ transverse to the foliation of the plane $\tilde{P}$ by vertical lines, induced by $\tilde{\Pi}$.*

Proof. Since the given curve $\mathcal{C}$ is a connected component of a real algebraic curve, that is, it is an analytic curve, it has finitely many points of vertical tangency. In other words, there are finitely many critical levels of the projection $\Pi_{|\mathcal{C}} : \mathcal{C} \to \mathbb{R}$. Locally near a critical point, one may have a tangency point of even order (see Figure 2.16a) or of odd order (see Figure 2.16b):

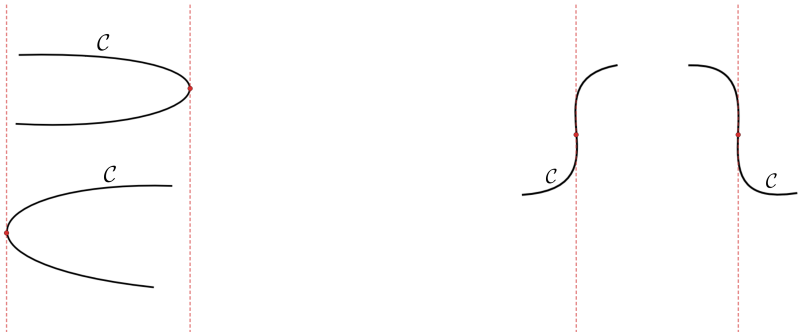

(a) Points on $\mathcal{C}$ of vertical even tangency (b) Points on $\mathcal{C}$ of vertical odd tangency

Figure 2.16: Vertical tangents.

Between any two critical levels, we have only what we call "bands" of the initial disk $\mathcal{D}$. See, for a better comprehension, Figure 2.17 below.

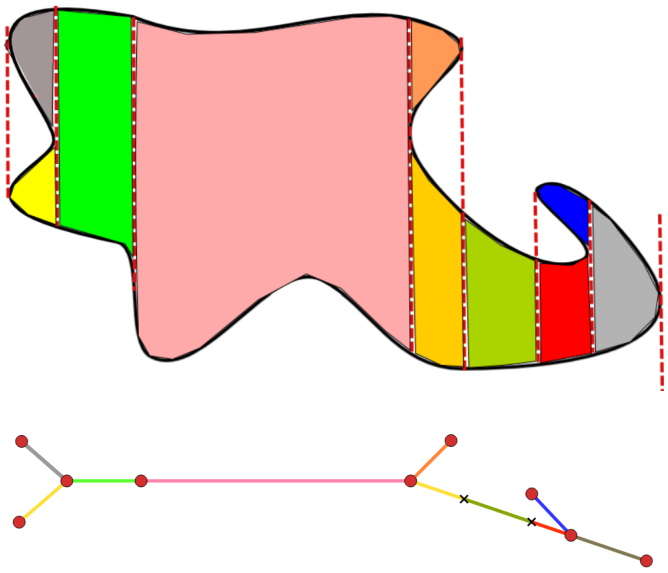

Figure 2.17: "Bands" of the disk $\mathcal{D}$, between two consecutive critical levels of the vertical projection Π. The bands contract into one-dimensional transverse arcs.

After taking the quotient, each band contracts into an arc of dimension one, transverse to the vertical foliation of the real plane $\tilde{P}$. Therefore, the topological space $\tilde{\mathcal{D}}$ is a graph, being a finite union of transverse arcs.

□

Definition 2.23. [Vic89, pages 13-14] A **preorder** on a set is a binary relation that is reflexive and transitive.

As we mentioned before, Definition 2.24 from below is adapted from the classical construction introduced by H. Poincaré (see [Poi10, 1904, Fifth supplement, page 221]), which was rediscovered

by G. Reeb (in [Ree46, p. 1946]). Both used it as a tool in Morse theory (see [Mat02]). Namely, given a Morse function on a closed manifold, they associated it a graph as a quotient of the manifold by the equivalence relation whose classes are the connected components of the levels of the function. We will perform an analogous construction for a special type of manifold with boundary, that is a topological disk $\mathcal{D}$ bounded by a smooth and compact connected component of a real algebraic curve.

Definition 2.24. Given the projection $\Pi : \mathbb{R}^2 \to \mathbb{R}$, let us consider the image $\tilde{\mathcal{D}} := q(\mathcal{D})$, of the topological disk $\mathcal{D}$ bounded by the smooth and compact connected component of a real algebraic curve $\mathcal{C}$, where q the quotient map introduced before. The image $\tilde{\mathcal{D}}$, endowed with special vertices, namely the finitely many points corresponding to the critical points of Π on $\mathcal{C}$ is called **the Poincaré-Reeb graph** associated to the curve $\mathcal{C}$ and to Π, denoted by $\mathcal{R}(\mathcal{C}, \Pi)$. Endow the real plane with the trivial fibre bundle $\tilde{P}$, then endow the vertices of the graph with the induced preorder.

In conclusion, the Poincaré-Reeb construction gives us a plane connected graph, embedded in a surface that is homeomorphic to $\mathbb{R}^2$. We will prove in the next section that it is in fact a tree.

2.4.2 Constructible functions and a Fubini type theorem

In this section we will recall the integration of constructible functions with respect to the Euler characteristic and a Fubini-type theorem for it. Then we will apply it to the proof of Proposition 2.36.

We will first introduce the necessary tools: constructible functions. We shall follow the definitions and results from [Cos05, Chapter 3, pages 21-22]. For more details, the reader should refer to [Wal04, page 162]. Constructible functions have applications in the study of the topology of singular real algebraic sets. The main tool is the integration against the Euler characteristic, which was first described in Viro's paper [Vir88].

Definition 2.25. [Cos02, page 25] A **basic semialgebraic set** is a subset of $\mathbb{R}^n$ satisfying a finite number of polynomial equations and inequations with real coefficients.

Example 2.26.
- All algebraic sets are basic semialgebraic.
- Unions of finitely many points and open intervals in $\mathbb{R}$ are basic semialgebraic sets.

Definition 2.27. [Cos02, page 29] Let us consider two basic semialgebraic sets $M \subset \mathbb{R}^m$ and $N \subset \mathbb{R}^n$. We say that a continuous map $s : M \to N$ is a **semialgebraic map** if its graph $\{(x, y) \in M \times N \mid y = s(x)\}$ is a semialgebraic subset of $\mathbb{R}^m \times \mathbb{R}^n$.

Definition 2.28. [Cos05, Chapter 3, page 21] A **constructible function** on a semialgebraic set A is a function $\varphi : A \to \mathbb{Z}$ which takes finitely many values and such that, for every $n \in \mathbb{Z}$, $\varphi^{-1}(n)$ is a semialgebraic subset of A.

Remark 2.29. [Wal04, page 162] Each constructible function is an integer linear combination of characteristic functions of constructible sets X_i, i.e. of semialgebraic subsets of A:

$$\varphi = \sum_{i \in I} m_i \mathbf{1}_{X_i},$$

where $m_i \in \mathbb{Z}$ and $\mathbf{1}_{X_i}$ is the characteristic function of X_i.

Definition 2.30. [Cos05, Chapter 3, page 22] Let φ be a constructible function on a semialgebraic set X. The **integral** of φ **with respect to the Euler characteristic** χ is by definition:

$$\int_X \varphi \mathrm{d}\chi := \sum_{n\in\mathbb{Z}} n\chi(\varphi^{-1}(n)\cap X),$$

where χ denotes the Euler characteristic.

Definition 2.31. [Cos05, Chapter 3, page 22] Let us consider a continuous semialgebraic map $f : A \to B$ and let φ be a constructible function on A. The **pushforward** of φ **along** f (see Figure 2.18) is the function $f_*\varphi : B \to \mathbb{Z}$,

$$f_*\varphi(y) := \int_{f^{-1}(y)} \varphi \mathrm{d}\chi.$$

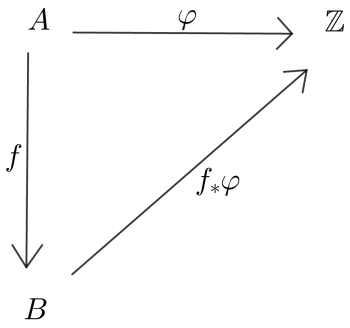

Figure 2.18: The pushforward $f_*\varphi$ of φ along f.

Remark 2.32. If we apply the definition of push-forward to the application from a set A towards a point, we obtain the function that associates at this point the integral with respect to the Euler characteristic of the starting function on A.

Remark 2.33. The diagram from Figure 2.18 is not commutative. If, for example, $A := \{a, b\}$, $B := \{c\}$, where a, b, c are points in $\mathbb{R}^2$, $f : A \to B$ a semialgebraic map such that $f(a) = f(b) := c$ and φ a constructible function on A such that $\varphi(a) := -1$, $\varphi(b) := 1$, then by definition we compute $f_*\varphi(b) = \int_{f^{-1}(c)} \varphi \mathrm{d}\chi = -1 + 1 = 0$. Thus $f_*\varphi \circ f(a) = 0$ while $\varphi(a) = -1$. Therefore $f_*\varphi \circ f \neq \varphi$.

Remark 2.34. The following proofs can be extended to semianalytic sets, with the more general hypothesis that f is analytic.

Theorem 2.35. *[Cos05, Chapter 3, page 22] **Fubini Type Theorem:** Let $f : A \to B$ be a semialgebraic map and φ a constructible function on A. Then*

$$\int_B f_*\varphi \mathrm{d}\chi = \int_A \varphi \mathrm{d}\chi.$$

We are ready now to prove the main result of this section, namely Proposition 2.36.

Proposition 2.36. *The Poincaré-Reeb graph of a topological disk $\mathcal{D}$ bounded by a smooth and compact connected component of a real algebraic curve in $\mathbb{R}^2$ is a tree.*

Proof. In Definition 2.31 let us replace A with the disk $\mathcal{D}$, B with the graph G obtained after the Poincaré-Reeb contraction π, the function f with the Poincaré-Reeb contraction π and φ with the characteristic function $\mathbf{1}_{\mathcal{D}}$, as in Figure 2.19:

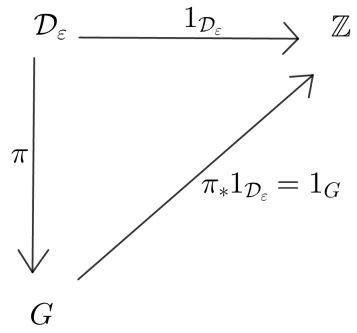

Figure 2.19: The pushforward $\pi_*\mathbf{1}_{\mathcal{D}}$ of $\mathbf{1}_{\mathcal{D}}$ along π.

In other words, we apply the Fubini Type Theorem 2.35 for the pushforward of the constructible function $\mathbf{1}_{\mathcal{D}}$.

Now for $g \in G$, we obtain:

$$\pi_*\mathbf{1}_{\mathcal{D}}(g) = \int_{\pi^{-1}(g)} \mathbf{1}_{\mathcal{D}} \mathrm{d}\chi = \sum_{n\in\mathbb{Z}} n\chi(\mathbf{1}_{\mathcal{D}}^{-1}(n) \cap \pi^{-1}(g)) = \chi(\pi^{-1}(g)) = 1,$$

since $\pi^{-1}(g)$ is a connected component of the fibre, i.e. a segment. Thus

$$\pi_*\mathbf{1}_{\mathcal{D}} = \mathbf{1}_G.$$

By Theorem 2.35, we have now

$$\int_{\mathcal{D}} \mathbf{1}_{\mathcal{D}} \mathrm{d}\chi = \int_G \pi_*\mathbf{1}_D \mathrm{d}\chi.$$

Since $\pi_*\mathbf{1}_{\mathcal{D}} = \mathbf{1}_G$, we obtain:

$$\int_{\mathcal{D}} \mathbf{1}_{\mathcal{D}} \mathrm{d}\chi = \int_G \mathbf{1}_G \mathrm{d}\chi.$$

Therefore, $\chi(\mathcal{D}) = \chi(G)$. Since $\mathcal{D}$ is a disk, we have $\chi(\mathcal{D}) = 1$. In Section 2.4 we proved that G is a connected graph, thus the Betti number $b_0 = 1$. We have $\chi(G) = b_0 - b_1$. Since we proved that its Euler characteristic is $\chi(G) = 1$, we get that the Betti number $b_1 = 0$. Thus we conclude that G has no cycles, hence G is a tree.

□

Corollary 2.37. *The Poincaré-Reeb graph associated to a compact and smooth connected component of a real algebraic plane curve and to a direction of projection x is a plane tree whose open edges are transverse to the foliation induced by the function x. Its vertices are endowed with a total preorder relation induced by the function x.*

Definition 2.38.
• A **transversal tree** is a finite tree embedded in a real oriented plane P endowed with a trivialisable fibre bundle $\Pi : P \to \mathbb{R}$, such that each one of its edges is transversal to the fibres of Π.
• Two transversal trees (P_1, T_1) and (P_2, T_2) are considered to be **equivalent** if there exists an orientation preserving homeomorphism ψ sending one pair into the other one and one fibre bundle into the other one (in the sense that there exists an orientation-preserving homeomorphism $\lambda : \mathbb{R} \to \mathbb{R}$ such that $\Pi_2 \circ \psi = \lambda \circ \Pi_1$).

Remark 2.39. We introduce Definition 2.38 since one of the main objectives of this thesis is to characterise the Poincaré-Reeb trees. To this end, in the following chapters our aim is to discover which transversal trees we can realise explicitly as Poincaré-Reeb trees by a strict local minimum of a polynomial function.

2.5 Asymptotic properties near a strict local minimum

Let us consider a polynomial function $f : \mathbb{R}^2 \to \mathbb{R}$ with a strict local minimum at the origin (see Section 2.1). The aim of this section is to prepare our study in the next Section 2.6. There, we shall focus of the asymptotic shape of the Poincaré-Reeb trees of its sufficiently small levels and we will prove that their shapes stabilise to a limit shape which we shall call the "asymptotic Poincaré-Reeb tree of the strict minimum with respect to the function x". Moreover, we prove several general properties of those trees.

2.5.1 Nested Jordan curves

The following definition and theorem are well-known:

Definition 2.40. [Kra99, page 19] A **Jordan curve** is the image of a continuous application $\gamma : [a, b] \to \mathbb{R}^2$, where $a, b \in \mathbb{R}$ are distinct real numbers, such that $\gamma(a) = \gamma(b)$ and $\gamma_{|[a,b[}$ is injective.

Theorem 2.41. *The complement in $\mathbb{R}^2$ of a Jordan curve J consists of two connected components, each of which has J as its boundary (see Figure 2.20). Both components are path-connected and open and exactly one is unbounded.*

Proofs of Theorem 2.41 can be found in [Wal72, pages 119, 133].

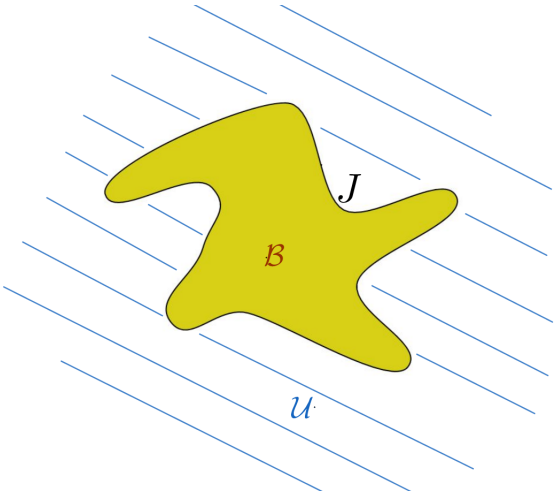

Figure 2.20: A Jordan Curve J: the bounded component of the real plane is $\mathcal{B}$, while the unbounded component is $\mathcal{U}$.

Lemma 2.42. *Under the notations and hypotheses listed in Section 2.1, for all sufficiently small $\varepsilon > 0$, the curve $\mathcal{C}_\varepsilon$ is a Jordan curve; more precisely, $\mathcal{C}_\varepsilon$ is diffeomorphic to S^1 and $\mathcal{D}_\varepsilon$ is diffeomorphic to a disk. If one denotes by* Int $\mathcal{C}_\varepsilon$ *the bounded connected component of $\mathbb{R}^2 \setminus \mathcal{C}_\varepsilon$, then $(0,0) \in$ Int $\mathcal{C}_\varepsilon$.*

Proof. Let us start by giving a slightly different definition of $\mathcal{C}_\varepsilon$. At the end of this proof, we will have justified Definition 2.2.

Suppose that $\mathcal{C}_\varepsilon$ is the union of connected components of $f^{-1}(\varepsilon)$, near the origin.

First step: let us prove that $\mathcal{C}_\varepsilon$ is a one-dimensional manifold.

By hypothesis (Section 2.1), $\mathcal{C}_0 = \{(0,0)\}$ is an isolated local minimum of f, thus for a sufficiently small ε, the level curve $\mathcal{C}_\varepsilon$ has no critical points. Therefore, $\mathcal{C}_\varepsilon$ is a one-dimensional manifold. By [Mil65, Appendix "Classifying 1-manifolds", page 65], the manifold $\mathcal{C}_\varepsilon$ is diffeomorphic to a disjoint union of circles S^1, or of some intervals of real numbers: the real line $\mathbb{R}$, the half-line $\mathbb{R}_+$ or the closed interval $[0,1]$.

Second step: we prove that one cannot obtain components of $\mathcal{C}_\varepsilon$ which are diffeomorphic to closed or semiclosed segments in $\mathbb{R}$.

Let us show that $\mathcal{C}_\varepsilon$ has no connected components diffeomorphic to $[0,1]$ or $[0,+\infty[$. The reader should recall that $0 < \varepsilon \ll 1$ is a regular value of f, thus (see [GP74, Preimage Theorem, page 21]) the set $\mathcal{C}_\varepsilon = f^{-1}(\varepsilon)$ is a submanifold of $\mathbb{R}^2$ of dimension 1. Let $P \in \mathcal{C}_\varepsilon$ be a point. If B_P is an open disk centered at P, then $\mathcal{C}_\varepsilon \cap B_P$ is diffeomorphic to an open interval $]a,b[$, where the image of P is in $]a,b[$. Since the point P was chosen arbitrarily, we conclude that one cannot obtain connected components of $\mathcal{C}_\varepsilon$ diffeomorphic to either closed or semiclosed segments in $\mathbb{R}$.

Third step: let us prove that $\mathcal{C}_\varepsilon$ is a disjoint union of connected components which are all diffeomorphic to the circle S^1.

We fix $r \in \mathbb{R}$ small enough, $r > 0$ and we fix the neighbourhood V to be $D_r := \{(x,y) \in \mathbb{R}^2 \mid ||(x,y)|| \leq r\}$ such that $(0,0)$ is the only critical point of f in the disk D_r. Firstly, we have $\mathcal{C}_\varepsilon$ is a closed set, since the preimage of a closed set by the continuous function f is closed. Since $\mathcal{C}_\varepsilon$ is also bounded, it is compact.

Secondly, we will show that $\mathcal{C}_\varepsilon \cap \partial D_r = \emptyset$. Since for ε sufficiently small, the curve $(f = \varepsilon)$ lies sufficiently close to the origin $(0,0)$, there exists $0 < \varepsilon_1 \ll 1$ such that $\mathcal{C}_\varepsilon \cap D_{\frac{r}{2}} \neq \emptyset$ for all $\varepsilon < \varepsilon_1$. We want to prove that there exists $0 < \varepsilon_2 \ll \varepsilon_1$ such that $\mathcal{C}_\varepsilon \subset D_{\frac{r}{2}}$ for all $\varepsilon < \varepsilon_2$. We argue by contradiction. Suppose there exists a sequence $\varepsilon_n \to 0$ such that $\mathcal{C}_{\varepsilon_n} \not\subset D_{\frac{r}{2}}$, namely $\mathcal{C}_{\varepsilon_n} \cap D_r \setminus D_{\frac{r}{2}} \neq \emptyset$. Hence, for any ε_n, there exists a point $(x_{\varepsilon_n}, y_{\varepsilon_n}) \in \mathcal{C}_{\varepsilon_n}$, namely $f(x_{\varepsilon_n}, y_{\varepsilon_n}) = \varepsilon_n$, such that $(x_{\varepsilon_n}, y_{\varepsilon_n}) \in D_r \setminus D_{\frac{r}{2}}$. If $\varepsilon := \frac{1}{n}$, then one obtains a sequence (x_n, y_n) with the following properties:

(a) $(x_n, y_n) \in D_r \setminus D_{\frac{r}{2}}$;

(b) $f(x_n, y_n) = \frac{1}{n}$.

Since $D_r \setminus D_{\frac{r}{2}}$ is a compact, there exists a convergent subsequence $(x_{\phi(n)}, y_{\phi(n)})$ of (x_n, y_n). More precisely, $\phi(n)$ is a strictly increasing and unbounded sequence of natural numbers.Let us denote by $\lim_{n\to\infty}(x_{\phi(n)}, y_{\phi(n)}) = (x_\infty, y_\infty) \in \overline{D_r} \setminus D_{\frac{r}{2}}$. One obtains $f(x_{\phi(n)}, y_{\phi(n)}) = \frac{1}{\phi(n)}$ and by the continuity of f, $f(x_\infty, y_\infty) = \lim_{n\to\infty} f(x_{\phi(n)}, y_{\phi(n)}) = \lim_{n\to\infty} \frac{1}{\phi(n)} = 0$. Therefore, there exists $(x_\infty, y_\infty) \neq (0,0)$, $(x_\infty, y_\infty) \in D_r$, such that $f(x_\infty, y_\infty) = 0$. This gives a contradiction with our hypothesis that $(0,0)$ is the isolated local minimum of f in D_r. Hence, $\mathcal{C}_\varepsilon$ is bounded.

In conclusion, we proved that $\mathcal{C}_\varepsilon \cap \partial D_r = \emptyset$. Hence we conclude that the level set $\mathcal{C}_\varepsilon$ could be a disjoint union of connected components which are either diffeomorphic to the segment $[0,1]$, or to the circle S^1. Since we have excluded the closed segments at the first step of our proof, $\mathcal{C}_\varepsilon$ is a disjoint union of connected components which are all diffeomorphic to the circle S^1.

Fourth and last step: we prove that $\mathcal{C}_\varepsilon \overset{\text{diffeo}}{\simeq} S^1$.

We argue by contradiction. Let us suppose that $\mathcal{C}_\varepsilon$ is a disjoint union of at least two distinct connected components, say S_1 and S_2, which are both diffeomorphic to the circle S^1. By the

Extreme Value Theorem, in the interiors of both these two connected components there is a local extremum of f. Since locally the origin is the only critical point in V that f admits by hypothesis, we obtain $(0,0) \in \text{Int } \mathrm{S}_1$ and $(0,0) \in \text{Int } \mathrm{S}_2$. Since $\mathcal{C}_\varepsilon$ is not self-intersecting, the configuration from Figure 2.21(a) below is impossible.

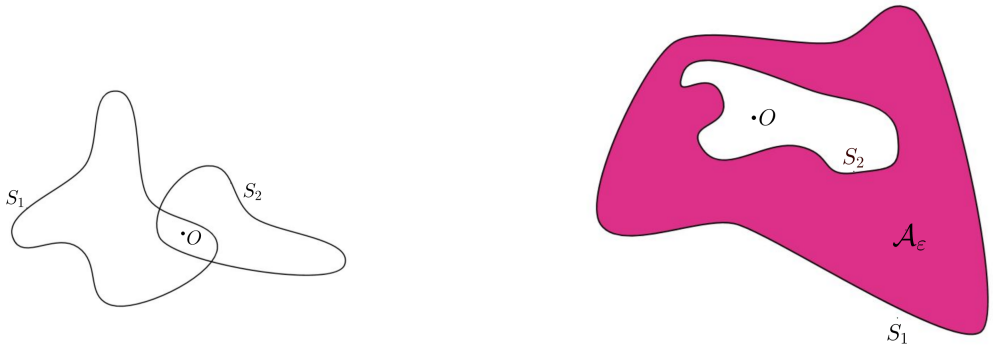

(a) Impossible configuration for $\mathcal{C}_\varepsilon$. (b) The annulus $\mathcal{A}_\varepsilon$ in pink.

Figure 2.21: Configurations for S_1 and S_2.

Hence the only two possible situations would be either $\mathrm{S}_1 \subset \text{Int } \mathrm{S}_2$ or $\mathrm{S}_2 \subset \text{Int } \mathrm{S}_1$. Without any loss of generality, let us choose $\mathrm{S}_2 \subset \text{Int } \mathrm{S}_1$. We have $(0,0) \in \text{Int } \mathrm{S}_2$. Let us consider the closed annulus bounded by the two circles, namely $\mathcal{A}_\varepsilon := \mathrm{S}_1 \cup (\text{Int } \mathrm{S}_1 \setminus \text{Int } \mathrm{S}_2)$. See Figure 2.21(b) above.

Since $\mathcal{A}_\varepsilon$ is compact, by the Extreme Value Theorem, the function f must attain a maximum value and a minimum value on $\mathcal{A}_\varepsilon$. We recall that f is not constant, since $(0,0) = f^{-1}(0)$ is a strict local minimum of f. If one extremum value is attained by f on S_1 and on S_2 ($f = \varepsilon$ both on S_1 and on S_2), then the other extremum value will necessarily be attained in Int $\mathcal{A}_\varepsilon$. Hence we obtain a contradiction with the hypothesis of the unique singularity of f in a neighbourhood of the origin. Therefore, we conclude that $\mathcal{C}_\varepsilon$ cannot have more than one connected component diffeomorphic to the circle S^1, thus $\mathcal{C}_\varepsilon \overset{\text{diffeo}}{\simeq} S^1$ and $(0,0) \in \mathcal{C}_\varepsilon$.

□

2.5.2 The polar curve

The notion of a polar curve goes back to the XIXth century, appearing in the work of J.-V. Poncelet ([Pon17]) and M. Plücker ([Plü37]) in the period of 1813-1830 (see for instance [Tei90], [Tei77], [TF16]). Starting with the 1970s, the theory of polar curves (see [BK86, page 589]) was renewed by important investigations and contributions due to Lê ([LMW89]), Teissier, Merle, Eggers, Delgado, García Barroso ([GB00], [GB98], [GB96]), Płoski, Gwoździewicz, Casas-Alvero, Michel, Weber, Maugendre ([Mau99]), Hefez among others. Considerable research on the polar curves has been carried out in the complex setting. However, less is known about the real polar curves.

Definition 2.43. [GB00, Section 4] Let $f : \mathbb{R}^2 \to \mathbb{R}$ be a polynomial function. The set

$$\Gamma(f,x) = \left\{ (x,y) \in \mathbb{R}^2 \mid \frac{\partial f}{\partial y}(x,y) = 0 \right\}$$

is called **the polar curve of f with respect to x**.

REMARK 2.44. The polar curve $\Gamma(f,x)$ consists of the points $(x,y) \in \mathbb{R}^2$ where the level curves of f have a vertical tangent. However, if f has a strict local minimum, then the polar curve does not contain the projection direction (see Proposition 2.45).

Proposition 2.45. *If $f : \mathbb{R}^2 \to \mathbb{R}$ has a strict local minimum at the origin and $f(0,0) = 0$, then the polar curve $\Gamma(f,x)$ does not contain the line $x = 0$.*

Proof. We argue by contradiction. If the line $x = 0$ is contained in $\Gamma(f,x)$, then we may write $\frac{\partial f}{\partial y}(x,y) = xg(x,y)$, where $g \in \mathbb{R}[x,y]$. Then $f(x,y) = f(x,0) + \int_0^y xg(x,t)\mathrm{d}t = x\varphi(x,y)$, since $f(0,0) = 0$. Hence f does not have a strict local minimum at the origin, because it vanishes on $x = 0$. Contradiction. □

EXAMPLE 2.46. In Figure 2.22 is represented the polar curve $\Gamma(f,x)$ of Coste's example (see Example 2.10: $f(x,y) := x^2 + (y^2 - x)^2$). It has two irreducible components, with equations $(y = 0) \cup (y^2 - x = 0)$.

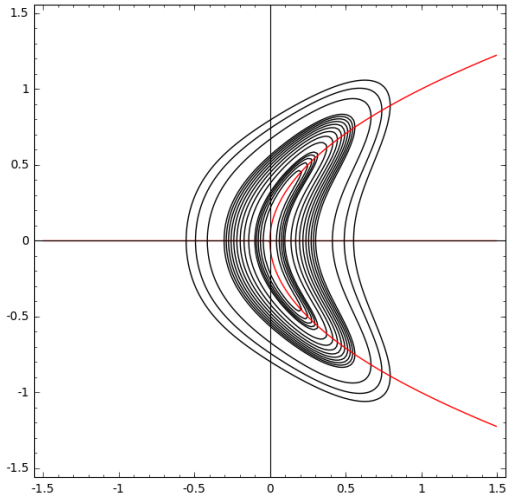

Figure 2.22: The polar curve $(y = 0) \cup (y^2 - x = 0)$ for Example 2.10, namely Coste's example

EXAMPLE 2.47. Recall our Example 2.12: $f(x,y) := x^{16} + (y^2 + x)^2(y^2 - x)^2$. In Figure 2.23, the polar curve $\Gamma(f,x)$ has three components $(y = 0) \cup (y^2 + x = 0) \cup (y^2 - x = 0)$.

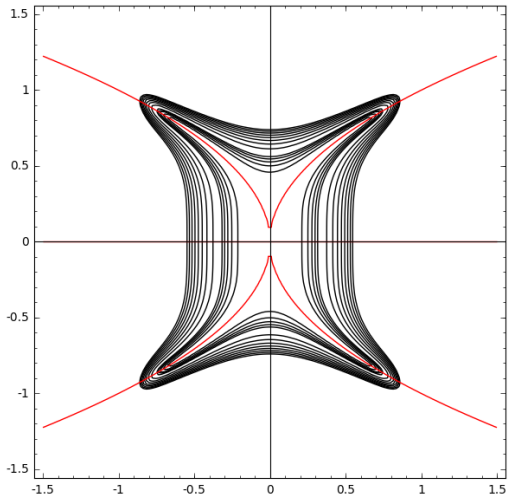

Figure 2.23: The polar curve $(y = 0) \cup (y^2 + x = 0) \cup (y^2 - x = 0)$ for Example 2.12.

EXAMPLE 2.48. We can create new examples starting from Coste's example by taking the parametrisation of a branch γ of the polar curve $\Gamma(f,x)$, namely $t \mapsto (t^2,t)$, and modify it, as follows.

Consider the new parametrisation $(t \mapsto p(t),q(t))$, where $p(t)=t^2+t^3$ and $q(t):=t$. Let us compute the resultant of the polynomials $g(t):=x-p(t)$ and $h(t):=y-q(t)$, in order to find the implicit polynomial whose zero locus is γ. We have the resultant (see for instance [BK86, page 178])

$$\mathrm{Res}_t(x,y)=\det\begin{bmatrix}-1 & -1 & 0 & x\\ -1 & y & 0 & 0\\ 0 & -1 & y & 0\\ 0 & 0 & -1 & y\end{bmatrix}=x-y^3-y^2.$$

Thus, (see [BK86, page 181]) we have a new algebraic branch $\tilde{\gamma}:=\{(x,y)\in\mathbb{R}^2 \mid x-y^3-y^2=0\}$.

Take now $\tilde{f}(x,y):=x^2+(x-y^3-y^2)^2(x-y^2)^2$ and obtain the local situation of the polar curve in a small enough neighbourhood of the origin as presented in Figure 2.24 below.

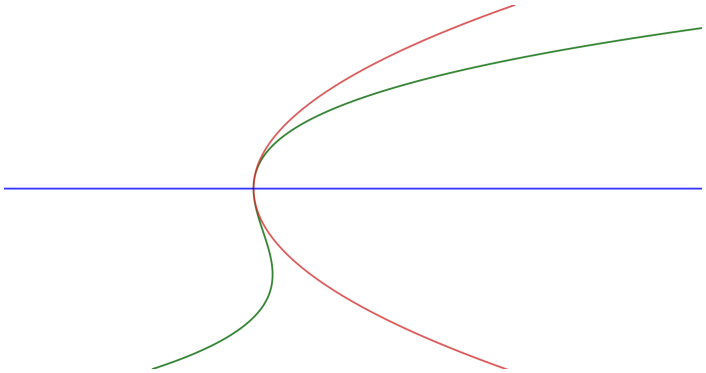

Figure 2.24: We modified the initial parabola γ (in red) into $\tilde{\gamma}$ (in green), both branches of the polar curve $\Gamma(\tilde{f},x)$, to obtain a different local shape of $\mathcal{C}_\varepsilon$ when compared to the initial one in Coste's example.

EXAMPLE 2.49. Recall our Example 2.13: $f(x,y):=x^6+(y^4+y^2-x)^2(y^2-x)^2$. In Figure 2.25, the polar curve $\Gamma(f,x)$ has four components.

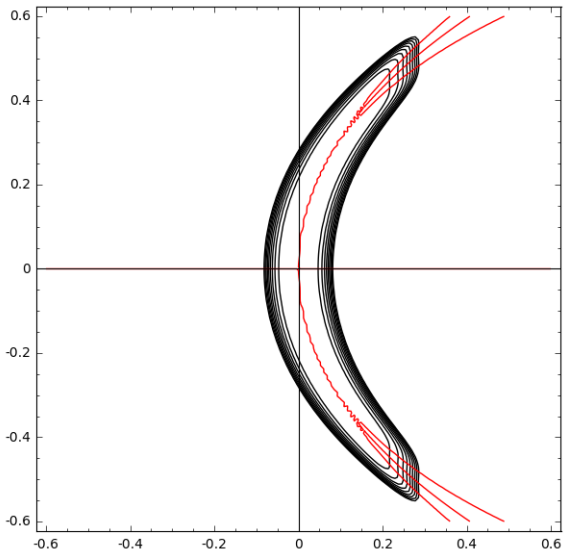

Figure 2.25: The polar curve for our Example 2.13.

For more details about the next Lemma 2.50, one should see [Ghy17, page 105].

Lemma 2.50. *[Mil68] Let Γ be a real algebraic curve. Firstly, there exists a Milnor disk for Γ at the origin: a Euclidean disk such that the boundaries of all the concentric disks inside the Milnor disk are transverse to the curve. Secondly, if the curve is analytically irreducible at the origin, then in such a disk the curve is homeomorphic to a segment.*

A proof can be found in [Mil68, Lemma 3.3, page 28] and [Ghy17, page 105].

Definition 2.51. [Ghy17, page 2] A **real branch** is the germ at the origin of an analytically irreducible curve at this point.

A definition similar to Definition 2.52 can be found, for instance, in [Cas15, page 97].

Definition 2.52. A **half-branch** (see Figure 2.26 below) is the germ at the origin of the closure of one of the connected components of the complementary of the origin in a Milnor representative of a branch.

Remark 2.53. We can choose to denote one half-branch by γ_i^+ and the other one by γ_i^-.

Definition 2.54 is inspired by [CP01, Section 2].

Definition 2.54. We call **polar half-branches** the half-branches of the polar curve $\Gamma := \Gamma(f, x)$, in the sense of Definition 2.52. Let $\gamma^* \subset \Gamma$ be a polar half-branch and let V be a good neighbourhood of the origin, as in Definition 2.67. We say that γ^* in V is a **right polar half-branch** if $x_{|\gamma^*} \geq 0$. If $x_{|\gamma^*} \leq 0$, we say that γ^* in V is a **left polar half-branch**.

Remark 2.55. By Corollary 2.62, in a sufficiently small V we always have that x is strictly increasing when restricted to the right polar half-branches and strictly decreasing when restricted to the left polar half-branches.

Remark 2.56. We sometimes call the union of the right polar half-branches the **positive** polar curve.

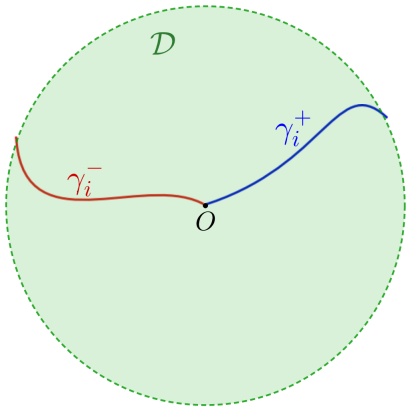

Figure 2.26: A branch γ_i of Γ has exactly two half-branches: γ_i^- and γ_i^+.

A result similar to the following lemma can be found in [FCP96, Lemma 1.1].

Lemma 2.57. *Let $g : \mathbb{R}^2 \to \mathbb{R}$ be a polynomial function with a strict local minimum at the origin $O = (0, 0)$ and let Γ be an algebraic curve passing through the origin. In a small enough neighbourhood V of the origin, for any half-branch $\gamma^* \subset \Gamma$, the restriction $g_{|\gamma^*}$ is strictly monotone. In particular, in the sufficiently small neighbourhood V, for a small enough $\varepsilon > 0$, the intersection $(g = \varepsilon) \cap \gamma^*$ consists of exactly one point, for each half-branch γ^* (see Figure 2.27). Here the symbol $* \in \{+, -\}$.*

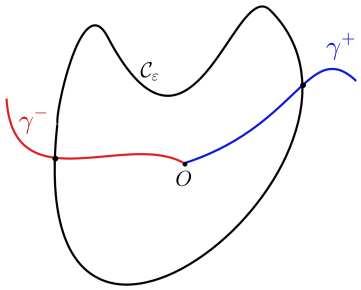

Figure 2.27: For a small enough neighbourhood V and for a sufficiently small $\varepsilon > 0$, the intersection $\mathcal{C}_\varepsilon \cap \gamma^-$ (respectively $\mathcal{C}_\varepsilon \cap \gamma^+$) consists of exactly one point.

Proof. Let us choose, without loss of generality, to study the behaviour of g on γ^+. Suppose that $g_{|\gamma^+}$ is not constant. Since Γ is an algebraic curve, it has only a finite number of critical points. Therefore one can assume that in a small enough neighbourhood V of the origin $O = (0,0)$, the half-branch γ^+ has no critical points except maybe the origin $O = (0,0)$. By [Mil68, Lemma 2.7], applied to the polynomial function g and to the one-dimensional manifold γ^+, which is a subset of the algebraic curve Γ, in the sufficiently small neighbourhood of $O = (0,0)$, the set of the local extrema of $g_{|\gamma^+}$ is an algebraic set of dimension zero. Thus, by [Eis95, Corollary 9.1, page 227], the set of local extrema is finite. Now let us choose V sufficiently small such that in V there are no local extrema of the function $g_{|\gamma^+\setminus\{(0,0)\}}$. Thus, in V, $g_{|\gamma^+}$ is strictly monotone. □

Corollary 2.58. *Given a polynomial function f with a strict local minimum at the origin and its polar curve $\Gamma(f,x)$, if γ^+ is a right polar half-branch, then f_{γ^+} is always strictly increasing in V, when going further from the origin.*

Proof. Apply Lemma 2.57 for the function f and the polar curve $\Gamma(f,x)$, taking into account that $(0,0)$ is a strict local minimum. □

Example 2.59. Let us present in Figure 2.28 a configuration which is **impossible** asymptotically (i.e. for $\varepsilon > 0$ sufficiently small) in V: even if $x_{|\gamma^+}$ is strictly increasing, we have $f_{|\gamma^+}$ not strictly increasing.

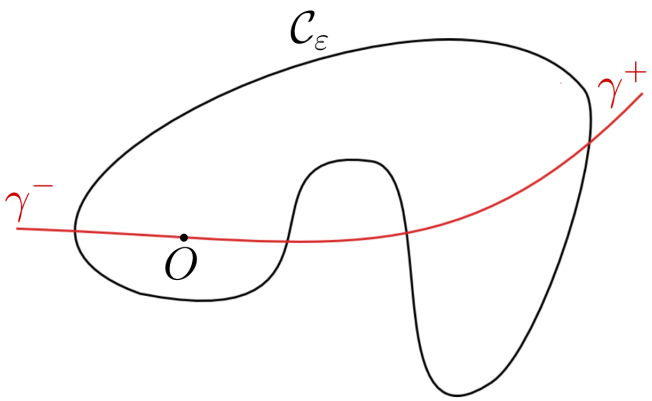

Figure 2.28: Locally impossible configuration in V: $f_{|\gamma^+}$ not strictly increasing.

Corollary 2.60. *In particular, the shape of $\mathcal{C}_\varepsilon$ in a sufficiently small enough V cannot go backwards or be spiral shaped.*

Corollary 2.61. *We can choose a sufficiently small neighbourhood V such that the intersection $\gamma^* \cap \mathcal{C}_\varepsilon$ consists of exactly one point, where $\mathcal{C}_\varepsilon := (f = \varepsilon) \cap V$.*

Proof. By Corollary 2.58, for any polar half-branch γ^* one has f_{γ^*} is locally strictly increasing, thus for sufficiently small ε, the intersection $(f = \varepsilon) \cap \gamma^*$ consists of at most one point. □

A consequence of Lemma 2.57, applied to the polar curve $\Gamma(f, x)$ of f and for the function $g : \mathbb{R}^2 \to \mathbb{R}$, $g(x, y) := x$ is the following result.

Corollary 2.62. *Let f be a polynomial function with a strict local minimum at the origin and let $\Gamma(f, x) := \left\{(x, y) \in \mathbb{R}^2 \;\middle|\; \frac{\partial f}{\partial y}(x, y) = 0\right\}$ be its polar curve with respect to x. In a small enough neighbourhood V of the origin, for any polar half-branch $\gamma^* \subset \Gamma$, the restriction $x_{|\gamma^*}$ is strictly monotone. Here the symbol $* \in \{+, -\}$.*

Proof. Since x is not constant on $\Gamma(f, x)$ by Proposition 2.45, we can apply Lemma 2.57. □

Example 2.63. Let us present in Figure 2.29 a locally **impossible** configuration in V of $\mathcal{C}_\varepsilon$ with a polar half-branch γ^+: even if $f_{|\gamma^+}$ is strictly increasing, we have $x_{|\gamma^+}$ not strictly increasing.

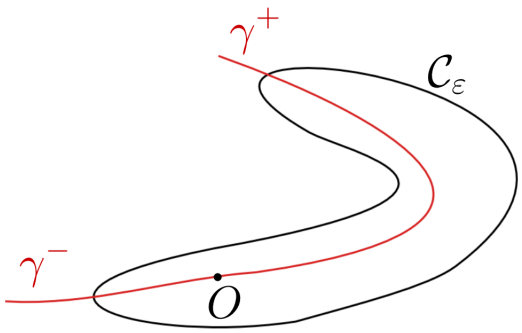

Figure 2.29: Impossible asymptotic configuration in V, since $x_{|\gamma^+}$ is not strictly increasing.

Remark 2.64. In particular, the shape of $\mathcal{C}_\varepsilon$ in a sufficiently small enough V cannot "go backwards". More rigorously, if we choose V small enough, then the polar curve $\Gamma(f, x)$ has no vertical tangents in V. A vertical tangent of a polar half-branch γ^* would correspond to a local extremum of the function $x_{|\gamma^*}$, which is impossible.

A consequence of Lemma 2.57, applied to the polar curve $\Gamma(f, x)$ of a polynomial function f with a strict local minimum at the origin and to the function square of the distance to the origin, namely $x^2 + y^2$ is the following result.

Corollary 2.65. *Let f be a polynomial function f with a strict local minimum at the origin and let $\Gamma(f, x)$ be its polar curve with respect to x. In a small enough neighbourhood V of the origin, for any polar half-branch $\gamma^* \subset \Gamma$, the restriction $x^2 + y^2{}_{|\gamma^*}$ is strictly monotone. Here the symbol $* \in \{+, -\}$.*

Corollary 2.66. *We can choose a sufficiently small neighbourhood V such that for any polar half-branch γ^*, the intersection $\gamma^* \cap \partial V$ consists of exactly one point.*

2.6 The asymptotic Poincaré-Reeb tree

The Poincaré-Reeb tree stabilises up to equivalence (see Definition 2.38) when the level gets small enough. This "limit" transversal tree is called **"the asymptotic Poincaré-Reeb tree" of f relative to x**. It has the following properties:

- the image of the origin is a point of valency 2, which will be considered to be the root of the tree;

- the preorder on the set of vertices induced by the function x is strictly monotonous on each geodesic starting from the root.

Here "limit" means for a sufficiently small $\varepsilon > 0$.

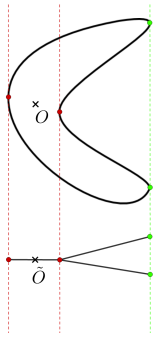

Figure 2.30: An asymptotic Poincaré-Reeb tree.

Definition 2.67. Let us consider a polynomial function $f : \mathbb{R}^2 \to \mathbb{R}$ with a strict local minimum at the origin, such that $f(0,0) = 0$. Denote by $\Gamma(f,x)$ the polar curve of f with respect to the direction x. Let V be a neighbourhood of the origin $O(0,0)$. We say that the neighbourhood V is a **good neighbourhood of the origin for the couple** (f,x) if V satisfies:

(i) the point $(0,0)$ is **the only strict local minimum** of f in V;

(ii) we have $V \cap (f = 0) = \{(0,0)\}$.

(iii) $\mathrm{Sing}(\Gamma(f,x)) \cap V \subseteq \{(0,0)\}$;

(iv) V is small enough such that on each polar half-branch γ^* of $\Gamma(f,x)$ we have $f_{|\gamma^*}$ is strictly monotone;

(v) V is small enough such that on each polar half-branch γ^* of $\Gamma(f,x)$ we have $x_{|\gamma^*}$ is strictly monotone.

(vi) V is small enough such that for any polar half-branch γ^*, the intersection $\gamma^* \cap \partial V$ consists of exactly one point

Remark 2.68. Condition (i) implies for any two distinct polar half-branches γ_i^* and γ_j^*, we have

$$(\gamma_i^* \cap \gamma_j^*) \cap V = \{(0,0)\}.$$

Definition 2.69. Consider a polynomial function f with a strict local minimum at the origin, such that $f(0,0) = 0$. The **asymptotic Poincaré-Reeb tree** of f relative to x is the "limit" Poincaré-Reeb tree of its sufficiently small levels near the origin with respect to x. Here by "limit" we mean: for a sufficiently small $\varepsilon > 0$.

Theorem 2.70. *Besides the properties of the Poincaré-Reeb tree (see Corollary 2.37),* ***the asymptotic Poincaré-Reeb tree*** *stabilises up to equivalence (see Definition 2.38) when the level gets small enough. It is a* ***rooted*** *plane tree, the root being the image of the origin. The total preorder relation on its vertices, induced by the function x, is* ***strictly monotone*** *on each geodesic starting from the root. In addition, the asymptotic Poincaré-Reeb tree is a union of* ***a positive tree*** *(at the right of the origin) and* ***a negative tree*** *(at the left of the origin), the latter two having a common root, that is the image of the origin.*

Proof. Let us first prove the stabilisation. Take two right polar half-branches γ_i and γ_j. Denote by $(x_i(t), y_i(t))$, respectively $(x_j(t), y_j(t))$ their corresponding Newton-Puiseux parametrisations (see [Wal04, Theorem 2.1.1]). Here $x_1(t), y_1(t), x_2(t), y_2(t) \in \mathbb{R}\{t\}$ are convergent analytic parametrisations. Now denote by $g(t) := x_i(t) - x_j(t)$. We have two possibilities: either $g(t) \equiv 0$, i.e. we have a vertical bitangent, or $g(t) \not\equiv 0$. In the second case, by taking a sufficiently small t, the sign of the analytic function g does not change. Since there are finitely many polar half-branches, we can choose a sufficiently small t such that the total preorder stabilises.

In the asymptotic setting, if we consider a polynomial function $f : \mathbb{R}^2 \to \mathbb{R}$ with a strict local minimum at the origin such that $f(0,0) = 0$, then the root of the Poincaré-Reeb tree is the image of the origin by the quotient map (see Section 2.4). By Lemma 2.42, the origin is in the interior of the disk $\mathcal{D}_\varepsilon$. Since the real plane is cooriented, we distinguish without ambiguity between the positive tree (at the right of the origin) and the negative tree (at the left of the origin), the latter two having the common root, that is the image of the origin.

Moreover, we have the induced application $\tilde{x} := x$ of the projection function $x : \mathbb{R}^2 \to \mathbb{R}$ to the embedded Poincaré-Reeb tree. By Corollary 2.62: for any polar half-branch $\gamma^* \subset \Gamma(f, x)$, the restriction $x_{|\gamma^*}$ is strictly monotone. Thus, $\tilde{x}$ has no internal local extremum on an edge of $\mathcal{R}(f, x)$. To the right, $\tilde{x}$ only attains its local maxima on the leaves of $\mathcal{R}(f, x)$. Similarly, to the left, $\tilde{x}$ only attains its local minima on the leaves of $\mathcal{R}(f, x)$. In other words, there are no edges of $\tilde{x}$ only attains its local maxima on the leaves of $\mathcal{R}(f, x)$ which "go backwards".

□

Remark 2.71. Since we did not impose any condition of genericity for the direction of projection, one can obtain several vertices of the asymptotic Poincaré-Reeb tree on the same level of the foliation of the plane given by x (namely they are points on a vertical bitangent, see Figure 2.31), thus we only have a total preorder relation, not a total order relation on the vertices.

Example 2.72. A Poincaré-Reeb tree whose vertices are in a total preorder relation, which is not a total order relation, since there exist vertical bitangents (in blue and in pink, see Figure 2.31). Thus the vertices v_1 and v_2 (in blue) have the same x-coordinate and $\tilde{x}$-coordinate. Similarly, the points v_3, v_4 and v_5 (in pink) have the same x-coordinate and $\tilde{x}$-coordinate.

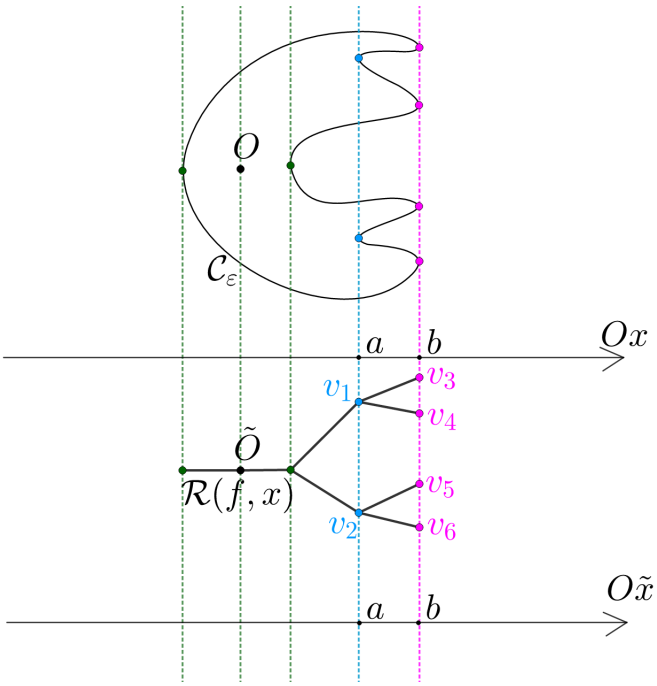

Figure 2.31: A total preorder relation, which is not a total order relation.

REMARK 2.73. If the asymptotic Poincaré-Reeb tree is generic (see Section 2.8 below), we do not have the phenomenon from Example 2.72.

REMARK 2.74. The strict monotonicity on the geodesics starting from the root implies that the small enough level curves $\mathcal{C}_\varepsilon$ have no turning back or spiralling phenomena. In particular, for $\varepsilon > 0$ sufficiently small, there are no shapes $\mathcal{C}_\varepsilon$ like the one in Figure 2.32.

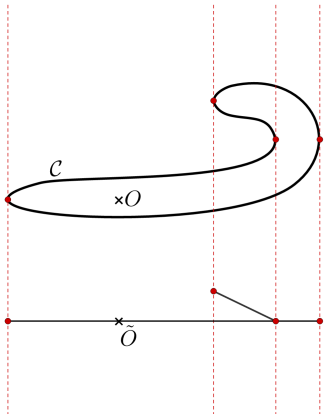

Figure 2.32: Forbidden shape for small enough $\varepsilon > 0$: there are no going backwards like this.

2.6.1 Positive tree, negative tree, union tree

The image of the origin will be the root of the Poincaré-Reeb tree. The real line is oriented, thus once the root is fixed, the root will separate without ambiguity between the negative side (i.e. left side) and the positive side (i.e. right side), as we shall see in the sequel.

Definition 2.75. If $v_1(x_1, y_1)$ and $v_2(x_2, y_2)$ are two points in a real plane P endowed with a trivial fibre bundle $\Pi : P \to \mathbb{R}$, we say that v_2 is **to the right of** v_1 if $x_2 > x_1$. If $x_2 < x_1$, we say that v_2 is **to the left of** v_1.

Definition 2.76. We call **a positive tree** a plane tree in which every vertex has its children to the right. We call **positive edges** the edges belonging to a complete plane binary positive tree.

EXAMPLE 2.77. The following Figure 2.33 shows a complete plane binary positive tree. For instance, the vertex v_2 is to the right of the vertex v_1.

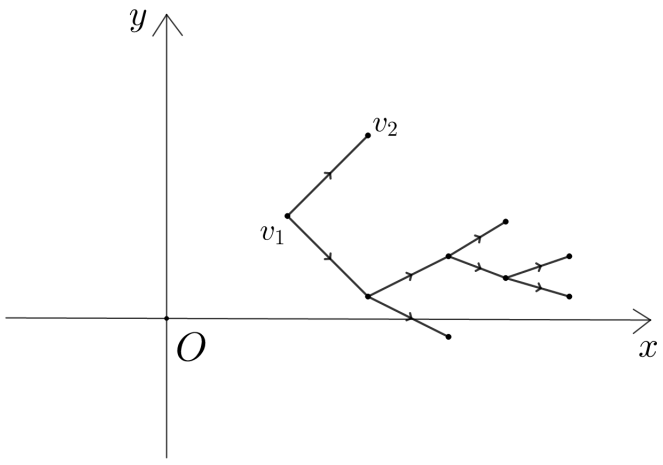

Figure 2.33: A complete plane binary positive tree.

Definition 2.78. We call **a negative tree** a plane tree in which every vertex has its children to the left. We call **negative edges** the edges belonging to a complete plane binary negative tree.

Definition 2.79. Let $\mathcal{T}_+$ be a positive tree and $\mathcal{T}_-$ be a negative tree. We call **the union tree** between $\mathcal{T}_-$ and $\mathcal{T}_+$, denoted by $\mathcal{T}_- - O - \mathcal{T}_+$, the plane tree obtained by making the connected sum of the two trees: we glue their roots into a point O, which becomes the root of the union-tree.

Example 2.80. We show in Figure 2.34 how we make the union tree, by making the connected sum of two half-planes. The arrows show the orientation of the half-planes, such that at the glued line the orientations are reversed.

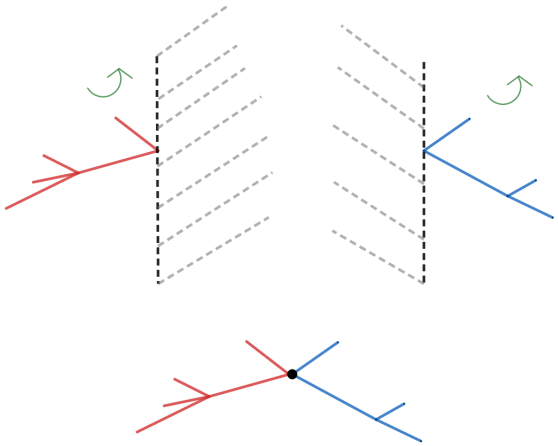

Figure 2.34: The union tree of a negative tree and a positive tree.

Remark 2.81. The asymptotic Poincaré-Reeb tree is a union tree of a positive tree and a negative tree (see Figure 2.35).

Since the plane is cooriented the image of the origin by the quotient map q separates the asymptotic Poincaré-Reeb tree in a negative tree and a positive tree. They form a union tree, whose root is the image of the origin.

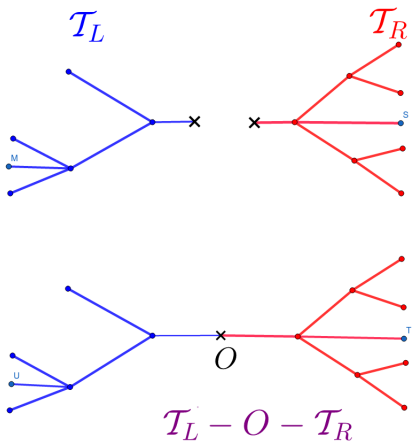

Figure 2.35: The asymptotic Poincaré-Reeb tree is a union of a negative tree and a positive tree.

REMARK 2.82. The root is a special vertex of the union tree. More precisely, the root of the union tree will be the only vertex with valency equal to two.

2.7 Generic directions of projection

2.7.1 Choosing the direction of a generic projection for one level curve

Definition 2.83. [Fis01, page 74] Let $\mathcal{C} \subset \mathbb{CP}^2$ be an algebraic curve. Then

$$\mathcal{C}^* := \left\{ L \in \mathbb{CP}^2 \mid L \text{ is tangent to } \mathcal{C} \text{ at some point } p \in \mathcal{C} \right\}$$

is called **the dual curve of** $\mathcal{C}$.

REMARK 2.84. Definition 2.83 is standard (see for instance [Fis01, pages 73-74], [BK86, page 252]). We denote the dual projective space by $(\mathbb{CP}^2)^*$. To a point

$$y = [y_0 : y_1 : y_2] \in (\mathbb{CP}^2)^*,$$

it corresponds the line $V(y_0X_0 + y_1X_1 + y_2X2) \subset \mathbb{CP}^2$.

The dual curve can be visually constructed by using the theory of pole-polar relation in a circle, see Figure 2.36 below and [BK86, pages 577-583].

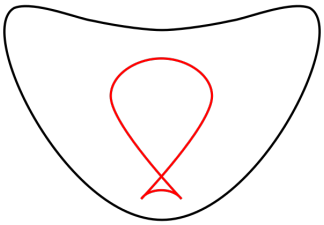

Figure 2.36: A curve and its dual (see [Wv]).

The three next results are classical. The proofs can be found, for instance, in [Fis01, Chapter 5], [Wal04, Chapter 7] or [GKZ94, Chapter 1].

Proposition 2.85. *[Fis01, page 74] Let $\mathcal{C} \subset \mathbb{CP}^2$ be an algebraic curve that has no lines as components. Then:*

(a) the dual curve of $\mathcal{C}$, denoted by $\mathcal{C}^*$, is an algebraic curve;

(b) $\mathcal{C}^{**} = \mathcal{C}$;

(c) if $\mathcal{C}$ is irreducible, then $\mathcal{C}^*$ is irreducible and $\deg \mathcal{C}^* \geq 2$.

Lemma 2.86. *[GKZ94, page 20] For a smooth curve $\mathcal{C}$, cusps of $\mathcal{C}^*$ correspond to the simple inflection points of $\mathcal{C}$, i.e. such points where the tangent line has tangency to $\mathcal{C}$ of exactly the second order and is not tangent to $\mathcal{C}$ anywhere else. Similarly, nodes of $\mathcal{C}^*$ correspond to simple bitangents of $\mathcal{C}$, i.e. such that both tangencies are of first order and there are no other points of tangency.*

Lemma 2.87. *[Fis01, page 49] An irreducible algebraic curve $\mathcal{C} \subset \mathbb{CP}^2$ of degree n has at most $\frac{1}{2}(n-1)(n-2)$ singularities.*

In the sequel, let us prove that any irreducible algebraic curve $\mathcal{C} \subset \mathbb{CP}^2$ has a finite number of bitangent lines and finitely many inflection points. These proofs will lead us to the choice of the direction of a generic projection with respect to $\mathcal{C}_\varepsilon$, for a small enough $\varepsilon > 0$, as we shall see at the end of this section.

Lemma 2.88. *An irreducible algebraic curve $\mathcal{C} \subset \mathbb{CP}^2$ has a finite number of bitangent lines.*

Proof. By Proposition 2.85, (b), we have $\mathcal{C}^*$ is also an algebraic curve. Thus, by Lemma 2.87, the dual algebraic curve $\mathcal{C}^*$ has a finite number of double nodes, namely $\frac{1}{2}(n^*-1)(n^*-2)$, where $n^* := \deg \mathbb{C}^*$. By Lemma 2.86, the bitangents of $\mathcal{C}$ correspond to the double nodes of $\mathcal{C}^*$. □

A similar result for the inflection points can be given, but [Fis01] gave a better result, in function of $n := \deg \mathcal{C}$, as follows:

Lemma 2.89. *[Fis01, page 68] An algebraic curve $\mathcal{C} \subset \mathbb{CP}^2$ of degree $\deg \mathcal{C} \geq 2$ that contains no lines has at most $3n(n-2)$ inflection points.*

Since we have the finiteness conditions given by Lemma 2.88 and Lemma 2.89, we are ready to introduce the following Definition 2.90 of a **generic projection**, which will be used in the next sections, followed by Proposition 2.91.

Definition 2.90. Let us consider a polynomial function $f : \mathbb{R}^2 \to \mathbb{R}$ and let us denote by $\mathcal{C}_\varepsilon := \{(x,y) \in \mathbb{R}^2 \mid f(x,y) = \varepsilon\}$, for a sufficiently small fixed $0 < \varepsilon \ll 1$. We call a **generic direction with respect to $\mathcal{C}_\varepsilon$**, a direction d which satisfies the following conditions:
(i) d is not the direction of any bitangent of $\mathcal{C}_\varepsilon$;
(ii) d is not the direction of any tangent which passes through any inflection point of $\mathcal{C}_\varepsilon$;

Proposition 2.91. *All but finitely many directions of projection are generic, for a fixed $\varepsilon > 0$.*

Proof. The proof is a consequence of Lemma 2.88 and Lemma 2.89, using Definition 2.90. □

Lemma 2.92. *In a good neighbourhood of the origin (see Definition 2.67), if the direction x is generic, then the Poincaré-Reeb tree is a rooted plane tree whose vertices are in a **total order relation** given by the induced application $\tilde{x} := x$ (see Definition 2.24), such that this total order is strictly increasing (respectively decreasing) on any geodesic going from the root to the right (respectively left).*

Proof. It is a corollary of Theorem 2.70, but in the case of a generic projection, the total preorder relation between the vertices of the Poincaré-Reeb tree becomes a total order relation, since for a generic direction x there will be no bitangents, namely no two vertices which have the same x-coordinate. □

2.7.2 Choosing the direction of a generic projection for a family of level curves

The purpose of this section is to prove that, except for finitely many small intervals on the circle of projection directions, all the directions are generic (in the sense of Definition 2.90) for all $\mathcal{C}_\varepsilon$, where $\varepsilon > 0$ is sufficiently small.

Theorem 2.93. *There exists $\nu > 0$, there are finitely many intervals $U_i \subset \mathbb{RP}^1$, of length ν, such that for any $0 < \varepsilon \ll \nu$, all the projection directions of $\mathbb{RP}^1 \setminus \bigcup_i U_i$ are generic (as in Definition 2.90).*

Remark 2.94. We consider the metric on $\mathbb{RP}^1$ to be the one induced by the one on $\mathrm{S}^1/\!\sim$, where $\sim$ is the antipodal equivalence relation.

Proof. • Firstly, let us consider the Hessian matrix of f, namely

$$\text{Hess } (f)(x,y) := \begin{bmatrix} \frac{\partial^2 f}{\partial x^2}(x,y) & \frac{\partial^2 f}{\partial x \partial y}(x,y) \\ \frac{\partial^2 f}{\partial y \partial x}(x,y) & \frac{\partial^2 f}{\partial y^2}(x,y) \end{bmatrix}.$$

Denote by $\mathcal{H} := \{(x,y) \in \mathbb{R}^2 \mid \det \text{Hess } (f) = 0\}$ the set of inflection points of the level sets of f. Thus $\mathcal{H} \subset \mathbb{R}^2$ is a real algebraic set of dimension less or equal to 1 (see Figure 2.37, in green).

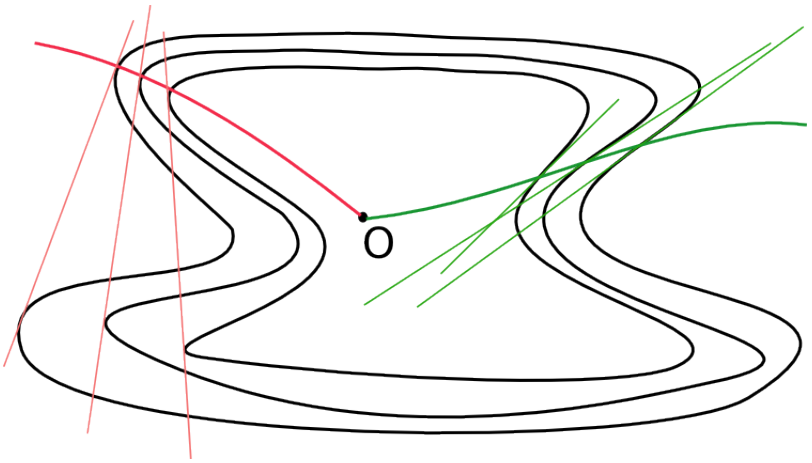

Figure 2.37: In green, an arc $\gamma_{\mathcal{H}} \subset \mathcal{H}$. In red, an arc $\gamma_{\mathcal{B}} \subset \mathcal{B}$. The curves in black represent three curves $\mathcal{C}_\varepsilon$, for sufficiently small $\varepsilon > 0$.

• Secondly, let $\mathcal{B} := \{P \in \mathbb{R}^2 \mid \exists Q \in \mathbb{R}^2, Q \neq P, \exists \varepsilon > 0$ such that $f(P) = f(Q) = \varepsilon$ and $P + T_P\mathcal{C}_\varepsilon = Q + T_Q\mathcal{C}_\varepsilon\}$ be the set of points where there exists a bitangent to a level set of f. Here $T_P\mathcal{C}_\varepsilon$ is the tangent to $\mathcal{C}_\varepsilon$ at the point P. We want to prove that $\mathcal{B}$ is a semialgebraic set of dimension less or equal to 1 (see Figure 2.37, in red).

Let $\Sigma := \{(P, Q) \in \mathbb{R}^2 \times \mathbb{R}^2 \mid \exists \varepsilon > 0$ such that $f(P) = f(Q) = \varepsilon$ and $P + T_P\mathcal{C}_\varepsilon = Q + T_Q\mathcal{C}_\varepsilon\}$ and $\delta = \{(P, P) \in \mathbb{R}^2 \times \mathbb{R}^2 \mid \exists \varepsilon > 0$ such that $f(P) = \varepsilon$ and $P + T_P\mathcal{C}_\varepsilon = P + T_P\mathcal{C}_\varepsilon\}$ the diagonal of Σ. Thus $\Sigma \setminus \delta$ is a semialgebraic set of $\mathbb{R}^2 \times \mathbb{R}^2$. Let us consider the projection $\Pi : \mathbb{R}^2 \times \mathbb{R}^2 \to \mathbb{R}^2$, $\Pi(P, Q) = P$. By Tarski-Seidenberg principle (see [Cos02, Section 2.1.2]), $\Pi(\Sigma \setminus \delta)$ is a semialgebraic set of $\mathbb{R}^2$. Since $\Pi(\Sigma \setminus \delta) = \mathcal{B}$, we have that $\mathcal{B}$ is a semialgebraic set.

Let us argue by contradiction to prove that the set $\mathcal{B}$, has dimension at most 1. Suppose $\mathcal{B}$ had dimension 2. Take $P \in \mathcal{B}$ then there exists a disk centred at P included in $\mathcal{B}$. If $\varepsilon_P := f(P) > 0$, we obtain that there exists a level curve $\mathcal{C}_{\varepsilon_P}$, which intersects this disk in infinitely many points. This in impossible, by Proposition 2.91: for a fixed $\varepsilon_P > 0$ there is a finite number of bitangents to $\mathcal{C}_\varepsilon$. In conclusion $\dim(\Pi(\Sigma \setminus \delta)) \leq 1$.

• Therefore we have $\mathring{\mathcal{H}} := \mathcal{H} \setminus \{O\}$ and $\mathring{\mathcal{B}} := \mathcal{H} \setminus \{O\}$ are semialgebraic sets of dimension less or equal to 1. Hence the set $\mathring{\mathcal{H}} \cup \mathring{\mathcal{B}}$ is also a semialgebraic set of dimension at most 1 of $\mathbb{R}^2 \setminus \{O\}$. Therefore, it has a finite number of arcs at the origin.

• The next step of the proof is to define the polynomial map $\Phi : \mathbb{R}^2 \to \mathbb{R}^2$,

$$\Phi(x, y) := \left(\frac{\partial f}{\partial x}(x, y), \frac{\partial f}{\partial y}(x, y)\right).$$

The set $\mathring{\mathcal{H}} \cup \mathring{\mathcal{B}}$ is semialgebraic of dimension at most 1, it is the union of finitely many half-branches: $\mathring{\mathcal{H}} \cup \mathring{\mathcal{B}} = \cup\gamma_i$, for finitely many i. Namely we have $\gamma_i : \mathbb{R} \to \mathbb{R}^2$.

Let us fix i_0. The image by Φ of the arc $\gamma_{i_0}(t)$ is the arc $\Phi(\gamma_{i_0}(t))$. The slope of a secant of the arc $\Phi(\gamma_{i_0}(t))$ is given by $\frac{\frac{\partial f}{\partial y}(\gamma_{i_0}(t)) - 0}{\frac{\partial f}{\partial x}(\gamma_{i_0}(t)) - 0}$. Since γ_{i_0} is a semialgebraic arc, there exists the limit

$$\lim_{t \to 0} \frac{\frac{\partial f}{\partial y}(\gamma_{i_0}(t))}{\frac{\partial f}{\partial x}(\gamma_{i_0}(t))} := p_{i_0},$$

which is the slope of the tangent at the origin. In other words, we use the well-known fact that an algebraic arc never reaches the origin as an infinite spiral (see for instance [Ghy17, p. 105]). If $p_{i_0} = \infty$, then make a change of coordinates. Therefore we can suppose that $p_{i_0} \in \mathbb{R}$ without loss of generality.

- The next step is to consider the map $\psi : \mathbb{R}^2 \to \mathbb{RP}^1$, defined by

$$\psi(x,y) := \left[\frac{\partial f}{\partial y}(x,y) : \frac{\partial f}{\partial x}(x,y)\right].$$

Thus

$$\lim_{t\to 0}\psi(\gamma_{i_0}(t)) = \lim_{t\to 0}\left[\frac{\partial f}{\partial y}(\gamma_{i_0}(t)) : \frac{\partial f}{\partial x}(\gamma_{i_0}(t))\right] = \lim_{t\to 0}\left[\frac{\frac{\partial f}{\partial y}(\gamma_{i_0}(t))}{\frac{\partial f}{\partial x}\gamma_{i_0}(t))} : 1\right] = [p_{i_0} : 1].$$

Since there are finitely many half-branches, we obtain finitely many points $[p_i : 1]$. For each of them, let us define a small neighbourhood $U_i \subset \mathbb{RP}^1$. There exists a real number $\nu > 0$ such that the directions corresponding to $\mathbb{RP}^1 \setminus \cup_i U_i$ are all generic directions (in the sense of Definition 2.90).

□

2.7.3 Geometric hypotheses for having a generic direction

In the asymptotic case, i.e. for $\varepsilon > 0$ sufficiently small, the level curve $\mathcal{C}_\varepsilon$ does not have tangents that pass through the origin.

Proposition 2.95. *There are no vertical tangents to $\mathcal{C}_\varepsilon$, for $\varepsilon > 0$ sufficiently small, that pass through the origin.*

Proof. Let $M_0(x_0, y_0) \in \mathcal{C}_\varepsilon$ be a point such that $\mathcal{C}_\varepsilon$ has a vertical tangent at M_0 and such that this tangent passes through the origin. Hence the equation of the tangent is $x_0\frac{\partial f}{\partial x}(x_0,y_0) + y_0\frac{\partial f}{\partial y}(x_0,y_0) = 0$. In other words, the vectors $\overrightarrow{OM_0}$ and $\text{grad}_f(x_0,y_0)$ are perpendicular, since their scalar product is zero. Since the tangent is vertical, the vector $\text{grad}_f(x_0,y_0)$ is horizontal, thus $\overrightarrow{OM_0}$ is a vertical vector.

Since M_0 was arbitrarily chosen, we conclude that there exists a sequence of points M_i that satisfy this property, namely that the Oy-axis is included in the polar curve $\Gamma(f,x)$. By Proposition 2.45, we obtain a contradiction. □

Recall Theorem 2.93, where we proved that the directions of projections which avoid bitangents and inflection tangents are generic.

We are now going to give two hypotheses that imply that there are no vertical bitangents and no vertical inflection tangents on $\mathcal{C}_\varepsilon$.

Proposition 2.96. *If the polar curve of f with respect to x, that is $\Gamma(f,x)$, is reduced, then there are no vertical inflection tangents to the curve $\mathcal{C}_\varepsilon$, for $\varepsilon > 0$ sufficiently small.*

Proof. Fix $x_0 > 0$. The vertical tangent at $(x_0, y_0, 0)$ to $\mathcal{C}_\varepsilon$ in the xOy plane, if it exists, is the projection of the horizontal tangent at the point (x_0, y_0, ε) to the graph of the one variable polynomial $f(x_0, y)$ in the $x = x_0$ plane. See Figure 2.38.

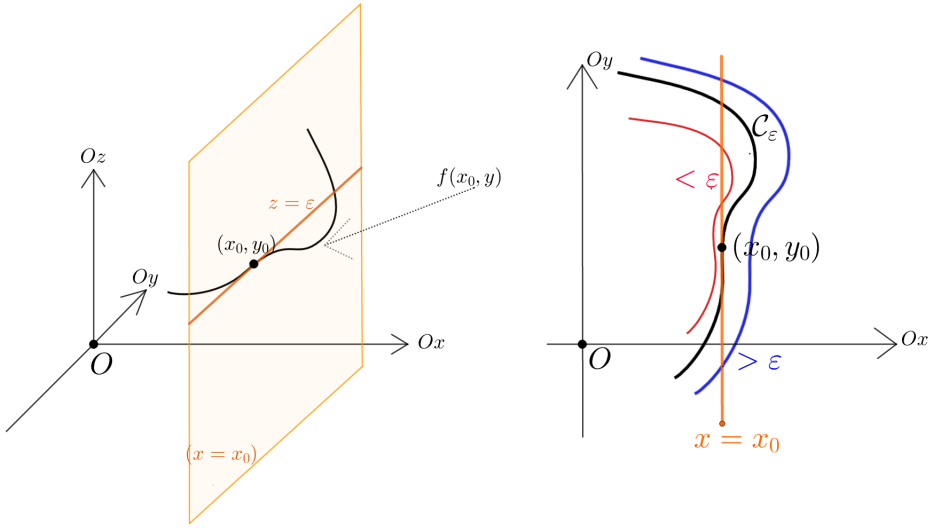

Figure 2.38: An inflection point of the one variable polynomial $f(x_0, y)$ corresponding to a vertical inflection tangent of $\mathcal{C}_\varepsilon$.

For fixed $x_0 > 0$, we have $(x_0, y_0) \in \mathcal{C}_\varepsilon$, that is $f(x_0, y_0) = \varepsilon$. Since (x_0, y_0) is a vertical inflection point, we have:

-if $y < y_0$, $f(x_0, y) > \varepsilon$;

-if $y > y_0$, $f(x_0, y) < \varepsilon$

(or its symmetric situation, that can be treated similarly).

This means that on the surface graph$(f) := \{(x, y, z) \in \mathbb{R}^3 \mid z = f(x, y)\}$ we have the corresponding two cases:

-if $y < y_0$, the graph of the one variable polynomial $f(x_0, y)$ is above $z = \varepsilon$;

-if $y > y_0$, the graph of the one variable polynomial $f(x_0, y)$ is below $z = \varepsilon$.

In other words, for a fixed sufficiently small $x_0 > 0$, the vertical inflection points of $\mathcal{C}_\varepsilon$ correspond to the inflection points of the one variable polynomial $f(x_0, y)$, since in the univariate case, the polynomial $f(x_0, y)$ has an inflection point (x_0, y_0) if and only if (x_0, y_0) is a double root of the derivative of $f(x_0, y)$, that is a double root of the equation $\frac{\partial f}{\partial y}(x_0, y) = 0$.

Since the above mentioned is true for any $x_0 > 0$ small enough, this means there is a family of double roots of $\frac{\partial f}{\partial y}(x, y) = 0$. In other words, the equation of the polar curve has factors with multiplicity greater than one, that is the polar curve is not reduced.

In conclusion, if the polar curve $\Gamma(f, x) := \left\{(x, y) \in \mathbb{R}^2 \;\middle|\; \frac{\partial f}{\partial y}(x, y) = 0\right\}$ is reduced, there are no vertical inflection tangents to $\mathcal{C}_\varepsilon$, for sufficiently small $\varepsilon > 0$. □

Corollary 2.97. *If the polar curve is reduced, then the asymptotic Poincaré-Reeb tree has no vertices of valency equal to two, except for the root.*

Proposition 2.98. *Let us consider the polar curve of f with respect to x, that is*

$$\Gamma := \left\{(x, y) \in \mathbb{R}^2 \;\middle|\; \frac{\partial f}{\partial y}(x, y) = 0\right\},$$

and the map

$$\phi : \mathbb{R}^2_{x,y} \to \mathbb{R}^2_{x,z}, \phi(x, y) := (x, f(x, y)).$$

If the restriction of the map ϕ to the polar curve is a homeomorphism on the image $\phi(\Gamma)$, then there are no vertical bitangents to the curve $\mathcal{C}_\varepsilon$, for $\varepsilon > 0$ sufficiently small.

REMARK 2.99. The fact that the restriction of ϕ to Γ is a homeomorphism onto $\phi(\Gamma)$ means that any two distinct polar branches of Γ have different images by ϕ.

Proof. Let us suppose there existed vertical bitangents to $\mathcal{C}_\varepsilon$, i.e. there exists $x_0 \in \mathbb{R}$, $x_0 > 0$ sufficiently small and there exist $y_1 \neq y_2$ such that $f(x_0, y_1) = f(x_0, y_2)$, with vertical tangent at both (x_0, y_1) and at (x_0, y_2). To be more precise, this means that there exist two different polar branches $\gamma_1 \neq \gamma_2$, with $(x_0, y_1) \in \gamma_1$, $(x_0, y_2) \in \gamma_2$ such that $(x_0, y_1) \neq (x_0, y_2)$ (see Figure 2.39) but $\phi(x_0, y_1) = \phi(x_0, y_2)$. Hence ϕ is not a homeomorphism when restricted to Γ on its image.

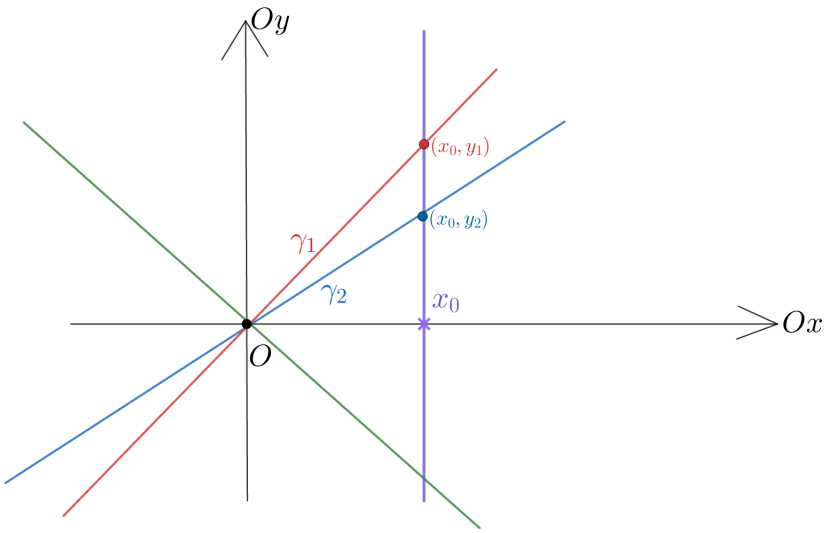

Figure 2.39: Two different polar branches $\gamma_1 \neq \gamma_2$, with $(x_0, y_1) \in \gamma_1$, $(x_0, y_2) \in \gamma_2$ such that $(x_0, y_1) \neq (x_0, y_2)$.

□

Corollary 2.100. *Let us consider the polar curve* $\Gamma(f, x) := \left\{(x, y) \in \mathbb{R}^2 \;\middle|\; \frac{\partial f}{\partial y}(x, y) = 0\right\}$, *and the map* $\phi : \mathbb{R}^2_{x,y} \to \mathbb{R}^2_{x,z}$, $\phi(x, y) := (x, f(x, y))$. *If the restriction of the map* ϕ *to the polar curve is a homeomorphism on the image* $\phi(\Gamma)$, *then the asymptotic Poincaré-Reeb tree has no vertices of valency strictly bigger than* 3.

2.8 The generic asymptotic Poincaré-Reeb trees

If the direction x of projection we consider is generic, namely if it is a direction that avoids bitangents to $\mathcal{C}_\varepsilon$ and tangents to inflection points, then we obtain what we call **a generic asymptotic Poincaré-Reeb tree**. We proved in Subsection 2.7.3 that if some hypotheses on the polar curve are satisfied, the direction is generic in the sense of Definition 2.90. Besides the properties of an asymptotic Poincaré-Reeb tree, a generic asymptotic Poincaré-Reeb tree (see Figure 2.40) has the following characteristics:

- the preorder induced by x on its set of vertices is **a total order**;
- it is a **complete binary** tree (i.e. each internal vertex has exactly two children).

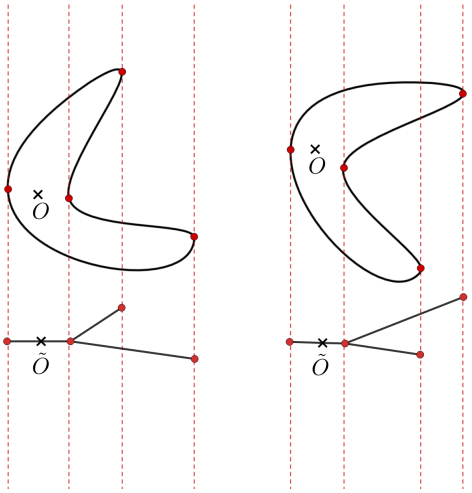

Figure 2.40: Two topologically inequivalent generic asymptotic Poincaré-Reeb trees.

Definition 2.101. If the direction of projection x is generic, then the asymptotic Poincaré-Reeb tree is called **a generic asymptotic Poincaré-Reeb tree** of f with respect to the generic direction.

Remark 2.102. The aim of this section is to prove that the generic asymptotic Poincaré-Reeb tree, besides being an asymptotic Poincaré-Reeb tree, it is complete binary and such that the preorder defined by x on its vertices is a total order.

Example 2.103. In Figure 2.41 we show an example of a generic asymptotic Poincaré-Reeb tree.

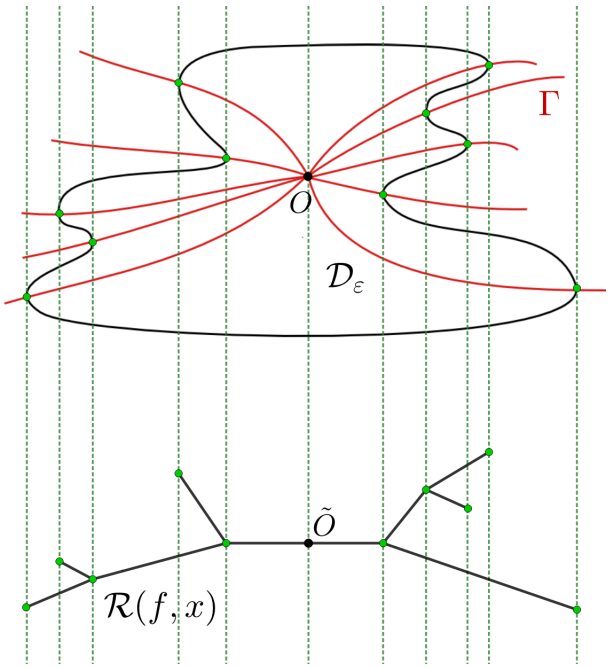

Figure 2.41: A generic asymptotic Poincaré-Reeb tree.

Remark 2.104. A generic asymptotic Poincaré-Reeb tree is a generic rooted transversal tree, in the sense of the following definition:

Definition 2.105. A **generic rooted transversal tree** is a complete binary transversal tree such that the preorder defined by x on its vertices is a total order which is strictly monotone on the geodesics starting from the root.

Remark 2.106. We introduce Definition 2.105 because in the next chapters we are interested in which (generic rooted) transversal trees (see also Definition 2.38) we can realise explicitly as generic asymptotic Poincaré-Reeb trees by a strict local minimum of a polynomial function.

Example 2.107. An example of two topologically inequivalent generic asymptotic Poincaré-Reeb trees is shown in Figure 2.42 below.

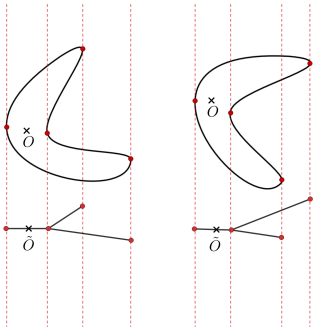

Figure 2.42: Two topologically inequivalent generic asymptotic Poincaré-Reeb trees.

The lack of equivalence (see 2.38) is due to the fact that in order to pass from one tree to the other one, we reach a non-generic tree, where the two leaves have the same $x-$coordinate, see Figure 2.43.

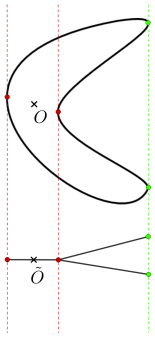

Figure 2.43: A non-generic tree: the two leaves are situated on the same x-level.

2.8.1 Crests and valleys

Let us suppose from now on that the polar curve $\Gamma(f,x)$ is reduced. This is equivalent to the fact that the levels of f have only order 2 intersections with their vertical tangents.

Let γ^* be a polar half-branch and let $(x_0,y_0) := \gamma^* \cap \mathcal{C}_\varepsilon$. By Definition 2.43 of the polar curve $\Gamma(f,x)$, the tangent to $\mathcal{C}_\varepsilon$ at the point (x_0,y_0), say $T_{(x_0,y_0)}\mathcal{C}_\varepsilon$, is the vertical line $(x=x_0)$. In the following, we shall use the notations introduced in the previous sections.

The terminology of **crest** and **valley** is inspired by [CP01, Definition 2], where Coste and de la Puente used it to study atypical values of real bivariate polynomial functions at infinity.

Definition 2.108. Let γ^* be a polar half-branch. We say that a point $(x_0,y_0) := \gamma^* \cap \mathcal{C}_\varepsilon$ is a **right crest** (respectively **right valley**) of $\mathcal{C}_\varepsilon$ if and only if $x_0 > 0$ and $\mathcal{C}_\varepsilon$ is situated to the right (respectively, left) of the vertical line $(x=x_0)$, in a small enough neighbourhood of (x_0,y_0).

Let γ^* be a polar half-branch. We say that a point $(x_0, y_0) := \gamma^* \cap \mathcal{C}_\varepsilon$ is a **left crest** (respectively **left valley**) of $\mathcal{C}_\varepsilon$ if and only if $x_0 < 0$ and $\mathcal{C}_\varepsilon$ is situated to the left (respectively, right) of the vertical line $(x = x_0)$, in a small enough neighbourhood of (x_0, y_0).

See Figure 2.44.

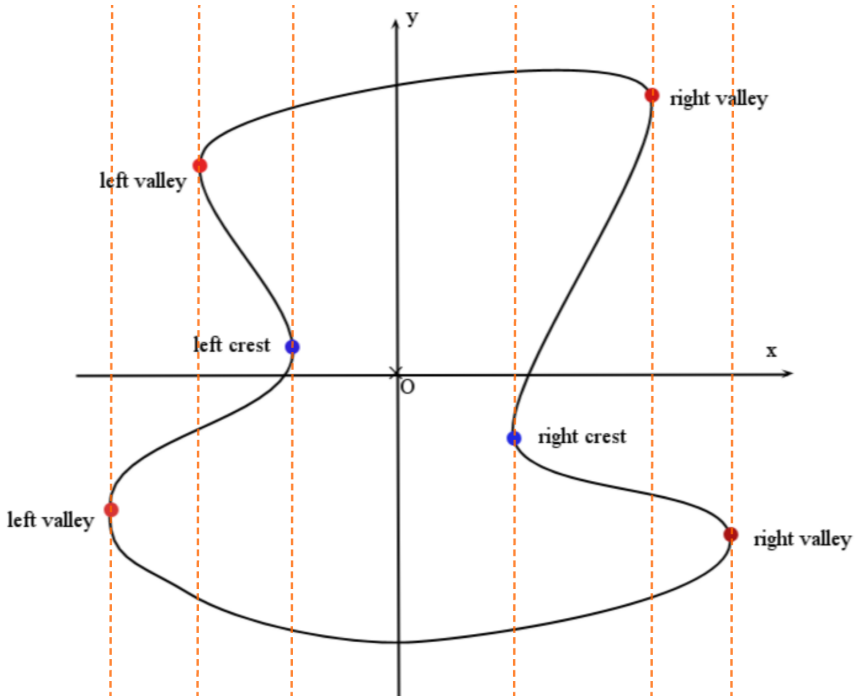

Figure 2.44: Left and right crests in blue; left and right valleys in red.

Remark 2.109. The reason we chose these names is to be consistent with the legends of geographical maps (see, for instance, [Geoa] and [Geob]). However, in our case the observer who is studying the topographic map of the three-dimensional landscape is situated at infinity in the vertical direction of the Oz axis. So our terminology of "valley" and "crest" is not intrinsic, since it depends on the position of the observer, as one will see later in Proposition 3.17.

Remark 2.110. By Definition 2.108, one has the following properties in a small enough neighbourhood of (x_0, y_0) :

(i) $(x_0, y_0) = \mathcal{C}_\varepsilon \cap \gamma^*$ is a right crest if and only if $x_0 > 0$ and $x_{|\mathcal{C}_\varepsilon} \geq x_0$.
(ii) $(x_0, y_0) = \mathcal{C}_\varepsilon \cap \gamma^*$ is a right valley if and only if $x_0 > 0$ and $x_{|\mathcal{C}_\varepsilon} \leq x_0$.
(iii) $(x_0, y_0) = \mathcal{C}_\varepsilon \cap \gamma^*$ is a left crest if and only if $x_0 < 0$ and $x_{|\mathcal{C}_\varepsilon} \leq x_0$.
(iv) $(x_0, y_0) = \mathcal{C}_\varepsilon \cap \gamma^*$ is a left valley if and only if $x_0 < 0$ and $x_{|\mathcal{C}_\varepsilon} \geq x_0$.

Let us define two total order relations: on the sets of right polar half-branches and of left polar half-branches. This is possible by Corollary 2.66, if we are in a good neighbourhood V of the origin (see Definition 2.67).

Definition 2.111. The **canonical total order on the set of right polar half-branches** is the restriction of the trigonometric order to it. The **canonical total order on the set of left polar half-branches** is the restriction of the anti-trigonometric order to it.

Remark 2.112. The order relation from Definition 2.111 is well-defined, since we are in a good neighbourhood V of the origin. Recall Corollary 2.66 and Remark 2.68. Thus all the inequalities are strict and we have a total order relation between the right polar half-branches and a total order relation between the left polar half-branches.

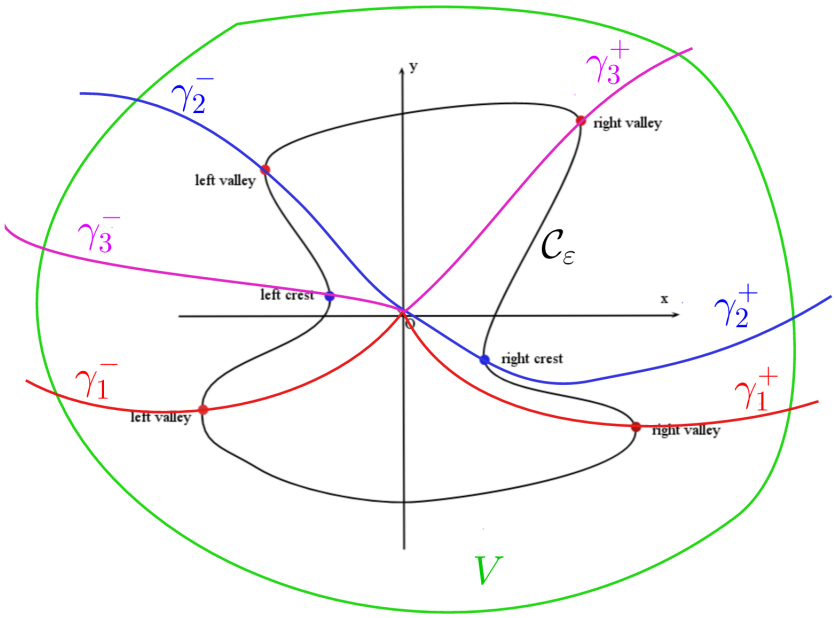

Figure 2.45: Right half-branches: $\gamma_1^+ < \gamma_2^+ < \gamma_3^+$ and left half-branches: $\gamma_1^- < \gamma_3^- < \gamma_2^-$ of the polar curve $\Gamma(f, x)$.

Proposition 2.113. *Let $\gamma_1^+ < \gamma_2^+ < \ldots < \gamma_k^+$ be all the right polar half-branches of $\Gamma(f, x)$. If $P_i := \mathcal{C}_\varepsilon \cap \gamma_i^+$, $P_i(x_i, y_i)$ in a good neighbourhood V of the origin, then the points $P_1, P_2, \ldots, P_k$, in this order, consist of an alternation of right valleys and right crests, i.e. there are no two consecutive right valleys and no two consecutive right crests.*

To the left there is an alternation of left valleys and left crests, i.e. there are no two consecutive left valleys and no two consecutive left crests.

Proof. It is sufficient to prove the statement only for the right side, and only for two consecutive right polar half-branches.

We shall prove that there are no two consecutive right polar half-branches γ_{i_0} and γ_{i_0+1} such that the points $P_{i_0}(x_{i_0}, y_{i_0}) := \mathcal{C}_\varepsilon \cap \gamma_{i_0}$ and $P_{i_0+1}(x_{i_0+1}, y_{i_0+1}) := \mathcal{C}_\varepsilon \cap \gamma_{i_0+1}$ are both right valleys of $\mathcal{C}_\varepsilon$.

We argue by contradiction. Let us suppose the contrary, namely that P_{i_0} and P_{i_0+1} are both right valleys. Furthermore, assume without loss of generality that $x_{i_0+1} < x_{i_0}$.

Let us consider $a \in]x_{i_0+1}, x_{i_0}[$ and the vertical line $x = a$. Recall Definition 2.67 and let us choose a good neighbourhood V of the origin. Then there is a unique intersection point $A := \gamma_{i_0+1}^+ \cap (x = a)$ and a unique intersection point $B := \gamma_{i_0}^+ \cap (x = a)$. Hence one obtains the points $A(a, y_A)$ and $B(a, y_B)$. By Corollary 2.58 and Definition 2.67, since $f_{|\gamma_{i_0}^+}$ and $f_{|\gamma_{i_0+1}^+}$ are strictly increasing in V, we have $f(A) > f(P_{i_0+1}) = \varepsilon$ and $f(B) < f(P_{i_0}) = \varepsilon$. See Figure 2.46.

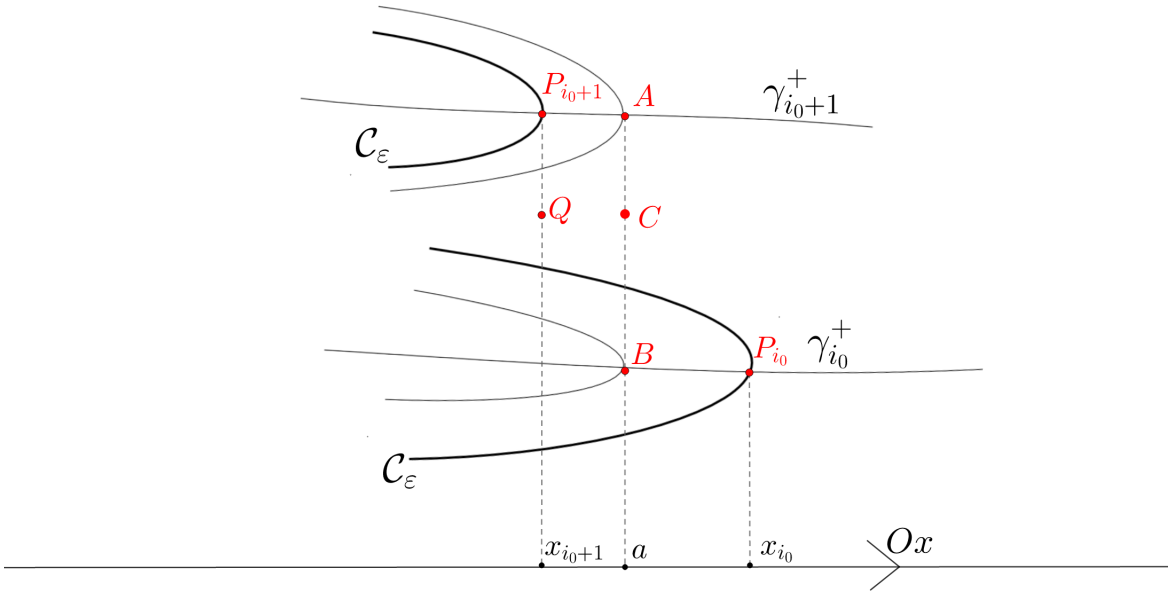

Figure 2.46: No two consecutive right valleys.

If we denote by $F : \mathbb{R} \to \mathbb{R}$ the function

$$F(y) := f(a, y) - \varepsilon,$$

then $F(y_A) > 0$ and $F(y_B) < 0$. By the continuity of the polynomial function F, there exists $b \in \mathbb{R}$, $y_B < b < y_A$, such that $F(b) = 0$. Namely, there exists a point $C(a, b)$ with $y_B < b < y_A$, such that $C(a, b) \in \mathcal{C}_\varepsilon$.

Now since the above holds for any $a \in]x_{i_0+1}, x_{i_0}[$, let us consider a continuous sequence $(a_k) \in]x_{i_0+1}, x_{i_0}[$. We obtain a sequence of points $C_k(a_k, b_k)$ with $y_B < b_k < y_A$, such that $C(a_k, b_k) \in \mathcal{C}_\varepsilon$. Therefore we have just proved that for all $a_k \in]x_{i_0+1}, x_{i_0}[$, there exists a point $C(a_k, b_k) \in \mathcal{C}_\varepsilon$, i.e. $F(a_k, b_k) = 0$. Thus one obtains a continuous sequence of points $C(a_k, b_k)$ in the compact set $\mathcal{C}_\varepsilon$, hence one can subtract a convergent subsequence $C'(a_k, b_k)$ which has its limit in $\mathcal{C}_\varepsilon$. Denote this limit by $L := \lim_{a_k \to x_i} C'(a_k, b_k)$.

Now there are two possibilities:

(a) if $L \equiv P_{i_0+1}$, then one obtains a contradiction with Remark 2.110, (ii), namely with the definition of a valley at P_{i_0+1};

(b) if $L \equiv Q \neq P_{i_0+1}$, $Q(x_{i_0+1}, y_Q)$:

let us first redefine the function $F : \mathbb{R} \to \mathbb{R}$, namely

$$F(y) := f(x_{i_0+1}, y) - \varepsilon;$$

since both $Q \in \mathcal{C}_\varepsilon$ and $P_{i_0+1} \in \mathcal{C}_\varepsilon$, i.e. $F(y_Q) = F(y_{i_0+1}) = 0$, one can apply Rolle's theorem to the continuous and differentiable function F. Hence there exists $y_S \in]y_Q, y_{i_0+1}[$ such that $F'(y_S) = 0$. But $F'(y_S) = \frac{\partial f}{\partial y}(x_{i_0+1}, y_s)$, thus the point $S(x_{i_0+1}, y_s) \in \Gamma$This is in contradiction with the hypothesis that $\gamma^+_{i_0}$ and $\gamma^+_{i_0+1}$ are **consecutive** right polar half-branches.

In conclusion, we have proved that two consecutive right polar half-branches cannot determine two right-valleys of $\mathcal{C}_\varepsilon$.

Using a similar reasoning, one can prove that two consecutive right polar half-branches cannot give two right-crests of $\mathcal{C}_\varepsilon$.

We conclude that the right valleys and the right crests must alternate. A similar result can be established for left valleys and left crests. □

We saw in Subsection 2.7.3 that if the polar curve Γ is reduced and the restriction of the map $\phi : \mathbb{R}^2_{x,y} \to \mathbb{R}^2_{x,z}$, $\phi(x,y) := (x, f(x,y))$ to the polar curve is a homeomorphism onto the image $\phi(\Gamma)$, then the generic asymptotic Poincaré-Reeb tree has a total order relation on its vertices and is complete and binary. Another way to see the generic Poincaré-Reeb tree (we will prove this in Chapter 3) is the snake to the right, that we define below. The conclusions from Subsection 2.7.3 are still true if we restrict our attention only to the right, namely for $x > 0$.

Definition 2.114. The **right asymptotic snake** of f at the origin relative to a generic direction x is given by the two total order relations endowing the right crests and right valleys, as follows: one is the order induced by the total order of the right polar half-branches, i.e. the one we obtain by reading the right crests and right valleys along the curve $\mathcal{C}_\varepsilon$. The other order is the one given by the x-coordinate of the right crests and right valleys.

Example 2.115. See Figure 2.47. the one obtained by reading the right crests and right valleys along the curve (i.e. in the order given by the right polar half-branches) and the other order given by the x-coordinate.

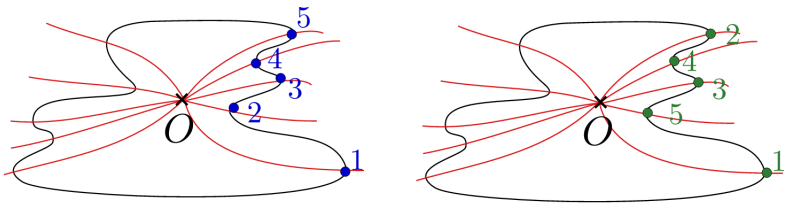

Figure 2.47: Two total order relations on the set of right crests and right valleys.

It is a biordered set of five points, to which we associate the snake $\sigma = \begin{pmatrix} 1 & 2 & 3 & 4 & 5 \\ 1 & 5 & 3 & 4 & 2 \end{pmatrix}$, by choosing the convention of reading the labels given by the order along the curve, from right to left. See Figure 2.48.

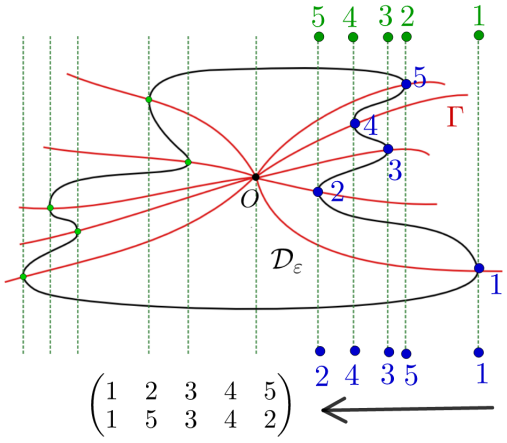

Figure 2.48: The snake to the right of the curve $\mathcal{C}_\varepsilon$.

Remark 2.116. However, the order given by the $y-$coordinate may not always correspond to the one along the curve, as the below Figure 2.49 shows.

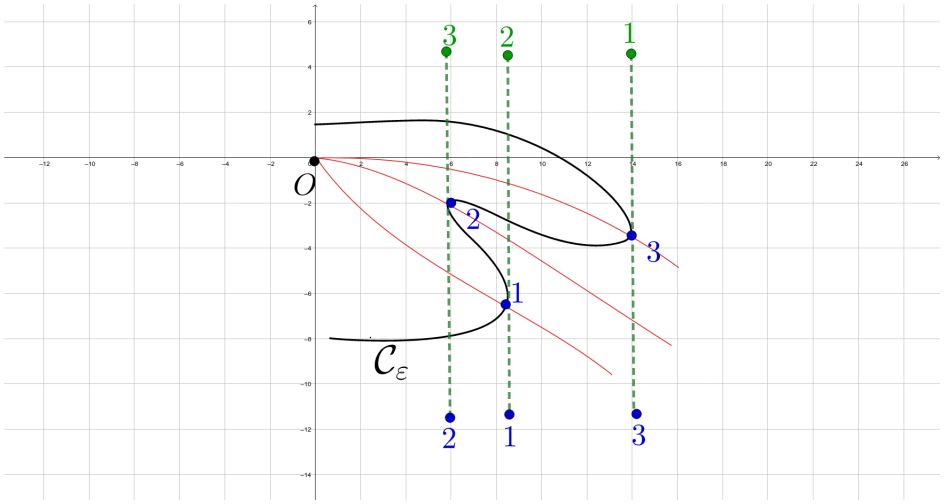

Figure 2.49: The canonical order is the one obtained by reading the crests and valleys along the curve, not by their $y-$coordinate.

Corollary 2.117. *If γ_i^+ and γ_{i+1}^+ are two consecutive right polar half-branches with $P_i := \mathcal{C}_\varepsilon \cap \gamma_i^+$ and $P_{i+1} := \mathcal{C}_\varepsilon \cap \gamma_{i+1}^+$, $0 < \varepsilon \ll 1$, in a good neighbourhood V of the origin (see Definition 2.67), then the following implications hold:*

(a) *If P_{i+1} is a right-crest and P_i is a right-valley, then $x_{i+1} < x_i$.*

(b) *If P_{i+1} is a right-valley and P_i is a right-crest, then $x_i < x_{i+1}$.*

Proof. (a) We argue by contradiction. If we suppose that $x_{i+1} > x_i$, then we apply the same steps as in Proposition 2.113 and by Rolle's theorem we obtain a contradiction with the hypothesis that γ_i^+ and γ_{i+1}^+ are consecutive right polar half-branches.

(b) Analogous reasoning.

□

Lemma 2.118. *The point $P_1 := \mathcal{C}_\varepsilon \cap \gamma_1^+$, $P_1(x_1, y_1)$ determined by the first right polar half-branch γ_1^+ and the point $P_k := \mathcal{C}_\varepsilon \cap \gamma_k^+$, $P_k(x_k, y_k)$ determined by the last right polar half-branch γ_k^+ are both right-valleys of $\mathcal{C}_\varepsilon$, in a good neighbourhood of the origin, denoted by V.*

Proof. We argue by contradiction. Let us suppose that P_k is a right-crest of $\mathcal{C}_\varepsilon$, as in Figure 2.50.

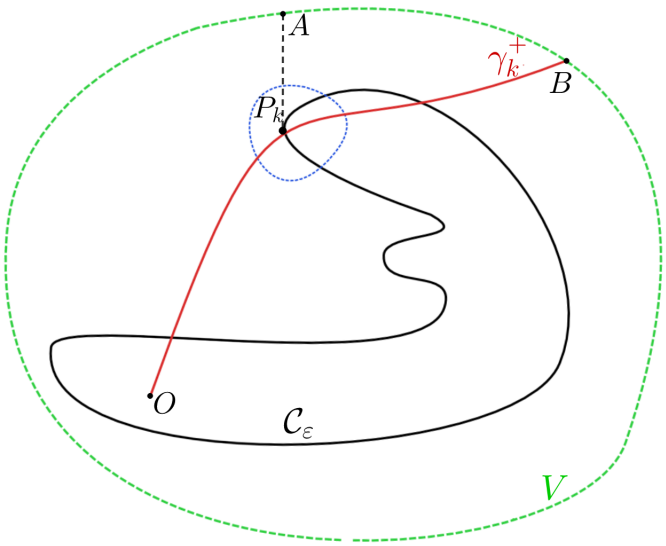

Figure 2.50: Arguing by contradiction: if P_k were a right crest.

Let us denote by $\delta := \{(x, y) \in \mathcal{C}_\varepsilon \mid x > x_k \text{ and } y > y_k\} \cap V$.

Let $A := (x = x_k) \cap \partial V$ and $B := \gamma_k^+ \cap \partial V$. In the following we shall prove that $P_k AB$ is a "triangular" sector of V. This follows directly from Definition 2.67 of a good neighbourhood, since the polar curve $\Gamma(f, x)$ has no vertical tangents in V. Namely, since $\Gamma(f, x)$ has no vertical tangents, neither the right polar half-branch $\gamma_k^+ \subset \Gamma(f, x)$ has vertical tangents (see impossible Figure 2.51).

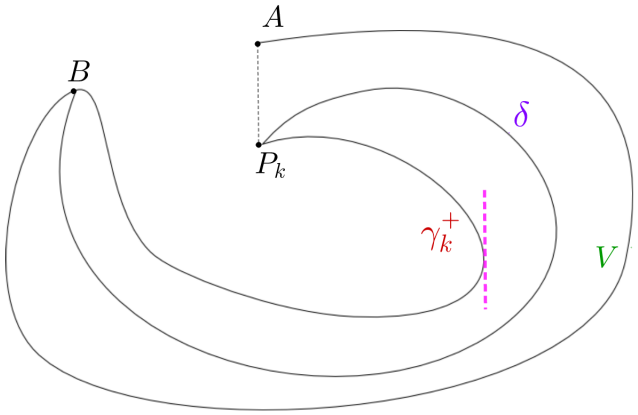

Figure 2.51: No vertical tangents of γ_k^+ in V.

Moreover, since $\mathcal{C}_\varepsilon$ is a compact curve, δ has to escape from the triangular sector $P_k AB$. We want to prove that this leads us to a contradiction, in three steps, as follows.

(a) We shall prove that $\delta \cap (x = x_k) = \emptyset$. We argue by contradiction. If there exists a point $Q(x_Q, y_Q) \in \mathcal{C}_\varepsilon$ with $x_Q = x_k$ and $y_Q > y_k$, then by Rolle's theorem one obtains another

right polar half-branch $\gamma^+_{k+1} > \gamma^+_k$. We have obtained a contradiction.

(b) Since by hypothesis $\delta \subset \mathcal{C}_\varepsilon \subset V$, one has $\delta \cap \partial V = \emptyset$.

(c) We prove now that $\delta \cap \gamma^+_k = \emptyset$. This follows from the fact that in a good neighbourhood V of the origin, the right polar half-branch γ^+_k intersects $\mathcal{C}_\varepsilon$ in precisely one point P_k, for $0 < \varepsilon \ll 1$.

Hence we obtain a contradiction with the fact that $\mathcal{C}_\varepsilon$ has to escape from the triangular sector $P_k AB$, thus P_k is a right- valley of $\mathcal{C}_\varepsilon$.

We argue by contradiction. If P_1 is a right-crest, we apply the same steps as above to prove that we obtain a contradiction, thus P_1 must also be a right-valley of $\mathcal{C}_\varepsilon$. □

In conclusion, to the right we have alternating right crests and right valleys, starting and ending with a right valley. Similarly, to the left.

Lemma 2.119. *Let $\gamma^+ \subset \Gamma(f,x)$ be a right polar half-branch and let $P := \gamma^+ \cap \mathcal{C}_\varepsilon$, with $0 < \varepsilon \ll 1$ be a right-valley of $\mathcal{C}_\varepsilon$. If $\mathcal{R}(f,x)$ denotes the Poincaré-Reeb tree of $\mathcal{D}_\varepsilon$, then the vertex corresponding to P is a leaf, i.e. it has no children.*

Proof. Let us consider a small enough neighbourhood of P, namely let us study $\mathcal{D}_\varepsilon$ locally around P.

By Lemma 2.42 $\mathcal{C}_\varepsilon$ is a Jordan curve. Apply the classical Jordan Theorem (see 2.41) and thus the set Int $\mathcal{C}_\varepsilon := \{f < \varepsilon\}$ is either the bounded or the unbounded component of $\mathbb{R}^2 \setminus \mathcal{C}_\varepsilon$, as it is shown in Figure 2.52 below.

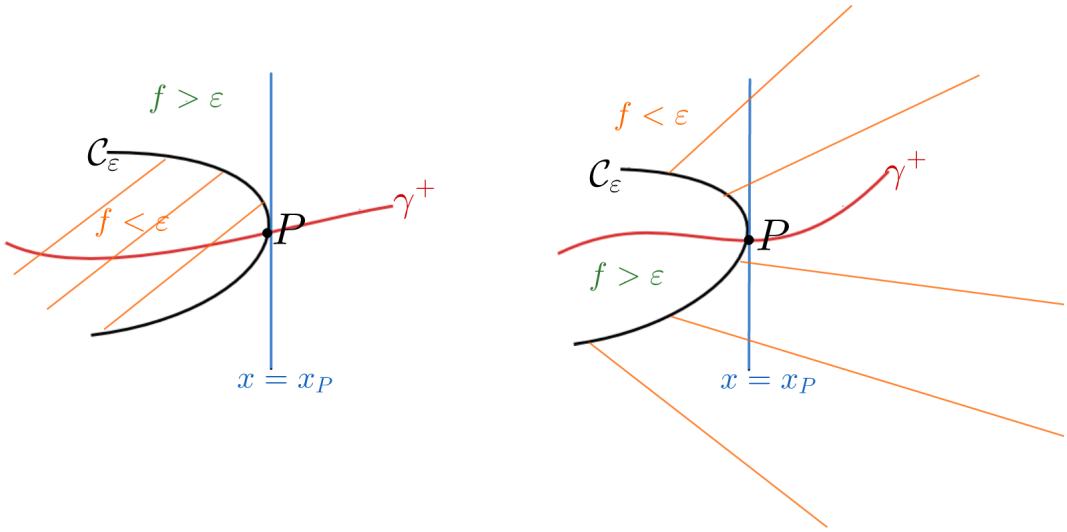

Figure 2.52: Local study in a neighbourhood of a right valley of $\mathcal{C}_\varepsilon$.

By Lemma 2.57, one has $f_{|\gamma^+}$ is strictly increasing as one goes to the right, further from the origin. Hence, the only possible configuration is the one where the line $x = x_P$ does not intersect any point of Int $\mathcal{C}_\varepsilon$ (see Figure 2.52, the left case).

Let us now study the construction of the Poincaré-Reeb tree using Definition 2.24, locally, in a neighbourhood of a point P. After passing to the quotient, the image of the point P is a vertex of $\mathcal{R}(f,x)$, say $P' \in \mathcal{R}(f,x)$ corresponding to the right-valley P. Since locally at P there is only one connected component of $\mathcal{D}_\varepsilon$, we obtain that the vertex P' has no children, i.e. P' is a leaf of $\mathcal{R}(f,x)$. □

REMARK 2.120. A similar reasoning can prove that the vertices of $\mathcal{R}(f,x)$ which correspond to left valleys of $\mathcal{C}_\varepsilon$ are also leaves of $\mathcal{R}(f,x)$. Nevertheless, the vertices corresponding to left crests or to right crests are always internal vertices. (For this proof, see Lemma 2.121, proven under the hypothesis of a generic projection.)

Lemma 2.121. *Let γ^+ be a right polar half-branch and let $P := \gamma^+ \cap \mathcal{C}_\varepsilon$, $0 < \varepsilon \ll 1$, be a right-crest of $\mathcal{C}_\varepsilon$. Let $\mathcal{R}(f,x)$ denote the Poincaré-Reeb tree. If the direction x is a generic direction, then the vertex $P' \in \mathcal{R}(f,x)$ which is the image of P by the quotient map, has exactly two children. In addition, both children will be situated to the right of P'.*

REMARK 2.122. Note that if the positive polar curve is reduced and if the map ϕ is a homeomorphism onto its image by ϕ, then x is a generic direction.

Proof. By applying the same reasoning as in the proof of Lemma 2.119, one concludes that locally the line $x = x_P$ has no common point with $(f > \varepsilon)$.

Moreover, we shall construct the Poincaré-Reeb tree by using Definition 2.24 locally in a neighbourhood of the point P. Thus, we obtain the vertex P' which corresponds to the right crest P and we take into account the fact that to the left of the vertical line $x = x_P$ there is one connected component to project, while to the right of the line $x = x_P$ there are two connected components to project. Therefore, P' has two children and they are both oriented to the right of P. See Figure 2.53.

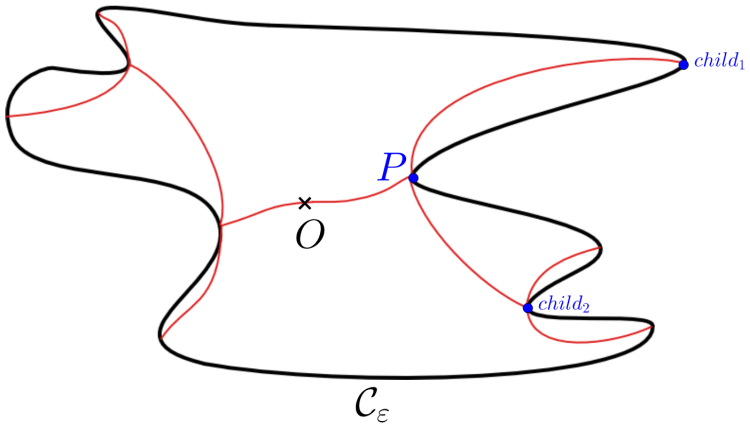

Figure 2.53: The vertex corresponding to a right crest P has two children to the right.

□

REMARK 2.123. Similar reasoning to prove that the vertices corresponding to left crests have two children, both oriented to the left.

Let us now gather into one theorem all the results of this chapter, in order to prove our new result, namely Theorem 2.124.

Theorem 2.124. *Let us consider the polar curve of f with respect to x, that is $\Gamma(f,x) := \left\{(x,y) \in \mathbb{R}^2 \mid \frac{\partial f}{\partial y}(x,y) = 0\right\}$, and the map $\phi : \mathbb{R}^2_{x,y} \to \mathbb{R}^2_{x,z}$, $\phi(x,y) := (x, f(x,y))$.*

If the following two hypotheses are satisfied:

- *the polar curve is reduced,*
- *the restriction of the map ϕ to the polar curve is a homeomorphism on the image $\phi(\Gamma)$,*

then the generic asymptotic Poincaré-Reeb tree of f relative to x is a complete binary transversal tree such that the preorder defined by x on its vertices is a total order which is strictly monotone on the geodesics starting from the root.

Proof. It follows from Corollary 2.97 and Corollary 2.100. □

2.8.2 Examples of generic asymptotic Poincaré-Reeb trees

Example 2.125. Consider Example 2.12. In Figure 2.54 is shown its Poincaré-Reeb tree, which is generic.

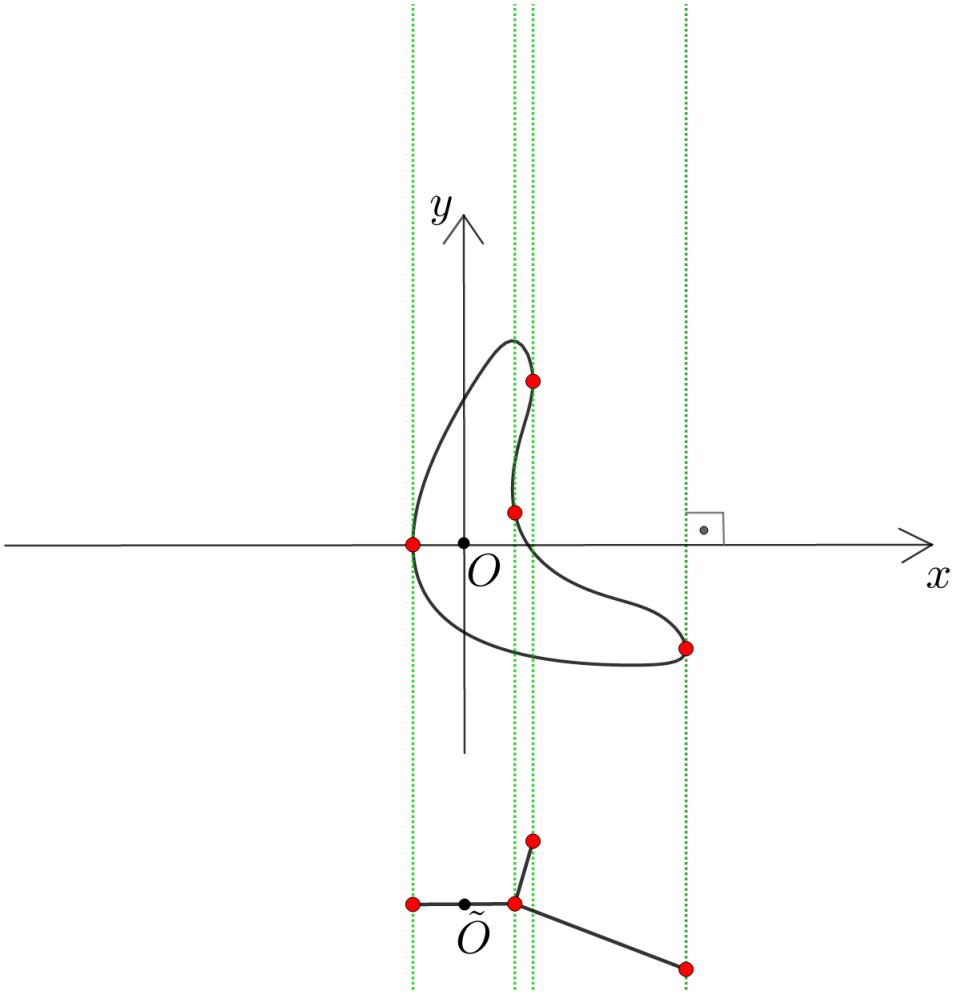

Figure 2.54: A generic asymptotic Poincaré-Reeb tree of Coste's example from Example 2.12.

Example 2.126. Consider Example 2.13. In Figure 2.55 is shown its Poincaré-Reeb tree, which is generic.

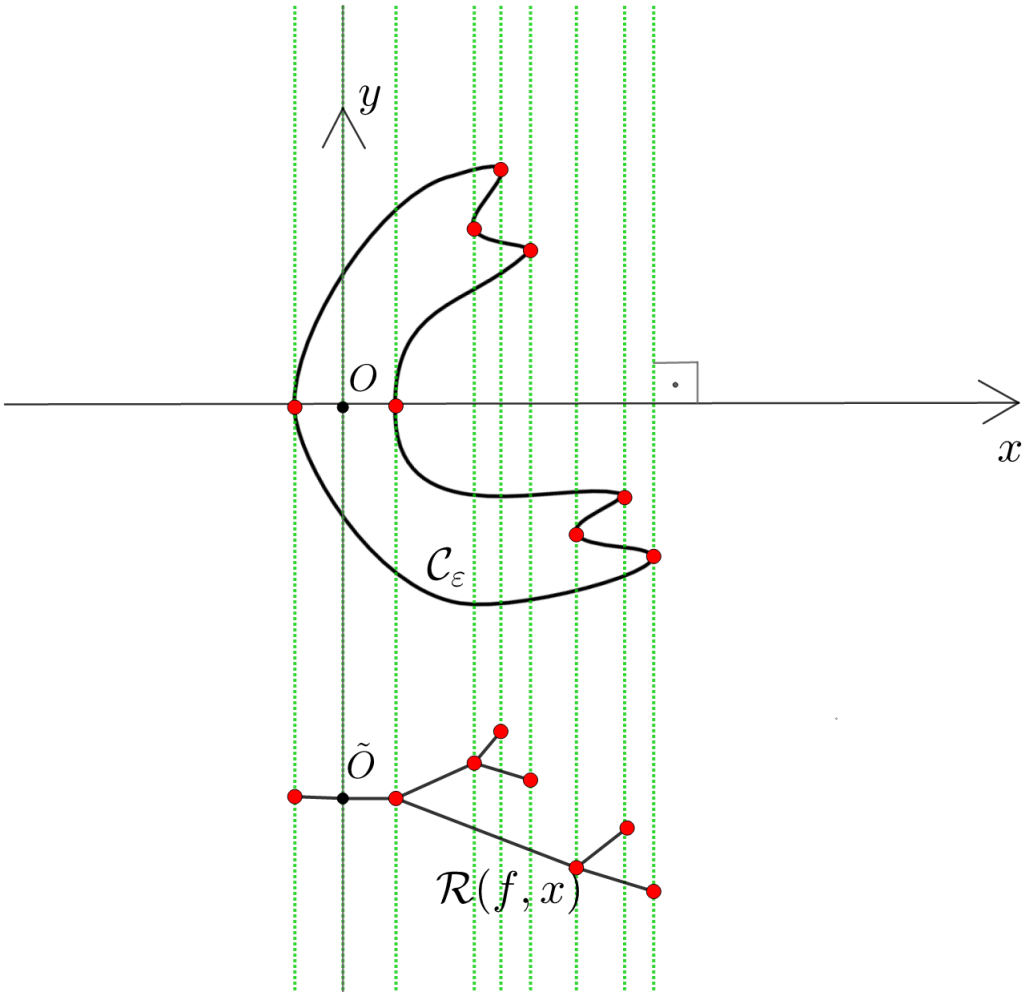

Figure 2.55: A generic asymtotic Poincaré-Reeb tree of the double banana from Example 2.13.

2.8.3 Example of non-generic asymptotic Poincaré-Reeb trees

If one considers polar curves Γ that are not reduced or the restriction of the map ϕ on Γ is not a homeomorphism on its image, then there exist also non-generic Poincaré-Reeb trees, since they have vertices whose valencies are not 3, due to either bitangents or inflection tangents.

EXAMPLE 2.127. **Bitangents:**

If the restriction of the map ϕ on Γ is not a homeomorphism on its image, then we may obtain non-generic Poincaré-Reeb trees, since we do not have a total order on the vertices of the asymptotic Poincaré-Reeb tree. Thus there might exist vertices whose valencies are not 3.

Let us consider the polynomial $f : \mathbb{R}^2 \to \mathbb{R}$,

$$f(x,y) := x^{10} + \frac{y^6}{6} - 3x\frac{y^4}{4} + x^2y^2.$$

The Poincaré-Reeb tree of f contains a vertex with valency equal to 4. For a small enough $\varepsilon > 0$, the curve $\mathcal{C}_\varepsilon$ is represented in blue in Figure 2.56. The polar curve (in red) is

$$\Gamma(f,x) = \{(x,y) \in \mathbb{R}^2 \mid y(x-y^2)(2x-y^2) = 0\}.$$

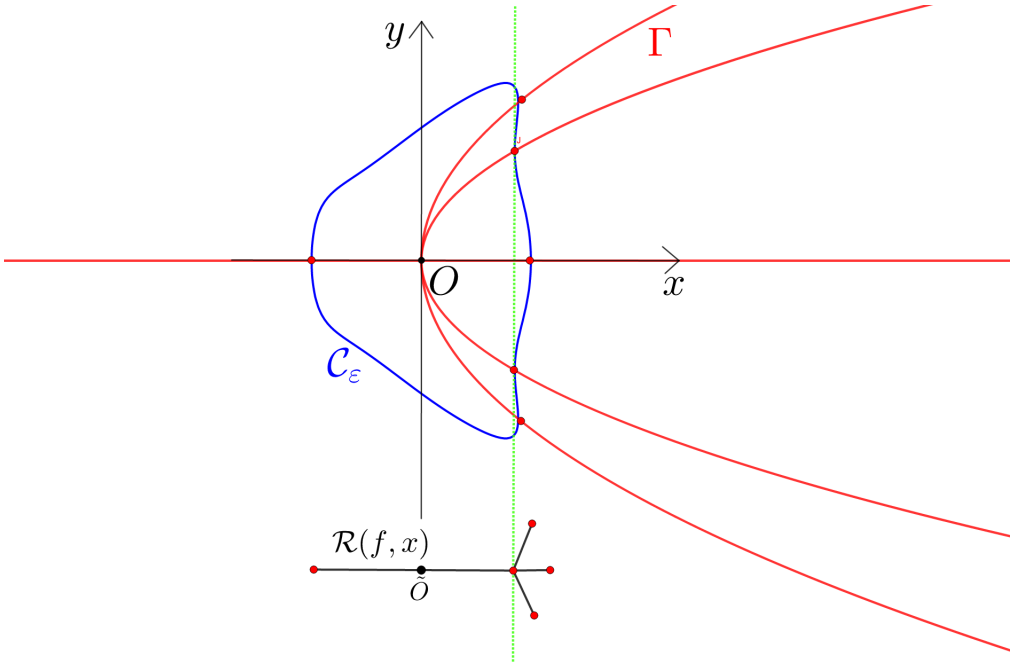

Figure 2.56: A projection which is not generic can lead to vertices of valency greater than 3 in the Poincaré-Reeb tree.

EXAMPLE 2.128. **Inflections:**

If one considers polar curves Γ that are not reduced, then we may obtain non-generic Poincaré-Reeb trees, since we can have vertical inflection tangents.

Consider the polynomial $f : \mathbb{R}^2 \to \mathbb{R}$,

$$f(x,y) := x^{12} + \int_0^y t^2(t-x^2)\mathrm{d}t.$$

Namely, the polar curve is in red:

$$\Gamma(f,x) = \{(x,y) \in \mathbb{R}^2 \mid y^2(y-x^2) = 0\},$$

as one can see in Figure 2.57 below.

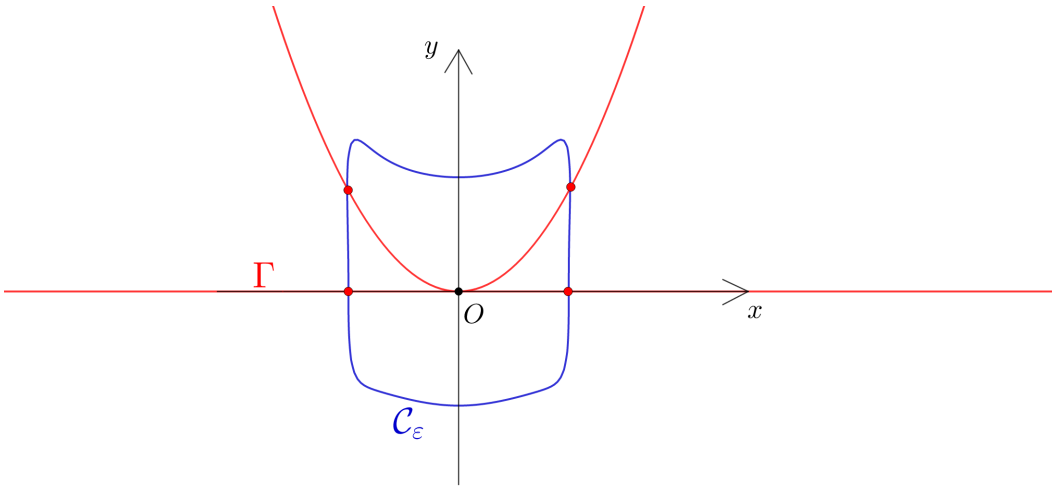

Figure 2.57: The level curve $\mathcal{C}_\varepsilon$ of $f(x,y) := x^{12} + \int_0^y t^2(t-x^2)\mathrm{d}t$ and its non reduced polar curve $\Gamma(f,x) = \{(x,y) \in \mathbb{R}^2 \mid y^2(y-x^2) = 0\}$, in red.

There are two vertical inflection points on the Ox axis, that will give two vertices of valency 2 in the Poincaré-Reeb tree, thus a non-generic asymptotic Poincaré-Reeb tree. The non-generic asymptotic Poincaré-Reeb tree $\mathcal{R}(f, x)$ is shown in Figure 2.58.

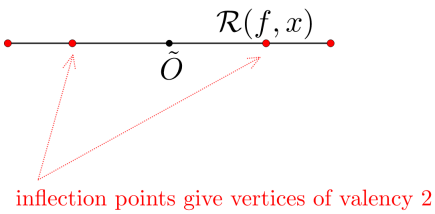

Figure 2.58: Non-generic asymptotic Poincaré-Reeb tree $\mathcal{R}(f, x)$ with two vertices of valency 2, which correspond to two vertical inflection points.

Chapter 3

Realising separable positive Poincaré-Reeb trees in two variables

Contents

QUESTION 3.1. Which generic rooted transversal trees (see Definition 2.105) can be realised as generic asymptotic Poincaré-Reeb trees (see Definition 2.101) of a connected component of a real algebraic level curve $\mathcal{C}_\varepsilon$, in sufficiently small neighbourhoods of strict local minima? More precisely, given a transversal tree T, can we construct a bivariate polynomial $f(x,y) \in \mathbb{R}[x,y]$ such that the generic asymptotic Poincaré-Reeb tree associated to f and to the direction x is T?

The following two chapters are dedicated to answering Question 3.1. We will construct a large family of polynomials that realise the separable generic rooted transversal trees as their Poincaré-Reeb trees.

QUESTION 3.2. We consider a polynomial function $f : \mathbb{R}^2 \to \mathbb{R}$ that has a strict local minimum at the origin O and such that $f(0,0) = 0$. Let us fix a neighbourhood V of O such that O is the only critical point of f in V. For sufficiently small $\varepsilon > 0$, consider the set $f^{-1}([0,\varepsilon])$ and denote the connected component that contains the origin by $\mathcal{D}_\varepsilon$. Denote by $\mathcal{C}_\varepsilon := \mathcal{D}_\varepsilon \setminus \operatorname{Int} \mathcal{D}_\varepsilon$. Let us fix a small enough $0 < \varepsilon \ll 1$ such that $\mathcal{C}_\varepsilon$ is a Jordan curve. From now on we study only the phenomena in V. Let us denote by $\pi_{\mathcal{D}_\varepsilon} : \mathcal{D}_\varepsilon \to \mathbb{R}$ a projection, which is a generic direction with respect to $\mathcal{C}_\varepsilon$ (see Definition 2.90). In particular, the question we are going to answer in this Chapter is: **can one realise any (generic rooted) transverse tree?** We give a partial but constructive affirmative answer in the following chapters. Namely, we shall present our original construction of polynomials f whose asymptotic positive Poincaré-Reeb trees correspond to **separable** snakes (see Definition 1.6 and Definition 1.128).

3.1 Strict local minima

Consider a non-degenerate (i.e. Morse) singular point (that is to say the Hessian matrix at that point has non-zero determinant). The classical second partial derivatives test determines if the non-degenerate singular point is a strict local minimum. But for degenerate singularities, this second partial derivatives test is inconclusive, thus one must use other techniques. In this

section we give a new method of constructing real polynomials $f \in \mathbb{R}[x, y]$ with a strict local minimum at the origin.

3.1.1 Newton polygon criterion for a strict local minimum

We want to construct a polynomial $f \in \mathbb{R}[x, y]$ such that f has a strict local minimum at the origin $(0, 0)$. In this construction, our main idea is to consider the polar curve $\Gamma(f, x)$ to be given by

$$\Gamma = \left\{ (x, y) \in \mathbb{R}^2 \mid \prod_{i=1}^{m+1} (y - a_i(x)) = 0 \right\},$$

where $a_i(x) \in \mathbb{R}[x]$ are distinct polynomials with valuation $\nu_x(a_i(x)) \geq 1$ and m is an even integer. More precisely, f is chosen such that all the branches of its polar curve $\Gamma := \left\{ (x, y) \in \mathbb{R}^2 \mid \frac{\partial f}{\partial y} = 0 \right\}$ are real, smooth and transverse to the Oy-axis. We will prove that

$$f(x, y) = x^2 + \int_0^y \frac{\partial f}{\partial y}(x, t)\mathrm{d}t$$

has the desired property (see Proposition 3.12).

Definition 3.3. [Ber09, page 338] Let A be a subset of $\mathbb{R}^2$. Then the smallest convex set containing A is called **the convex hull of** A.

We now present the classical notion of Newton polygon and Proposition 3.10 (see e.g. [Fis01, Appendix 4, page 197]).

Definition 3.4. [Fis01, Appendix 4, page 197] Let

$$f = \sum_{\mu,\nu \geq 0} c_{\mu\nu} x^\mu y^\nu \in \mathbb{R}\{x, y\}$$

be a power series in two variables. We define the **support** of f as the following set of lattice points in the plane:

$$\mathrm{supp}(f) := \{(\mu, \nu) \in \mathbb{N}^2 \mid c_{\mu,\nu} \neq 0\}.$$

The Newton diagram of f, denoted by $\tilde{\mathcal{N}}(f)$, is the convex hull of

$$\bigcup_{(\mu,\nu) \in \mathrm{supp}(f)} \left\{ (\mu, \nu) + \mathbb{R}^2_{\geq 0} \right\}.$$

The Newton polygon $\mathcal{N}(f)$ of f is the union of the compact edges of $\partial\tilde{\mathcal{N}}(f)$ (see Figure 3.2).

Definition 3.5. [Fis01, Appendix 4, page 197] Let

$$f = \sum_{\mu,\nu \geq 0} c_{\mu\nu} x^\mu y^\nu \in \mathbb{R}\{x, y\}$$

be a power series in two variables. If $\mathcal{N}(f)$ is its Newton polygon and $\mathcal{E}$ is an edge of $\mathcal{N}(f)$, then we define **the restriction of** f **to** $\mathcal{E}$ by

$$f_{|\mathcal{E}} := \sum_{\{(\mu,\nu) \in \mathcal{E}\}} c_{\mu\nu} x^\mu y^\nu.$$

EXAMPLE 3.6. Let us study Figure 3.1: the four-leaf clover defined by the polynomial (see [Fis01, page 38] and [Wal04, page 58, Example 7])

$$f(x,y) = (x^2+y^2)^3 - 4x^2y^2 = x^6 + 3x^4y^2 + 3x^2y^4 + y^6 - 4x^2y^2.$$

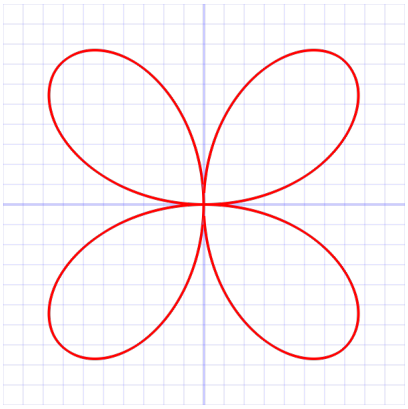

Figure 3.1: The four-leaf clover.

The Newton polygon associated to the four-leaf clover is shown in Figure 3.2. Firstly, the support of f is:

$$\operatorname{supp}(f) = \{(6,0),(4,2),(2,4),(0,6),(2,2)\}.$$

There are two compact edges and two non-compact edges in the boundary of the Newton diagram. By Definition 3.4, the Newton polygon is the union of the two compact red edges.

In addition, if $\mathcal{E}$ is the edge defined by joining the vertices $(0,6)$ and $(2,2)$, then

$$f_{|\mathcal{E}} = y^6 - 4x^2y^2.$$

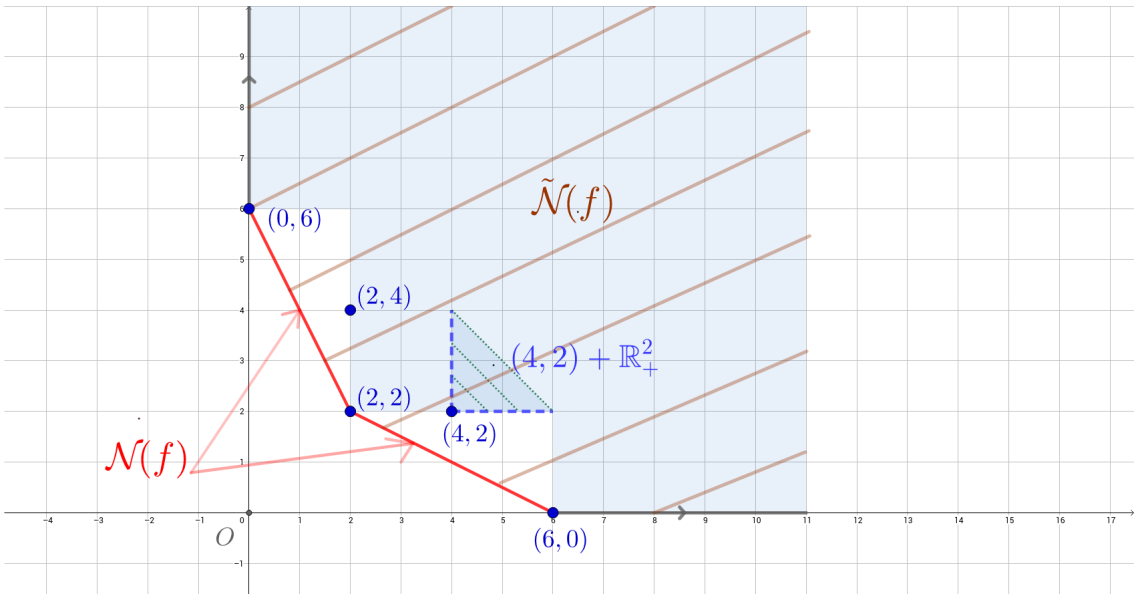

Figure 3.2: The Newton polygon (in red) of the four-leaf clover given by the equation $f(x,y) = (x^2+y^2)^3 - 4x^2y^2$.

REMARK 3.7. See two more examples in [Coo59, pages 47-48].

Notation 3.8. *If $g, h \in \mathbb{R}\{t\}$ are convergent series, we say that $g(t) = o(h(t))$ if and only if $\lim_{t\to 0} \frac{g(t)}{h(t)} = 0$.*

Notation 3.9. *By $f(0,y) \not\equiv 0$ we mean that there exists $y_0 \in \mathbb{R}$ such that $f(0,y_0) \neq 0$. Similarly, for $f(x,0) \not\equiv 0$.*

A connection between $\mathrm{supp}(f)$ and the factorization of the series of f was presented in [Fis01, Proposition, page 198], as follows.

Proposition 3.10. *[Fis01, pages 197-198] Let $f(x,y) \in \mathbb{R}\{x,y\}$ such that $f(0,0) = 0$ and $f(0,y) \not\equiv 0$, $f(x,0) \not\equiv 0$. Assume that $x(t) \in \mathbb{R}\{t\}$, $y(t) \in \mathbb{R}\{t\}$ are convergent series such that $x(0) = y(0) = 0$ and $f(x(t),y(t)) \equiv 0$. Namely the series $x(t)$ and $y(t)$ parametrise a real branch of $(f = 0)$. If $x(t) = at^\alpha + o(t^\alpha)$ and $y(t) = bt^\beta + o(t^\beta)$ where $a, b \in \mathbb{R}^*$ and $\alpha > 0, \beta > 0$, then there exists an edge $\mathcal{E}$ (of slope $-\frac{\alpha}{\beta}$) of the Newton polygon of f such that $f_{|\mathcal{E}}(a,b) = 0$.*

Proof. We have

$$f(x(t),y(t)) = \sum_{m,n} c_{m,n}(at^\alpha + o(t^\alpha))^m(bt^\beta + o(t^\beta))^n = \sum_{m,n} c_{m,n}a^m b^n t^{\alpha m+\beta n} + o(t^{\alpha m+\beta n}) \equiv 0.$$

Denote by

$$\ell := \min\{\alpha m + \beta n \mid (m,n) \in \mathrm{supp}(f)\}.$$

Then

$$f(x(t),y(t)) = \left(t^\ell \sum_{\alpha m+\beta n=l} c_{m,n}a^m b^n \right) + o(t^\ell) \equiv 0.$$

For the above equality to take place, the term with the lowest order in the series must vanish. Hence $(x,y) = (a,b)$ is a solution of the equation $g(x,y) = 0$, where $g(x,y) := \sum_{\alpha m+\beta n=\ell} c_{m,n}x^m y^n$ (note that $(m,n) \in \mathrm{supp}(f)$). Since both a and b are non-zero, g must have at least two non-zero coefficients. Therefore there must be at least two points (m_1,n_1) and $(m_2,n_2) \in \mathrm{supp}(f)$ that lie on the line $\alpha m + \beta n = \ell$. By the minimality of ℓ, this line contains a segment of the Newton polygon of f, say the segment $\mathcal{E}$, with slope $-\frac{\alpha}{\beta}$. In addition, (a,b) verifies $g(a,b) = 0$, namely $f_{|\mathcal{E}}(a,b) = 0$. □

Example 3.11. In Example 3.6 we have four real analytic branches at the origin. Let us consider the branch given by the parametrisation $x(t) = 2t^2 + o(t^2) \in \mathbb{R}\{t\}$ and $y(t) = 2t + o(t) \in \mathbb{R}\{t\}$. In this case, by the notations introduced in Proposition 3.10, we get $a = b = 2$. Denote the edge given by the points $(0,6)$ and $(2,2)$ by $\mathcal{E}$. We have $f_{|\mathcal{E}}(x,y) = y^6 - 4x^2y^2$. The pair $(a,b) = (2,2)$ verifies the equation $f_{|\mathcal{E}} = 0$, namely $f_{|\mathcal{E}}(2,2) = b^6 - 4a^2b^2 = 0$.

As a remark, we underline the fact that if we take two other series $\tilde{x}(t) = 2t^2$, $\tilde{y}(t) = 2t + t^2 \in \mathbb{R}\{t\}$, such that $\tilde{a} = \tilde{b} = 2$ (with the notations from above), then $f(\tilde{a},\tilde{b}) = f(2,2) = 0$, although we have $f(\tilde{x}(t),\tilde{y}(t)) \not\equiv 0$.

3.1.2 Application of the Newton polygon criterion

We apply Proposition 3.10 to obtain our main result of Subsection 3.1, i.e. Proposition 3.12:

Proposition 3.12. *Let us consider an even integer $m \geq 2$ and the polynomial function $f : \mathbb{R}^2 \to \mathbb{R}$ defined by*

$$f(x,y) := x^2 + \int_0^y \prod_{i=1}^{m+1} (t - a_i(x))\mathrm{d}t,$$

where $a_i(x) \in \mathbb{R}[x]$, $a_i(0) = 0$. Then f has a strict local minimum at $(0,0)$.

REMARK 3.13. For $m = 0$, we obtain the function

$$f(x, y) = x^2 + \int_0^y (t - a_1(x))\mathrm{d}t = x^2 + \frac{y^2}{2} - a_1(x)y.$$

Thus f has a non-degenerated critical point, so one could apply the second derivative test. Note that in this case, f has not necessarily a strict local minimum at $(0, 0)$.

Proof. By construction, we have $f(0, 0) = 0$. We argue by contradiction. We suppose that the origin $(0, 0)$ is not a strict local minimum of f, hence in the neighbourhood of the origin, f would take non-positive values: for any $\varepsilon > 0$, there exists a point of coordinates $(x_\varepsilon, y_\varepsilon)$ in the disk of radius ε, centered at the origin, namely $(x_\varepsilon, y_\varepsilon) \in D^2_\varepsilon(0, 0) \setminus \{(0, 0)\}$ such that $f(x_\varepsilon, y_\varepsilon) \leq 0$.

• **First step: we find some convergent series $x(t)$, $y(t)$ such that $f(x(t), y(t)) \equiv 0$.**

Consider $\varepsilon := \frac{1}{n}$. We obtain a sequence of points $(x_n, y_n) \neq (0, 0)$ arbitrarily close to the origin such that $f(x_n, y_n) \leq 0$. We can now apply the Curve selection lemma (see [Mil68, page 25]), which allows us to construct a real analytic curve $\varphi : [0, \varepsilon[\to \mathbb{R}^2$ such that $\varphi(0) = 0$ and $f(\varphi(t)) < 0$ for any $t \in]0, \varepsilon[$ (see Figure 3.3).

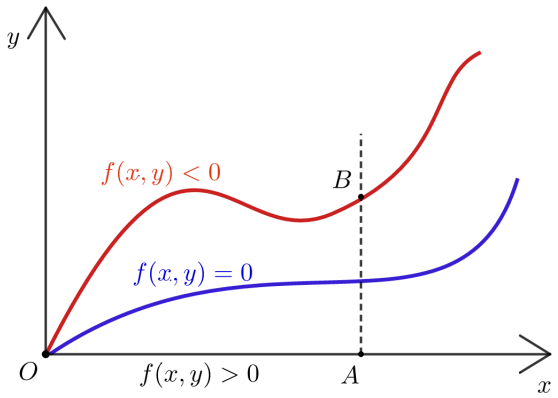

Figure 3.3: In a sufficiently small neighbourhood of the origin there exists a real analytic arc (in blue) denoted by δ such that $f(\delta(t)) = 0$, where f is the function defined in Proposition 3.12.

Note that for $(x, y) \in (Ox) \setminus \{(0, 0)\}$ we have $f(x, y) = x^2 > 0$.

Denote by $B \in \varphi(]0, \varepsilon[)$ a point such that $f(B) < 0$. Similarly, denote by $A \in (Ox) \setminus \{(0, 0)\}$ a point such that $f(A) > 0$. Suppose that A and B have the same $x-$coordinate.

Consider an arbitrarily fixed $x_n := \frac{1}{n} \ll 1$. Let us define $g : \mathbb{R} \to \mathbb{R}$, $g(y) := f(x_n, y)$. For $A \in (Ox) \setminus \{(0, 0)\}$, one has $g(0) > 0$. For $B \in \varphi(]0, \varepsilon[)$, one has $g(y_B) < 0$. Since g is a continuous function, we apply the intermediate value theorem, hence there exists $y_n \in \mathbb{R}$ such that $0 < y_n < y_B$ such that $g(y_n) = 0$. Thus there exists a sequence of points $(x_n, y_n) \neq (0, 0)$, arbitrarily close to the origin, such that $f(x_n, y_n) = 0$. By the Curve selection lemma, there exists a real analytic arc, say $\delta : [0, \varepsilon[\to \mathbb{R}^2$, such that $f(\delta(t)) \equiv 0$, for any $t \in [0, \varepsilon[$.

In other words, there exist $x(t) := at^\alpha + o(t^\alpha) \in \mathbb{R}\{t\}$ and $y(t) := bt^\beta + o(t^\beta) \in \mathbb{R}\{t\}$ such that $f(x(t), y(t)) \equiv 0$, where $a, b \in \mathbb{R}^*$, $\alpha > 0, \beta > 0$.

• **Second step: we obtain a contradiction, using the Newton criterion presented above.**

By definition,

$$f(x, y) = x^2 + \int_0^y \prod_{i=1}^{m+1} (t - a_i(x))\mathrm{d}t,$$

thus we have

$$f(x, 0) = x^2$$

and

$$f(0,y)=\int_0^y\prod_{i=1}^{m+1}(t-a_i(0))\mathrm{d}t=\frac{1}{m+2}y^{m+2},$$

because $a_i(0)=0$. Thus the points $A(2,0)$ and $B(0,m+2)$ belong to $\mathrm{supp}(f)$ (see Figure 3.4 below).

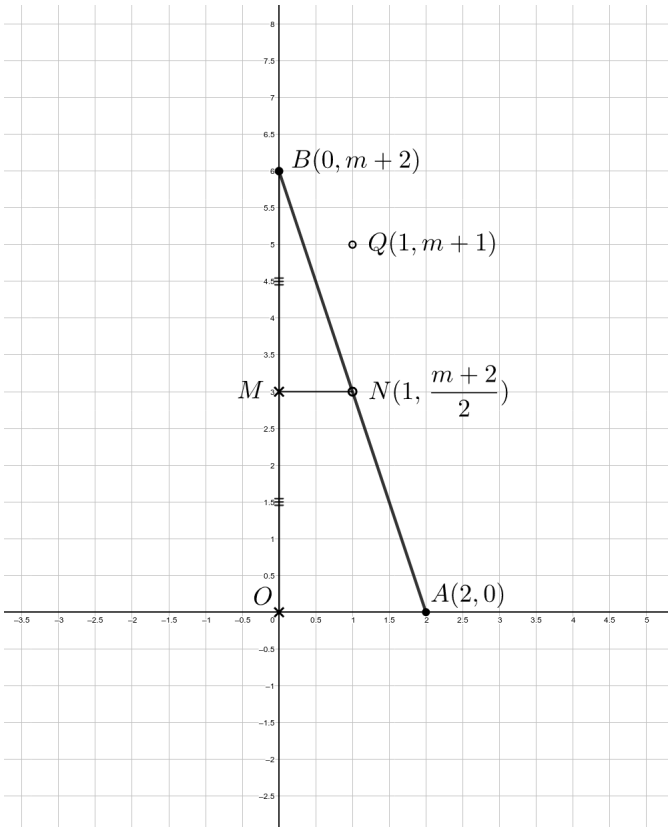

Figure 3.4: Edge of the Newton polygon of f.

If $a_i(x)=0+a_i^1x+a_i^2x^2+o(x^2)$, where $a_i^k\in\mathbb{R}$, then we have

$$f(x,y)=x^2+\int_0^y\prod_{i=1}^{m+1}\left(t-(0+a_i^1x+a_i^2x^2+o(x^2))\right)\mathrm{d}t=$$

$$=x^2+\int_0^y\left(t^{m+1}+c_1t^mx^1+\ldots+c_kt^kx^{m+1-k}+o(t^k)\right)\mathrm{d}t=$$

$$=x^2+\frac{1}{m+2}y^{m+2}+\frac{c_1}{m+1}y^{m+1}x+x^2h(x,y),$$

where $h(0,y)=0$.

Since by hypothesis $m>0$, the midpoint $N(1,\frac{m+2}{2})$ of the segment $[AB]$, is below the point $Q(1,m+1)$. Denote by $\triangle OAB$ the convex hull of the set $\{O,A,B\}$. Hence, $Q\notin\triangle OAB$ (although Q might belong to the support of f). In conclusion, we have

$$\mathrm{supp}(f)\cap\triangle OAB\subseteq\{A,B,N\}.$$

In addition, since we obtained $f(x,y)=x^2+\frac{1}{m+2}y^{m+2}+\frac{c_1}{m+1}y^{m+1}x+x^2h(x,y)$, if there are other points of $\mathrm{supp}(f)$, besides those on the segment $[AB]$, then those points are of the form (x,y) with $y\geq m+2$. Thus by Definition 3.4, the only edge of $\mathcal{N}(f)$ is $[AB]$.

By Proposition 3.10, if $(x(t), y(t))$ is a parametrisation of a branch of $(f = 0)$, then the pair of real numbers (a, b) verifies the equation $f_{|[AB]}(a, b) = 0$. Namely $a^2 + \frac{1}{m+2}b^{m+2} = 0$. Since by hypothesis $m > 0$ is even, we have a sum of squares which can only be zero if both its terms are zero. This is impossible, since $a, b \in \mathbb{R}^*$. In conclusion our supposition was false and f has a strict local minimum at the origin.

□

3.2 Construction to the right of a given separable snake

Note that the main purpose of Chapter 3 is to prove the following result, as we shall do in Subsection 3.2.4: Every separable positive generic rooted transversal tree is realisable in an effective way by a strict local minimum of a bivariate real polynomial function in a small enough neighbourhood of the origin.

Note that the construction in this section is made only to the right, namely for $x > 0$. We will treat left-right configurations only in Chapter 4.

3.2.1 The image of the apparent contour of a projection

The reader should remember Definition 2.43 of **the polar curve of** f with respect to x, namely

$$\Gamma(f, x) := \left\{ (x, y) \in \mathbb{R}^2 \mid \frac{\partial f}{\partial y}(x, y) = 0 \right\}.$$

Definition 3.14. Denote by

$$\tilde{\Gamma} := \left\{ (x, y, z) \in \mathbb{R}^3 \mid z = f(x, y), (x, y) \in \Gamma(f, x) \right\}.$$

Notation 3.15. *We denote by*

$$\mathrm{graph}(f) := \{(x, y, z) \in \mathbb{R}^3 \mid z = f(x, y)\}$$

the surface which is the graph of the polynomial function $f : \mathbb{R}^2 \to \mathbb{R}$.

Furthermore, let us present the following notions of "apparent contour" and "discriminant locus", which appeared for instance in [AGZV12, page 13]. A more visual explanation given by Ghys can also be found in [GL09, Le-pli-et-la-fronce].

Definition 3.16. Let $\Pi : \mathrm{graph}(f) \to \mathbb{R}^2_{x,z}$ be the projection $(x, y, z) \mapsto (x, z)$. The set of critical points of Π on $\mathrm{graph}(f)$ is called **the apparent contour at the source** of the projection Π.

Proposition 3.17. *The curve* $\tilde{\Gamma}$ *is the apparent contour of the projection*

$$\Pi : \mathrm{graph}(f) \to \mathbb{R}^2_{x,z}, \Pi(x, y, z) = (x, z).$$

Proof. By [Mil68, Lemma 2.7] and by Definition 3.16, the apparent contour of $\Pi = (\Pi_1, \Pi_2)$ (i.e. $\Pi_1(x, y, z) = x, \Pi_2(x, y, z) = z$), is given by the set

$$\mathrm{c} := \left\{ (x, y, z) \in \mathrm{graph}(f) \mid \mathrm{rank} \begin{pmatrix} -\frac{\partial f}{\partial x} & -\frac{\partial f}{\partial y} & 1 \\ \frac{\partial \Pi_1}{\partial x} & \frac{\partial \Pi_1}{\partial y} & \frac{\partial \Pi_1}{\partial z} \\ \frac{\partial \Pi_2}{\partial x} & \frac{\partial \Pi_2}{\partial y} & \frac{\partial \Pi_2}{\partial z} \end{pmatrix} \leq 2 \right\}.$$

Hence the apparent contour

$$\mathrm{c} = \left\{ (x, y, z) \in \mathrm{graph}(f) \mid \det \begin{pmatrix} -\frac{\partial f}{\partial x} & -\frac{\partial f}{\partial y} & 1 \\ 1 & 0 & 0 \\ 0 & 0 & 1 \end{pmatrix} = 0 \right\} = \left\{ (x, y, z) \in \mathrm{graph}(f) \mid -\frac{\partial f}{\partial y} = 0 \right\} = \tilde{\Gamma}.$$

□

Definition 3.18. We call the critical image of the projection $\Pi : \mathrm{graph}(f) \to \mathbb{R}^2_{x,z}$, $(x, y, z) \mapsto (x, z)$, the **discriminant locus** of this projection.

Thus

$$\Delta := \Pi(\tilde{\Gamma}) \subset \mathbb{R}^2_{x,z}$$

is the discriminant locus of the projection Π. This terminology is similar to the one found, for instance, in [Mau99, page 440].

3.2.2 Hypotheses

• We are in the context $x > 0$: we want to realise a given **right** separable generic rooted transversal tree.

• As in Subsection 1.7.1 let us consider the monic polynomial $P_x(y) \in \mathbb{R}[x][y]$, such that

$$P_x(y) := \prod_{i=1}^{m+1} (y - a_i(x)) \in \mathbb{R}[x][y],$$

where $m \in \mathbb{N}$, the roots $a_i(x) \in \mathbb{R}[x]$ for any $i = 1, \ldots, m+1$ and

$$a_1(x) \prec_+ a_2(x) \prec_+ \ldots \prec_+ a_{m+1}(x),$$

as one can see in Figure 3.5.

• Let a_i denote the graph of the polynomial $a_i(x)$, that is $a_i := \{(x, y) \in \mathbb{R}^2 \mid y = a_i(x)\}$ and

$$\tilde{a_i} := \{(x, y, z) \in \mathbb{R}^3 \mid z = f(x, y), y = a_i(x)\}.$$

The curves a_i are in the positive trigonometric order in the plane Oxy, as in Figure 3.5 below.

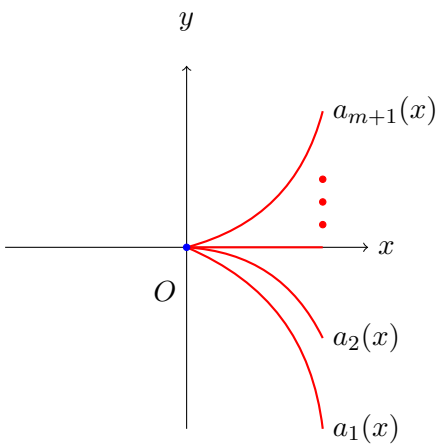

Figure 3.5: The right half-branches of a_i for $i = 1, \ldots, m+1$.

• In the sequel, we will consider only polynomials a_i such that

$$\nu_x(a_i) \geq 1,$$

i.e. $a_i(0) = 0$, for any $i = 1, \ldots, m+1$.

• We denote by

$$\Gamma := (P_x(y) = 0).$$

• In addition, we suppose that the map $\Pi : \mathrm{graph}(f) \to \mathbb{R}^2_{x,z}$, $(x, y, z) \mapsto (x, z)$ is a **homeomorphism** from $\tilde{\Gamma}_+ := \tilde{\Gamma} \cap (x > 0)$ to $\Pi(\tilde{\Gamma}_+)$, namely that there are $m+1$ half-branches in $\tilde{\Gamma}_+$ (i.e. $\tilde{a}_1, \tilde{a}_2, \ldots, \tilde{a}_{m+1}$) and $m+1$ half-branches in Δ (i.e. $\Pi(\tilde{a}_1), \Pi(\tilde{a}_2), \ldots, \Pi(\tilde{a}_{m+1})$ are distinct).

3.2.3 Projections

In Chapter 1 we defined the notion of snake (see Definition 1.6), then we explained how to draw it embedded in the real plane (see Example 1.8 and Figure 1.2). In what follows, we shall define another object that describes completely a snake, namely its *snake-sequence*.

Definition 3.19. Take an even integer number $m \in \mathbb{N}$ and consider the $(m+1)$-permutation

$$s : \{1, 2, \ldots, m+1\} \to \{1, 2, \ldots, m+1\}.$$

Consider its inverse permutation, $s^{-1} : \{1, 2, \ldots, m+1\} \to \{1, 2, \ldots, m+1\}$. The ordered sequence

$$(s^{-1}(1), s^{-1}(2), \ldots, s^{-1}(m+1))$$

is called **the sequence** of s and it is denoted by $\mathrm{seq}(s)$. If s is a snake, we call it **the snake-sequence** of s.

Remark 3.20. Given a snake, its snake-sequence is thus defined independently of the embedding plane. However, if one wants to construct the sequence geometrically, first label each critical point of the snake (see Definition 1.6) with an integer number from 1 to $m+1$, from left to right (see Figure 3.6). Then, project the critical points of s on a fixed axis in the plane. On this axis, we associate to each projection the label of its corresponding critical point in its preimage. At the end, we read the numbers starting from the one corresponding to the lowest point of the snake.

Example 3.21. Let us consider the 3-snake $s := \begin{pmatrix} 1 & 2 & 3 \\ 2 & 3 & 1 \end{pmatrix}$. Its inverse is $s^{-1} = \begin{pmatrix} 1 & 2 & 3 \\ 3 & 1 & 2 \end{pmatrix}$. Thus its snake-sequence $\mathrm{seq}(s) = (3, 1, 2)$ (see Figure 3.6).

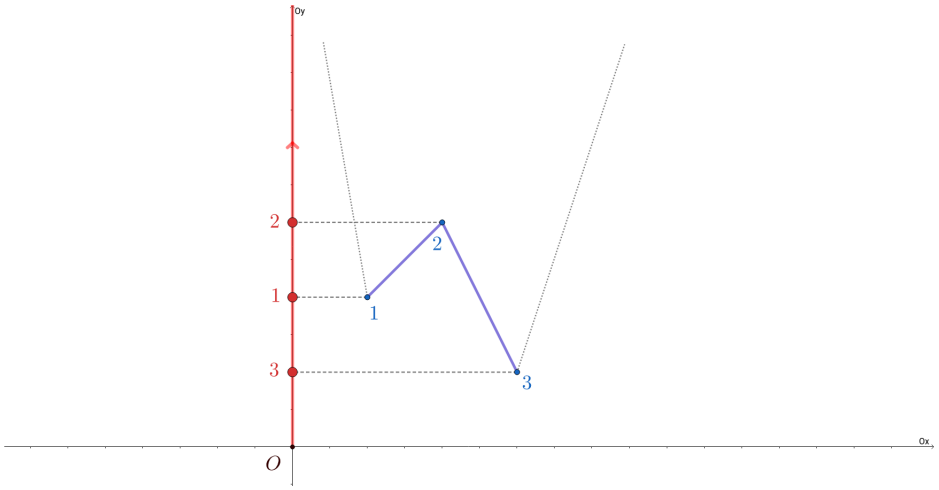

Figure 3.6: Construction of the snake-sequence, read on the vertical axis.

Lemma 3.22. *Two $(m+1)$-snakes are identical if and only if they have the same snake-sequences.*

Proof. If the snakes are identical, there is nothing to prove. If two snakes have the same snake-sequence, then by Definition 3.19, they have the same inverse. Thus, the given snakes are identical, since they represent the same permutation. □

In the following we consider a polynomial function $f : \mathbb{R}^2 \to \mathbb{R}$, like in Subsection 3.2.1 above.

For a general view of the geometric aspects, the reader should see Figure 3.7 and Figure 3.8 below.

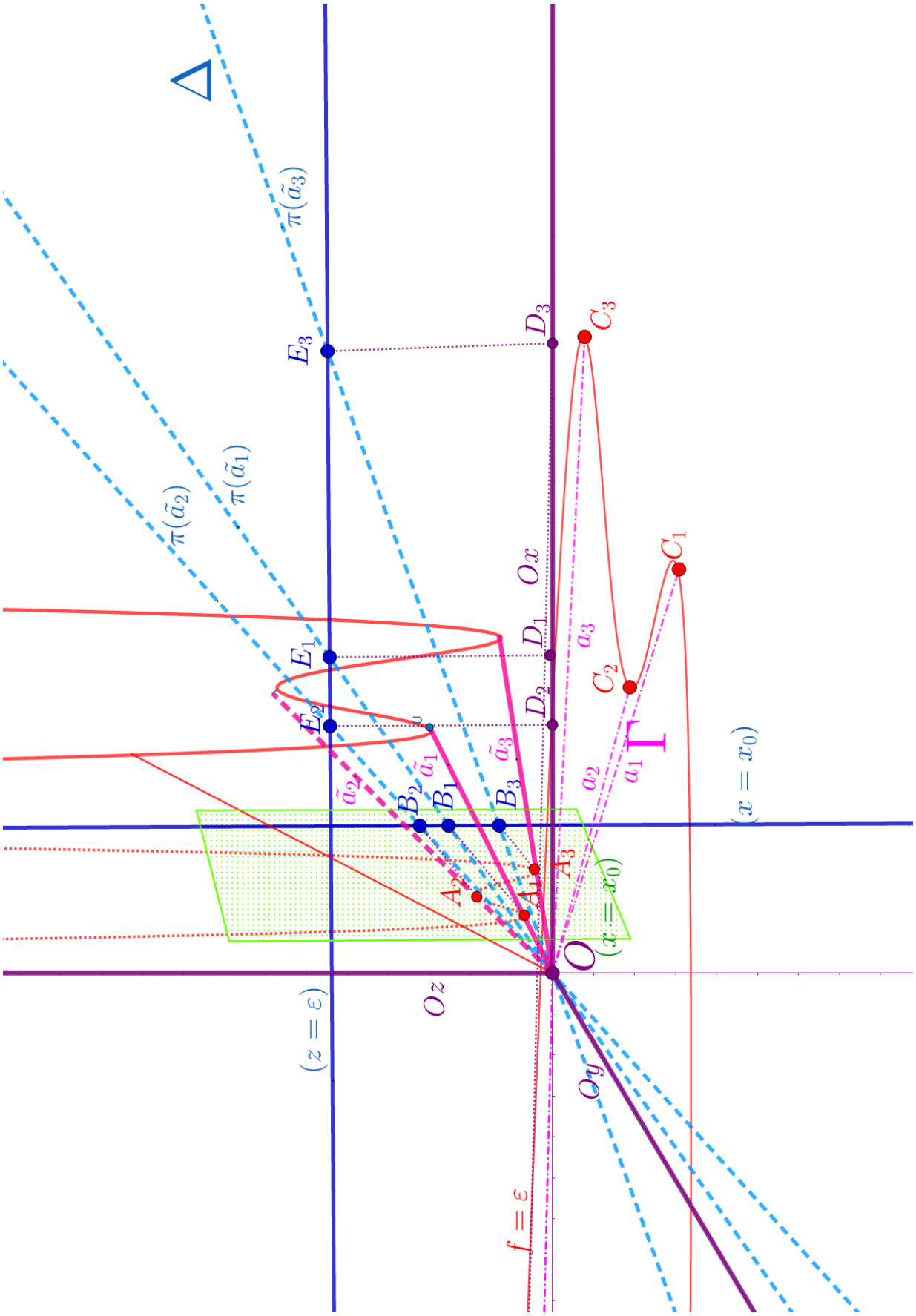

Figure 3.7: The geometric interpretation of the permutations σ_ε, π and τ. Conclusion: $\tau = \sigma_\varepsilon$ for $\varepsilon > 0$ and for $x_0 > 0$ small enough.

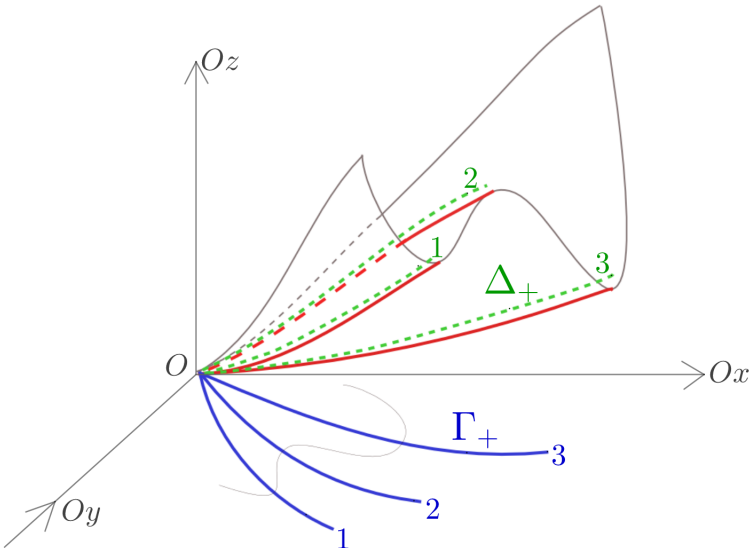

Figure 3.8: The homeomorphism between the reduced positive polar curve Γ_+ and its image Δ_+ gives the permutation π.

In the following, for a sufficiently small $x_0 > 0$ we have the notations: $A_k(x_0, y_k, z_k)$ and by $B_k(x_0, 0, z_k)$.

Definition 3.23. Denote by π the permutation given by $\pi(i) := j$ if and only if the half-branch $\Pi_{xz}(\tilde{a_j})$ is on the i-th position in the discriminant Δ, when considering the positive trigonometric order of the half-branches of Δ (see Figure 3.9) in the plane Oxz.

Remark 3.24. To obtain π, just read the labels of the half-branches in Δ in the trigonometric order.

Example 3.25. If the half-branches in Δ are ordered trigonometrically like in Figure 3.9, then $\pi := \begin{pmatrix} 1 & 2 & 3 \\ 3 & 1 & 2 \end{pmatrix}$. For instance, $\pi(1) = 3$ since the image of the half-branch a_3 appears in Δ as $\Pi(\tilde{a_3})$ in the first position (in the trigonometric order).

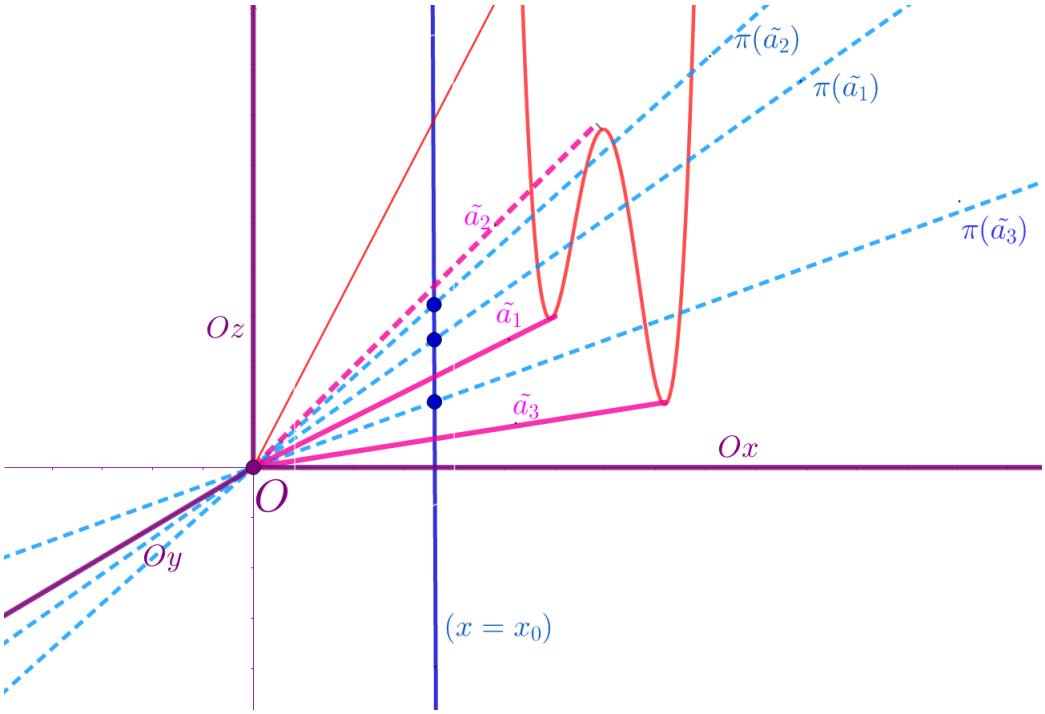

Figure 3.9: The permutation $\pi = (1, 2, 3) \mapsto (3, 1, 2)$, obtained by reading the projection of $\{\tilde{a}_i\}$, for $i = 1, 2, 3$ on the Oxz plane. Just read the indices j of $\Pi(\tilde{a}_j)$ in the Oxz plane in the trigonometric order: $3, 1, 2$.

Proposition 3.26. *The snake-sequence of π can be read on the line d defined by the intersection of the planes $(x = x_0)$ and Oxz, for a sufficiently small $x_0 > 0$. More precisely, π gives the order of the points $(x_0, 0, z(x_0, y_k))$ on the line d.*

Proof. For a sufficiently small $x_0 > 0$, the projected curves $\Pi(\tilde{a_k})$, $k = 1, \ldots, m + 1$ do not intersect, thus they do not change order. The trigonometric order is the same as the order in which they intersect the $(x = x_0)$ axis. The points $(x = x_0) \cap \Pi(\tilde{a_k})$ have coordinates $(x_0, 0, z(x_0, y_k))$. □

Definition 3.27. For fixed $x_0 > 0$ small enough, denote by τ (see Figure 3.17 and Figure 3.11) the snake associated to the one variable polynomial given by $y \mapsto z(x_0, y)$, where $z = f(x, y)$ is the height function (see Figure 3.10 for the convention of reading the snake τ).

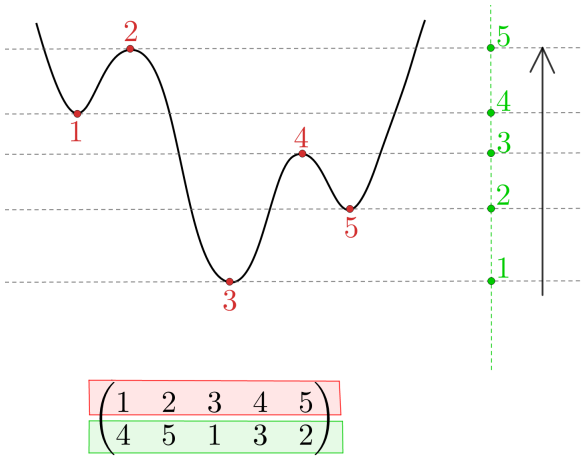

Figure 3.10: Convention for reading a Arnold snake τ.

Notation 3.28. *The critical points of the polynomial* $y \mapsto z(x_0, y)$, *where* $z = f(x, y)$ *are denoted by* $A_k := (x = x_0) \cap \tilde{a_k}$, *for* $k = 1, \ldots, m+1$. *We have*

$$A_k(x_0, y_k, z(x_0, y_k))$$

.

Proposition 3.29. *The snake-sequence* $\mathrm{seq}(\tau)$ *is* $(\pi(1), \pi(2), \ldots, \pi(m+1))$.

Proof. Let us project the points A_k on the line d. We obtain the points $B_k := \mathrm{proj}_{(x=x_0)} A_k$ (see Figure 3.11 below), namely

$$B_k(x_0, 0, z(x_0, y_k)).$$

The snake-sequence of τ is given by the indices of the points B_k on the line $(x = x_0)$ (the blue line), when one reads them in the increasing order of their z-coordinates.

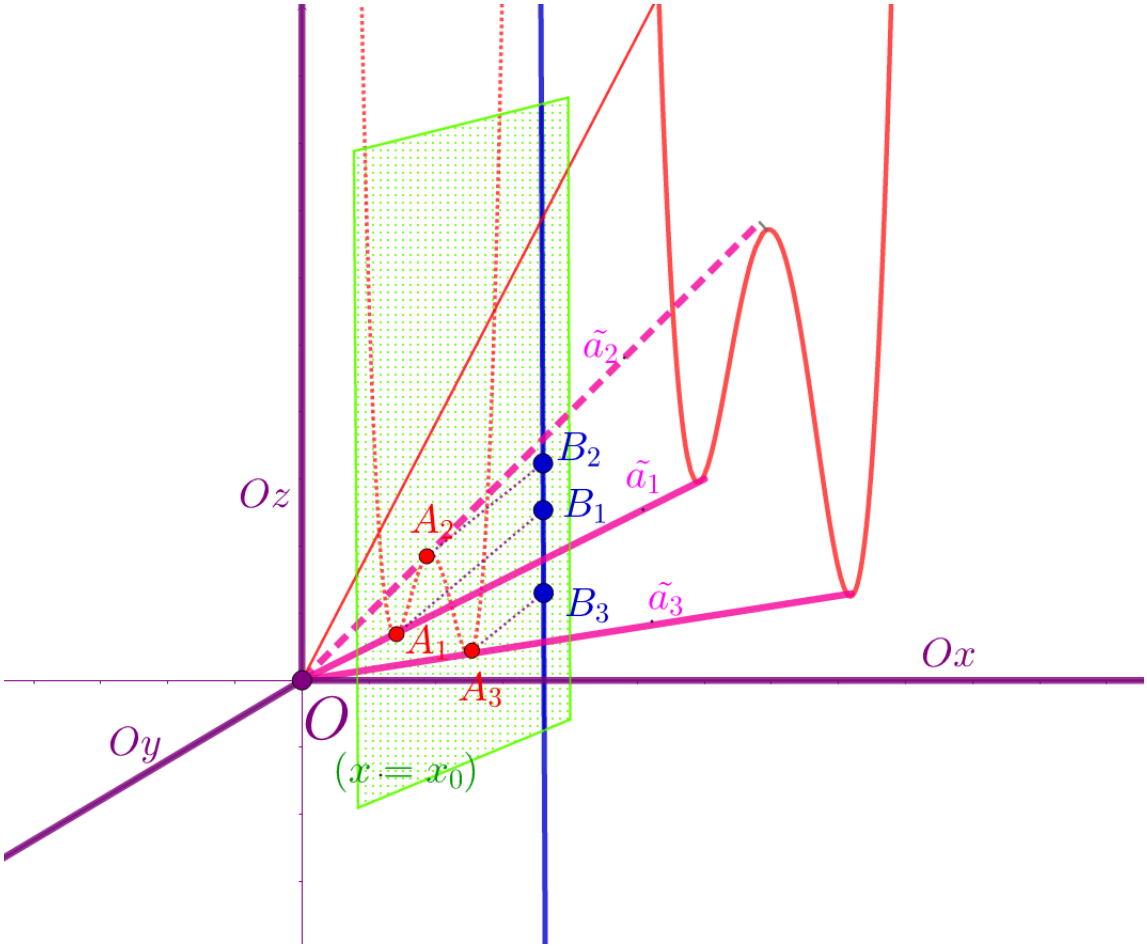

Figure 3.11: The snake $\tau = (1, 2, 3) \mapsto (3, 1, 2)$; we project the critical points $A_k(x_0, y_k, z_k)$ on the line d (in blue), situated in the green plane; we obtain the snake-sequence of τ, given by the ordering of the points $B_k(x_0, 0, z_k)$, $k = 1, 2, 3$.

Since B_k, obtained by projecting the point A_k, is the same one which appears in Proposition 3.26, we have now $\pi(i) = j$ if and only if B_j is on the i-th position on the $(x = x_0)$ axis.

In conclusion, $\mathrm{seq}(\tau) = (\pi(1), \ldots, \pi(m+1))$. □

The reader should remember Section 2.1, where we stated the following hypotheses and Definition 2.2:

(a) In this Chapter, the expressions "sufficiently small ε" or "small enough ε" mean: "there exists $\varepsilon_0 > 0$ such that, for any $0 < \varepsilon < \varepsilon_0$, one has ...." We will denote this often by $0 < \varepsilon \ll 1$.

(b) The function $f : \mathbb{R}^2 \to \mathbb{R}$ is a two variables polynomial function with $f(0,0) = 0$.

(c) Given f, let us **fix a neighbourhood** V of $(0,0)$ such that:

- the point $(0,0)$ is a strict local minimum of f in V;

- we have $V \cap (f = 0) = \{(0,0)\}$.

In this context, let us give the following Definition 3.30.

Definition 3.30. Consider we are in the plane $z = 0$. Let us define σ_ε (see Figure 3.17) to be the right asymptotic snake of f at the origin relative to a generic direction x (see Definition 2.114). That is the snake given by the points $C_k := \mathcal{C}_\varepsilon \cap a_k$ (in Chapter 2 the set of points C_k represents the set of right crests and right valleys) in the plane Oxy, where $x > 0$ (see Figure 3.12 for the convention of reading the snake).

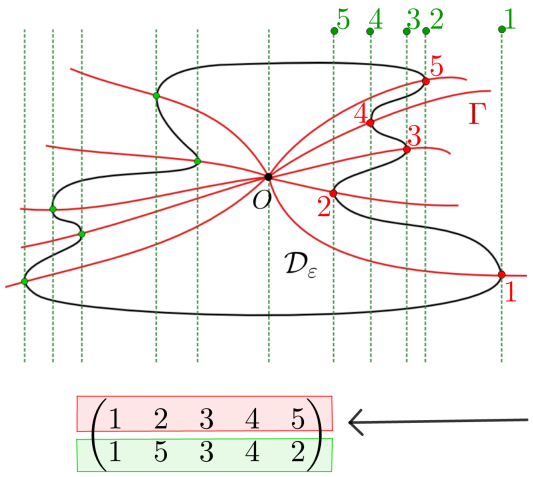

Figure 3.12: Convention for reading a right asymptotic snake σ_ε.

Remark 3.31. In the case of the snake-sequence associated to the snake of the right crests and right valleys of f, we use the following convention: we read the projections of the minima and maxima of the snake, starting with the furthest from the origin, on the Ox axis, as in Figure 3.13.

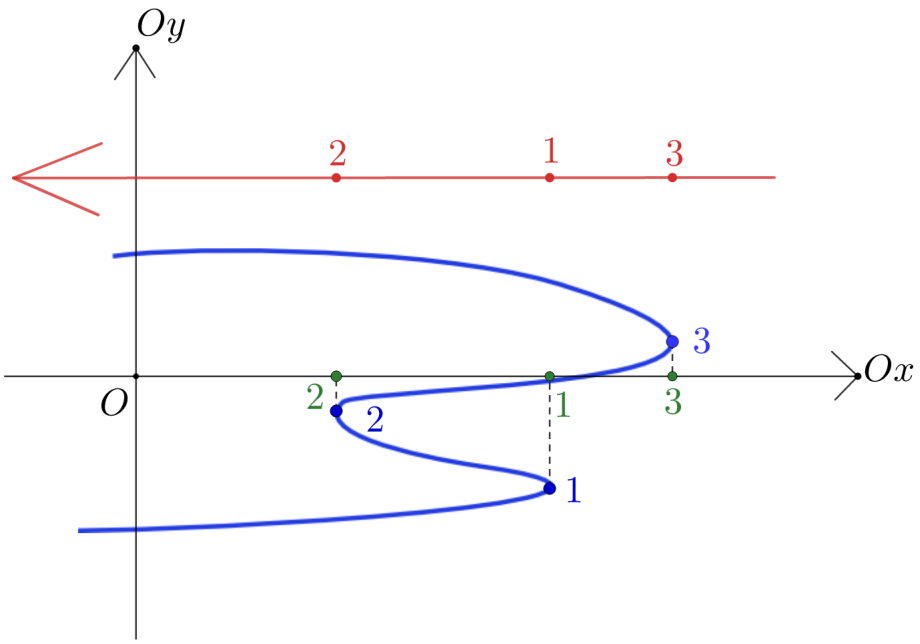

Figure 3.13: Convention for the snake-sequence of the snake of right crests and valleys of f.

Proposition 3.32. *The snake-sequence of* σ_ε *is* $\mathrm{seq}(\sigma_\varepsilon) = (\pi(1), \pi(2), \ldots, \pi(m+1))$ *(see Figure 3.15).*

Proof. Let us start by projecting the points $C_k(x_k, y_k, 0)$, $k = 1, \ldots, m+1$, with $f(x_k, y_k) = \varepsilon$, on the Ox-axis, like in Figure 3.15. We obtain the points $D_k := \mathrm{proj}_{Ox}(C_k)$, namely $D_k(x_k, 0, 0)$. By Definition 3.19, $\mathrm{seq}(\sigma_\varepsilon)$ is given by the ordered sequence of points $\{D_k\}_{k=1,\ldots,m+1}$, read on the Ox-axis, where the first point is the furthest from the origin.

Consider a fixed $\varepsilon > 0$ small enough. We call d_ε the line obtained as the intersection of the plane $(z = \varepsilon)$ with the plane Oxz. Let us denote by $E_k := (x_k, 0, \varepsilon)$. Hence, by their coordinates, we obtain the points $\{E_k\}$ in the same order on d_ε as the order of the points $\{D_k\}$ on the Ox-axis, going towards the origin. Note that here we only consider the case $x > 0$, as we stated in the beginning of this chapter.

One reads the snake π on the line d_ε as follows: we have $\pi(i) = j$ if and only if E_j is on the i-th position on the line d_ε, read in the trigonometric order of the half-branches $\pi(\tilde{a_k})$ of the discriminant set Δ.

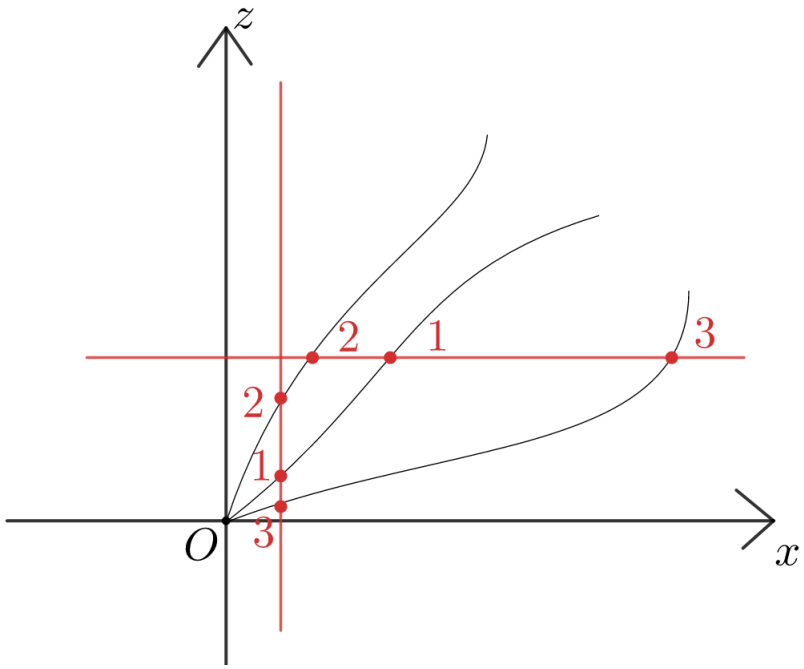

Figure 3.14: The main idea of the proof: the transversality of the vertical line d (respectively of the horizontal line d_ε) with the curves $\pi(\tilde{a}_i)$, $i = 1, \ldots, m+1$ of Δ, in the plane Oxz.

As shown in Figure 3.14, for a small enough $\varepsilon > 0$, the curves in Δ in the plane Oxz do not intersect under the line d_ε (except for the origin O, which is their common point). Therefore, we have $\pi(i) = j$ if and only if D_j is on the i-th position on the Ox-axis.

In conclusion, the points $\{D_k\}$ are ordered on Ox (the first one is the furthest from the origin O), as follows: $D_{\pi(1)}, D_{\pi(2)}, \ldots, D_{\pi(m+1)}$. Thus by Definition 3.19,

$$\mathrm{seq}(\sigma_\varepsilon) = (\pi(1), \pi(2), \ldots, \pi(m+1)).$$

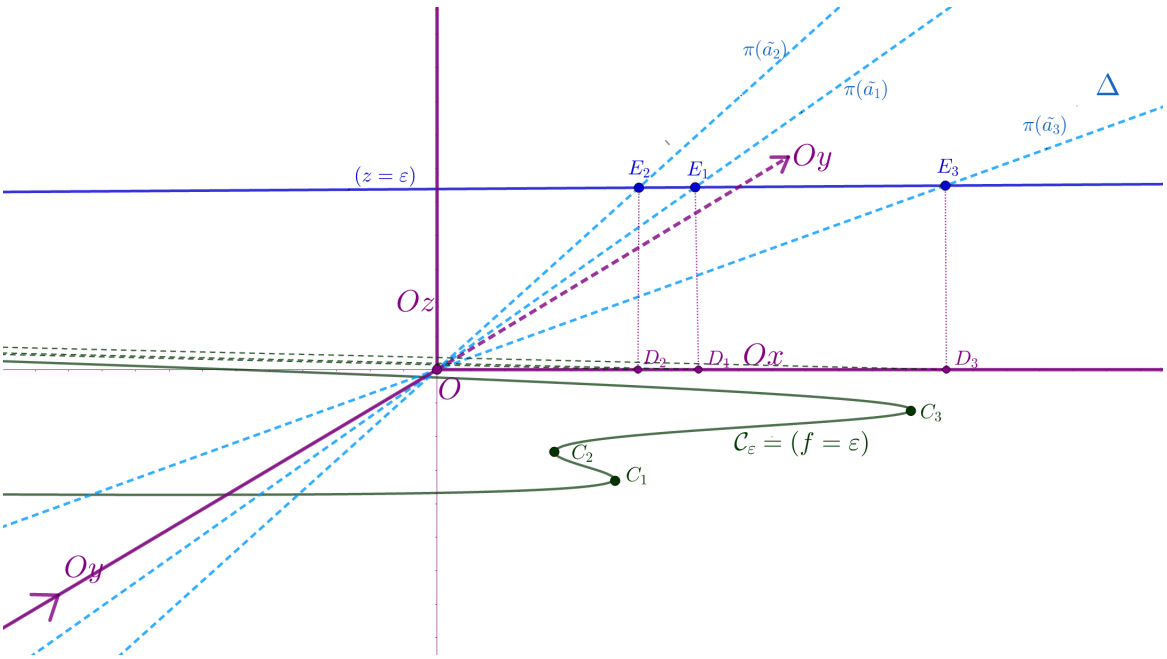

Figure 3.15: The snake-sequence of σ_ε is $(3, 1, 2)$. The points $C_k = (x_k, y_k, 0)$.

□

Theorem 3.33. *Let us take a sufficiently small $\varepsilon > 0$, a sufficiently small $x_0 > 0$. Moreover, as in Subsection 1.7.1 let us consider the monic polynomial $P_x(y) \in \mathbb{R}[x][y]$, such that*

$$P_x(y) := \prod_{i=1}^{m+1} (y - a_i(x)) \in \mathbb{R}[x][y],$$

where $m \in \mathbb{N}$, the roots $a_i(x) \in \mathbb{R}[x]$ for any $i = 1, \ldots, m+1$ and $a_1(x) \prec_+ a_2(x) \prec_+ \ldots \prec_+ a_{m+1}(x)$, such that $\nu_x(a_i) \geq 1$, i.e. $a_i(0) = 0$, for any $i = 1, \ldots, m+1$. Suppose that

$$\Gamma = (P_x(y) = 0).$$

Then we have the following equality of the snakes introduced in Definition 3.27 and Definition 3.30 (see Figure 3.16 and Figure 3.17):

$$\tau = \sigma_\varepsilon.$$

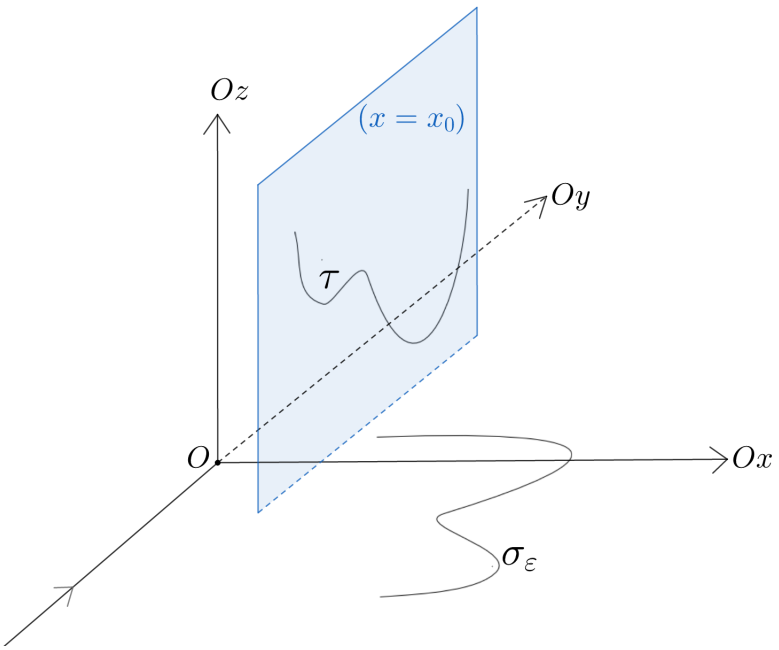

Figure 3.16: We have the equality $\tau = \sigma_\varepsilon$.

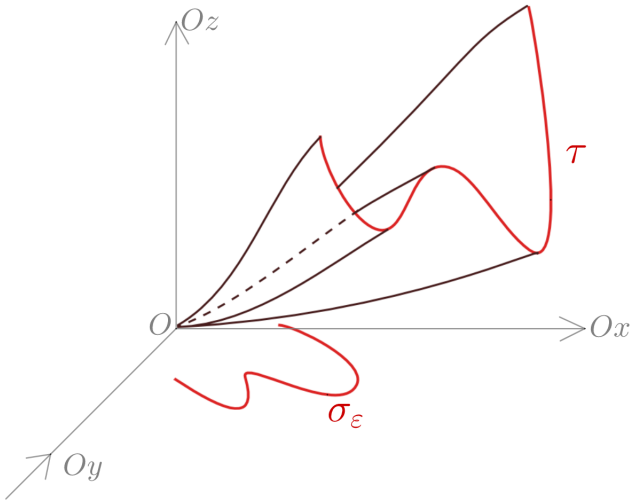

Figure 3.17: The snakes σ_ε and τ.

Proof. From Proposition 3.29 and Proposition 3.32, we have by transitivity the equality $\mathrm{seq}(\tau) = \mathrm{seq}(\sigma_\varepsilon)$. By Lemma 3.22, we conclude that τ and σ_ε are the same $(m+1)$-snake. □

3.2.4 The effective construction of the Poincaré-Reeb tree to the right

We are under the hypotheses from Subsection 3.2.2 and those from Section 2.1. The following Theorem 3.34 gives us an original construction of a given separable snake to the right, in two variables, for a strict local minimum at the origin. In other words, we realise a given separable positive Poincaré-Reeb tree of $f : \mathbb{R}^2 \to \mathbb{R}$, where f has a strict local minimum at the origin.

The main idea is to start from a given separable snake σ. Following the steps from Section 1.8, we construct the polynomials $a_i(x)$, $i = 1, \ldots, m+1$ such that the snake associated to the polynomial $Q_x(y) := \int_0^y \prod_{i=1}^{m+1}(y - a_i(x))$ is σ. Consider the bivariate polynomial $Q(x, y) := Q_x(y)$ and take $f(x, y) := x^2 + Q(x, y)$. The snake to the right (of the positive Poincaré-Reeb tree) of f (namely the one given by the alternating right crests and right valleys of $(f(x, y) = \varepsilon)$) will be exactly σ, as shown by:

Theorem 3.34. *Let σ be a separable $(m+1)$-snake, with m an even integer. The polynomial $f \in \mathbb{R}[x, y]$ constructed by the following steps (a) and (b) has a strict local minimum at the origin whose snake to the right, namely σ_ε, of its alternating sequence of right crests and right valleys is σ:*

(a) first, construct the one variable polynomial $Q_x(y) \in \mathbb{R}[x][y]$, by following the steps described in Theorem 1.149:

$$Q_x(y) := \int_0^y \prod_{i=1}^{m+1} \big(t - a_i(x)\big)\mathrm{d}t,$$

by choosing the polynomials $a_i(x) \in [R][x]$ such that their contact tree is one of the binary separating trees of σ.

(b) take $f(x, y) := x^2 + Q_x(y)$.

REMARK 3.35. We have $\frac{\partial f}{\partial y} = \frac{\partial Q_x(y)}{\partial y}$, which by construction (see Section 1.8) is equal to $\prod_{i=1}^{m+1}(y - a_i(x))$.

Proof. By Theorem 1.149, the polynomial $Q_x(y)$ is $(m+2)$-Morse (see Definition 1.14) and for sufficiently small $x > 0$, the snake associated to $Q_x(y)$ is σ. By Proposition 3.12, we know that the polynomial $f(x, y) := x^2 + Q_x(y)$ has a strict local minimum at the origin. Notice that the snake τ of $f(x_0, y) = x_0^2 + Q_{x_0}(y)$ is the same as the given snake σ for $Q_{x_0}(y)$ (up to a translation with x_0^2) for a sufficiently small $x_0 > 0$. In addition, by Theorem 3.33, we know that the snake $\sigma_\varepsilon = \tau$. This concludes the proof. □

3.2.5 Appendix 1: Generalisations

The results from Chapter 3 hold for a more general case, as follows:

Theorem 3.36. *Let us consider $f : \mathbb{R}^2 \to \mathbb{R}$ a polynomial function with a strict local minimum at the origin; $f(0,0) = 0$. Let $\phi : \mathbb{R}^2 \to \mathbb{R}^2$ be the map $(x, y) \mapsto (x, f(x, y))$. Let us denote by Γ_+ the right polar half-branches of the polar curve of $f : \mathbb{R}^2 \to \mathbb{R}^2$, with the notations and hypotheses from Section 2.1:*

-Suppose that Γ_+ is reduced.

-If we denote by $\Delta_+ := \phi(\Gamma_+)$, let us suppose that $\phi_{|\Gamma_+} : \Gamma_+ \to \Delta_+$ is a homeomorphism.

Then:

(i) $\mathcal{C}_\varepsilon$ represents a snake σ_ε to the right;

(ii) the snake σ_ε to the right is the permutation given by the comparison of the total order relation of the half-branches of Γ_+ and the total order relation of the half-branches of Δ_+.

REMARK 3.37. (a) In other words, if the two hypotheses from Theorem 3.36 are satisfied, then **the interplay between the positive polar curve and its image determines the positive generic asymptotic Poincaré-Reeb tree**.

(b) In addition, as we proved in Subsection 2.7.3,

- if the polar is reduced, then to the right of the origin $\mathcal{C}_\varepsilon$ consists of an alternation of crests and valleys, with no inflection points;

-if the restriction of ϕ to the positive polar curve is a homeomorphism on its image, then $\mathcal{C}_\varepsilon$ has no bitangents.

Namely, the two hypotheses imply also the existence of a **snake** to the right.

Theorem 3.38. *If the following hypotheses are satisfied:*

(a) $f : \mathbb{R}^2 \to \mathbb{R}$ polynomial function with a strict local minimum at the origin; $f(0,0) = 0$;

(b) the set $\Gamma := \left(\frac{\partial f}{\partial y} = 0\right)$ has only real smooth branches, which are transverse to the Oy axis;

(c) Γ is reduced;

(d) the (positive) contact tree of Γ is an end-rooted plane binary tree;

then the snake to the right of f is separable.

REMARK 3.39. (i) The hypothesis *(d)* (the (positive) contact tree of Γ is complete and binary) implies the fact that $\varphi_{|\Gamma_+} : \Gamma_+ \to \Delta_+$ is a homeomorphism.

(ii) If the (positive) contact tree of Γ is not complete and binary, then we might lose the separability property of the snake to the right of f (as shown in Example 1.158).

3.2.6 Appendix 2: Biordered sets

Let us consider a finite set $\mathcal{A}$, with $\#\mathcal{A} = n$. Let us take two total order relations on the set $\mathcal{A}$, denoted by $<_1$, respectively by $<_2$. To such a pair we can associate an automorphism. The advantage of working with total order relations on the set $\mathcal{A}$ is that one can restrain the total

order relations to subsets of $\mathcal{A}$, whereas one cannot restrain automorphisms of $\mathcal{A}$ to subsets of $\mathcal{A}$.

Let us use the combinatorists' notation $[n] := \{1, 2, \ldots, n\}$. Moreover, denote by $\mathrm{Aut}(\mathcal{A})$ (respectively $\mathrm{Aut}([n])$) the set of automorphisms of $\mathcal{A}$ (respectively of $[n]$).

A total order relation on $\mathcal{A}$ can be seen as a bijection from the set $[n]$ to the set $\mathcal{A}$. Thus the function $<_1 \colon [n] \to \mathcal{A}$ (respectively $<_2 \colon \mathcal{A} \to [n]$) has an inverse function, namely ${<_1}^{-1} : \mathcal{A} \to [n]$ (respectively ${<_1}^{-1} : [n] \to \mathcal{A}$). Therefore, we have the following examples of elements of the set $\mathrm{Aut}(\mathcal{A})$: the identity id, $<_2 \circ {<_2}^{-1}$ or $<_1 \circ {<_2}^{-1}$. Similarly, we have the following examples of elements of the set $\mathrm{Aut}([n])$: the identity id, ${<_2}^{-1} \circ <_1$ or ${<_1}^{-1} \circ <_2$. Figure 3.18 illustrates the total order relations viewed as bijections.

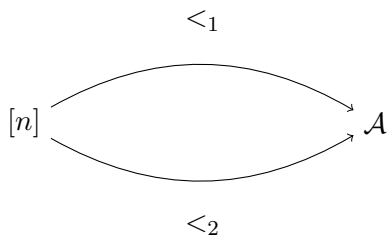

Figure 3.18: Two total order relations viewed as bijections.

In addition, in Figure 3.19 and Figure 3.20 below we can see the two ways of constructing automorphisms, given two total order relations $<_1$ and $<_2$ on the same set.

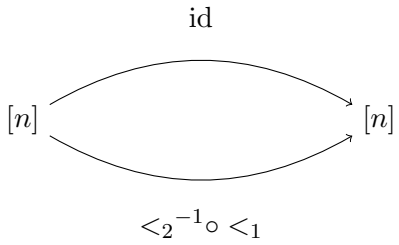

Figure 3.19: Two automorphisms of the set $[n]$, which give us the permutation $i \mapsto {<_2}^{-1} \circ <_1 (i)$.

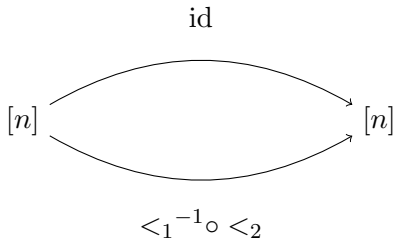

Figure 3.20: Two automorphisms of the set $[n]$, which give us the permutation $i \mapsto {<_1}^{-1} \circ <_2 (i)$.

By convention, we shall choose the automorphisms from Figure 3.19. We can now define the notion of biordered set (see [Ghy17]), viewed from the point of view of the comparison between two total order relations on the same set.

Definition 3.40. [Ghy17, pages 17-18] A **biordered set** is a finite set, say $\mathcal{A}$, endowed with

two total order relations. By convention, given a couple $\{<_1, <_2\}$ of total ordered relations, **the Knuth automorphism of the biordered set** $(\mathcal{A}, <_1, <_2)$ is defined by $\sigma(i) := {<_2}^{-1} \circ <_1 (i)$.

By abuse of language, we shall also call a biordered set a **permutation** when there is no ambiguity.

In other words, let us denote by a_i the element of $\mathcal{A}$ which appears in the position i in the first total order relation. Then let us find the position p of a_i in the second total order relation. Thus Definition 3.40 says that $\sigma(i) := p$.

EXAMPLE 3.41. Given the set $\mathcal{A} := \{a_1, a_2, a_3\}$ with the first total order relation $a_1 <_1 a_2 <_1 a_3$ and the second total order relation $a_1 <_2 a_3 <_2 a_2$, we have (see Figure 3.21):

$$\begin{aligned} {<_2}^{-1} \circ <_1 (1) &= {<_2}^{-1}(a_1) = 1; \\ {<_2}^{-1} \circ <_1 (2) &= {<_2}^{-1}(a_2) = 3; \\ {<_2}^{-1} \circ <_1 (3) &= {<_2}^{-1}(a_3) = 2. \end{aligned}$$

By Definition 3.40, the Knuth automorphism of $(\mathcal{A}, <_1, <_2)$ is $\sigma := \begin{pmatrix} 1 & 2 & 3 \\ 1 & 3 & 2 \end{pmatrix}$.

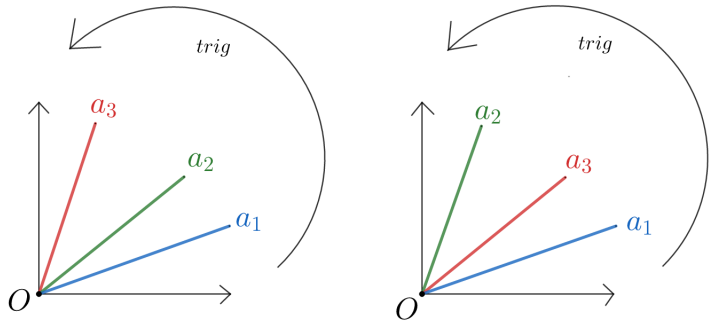

Figure 3.21: The set $\mathcal{A} := \{a_1, a_2, a_3\}$ with two total order relations.

3.2.7 Appendix 3: Second criterion for a strict local minimum at the origin

In this subsection we present another criterion for a polynomial function $f : \mathbb{R}^2 \to \mathbb{R}$ to have a strict local minimum at the origin. This criterion is independent of the Newton polygon criterion presented in Subsection 3.1.1. Its main advantage is that it may be applied to functions of the form:

$$f(x, y) := x^{2k} + \int_{a_{i_0}(x)}^{y} \prod_{i=1}^{m+1} (t - a_i(x)) \mathrm{d}t$$

for $k \in \mathbb{N}$, $k \geq 1$, while the Newton polygon criterion was studied above only for the case $k = 1$.

Lemma 3.42. *Let $f \in \mathbb{R}[x, y]$ such that $f(0, y)$ has a strict local minimum at the origin. Assume that its polar curve $\Gamma(f, x)$ is real, reduced, with an odd number of branches, which are all smooth and transversal to the y-axis. Assume moreover that the positive contact tree of $\Gamma(f, x)$ is binary. Then there exists a neighbourhood of the origin in $\mathbb{R}^2$ of the form $\mathrm{I} \times \mathrm{J}$, where I and J are compact*

intervals, and a branch C of $\Gamma(f,x)$ such that for all $x_0 \in \mathrm{I}$, the restrictions of f to the segments $\{x_0\} \times \mathrm{J}$ achieve their absolute minimum only at $(\{x_0\} \times \mathrm{J}) \cap C$.

As a consequence of the previous lemma, whose proof is left to the reader, we get the following criterion for a strict local minimum:

Proposition 3.43. *Assume the same hypotheses as in Lemma 3.42. Assume moreover that the restriction of f to C is positive in a pointed neighbourhood of O on C. Then f has a strict local minimum at O.*

As a direct consequence of the previous Proposition 3.43, of Theorem 3.33 and Theorem 1.149, we get the following Theorem 3.44 which generalises Theorem 3.34.

Theorem 3.44. *Let σ be a separable $(m+1)$-snake, where $m \in \mathbb{N}^*$ is even. Choose $(m+1)$ pairwise distinct polynomials $a_i(x) \in \mathbb{R}[x]$, $i \in \{1,\dots,m+1\}$, vanishing at 0, whose positive contact tree is one of the binary decomposition trees of σ. Let $i_0 \in \{1,\dots,m+1\}$ be the unique index such that the primitives of $y \mapsto \prod_{i=1}^{m+1}(y - a_i(x))$ achieve their absolute minimum at $a_{i_0}(x)$, for x varying in a neighbourhood of 0. Then for any $k \in \mathbb{N}^*$, the polynomial $f \in \mathbb{R}[x,y]$ defined by*

$$f(x,y) := x^{2k} + \int_{a_{i_0}(x)}^{y} \prod_{i=1}^{m+1} (t - a_i(x))\mathrm{d}t$$

has a strict local minimum at $(0,0)$ and its right asymptotic snake is the given snake σ.

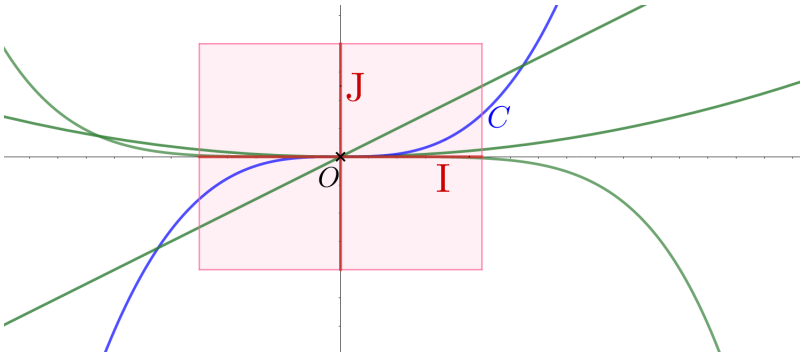

Figure 3.22: Second criterion for a strict local minimum at the origin.

Proof. It is enough to combine Proposition 3.43, Theorem 3.33 and Theorem 1.149. We leave the details of the proof to the reader. □

Chapter 4

Realising pairs of separable negative-positive Poincaré-Reeb trees

Contents

It is important to bear in mind that all along this chapter we will only work with end-rooted **complete binary** plane trees. In addition, note that we will consider sometimes different embeddings of the same plane tree, namely vertical and horizontal, depending on the context.

4.1 The flipped tree of a contact tree

The following Definition 4.1 and Definition 4.2 are inspired by [Ghy17, page 28]. By convention, in this section we shall represent the contact trees vertically, with the root on top.

Definition 4.1. Let us consider an end-rooted complete binary plane tree $\mathcal{T}$ such that each of its internal vertices is decorated with an even or an odd label. Let v be an internal vertex of $\mathcal{T}$ and let us denote by A the subtree (see Definition 1.46) rooted at the left child of v and by B the subtree rooted at the right child of v. The operation of **elementary flip** at the vertex v is defined as follows (see Figure 4.1) and concerns only the two subtrees of the vertex v:

(a) if v is decorated with an odd label, then after the flip, the subtrees A and B of v are interchanged.

(b) if v is decorated with an even label, then there is no change.

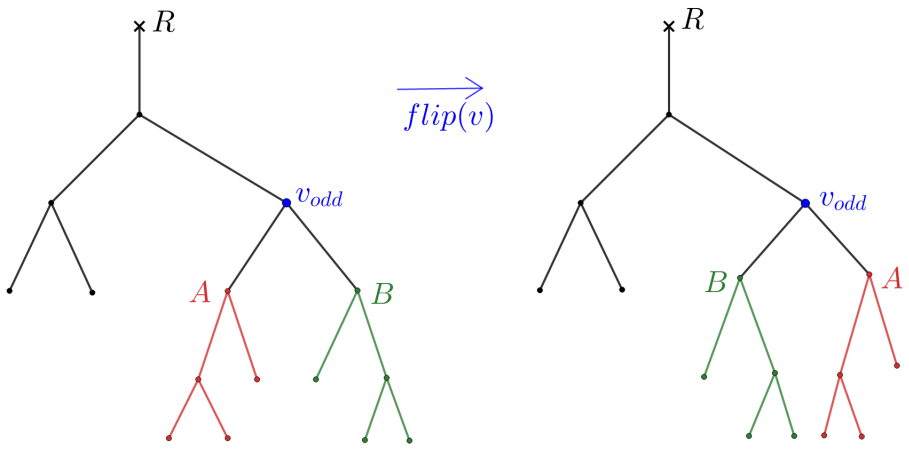

Figure 4.1: An elementary flip at a vertex decorated with an odd label.

Definition 4.2. Let us consider an end-rooted complete binary plane tree $\mathcal{T}$ such that each of its internal vertices is decorated by either an odd or an even parity. Let us apply an elementary flip at each of these internal vertices. The new tree obtained in this way, denoted by $\mathrm{flip}(\mathcal{T})$, is called **the flipped tree** of $\mathcal{T}$.

Remark 4.3. The order in which we apply the elementary flips does not matter, since an elementary flip only interchanges the left subtree of a vertex with the right subtree, without affecting the structure of the tree in any other way (neither above the vertex, nor inside the subtrees interchanged). In addition, the flipped tree of an end-rooted complete binary plane tree is also an end-rooted complete binary plane tree.

Example 4.4. In Figure 4.2, given the tree on the left side of the picture, we construct the flipped tree by applying elementary flips to each internal vertex of the given tree. Here the decoration of each vertex is the parity of the exponent of its associated monomial.

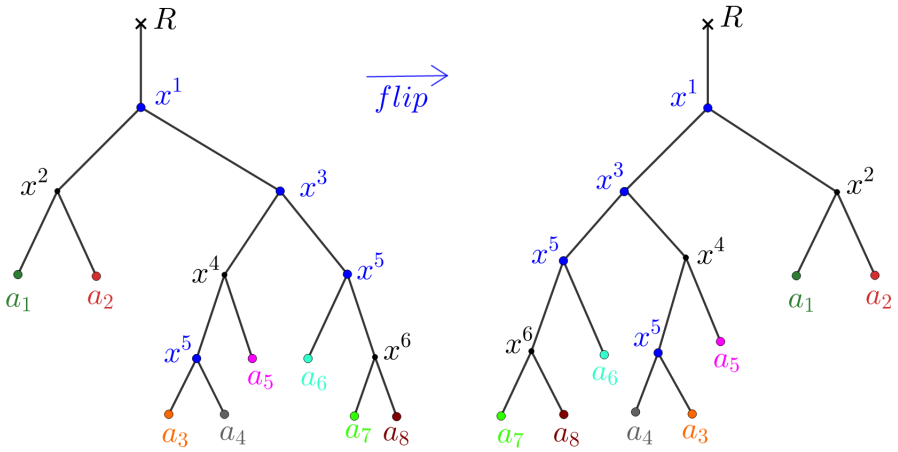

Figure 4.2: The flipped tree of a given tree.

Remark 4.5. In [Ghy17, Theorem, page 31], Ghys gave a characterisation of the pairs formed by a tree and its flipped tree. He proved that there exist impossible configurations of flipped trees. Note that Ghys also considered non binary trees.

Definition 4.6. Given an end-rooted complete binary plane tree $\mathcal{T}$, whose vertices are not decorated with parities, we denote by $\mathrm{Flip}(\mathcal{T})$ the set of all the possible flipped trees that one can obtain from $\mathcal{T}$ by decorating its internal vertices with odd and even parities. Let us call this set **the flipped forest of** $\mathcal{T}$.

Remark 4.7. The terminology of *forest* is inspired from [Knu05, p. 309] and it is a general accepted terminology of graph theory.

Remark 4.8. Note that $\mathcal{T} \in \mathrm{Flip}(\mathcal{T})$: we obtain $\mathcal{T}$ when we decorate all the internal vertices with an even parity.

4.2 The flopped trees of a binary separating tree

In Chapter 1, we gave Definition 1.126 of the direct sum and the skew sum of two permutations. Recall that both operations are associative.

Given a separable permutation σ, let us consider its maximal decomposition up to associativity (for the proof, see Lemma 4.13). Let us suppose that we can apply the associativity inside this decomposition. This allows us to define the following operation on a binary separating tree of a separable permutation (see Definition 1.133):

Definition 4.9. If two vertices of a binary separating tree $\mathcal{T}$ are adjacent and are decorated with the same sign in the decomposition of the separable permutation, then one can replace them by a different pair of vertices using the so-called *tree rotation operation* (see [STT88]) in a binary tree: contract an internal edge to a point (thus two vertices become a vertex with three children), and expand this point in the other side, as shown in Figure 4.3. We say then that we apply an **elementary flop** to the given tree $\mathcal{T}$.

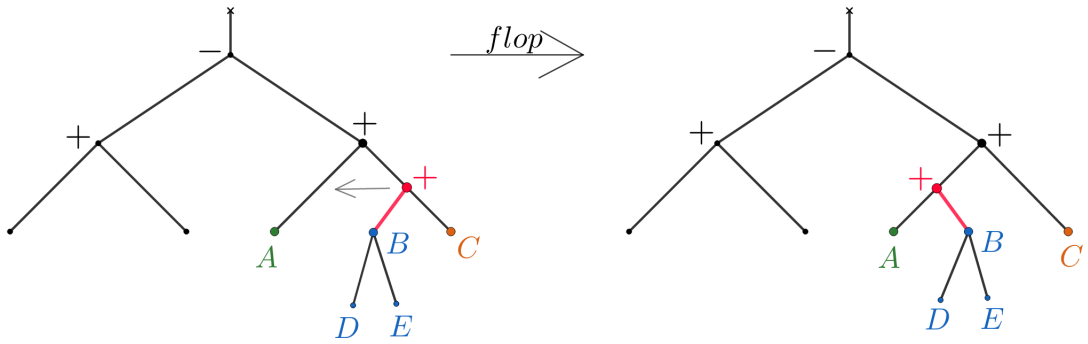

Figure 4.3: An elementary flop.

Definition 4.10. Two end-rooted complete binary plane trees, say t_1 and t_2, are called **flop equivalent** if one can obtain t_2 by applying a finite sequence of elementary flops to t_1.

Remark 4.11. A binary separating tree $\mathcal{T}$ can have several flop equivalent trees. Let us denote by $\mathrm{Flop}(\mathcal{T})$ the equivalence class of $\mathcal{T}$ with respect to the flop relation.

Definition 4.12. [AHP15, page 3] A permutation is called $\oplus$**-decomposable** (respectively $\ominus$**-decomposable**) if it can be written as a sum (respectively skew sum) of two permutations. We call it $\oplus$**-indecomposable** (respectively $\ominus$**-indecomposable**) otherwise.

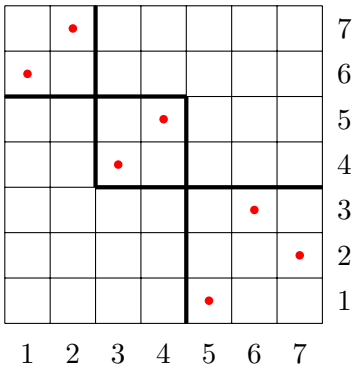

Figure 4.4: A separable permutation $\sigma := \left(\begin{smallmatrix} 1 & 2 & 3 & 4 & 5 & 6 & 7 \\ 6 & 7 & 4 & 5 & 1 & 3 & 2 \end{smallmatrix}\right)$.

As in Subsection 1.8.1, we shall represent separable permutations σ as matrices or blocks decorated with dots corresponding to the pairs $(i, \sigma(i))$, as inspired from [Kit11, page 4] (see Figure 4.4).

Lemma 4.13. *Let us consider a separable permutation $\sigma : \{1, 2, \ldots, n\} \to \{1, 2, \ldots, n\}$, $n \in \mathbb{N}$, $n \geq 2$. Then it has a unique decomposition (see Definition 1.129) up to the associativity of the $\oplus$ and of the $\ominus$ operations.*

Example 4.14. Let $\sigma := \begin{pmatrix} 1 & 2 & 3 & 4 & 5 & 6 & 7 \\ 6 & 7 & 4 & 5 & 1 & 3 & 2 \end{pmatrix}$ be the separable permutation from Example 1.135 (see Figure 4.4).

Then up to associativity, the unique decomposition of σ is

$$\sigma = \Big(\boxdot \oplus \boxdot \Big) \ominus \Big(\boxdot \oplus \boxdot \Big) \ominus \Big(\boxdot \oplus (\boxdot \ominus \boxdot) \Big).$$

However, σ has two binary decompositions, namely

$$\sigma = \Big((\boxdot \oplus \boxdot) \ominus (\boxdot \oplus \boxdot) \Big) \ominus \Big(\boxdot \oplus (\boxdot \ominus \boxdot) \Big)$$

and

$$\sigma = \Big(\boxdot \oplus \boxdot \Big) \ominus \Big((\boxdot \oplus \boxdot) \ominus \big(\boxdot \oplus (\boxdot \ominus \boxdot) \big) \Big),$$

which by Proposition 1.141 are in a bijective correspondence with the two binary separating trees of σ (see Figure 4.5). In other words, by Definition 4.9, one tree is obtained from the other one by applying an elementary flop.

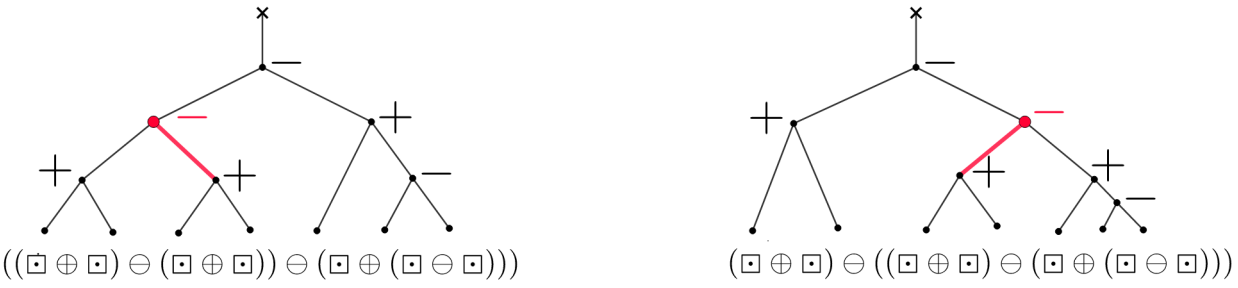

Figure 4.5: Two binary separating trees of the same permutation σ, which are obtained by applying a flop.

We present now the proof of Lemma 4.13.

Proof. Let us suppose without loss of generality that there exist $k, l \in \mathbb{N}^*$ such that

$$\sigma = A_1 \oplus A_2 \oplus \cdots \oplus A_k = B_1 \odot B_2 \odot \cdots \odot B_l,$$

where $\odot$ is either $\oplus$ or $\ominus$, A_i is $\oplus$-indecomposable, for $i = 1, \ldots, k$ and B_j is $\odot$-indecomposable, for $j = 1, \ldots, l$.

We shall prove that $\odot = \oplus$, $k = l$ and $A_i = B_i$, for $i = 1, \ldots, k$.

• First step: let us prove that σ cannot be both $\oplus$-decomposable and $\ominus$-decomposable, namely we show that

$$\odot = \oplus.$$

From the first decomposition of σ, we have $\sigma = A_1 \oplus A_2 \oplus \cdots \oplus A_k$, thus $\sigma(1) < \sigma(n)$. If $\odot = \ominus$, then $\sigma(1) > \sigma(n)$, thus we obtain a contradiction.

• Second step, we prove that $\#A_1 = \#B_1$. Denote by $k_1 := \#A_1$.

-First case: $k_1 \geq 2$. Since A_1 is $\ominus$-decomposable, because it is not $\oplus$-decomposable, we obtain $\sigma(1) > \sigma(k_1)$. Let us suppose that $\#B_1 < k_1$. Then $\sigma(k_1)$ must belong to the block B_2. Since between B_1 and B_2 there is $\oplus$ sign we obtain $\sigma(1) < \sigma(k_1)$. Contradiction. Analogously we prove that we cannot have $\#B_1 > k_1$.

-Second case: $k_1 = 1$, namely it is reduced to one element: $A_1 = \boxdot$. Since $\sigma = A_1 \oplus A_2 \oplus \cdots \oplus A_k$, for any $j \in \{2, \ldots, n\}$ we have $\sigma(j) > \sigma(1)$. Let us suppose that $\#B_1 > 1$. Since B_1 is a $\ominus$-decomposable block, there exists $j \in \{2, \ldots, \#B_1\}$ such that $\sigma(j) < \sigma(1)$. Contradiction.

In conclusion, $\#A_1 = \#B_1$.

• By taking the restriction of σ to the indices $k_1 + 1, \ldots, n$ we can prove as before that $\#A_2 = \#B_2$. Recursively, we obtain

$$\#A_i = \#B_i,$$

for $i = 1, \ldots, n$. As a consequence, we have

$$k = l.$$

• Recursively we apply the steps above to prove that the decomposition of A_i is the same as the decomposition of B_i, for $i = 1, \ldots, n$. □

Remark 4.15. See more about counting trees, decompositions and separable permutations in [Ghy17, page 35], [Sta97], [Sta15], [Wes95, Theorem 4.3], [SS00].

Proposition 4.16. *There is a bijection between the set of the separable generic rooted transversal trees and the quotient space of binary separating trees with respect to the flop equivalence.*

Proof. • Given any two binary separating trees that are flop-equivalent, by Definition 4.9 and Lemma 4.13, they provide a unique decomposition (up to associativity) which corresponds to a unique separable snake. By Proposition 1.69, this separable snake corresponds to a unique separable Poincaré-Reeb tree.

• Given a separable Poincaré-Reeb tree, by Proposition 1.69, it corresponds to a unique separable snake, say σ. By Lemma 4.13, the decomposition of σ is unique up to associativity of the $\oplus$ and of the $\ominus$ operations. If there are several binary decompositions possible, thanks to the associativity, then by Definition 4.9, they all give flop equivalent binary separating trees of σ. □

Remark 4.17. One of our main problems is to realise pairs (negative-positive) of (separable) Poincaré-Reeb trees in two variables by a strict local minimum of a polynomial function at the origin. In Chapter 1 the binary separating trees were used as contact trees in our construction of Poincaré-Reeb trees for one variable polynomials. Proposition 4.16 enables us to express our result in terms of pairs of negative-positive contact trees.

4.3 The negative contact tree of a set of polynomial functions in one real variable

Given a set of real univariate polynomials, we want to define its negative contact tree and then describe this tree, in terms of the flipped tree of its (positive) contact tree (see Definition 1.92).

Notation 4.18. *Let us consider $m \in \mathbb{N}$ and the polynomials $a_i(x) \in \mathbb{R}[x]$ for any $i = 1, \dots, m+1$ such that*

$$a_1(x) \prec_+ a_2(x) \prec_+ \dots \prec_+ a_{m+1}(x).$$

Denote by $\mathcal{A}_+ := \{a_1(x), \dots, a_{m+1}(x)\}$ and by $\mathcal{A}_- := \{a_1(-x), \dots, a_{m+1}(-x)\}$, where $x > 0$ is sufficiently small.

Definition 4.19.
• We define $\mathcal{CT}(\mathcal{A}_-)$ as the contact tree of the set of polynomials $\mathcal{A}_-$, as in Definition 1.92.
• The **negative contact tree** of the set of the given polynomials $\mathcal{A}_+$ is the symmetric of $\mathcal{CT}(\mathcal{A}_-)$ with respect to the Oy axis. We denote it by $\mathcal{CT}_-(\mathcal{A}_+)$.

Example 4.20. The contact tree (to the right of the origin) and the negative contact tree (to the left of the origin) of the following set of three real univariate polynomials $\mathcal{A}_+ := \{0, x^2, x^2 + x^3\}$ are shown in Figure 4.6. Note that here $\mathcal{A}_- := \{0, x^2, x^2 - x^3\}$

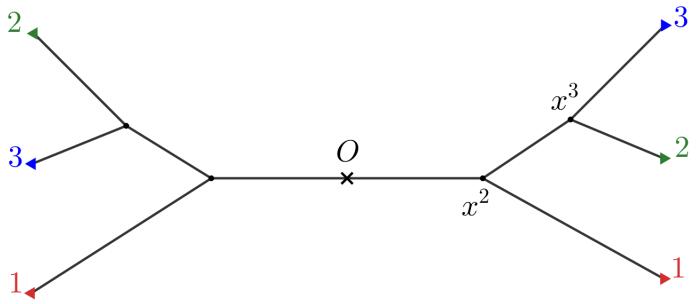

Figure 4.6: The (positive) contact tree (to the right of the origin) and the negative contact tree (to the left of the origin) of $\mathcal{A}_+ := \{0, x^2, x^2 + x^3\}$.

Proposition 4.21. *[Ghy13, page 237] The negative contact tree of $\mathcal{A}_+$ is the symmetric of the flip of the contact tree of $\mathcal{A}_+$ with respect to the Oy axis. Namely*

$$\mathcal{CT}_-(\mathcal{A}_+) = \mathrm{sym}_{Oy}\big(\mathrm{flip}(\mathcal{CT}(\mathcal{A}_+))\big).$$

Proof. All we need to show is that when we flip $\mathcal{CT}(\mathcal{A}_+)$ we obtain $\mathcal{CT}(\mathcal{A}_-)$. For each vertex labelled with an odd parity, a nontrivial elementary flip consists in interchanging the two subtrees of that vertex. By the construction of the contact tree (see Definition 1.92), this is equivalent to considering $-x$ instead of x, since this changes the order of the coefficients of the corresponding monomials, thus forcing an interchanged vertical order in the cartesian plane (see Figure 1.25). □

Example 4.22. Let us consider the following polynomials: $a_1(x) = 0$, $a_2(x) = x^3$, $a_3(x) = x^3 + x^4$, $a_4(x) = x^2$, $a_5(x) = x^2 + x^4$, $a_6(x) = x^1$, $a_7(x) = x^1 + x^3$, $a_8(x) = x^1 + x^3 + x^4$, $a_9(x) = x^1 + x^3 + x^4 + x^5$. For $x > 0$, let us denote by $\mathcal{A}_+ := \{a_1(x), a_2(x), \dots, a_9(x)\}$ and by $\mathcal{A}_- := \{a_1(-x), a_2(-x), \dots, a_9(-x)\}$.

See Figure 4.7 below. We have labelled the leaves of the trees in order to see better the corresponding position of the graphs of the polynomials $y = a_i(x)$, which change position for $x < 0$. To understand better why we sometime choose the horizontal embedding of the positive and negative contact tree of a set of polynomials; see Figure 4.8, where the graphs of the polynomials $y = a_i(x)$ are shown for $i = 1, \ldots, 9$.

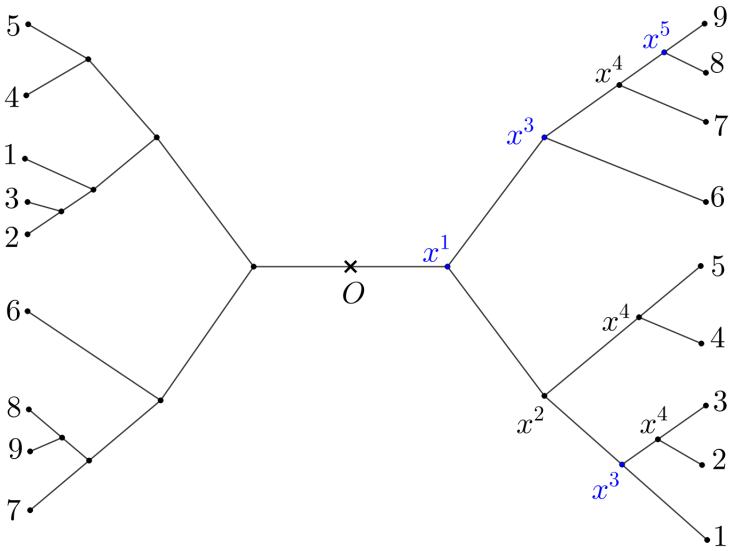

Figure 4.7: The positive contact tree of $\mathcal{A}_+$ is situated to the right of the root O, while the negative contact tree of $\mathcal{A}_+$ is situated to the left of the root O.

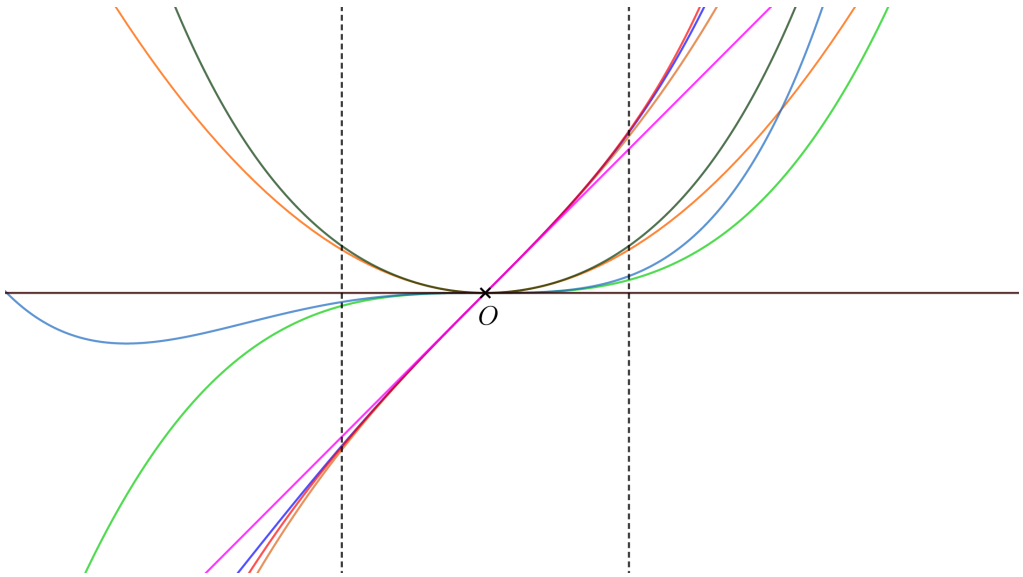

Figure 4.8: The graphs of $y = a_i(x)$ in a small enough neighbourhood of the origin. The position of the graphs corresponds to the labelling of the leaves in the negative, respectively the positive contact tree. Note that in order to get a good visual representation corresponding with the contact trees, one has to choose a sufficiently small neighbourhood of O.

4.4 Realising pairs of separable negative-positive Poincaré-Reeb trees

In what follows, by convention we draw the contact trees with the root on top. We will draw their flipped trees in the same manner, but we shall keep in mind that the negative contact tree is the symmetric of the flipped tree, as stated in Proposition 4.21. This convention allows us to have a total order relation of the given polynomials, which are ordered increasingly from left to right, namely the smallest polynomial corresponds to the leaf situated to the left.

EXAMPLE 4.23. Let us consider the three polynomials given in Example 4.20 in Figure 4.9.

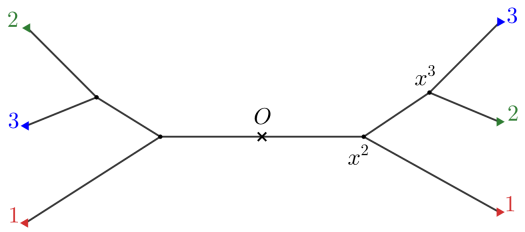

Figure 4.9: The contact tree (to the right of the origin) and the negative contact tree (to the left of the origin) of $\mathcal{A}_+ := \{0, x^2, x^2 + x^3\}$.

We shall draw the (positive) contact tree and the negative contact tree as shown in Figure 4.10 below.

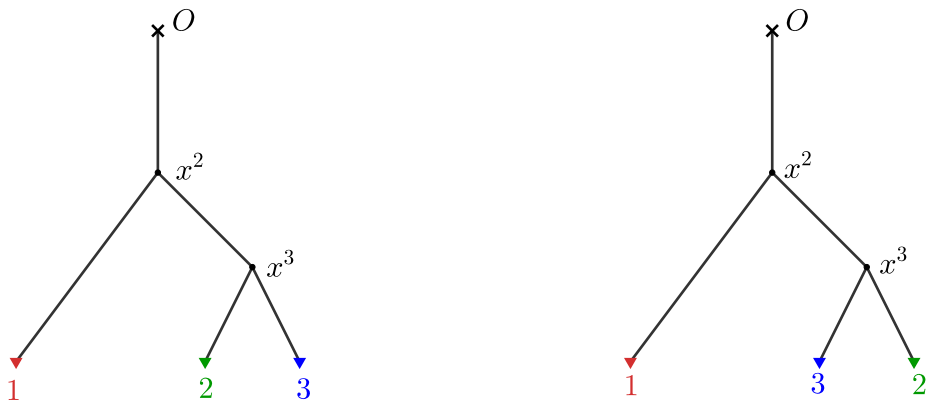

Figure 4.10: Convention for drawing vertically the positive contact tree (left side of the picture) and its flip (right side of the picture). This allows us to reconstruct Figure 4.6.

4.4.1 The algorithm

REMARK 4.24. By Lemma 1.153, for each chosen decoration there exist polynomials such that the decorated tree represents their contact tree.

Let us now present the algorithm that provides all the negative Poincaré-Reeb trees which form pairs with a given separable positive Poincaré-Reeb tree.

Algorithm 4.25.
INPUT: a separable positive Poincaré-Reeb tree.
OUTPUT: a set of negative Poincaré-Reeb trees, which will form pairs with the given separable positive Poincaré-Reeb tree; the pairs formed in this way are realisable as a union-tree, by a strict local minimum of a polynomial function of two real variables in a small enough neighbourhood of the origin.

• *Given a separable positive Poincaré-Reeb tree, let us first obtain its unique separable snake, denoted by σ. Let us consider all the binary separating trees of σ. They form a set of flop equivalent trees, denoted by* $\mathrm{Flop}(\sigma)$.

• *For each tree s in* $\mathrm{Flop}(\sigma)$*, let us decorate its internal vertices with either odd or even labels in all the possible ways in order to obtain the set* $\mathrm{Flip}(s)$*;*

- For each flipped tree $t \in \mathrm{Flip}(s)$, let us construct the separable snake, denoted by τ, that has t as a binary separating tree; we do this by decorating the internal vertices of t, from right to left (considering the natural order, see Definition 1.161) with $\ominus$ and $\oplus$ alternatively, starting with $\ominus$ to the right;

- For each separable snake τ obtained at the previous step, we construct its Poincaré-Reeb tree.

See Figure 4.11 below and Example 4.29.

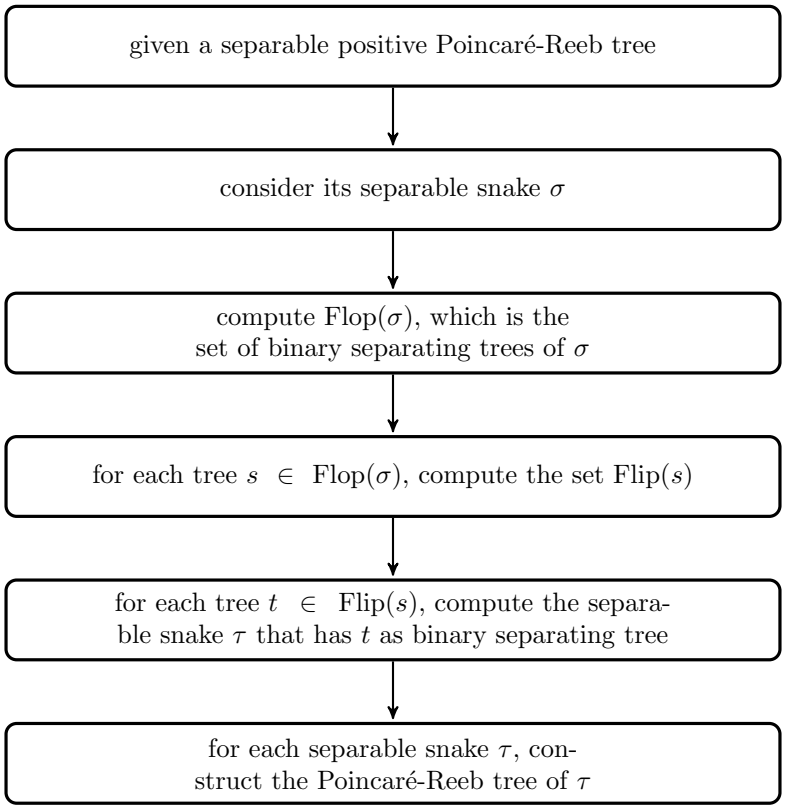

Figure 4.11: The algorithm for obtaining the set of negative Poincaré-Reeb trees, which form pairs with a given separable positive Poincaré-Reeb tree; the pairs are realisable by a strict local minimum of a polynomial function of two real variables in a small enough neighbourhood of the origin, by our family of polynomials.

To understand better the algorithm, see also Figure 4.12 below.

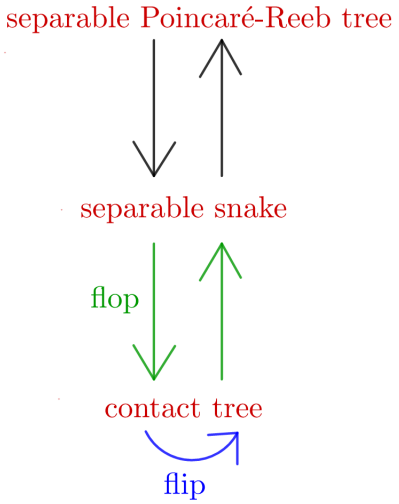

Figure 4.12: The combinatorial objects appearing in Algorithm 4.25.

4.4.2 The effective realisation of the pairs provided by the algorithm

Theorem 4.26. *Given a positive separable Poincaré-Reeb tree, the trees obtained by applying Algorithm 4.25 have the following properties:*

- *they are end-rooted complete binary plane trees;*
- *they are separable;*
- *they form pairs with the given separable positive Poincaré-Reeb tree such that each couple negative-positive is realisable as a union-tree, by a strict local minimum of a polynomial function of two real variables in a small enough neighbourhood of the origin.*

Proof.
• Since they are Poincaré-Reeb trees of snakes, they are end-rooted complete binary plane trees, by construction (see Definition 1.63).
• The permutations τ in the algorithm are by construction snakes because the signs $\oplus$ and $\ominus$ alternate in the decoration. In addition, τ is separable, since it is the sum and skew sum of $\boxdot$. Hence by Lemma 1.168, the Poincaré-Reeb tree of τ is also separable, because it is the snake-tree of a separable permutation.
• For each tree $s \in \mathrm{Flop}(\sigma)$, for any decoration of even/odd chosen, we can construct a set of polynomials $\mathcal{A}_+ := \{a_1(x), \dots, a_{m+1}(x)\}$, where $m+1$ is the number of leaves of s, such that the contact tree of $\mathcal{A}_+$ is s. By Theorem 3.34 the main idea is that following the steps from Section 1.8, we construct the polynomials $a_i(x)$, $i = 1, \dots, m+1$ such that the snake associated to the polynomial

$$Q_x(y) := \int_0^y \prod_{i=1}^{m+1} (y - a_i(x))$$

is σ. We denote now the two variable polynomial $Q(x, y) := Q_x(y)$ and we take

$$f(x, y) := x^2 + Q(x, y)$$

The right asymptotic snake of f (see Definition 2.114) of f (namely the one given by the alternating right crests and right valleys of $(f(x, y) = \varepsilon)$) will be exactly σ, by Theorem 3.33. For the negative contact tree, consider $x > 0$ sufficiently small, hence we have $f(-x, y) := x^2 + Q(-x, y)$.

By Proposition 4.21, the negative contact tree of $\mathcal{A}_+$ is obtained by taking the symmetric of the flip of the positive contact tree.

□

REMARK 4.27. In the sequel, by convention, we shall draw the positive and the negative Poincaré-Reeb trees for two-variable polynomials with the root on top and vertically. This makes it easier to apply the results from Chapter 1. However, the reader has to be aware of the fact that the embedding of the positive Poincaré-Reeb tree in the neighbourhood of the origin is obtained by applying a rotation of $\frac{\pi}{2}$ to the vertical embedding we use when we draw the tree vertically. The embedding of the negative Poincaré-Reeb tree is obtained after a rotation of $-\frac{\pi}{2}$ and a symmetry with respect to the Ox axis applied to the vertical embedding we use when we draw the tree vertically. This is due to Chapter 3, namely Theorem 3.33 (see Figure 3.16). Hence in the end, in the horizontal embedding, the positive Poincaré-Reeb tree is situated on the right of the origin, while the negative Poincaré-Reeb tree is situated on the left of the origin. The origin is their common root.

REMARK 4.28. We have to take into account all the flops of the binary separating tree of the given separable snake, as the following Example 4.29 shows.

EXAMPLE 4.29.

• Let us consider the separable snake $\sigma := \begin{pmatrix} 1 & 2 & 3 & 4 & 5 \\ 1 & 3 & 2 & 5 & 4 \end{pmatrix}$ and its corresponding (positive) Poincaré-Reeb tree (see Figure 4.13).

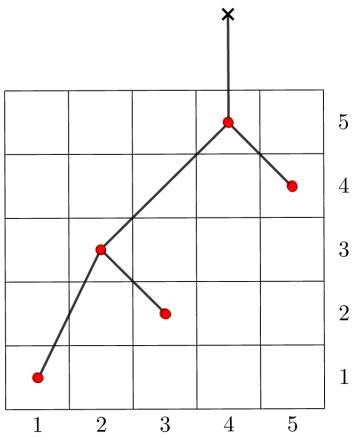

Figure 4.13: A given separable snake $\sigma := \left(\begin{smallmatrix} 1 & 2 & 3 & 4 & 5 \\ 1 & 3 & 2 & 5 & 4 \end{smallmatrix}\right)$ and its corresponding Poincare-Reeb tree.

The maximal decomposition of σ, up to associativity, is $\sigma = \boxdot \oplus (\boxdot \ominus \boxdot) \oplus (\boxdot \ominus \boxdot)$.

• Let us choose one of the binary decompositions of σ, say $\sigma = \Big(\boxdot \oplus (\boxdot \ominus \boxdot) \Big) \oplus (\boxdot \ominus \boxdot)$, which corresponds to the binary separating tree from Figure 4.14, called s_1.

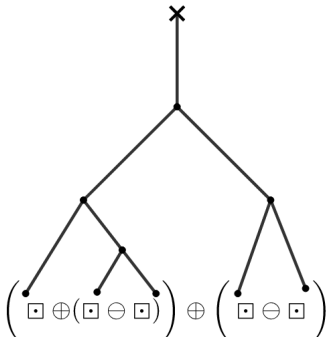

Figure 4.14: A binary separating tree s_1 of σ.

Consider all the possible combinations of odd/even labels for the internal vertices of s_1. Then let us construct the flipped tree for each possible labelling. Note that in this example we shall not label the internal vertices if they have the left subtree the same as the right subtree, since the flip would make no change for symmetry reasons. We obtain therefore the set of possible negative contact trees shown in Figure 4.15 (the trees on the middle column).

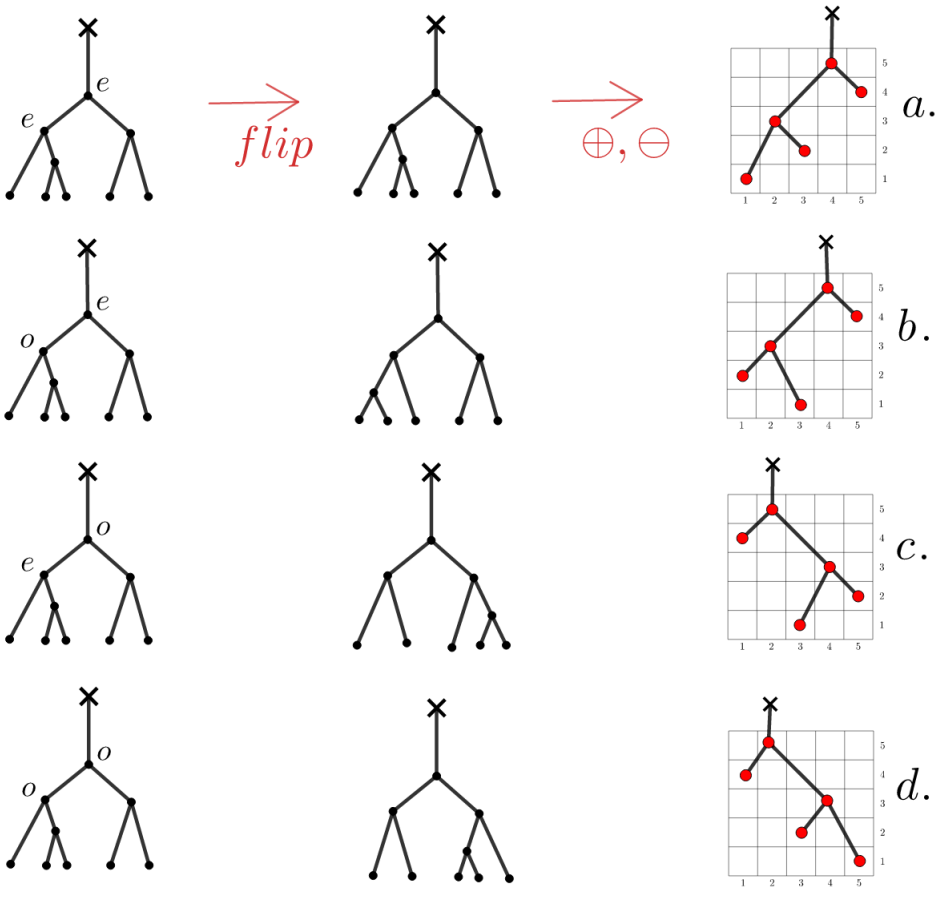

Figure 4.15: The decoration e means an even label, while o comes from odd. The negative contact trees after the possible flips of s_1 are the trees on the middle column. Then constructing the corresponding negative Poincaré-Reeb trees: the trees in the right column.

As one can see in Figure 4.15, each of the negative contact trees gives a negative Poincaré-Reeb tree (the trees obtained in the right column): these are the negative Poincaré-Reeb trees

associated to the given positive Poincaré-Reeb tree, when we consider s_1 the binary separating tree of σ.

In each of the four situations, let us construct a set $\mathcal{A}_+$ such that the corresponding tree in the left column in Figure 4.15 is the positive contact tree of $\mathcal{A}_+$. Once the polynomials a_i chosen, each case is realised by

$$f(x,y) := x^2 + \int_0^y \prod_{i=1}^{m+1} (t - a_i(x))\mathrm{d}t,$$

see Theorem 3.34.

- In the case **a.**, we can choose $a_1(x) := 0$, $a_2(x) := x^4$, $a_3(x) := x^4 + x^5$, $a_4(x) := x^2$, $a_5(x) := x^2 + x^3$.
- In the case **b.**, we can choose $a_1(x) := 0$, $a_2(x) := x^3$, $a_3(x) := x^3 + x^4$, $a_4(x) := x^2$, $a_5(x) := x^2 + x^4$.
- In the case **c.**, we can choose $a_1(x) := 0$, $a_2(x) := x^2$, $a_3(x) := x^2 + x^3$, $a_4(x) := x^1$, $a_5(x) := x^1 + x^2$.
- In the case **d.**, we can choose $a_1(x) := 0$, $a_2(x) := x^3$, $a_3(x) := x^3 + x^4$, $a_4(x) := x^1$, $a_5(x) := x^1 + x^2$.

Let us present in Figure 4.16 the pairs of negative-positive Poincaré-Reeb trees realised with our construction by a strict local minimum at the origin of a polynomial function in two real variables, given the positive Poincaré-Reeb tree.

Be aware that by convention, we drew the positive and the negative Poincaré-Reeb trees for two-variable polynomials with the root on top and vertically. This made it easier to apply the results from Chapter 1. However, the embedding of the positive Poincaré-Reeb tree that we constructed in the neighbourhood of the origin (see Remark 4.27) is shown in Figure 4.16.

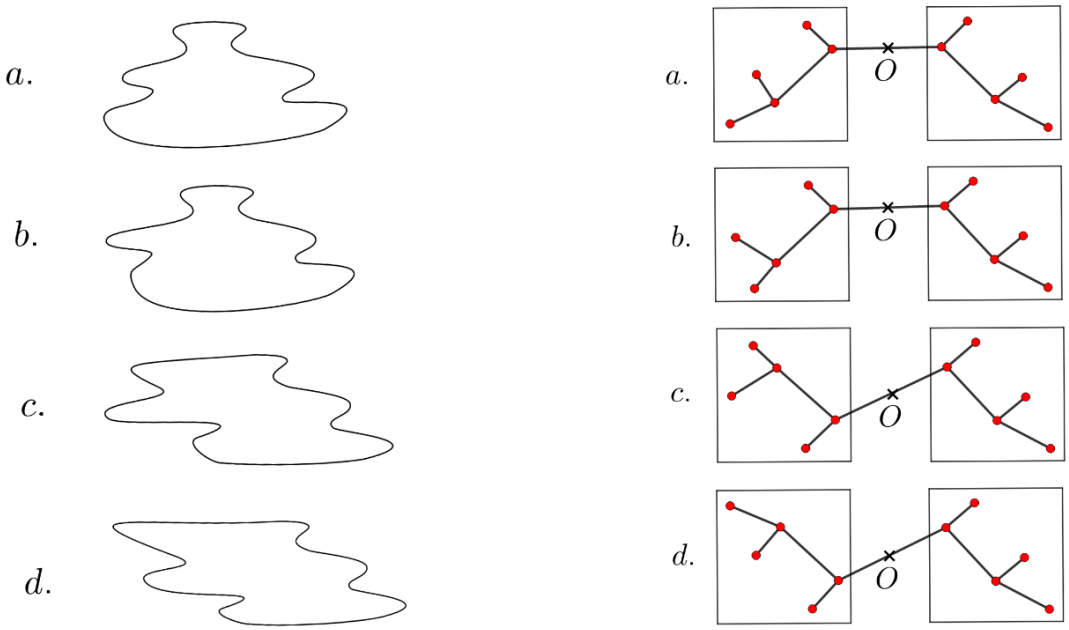

Figure 4.16: Non-convex level curves and their corresponding pairs of negative-positive Poincaré-Reeb trees realised with our construction by a strict local minimum at the origin of a polynomial function in two real variables, given the positive Poincaré-Reeb tree (the tree on the right side of the origin).

• Let us now choose another binary decomposition of σ, say $\sigma = \boxdot \oplus \Big((\boxdot \ominus \boxdot) \oplus (\boxdot \ominus \boxdot) \Big)$, which corresponds to the binary separating tree from Figure 4.17, called s_2.

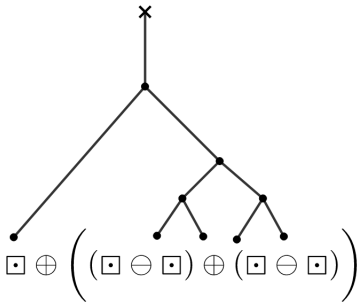

Figure 4.17: Another binary separating tree of σ, called s_2.

The possible flipped trees of s_2 (after the possible choices of parity labels) are the ones shown in Figure 4.18 (the trees in the middle column). The corresponding negative Poincaré-Reeb trees obtained using the binary separating tree s_2 are in the right column. Note that again we do not label the internal vertices of s_2 if their left subtree is the same as their right subtree, for symmetry reasons.

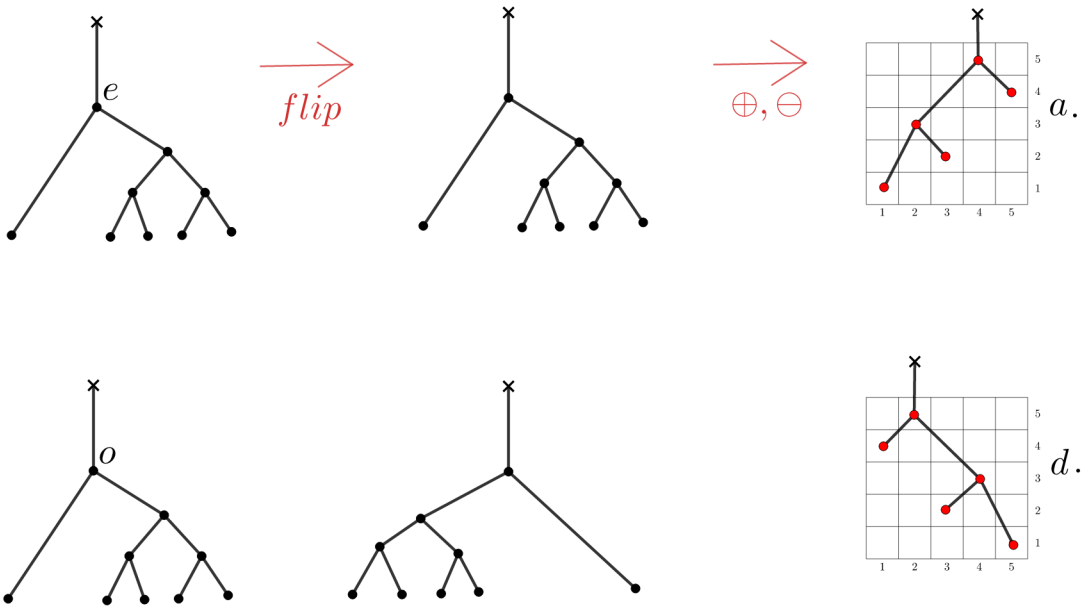

Figure 4.18: The negative contact trees after the possible flips of s_2 are the trees on the middle column. The corresponding negative Poincaré-Reeb trees: the trees in the right column.

• In our example we obtain less negative Poincaré-Reeb trees if we use the binary separating tree s_2 than if we use the flop of s_2, namely s_1. Therefore we always have to take into account all the set $\mathrm{Flop}(\sigma)$.

REMARK 4.30. There exist more complicated examples, where using a single decomposition is not enough. Namely, each tree $s \in \mathrm{Flop}(\sigma)$ may provide new negative Poincaré-Reeb trees.

[This page intentionally left blank]

Bibliography

[AB06] Charalambos Dionisios Aliprantis and Kim Christian Border. *Infinite dimensional analysis*. Third. A hitchhiker's guide. Springer, Berlin, 2006, pp. xxii+703 (cit. on pp. 71, 122).

[AF08] Colin Adams and Robert Franzosa. "Introduction to Topology: Pure and Applied, Person Education". In: *Inc, publishing: Prentice Hall* (2008) (cit. on p. 64).

[AGZV12] Vladimir Igorevich Arnold, Sabir Medgidovich Gusein-Zade, and Alexander Nicholaevich Varchenko. *Singularities of differentiable maps. Volume 1*. Modern Birkhäuser Classics. Classification of critical points, caustics and wave fronts, Translated from the Russian by Ian Porteous based on a previous translation by Mark Reynolds, Reprint of the 1985 edition. Birkhäuser/Springer, New York, 2012, pp. xii+382 (cit. on p. 169).

[AHP15] Michael Albert, Cheyne Homberger, and Jay Pantone. "Equipopularity classes in the separable permutations". In: *Electron. J. Combin.* 22.2 (2015), Paper 2.2, 18 (cit. on pp. 97, 99, 187).

[And79] Désiré André. "Développements de sec x et de tang x". In: *CR Acad. Sci. Paris* 88 (1879), pp. 965–967 (cit. on pp. 49, 50).

[And81] Désiré André. "Sur les permutations alternées". In: *Journal de mathématiques pures et appliquées* 7 (1881), pp. 167–184 (cit. on p. 49).

[Arn00] Vladimir Igorevich Arnold. "Nombres d'Euler, de Bernoulli et de Springer pour les groupes de Coxeter et les espaces de morsification : le calcul des serpents". In: *Leçons de mathématiques d'aujourd'hui (Éric Carpentier and Nicolas Nikolski, eds.), Cassini, Paris* (2000), pp. 61–98 (cit. on pp. 50, 51, 54, 55).

[Arn92] Vladimir Igorevich Arnold. "Snake calculus and the combinatorics of the Bernoulli, Euler and Springer numbers of Coxeter groups". In: *Uspekhi Mat. Nauk* 47.1(283) (1992), pp. 3–45, 240. DOI: 10.1070/RM1992v047n01ABEH000861. URL: https://doi.org/10.1070/RM1992v047n01ABEH000861 (cit. on pp. 19, 20, 37, 38, 51, 54, 55).

[Bas+18] Frédérique Bassino et al. "The Brownian limit of separable permutations". In: *Ann. Probab.* 46.4 (2018), pp. 2134–2189. DOI: 10.1214/17-AOP1223. URL: https://doi.org/10.1214/17-AOP1223 (cit. on pp. 13, 31).

[BBL98] Prosenjit Bose, Jonathan Frederick Buss, and Anna Lubiw. "Pattern matching for permutations". In: *Inform. Process. Lett.* 65.5 (1998), pp. 277–283. DOI: 10.1016/S0020-0190(97)00209-3. URL: https://doi.org/10.1016/S0020-0190(97)00209-3 (cit. on pp. 13, 31, 96, 97, 101).

[Ber09] Marcel Berger. *Geometry I*. Universitext. Translated from the 1977 French original by M. Cole and S. Levy, Fourth printing of the 1987 English translation [MR0882541]. Springer-Verlag, Berlin, 2009, pp. xiv+428 (cit. on p. 164).

[BK86] Egbert Brieskorn and Horst Knörrer. *Plane algebraic curves*. Translated from the German by John Stillwell. Birkhäuser Verlag, Basel, 1986, pp. vi+721. DOI: 10.1007/978-3-0348-5097-1. URL: https://doi.org/10.1007/978-3-0348-5097-1 (cit. on pp. 18, 36, 133, 135, 143).

[BM08] John Adrian Bondy and Uppaluri Siva Ramachandra Murty. *Graph theory*. Vol. 244. Graduate Texts in Mathematics. Springer, New York, 2008, pp. xii+651. DOI: 10.1007/978-1-84628-970-5. URL: https://doi.org/10.1007/978-1-84628-970-5 (cit. on p. 61).

[Bol80] Theodore S. Bolis. "Degenerate critical points". In: *Math. Mag.* 53.5 (1980), pp. 294–299. DOI: 10.2307/2689393. URL: https://doi.org/10.2307/2689393 (cit. on p. 119).

[Bol98] Béla Bollobás. *Modern graph theory*. Vol. 184. Graduate Texts in Mathematics. Springer-Verlag, New York, 1998, pp. xiv+394. DOI: 10.1007/978-1-4612-0619-4. URL: https://doi.org/10.1007/978-1-4612-0619-4 (cit. on p. 61).

[BR06] Mathilde Bouvel and Dominique Rossin. "The longest common pattern problem for two permutations". In: *Pure Math. Appl. (PU.M.A.)* 17.1-2 (2006), pp. 55–69 (cit. on p. 99).

[Cas15] Roberto Castellini. "The topology of A'Campo deformations of singularities: an approach through the lotus." PhD thesis. Université de Lille 1, 2015. URL: https://www.theses.fr/2015LIL10062 (cit. on p. 136).

[Coo59] Julian Lowell Coolidge. *A treatise on algebraic plane curves*. Dover Publications, Inc., New York, 1959, pp. xxiv+513 (cit. on p. 165).

[Cos02] Michel Coste. "An introduction to semialgebraic geometry". In: *RAAG network school* 145 (2002), p. 30 (cit. on pp. 128, 145).

[Cos05] Michel Coste. "Real algebraic sets". In: *Notes de cours* (2005) (cit. on pp. 128, 129).

[CP01] Michel Coste and María Jesús de la Puente. "Atypical values at infinity of a polynomial function on the real plane: an erratum, and an algorithmic criterion". In: *J. Pure Appl. Algebra* 162.1 (2001), pp. 23–35. DOI: 10.1016/S0022-4049(00)00111-0. URL: https://doi.org/10.1016/S0022-4049(00)00111-0 (cit. on pp. 21, 39, 136, 150).

[Dav57] Chandler Davis. "Extrema of a polynomial". In: *Amer. Math. Monthly* 64.9 (1957), pp. 679–680 (cit. on pp. 19, 37, 55–57).

[Die10] Reinhard Diestel. *Graph theory*. Fourth. Vol. 173. Graduate Texts in Mathematics. Springer, Heidelberg, 2010, pp. xviii+437. DOI: 10.1007/978-3-642-14279-6. URL: https://doi.org/10.1007/978-3-642-14279-6 (cit. on p. 61).

[Dou97] Adrien Douady. "Géométrie dans les espaces de paramètres". In: *IREM, Cahiers rouges,* 23_2 (1997) (cit. on pp. 19, 37, 61).

[Eis95] David Eisenbud. *Commutative algebra*. Vol. 150. Graduate Texts in Mathematics. With a view toward algebraic geometry. Springer-Verlag, New York, 1995, pp. xvi+785. DOI: 10.1007/978-1-4612-5350-1. URL: https://doi.org/10.1007/978-1-4612-5350-1 (cit. on p. 137).

[FCP96] Juan Ferrera Cuesta and María Jesús de la Puente. "The asymptotic values of a polynomial function on the real plane". In: *J. Pure Appl. Algebra* 106.3 (1996), pp. 263–273. DOI: 10.1016/0022-4049(95)00025-9. URL: https://doi.org/10.1016/0022-4049(95)00025-9 (cit. on p. 136).

[Fis01] Gerd Fischer. *Plane algebraic curves*. Vol. 15. Student Mathematical Library. Translated from the 1994 German original by Leslie Kay. American Mathematical Society, Providence, RI, 2001, pp. xvi+229. DOI: 10.1090/stml/015. URL: https://doi.org/10.1090/stml/015 (cit. on pp. 143, 144, 164–166).

[Fla73] Harley Flanders. "Differentiation under the integral sign". In: *Amer. Math. Monthly* 80 (1973), 615–627; correction, ibid. 81 (1974), 145. DOI: 10.2307/2319163. URL: https://doi.org/10.2307/2319163 (cit. on p. 59).

[Frè13] Pietro Giuseppe Frè. *Gravity, a geometrical course. Volume 1*. Development of the theory and basic physical applications. Springer, Dordrecht, 2013, pp. xviii+336 (cit. on p. 125).

[GB00] Evelia R. García Barroso. "Sur les courbes polaires d'une courbe plane réduite". In: *Proc. London Math. Soc. (3)* 81.1 (2000), pp. 1–28. DOI: 10.1112/S0024611500012430. URL: https://doi.org/10.1112/S0024611500012430 (cit. on pp. 18, 36, 133).

[GB96] Evelia R. García Barroso. "Invariants des singularités de courbes planes et courbure des fibres de Milnor". PhD thesis. Universidad de La Laguna, 1996. URL: http://ergarcia.webs.ull.es/tesis.pdf (cit. on pp. 18, 36, 133).

[GB98] Evelia R. García Barroso. "Un théorème de décomposition pour les polaires génériques d'une courbe plane". In: *C. R. Acad. Sci. Paris Sér. I Math.* 326.1 (1998), pp. 59–62. DOI: 10.1016/S0764-4442(97)82713-9. URL: https://doi.org/10.1016/S0764-4442(97)82713-9 (cit. on pp. 18, 36, 133).

[GBGPPP18] Evelia R. García Barroso, Pedro D González Pérez, and Patrick Popescu-Pampu. "Ultrametric spaces of branches on arborescent singularities". In: *Singularities, algebraic geometry, commutative algebra and related topics.* (2018). Ed. by L. Narvaéz G.-M. Greuel and S. Xambo-Descamps. Festschrift for Antonio Campillo on the occasion of his 65th birthday (cit. on pp. 66, 77).

[Geoa] URL: https://www.altituderando.com/Comment-lire-une-carte-IGN-de-randonnee (cit. on p. 151).

[Geob] URL: http://arwann.com/?page\textunderscoreid=1482 (cit. on p. 151).

[Ghy13] Étienne Ghys. "Intersecting curves (variation on an observation of Maxim Kontsevich)". In: *Amer. Math. Monthly* 120.3 (2013), pp. 232–242. DOI: 10.4169/amer.math.monthly.120.03.232. URL: https://doi.org/10.4169/amer.math.monthly.120.03.232 (cit. on pp. 77, 190).

[Ghy17] Étienne Ghys. *A singular mathematical promenade*. ENS Éditions, Lyon, 2017, pp. viii+302. URL: http://ghys.perso.math.cnrs.fr/bricabrac/promenade.pdf (cit. on pp. 13–15, 22, 31–33, 40, 77, 97, 103, 108–110, 136, 145, 182, 185, 186, 189).

[Gil91] George Thomas Gilbert. "Positive definite matrices and Sylvester's criterion". In: *Amer. Math. Monthly* 98.1 (1991), pp. 44–46. DOI: 10.2307/2324036. URL: https://doi.org/10.2307/2324036 (cit. on p. 118).

[GKZ94] Izrail Moiseevich Gelfand, Mikhail M. Kapranov, and Andrei Vladlenovich Zelevinsky. *Discriminants, resultants, and multidimensional determinants*. Mathematics: Theory & Applications. Birkhäuser Boston, Inc., Boston, MA, 1994, pp. x+523. DOI: 10.1007/978-0-8176-4771-1. URL: https://doi.org/10.1007/978-0-8176-4771-1 (cit. on p. 143).

[GL09] Étienne Ghys and Jos Leys. *Le pli et la fronce - un théorème de Whitney*. 2009. URL: http://images.math.cnrs.fr/Le-pli-et-la-fronce.html (cit. on p. 169).

[Gos09] Eric Gossett. *Discrete mathematics with proof*. John Wiley & Sons, 2009 (cit. on pp. 61–64).

[GP74] Victor Guillemin and Alan Pollack. *Differential topology*. Prentice-Hall, Inc., Englewood Cliffs, N.J., 1974, pp. xvi+222 (cit. on p. 132).

[JK11] Jennifer M. Johnson and János Kollár. "How small can a polynomial be near infinity?" In: *Amer. Math. Monthly* 118.1 (2011), pp. 22–40. DOI: 10.4169/amer.math.monthly.118.01.022. URL: https://doi.org/10.4169/amer.math.monthly.118.01.022 (cit. on p. 119).

[Kap93] Mikhail M. Kapranov. "The permutoassociahedron, Mac Lane's coherence theorem and asymptotic zones for the KZ equation". In: *J. Pure Appl. Algebra* 85.2 (1993), pp. 119–142. DOI: 10.1016/0022-4049(93)90049-Y. URL: https://doi.org/10.1016/0022-4049(93)90049-Y (cit. on p. 77).

[Kit11] Sergey Kitaev. *Patterns in permutations and words*. Monographs in Theoretical Computer Science. An EATCS Series. With a foreword by Jeffrey B. Remmel. Springer, Heidelberg, 2011, pp. xxii+494. DOI: 10.1007/978-3-642-17333-2. URL: https://doi.org/10.1007/978-3-642-17333-2 (cit. on pp. 13, 14, 31, 32, 95–97, 188).

[Knu05] Donald Ervin Knuth. *The art of computer programming. Vol. 1. Fasc. 1*. MMIX, a RISC computer for the new millennium. Addison-Wesley, Upper Saddle River, NJ, 2005, pp. vi+134 (cit. on pp. 63, 65, 187).

[Kra99] Steven George Krantz. *Handbook of complex variables*. Birkhäuser Boston, Inc., Boston, MA, 1999, pp. xxiv+290. DOI: 10.1007/978-1-4612-1588-2. URL: https://doi.org/10.1007/978-1-4612-1588-2 (cit. on p. 131).

[KS02] Vladimir Petrov Kostov and Boris Zalmanovich Shapiro. "On arrangements of roots for a real hyperbolic polynomial and its derivatives". In: *Bull. Sci. Math.* 126.1 (2002), pp. 45–60. DOI: 10.1016/S0007-4497(01)01106-X. URL: https://doi.org/10.1016/S0007-4497(01)01106-X (cit. on p. 53).

[Lan03] Sergei Konstantinovich Lando. *Lectures on generating functions*. Vol. 23. Student Mathematical Library. Translated from the 2002 Russian original by the author. American Mathematical Society, Providence, RI, 2003, pp. xvi+148. DOI: 10.1090/stml/023. URL: https://doi.org/10.1090/stml/023 (cit. on pp. 20, 37, 38, 50, 53–55).

[LG95] Leonid Libkin and Vladimir Gurvich. "Trees as semilattices". In: *Discrete Math.* 145.1-3 (1995), pp. 321–327. DOI: 10.1016/0012-365X(94)00046-L. URL: https://doi.org/10.1016/0012-365X(94)00046-L (cit. on p. 80).

[LMW89] Dũng-Tráng Lê, Françoise Michel, and Claude Weber. "Sur le comportement des polaires associées aux germes de courbes planes". In: *Compositio Math.* 72.1 (1989), pp. 87–113. URL: http://www.numdam.org/item?id=CM_1989__72_1_87_0 (cit. on pp. 18, 36, 133).

[Mat02] Yukio Matsumoto. *An introduction to Morse theory*. Vol. 208. Translations of Mathematical Monographs. Translated from the 1997 Japanese original by Kiki Hudson and Masahico Saito, Iwanami Series in Modern Mathematics. American Mathematical Society, Providence, RI, 2002, pp. xiv+219 (cit. on pp. 124, 128).

[Mau99] Hélène Maugendre. "Topologie comparée d'une courbe polaire et de sa courbe discriminante". In: *Rev. Mat. Complut.* 12.2 (1999), pp. 439–450. DOI: 10.5209/rev_REMA.1999.v12.n2.17149. URL: https://doi.org/10.5209/rev_REMA.1999.v12.n2.17149 (cit. on pp. 18, 36, 133, 170).

[Mil65] John Willard Milnor. *Topology from the differentiable viewpoint*. Based on notes by David W. Weaver. The University Press of Virginia, Charlottesville, Va, 1965 (cit. on p. 132).

[Mil68] John Willard Milnor. *Singular points of complex hypersurfaces*. Annals of Mathematics Studies, No. 61. Princeton University Press, Princeton, N.J.; University of Tokyo Press, Tokyo, 1968, pp. iii+122 (cit. on pp. 117, 136, 137, 167, 169).

[Myc70] Jan Mycielski. "Mathematical Notes: Polynomials with Preassigned Values at their Branching Points". In: *Amer. Math. Monthly* 77.8 (1970), pp. 853–855. DOI: 10.2307/2317021. URL: https://doi.org/10.2307/2317021 (cit. on pp. 55, 56, 61).

[Osb82] Howard Osborn. *Vector bundles. Vol. 1*. Vol. 101. Pure and Applied Mathematics. Foundations and Stiefel Whitney classes. Academic Press, Inc. [Harcourt Brace Jovanovich, Publishers], New York, 1982, pp. xii+371 (cit. on p. 126).

[Plü37] Julius Plücker. "Sur les points singuliers des courbes". In: *Journal de Mathématiques pures et appliquées (Journal de Liouville)* 2 (1837), pp. 11–15 (cit. on pp. 18, 36, 133).

[Poi10] Henri Poincaré. *Papers on topology, Cinquième complément à l'analysis situs*. Vol. 37. History of Mathematics. Rendiconti del Circolo Matematico di Palermo (1884-1940), 45–110, Springer, translated and with an introduction by John Stillwell, 1904. American Mathematical Society, Providence, RI; London Mathematical Society, London, 2010, pp. xx+228 (cit. on pp. 23, 41, 124, 127).

[Pon17] Jean-Victor Poncelet. "Théorie des polaires réciproques". In: *Annales de Mathématiques pures et appliqués* 8 (1817), pp. 201–232 (cit. on pp. 18, 36, 133).

[PP01] Patrick Popescu-Pampu. "Arbres de contact des singularités quasi-ordinaires et graphes d'adjacence pour les 3-variétés réelles". PhD thesis. Université Paris-Diderot-Paris VII, 2001. URL: https://tel.archives-ouvertes.fr/tel-00002800 (cit. on p. 61).

[Ree46] Georges Reeb. "Sur les points singuliers d'une forme de Pfaff complètement intégrable ou d'une fonction numérique". In: *C. R. Acad. Sci. Paris* 222 (1946), pp. 847–849 (cit. on pp. 23, 41, 124, 128).

[Rek+83] Gintaras Victor Reklaitis et al. *Engineering optimization*. A Wiley-Interscience Publication. Methods and applications. John Wiley & Sons, Inc., New York, 1983, pp. xvii+684 (cit. on pp. 117, 118).

[Ser80] Jean-Pierre Serre. *Trees*. Translated from the French by John Stillwell. Springer-Verlag, Berlin-New York, 1980, pp. ix+142 (cit. on p. 62).

[Sha] Niloufar Shafiei. *Recursive Definitions and Structural Induction*. URL: https://pdfs.semanticscholar.org/presentation/e31f/1cc1cbe4fe0819a326b66f8513f4fcb39df1.pdf (cit. on p. 65).

[SS00] Louis Welles Shapiro and Robert A. Sulanke. "Bijections for the Schröder numbers". In: *Math. Mag.* 73.5 (2000), pp. 369–376. DOI: 10.2307/2690814. URL: https://doi.org/10.2307/2690814 (cit. on p. 189).

[SS15] Ernest Shult and David Surowski. *Algebra—a teaching and source book*. Springer, Cham, 2015, pp. xxii+539 (cit. on pp. 80, 83).

[Sta10] Richard Peter Stanley. "A survey of alternating permutations". In: *Combinatorics and graphs*. Vol. 531. Contemp. Math. Amer. Math. Soc., Providence, RI, 2010, pp. 165–196. DOI: 10.1090/conm/531/10466. URL: https://doi.org/10.1090/conm/531/10466 (cit. on pp. 51, 64, 66, 67, 69).

[Sta12] Richard Peter Stanley. *Enumerative combinatorics. Volume 1*. Second. Vol. 49. Cambridge Studies in Advanced Mathematics. Cambridge University Press, Cambridge, 2012, pp. xiv+626 (cit. on pp. 64, 69).

[Sta15] Richard Peter Stanley. *Catalan numbers*. Cambridge University Press, New York, 2015, pp. viii+215. DOI: 10.1017/CBO9781139871495. URL: https://doi.org/10.1017/CBO9781139871495 (cit. on p. 189).

[Sta97] Richard Peter Stanley. "Hipparchus, Plutarch, Schröder, and Hough". In: *Amer. Math. Monthly* 104.4 (1997), pp. 344–350. DOI: 10.2307/2974582. URL: https://doi.org/10.2307/2974582 (cit. on p. 189).

[STT88] Daniel Dominic Sleator, Robert Endre Tarjan, and William Paul Thurston. "Rotation distance, triangulations, and hyperbolic geometry". In: *J. Amer. Math. Soc.* 1.3 (1988), pp. 647–681. DOI: 10.2307/1990951. URL: https://doi.org/10.2307/1990951 (cit. on p. 187).

[Tei77] Bernard Teissier. "Variétés polaires. I. Invariants polaires des singularités d'hypersurfaces". In: *Invent. Math.* 40.3 (1977), pp. 267–292. DOI: 10.1007/BF01425742. URL: https://doi.org/10.1007/BF01425742 (cit. on pp. 18, 36, 133).

[Tei90] Bernard Teissier. "Quelques points de l'histoire des variétés polaires, de Poncelet à nos jours". In: *Séminaire d'Analyse, 1987–1988 (Clermont-Ferrand, 1987–1988)*. Univ. Clermont-Ferrand II, Clermont-Ferrand, 1990, Exp. No. 4, 12 (cit. on pp. 18, 36, 133).

[TF16] Bernard Teissier and Arturo Giles Flores. "Local polar varieties in the geometric study of singularities". In: *arXiv preprint arXiv:1607.07979* (2016) (cit. on pp. 18, 36, 133).

[Tru93] Richard J. Trudeau. *Introduction to graph theory*. Corrected reprint of the 1976 original. Dover Publications, Inc., New York, 1993, pp. x+209 (cit. on pp. 61, 63).

[Tut84] William Thomas Tutte. *Graph theory*. Vol. 21. Encyclopedia of Mathematics and its Applications. With a foreword by C. St. J. A. Nash-Williams. Addison-Wesley Publishing Company, Advanced Book Program, Reading, MA, 1984, pp. xxi+333 (cit. on p. 61).

[Vic89] Steven Vickers. *Topology via logic*. Vol. 5. Cambridge Tracts in Theoretical Computer Science. Cambridge University Press, Cambridge, 1989, pp. xvi+200 (cit. on pp. 79, 80, 127).

[Vir88] Oleg Yanovich Viro. "Some integral calculus based on Euler characteristic". In: *Topology and geometry—Rohlin Seminar*. Vol. 1346. Lecture Notes in Math. Springer, Berlin, 1988, pp. 127–138. DOI: 10.1007/BFb0082775. URL: https://doi.org/10.1007/BFb0082775 (cit. on p. 128).

[Wal04] Charles Terence Clegg Wall. *Singular points of plane curves*. Vol. 63. London Mathematical Society Student Texts. Cambridge University Press, Cambridge, 2004, pp. xii+370. DOI: 10.1017/CBO9780511617560. URL: https://doi.org/10.1017/CBO9780511617560 (cit. on pp. 77, 118, 128, 140, 143, 165).

[Wal72] Charles Terence Clegg Wall. *A geometric introduction to topology*. Addison-Wesley Publishing Co., Reading, Mass.-London-Don Mills, Ont., 1972, pp. vii+168 (cit. on p. 131).

[Wal78] Robert John Walker. *Algebraic curves*. Reprint of the 1950 edition. Springer-Verlag, New York-Heidelberg, 1978, pp. x+201 (cit. on pp. 116, 117).

[Wes95] Julian West. "Generating trees and the Catalan and Schröder numbers". In: *Discrete Math.* 146.1-3 (1995), pp. 247–262. DOI: 10.1016/0012-365X(94)00067-1. URL: https://doi.org/10.1016/0012-365X(94)00067-1 (cit. on p. 189).

[Wi] URL: https://en.wikipedia.org/wiki/Tree_(graph_theory) (cit. on p. 63).

[Wil70] Stephen Willard. *General topology*. Addison-Wesley Publishing Co., Reading, Mass.-London-Don Mills, Ont., 1970, pp. xii+369 (cit. on p. 71).

[Woo26] Frederick Shenstone Woods. *Advanced calculus: a course arranged with special reference to the needs of students of applied mathematics*. Ginn, 1926 (cit. on p. 59).

[Wv] URL: https://wikivisually.com/wiki/Dual_curve (cit. on p. 143).

[This page intentionally left blank]

Index